A THERMAL STUDY OF SLAG SYSTEMS CONTAINING TITANIUM DIOXIDE.

THESIS

submitted to the

UNIVERSITY OF GLASGOW

for the degree of

DOCTOR OF PHILOSOPHY

by

JAMES GRIEVE.

JUNE 1940.

ProQuest LLC.
789 East Eisenhower Parkway
P.O. Box 1346
Ann Arbor, MI 48106 – 1346

CONTENTS.

INTRODUCTION.

Titania (TiO_2) with the composition Ti = 60%, O = 40% occurs in nature in different modifications as the minerals Rutile, Anatase and Brookite. It is an important constituent of many glazes and enamels; it also occurs in certain ferrous slags, and as an impurity in many fireclays, in which it acts as a flux.

In actual blast-furnace operation ores and fuels are often employed containing elements in small quantities which go into the slag or iron in varying proportions. One of the most common of these is titanium (Ti) which occurs in some cokes in fractional per cent, and in many ores in amounts varying from a trace up to 15 to 20% in the form of titania, which is extremely irreducible and infusible, its presence complicating the operation of the blast-furnace materially, for reasons which are only partly understood. The principal titaniferous iron ore is ilmenite ($FeTiO_3$), the mineral containing from 3 to 59% of titania (TiO_2), and it has been shown by Rossi and others that titaniferous iron ores can be smelted in the blast-furnace, and cast-irons containing titanium have been prepared by the blast-furnace-smelting of titanium ores with iron ores. The method is little used now, as much of the titanium enters the slag, and unless precautions are taken this leads to the production of higher-melting-constituents. In one example[1], of a high titanium

ore the blast furnace slag analysed 35% titania (Ti_2O_3) and the titanium (Ti) in the final steel ranged from 0·054% to 1%, although the steel was said to be cleaner and sounder than normal steel. However, copper-coloured infusible titanium cyano-nitride (TiCN) is liable to be formed in the hearth of the blast-furnace, and trouble from infusible accretions due to nitride formation have also been reported.

Mathesius[2], has patented a method for the production of titanium-bearing steels by melting pig-iron under a slag free from silica (Si_2O_2), containing not less than 70% Ti_2O_3 and reducing this with carbon (C); the titanium (Ti) liberated is said to remove nitrogen, oxygen, and sulphur from the iron. The slag is then removed and replaced by a fresh one containing titania (Ti_2O_3); it is claimed that the liberated titanium is sufficient to combine with the carbon in the molten iron, giving a steel containing 0·5% to 1% titanium carbide (TiC).

Early experiments on the addition of ferro-titanium to steel showed that improved steels could be obtained, but the amount of titanium (Ti) left in the steel was small, and it was recognised that the function of small additions was that of a scavenger or remover of impurities. Steels properly treated and containing a small amount of titanium have also been claimed to show a decreased sulphur content.

Comstock[3] found that there was an improvement in

mechanical properties of steels due to titanium, and that the microstructure of the titanium-treated steels was finer and more uniform, and there appeared to be less segregation of sulphides than when the same steel was treated with aluminium. The latter suffered from the presence of alumina (Al_2O_3) inclusions, whereas it is claimed by Comstock[4] that one of the advantages of titanium lies in the fluxing action of its oxide (TiO_2) on the furnace slags which may become mixed in the steel. From the viewpoint of deoxidation, titanium is claimed to be of value not only because titania (TiO_2) has a high heat of formation, but also because it has a low melting point (1560°C.), so that in liquid steel there is a greater chance of the oxide coalescing and rising to the surface, than there is with say, alumina. However, according to the investigations of the melting point of the titania used in the present work, it appears to be above 1650°C. (see Chapter 2.). According to Benedicks and Lofquist[6] the titanium dioxide formed during the deoxidation facilitates the removal of silicate slag present by considerably lowering the melting point.

Comstock[4] determined the solidification temperatures of basic open-hearth slags to which the addition of titania (TiO_2) had been made. The effect of titania in lowering the temperatures may be seen from the table below:

Slag.	Solidification Temperature.
Plain Slag	1065° C. - 1085° C.
Slag + 0·33% TiO_2	1085° C.
Slag + 1·33% TiO_2	1055° C. - 1060° C.
Slag + 2·67% TiO_2	1025° C.

Similar results were obtained with a higher melting point slag.

A still greater lowering will probably occur in a deoxidation product composed of silicates. Hence, it is probable that the beneficial effect of titanium (Ti) depends upon its slag-eliminating action, due to its fluxing action on the inclusions, almost as much as to actual deoxidation and denitrification (free titania has scarcely ever been observed in steel). Comstock[4] experimentally established the fact that the slag becomes less viscous and more easily removed. The latter being facilitated by the heat developed by the oxidation of titanium.

It is interesting to note that Benedicks and Lofquist[5], state that the presence of titania does not bring about any characteristic change in the appearance of silicate slags.

In recent years the binary system TiO_2 - SiO_2, and the titania-rich side of the diagram Ti_2O_3 - Na_2O have been

investigated by Bogatzky[6], and Junker[7] respectively, and the existence of the compound $Na_2O,3TiO_2$ confirmed. Moreover, the behaviour of titania on heating and its relation to ferric oxide (Fe_2O_3), and magnesium oxide (MgO) have also been partly investigated by Junker[7]. Nevertheless, few systematic investigations of the behaviour of titania at high temperatures have been made, though a number of systems involving compounds of titania that occur in glazes have recently been examined[8].

The present work was undertaken primarily with the object of throwing some light on the constitution and properties of ferrous slags containing titania, for which purpose thermal investigations of the systems $FeO - TiO_2$, $MnO - TiO_2$ and $FeO - MnO - TiO_2$ have been carried out.

CHAPTER 1.

DESCRIPTION OF APPARATUS EMPLOYED.

FURNACE.

The requirements of a furnace for work of this type are threefold and as follows:-

1. The distribution of temperature in the interior of the furnace must be sufficiently uniform to ensure that all parts of the melt to be investigated are sensibly equal in temperature.
2. The temperature of the interior must be capable of continuous variation throughout a considerable range, and it must be capable to make the rate of cooling and in certain cases of heating so slow, that equilibrium is approached in the melt.
3. It should be possible to heat the melt out of contact with gases capable of acting upon it chemically, or of dissolving in it to a notable extent.

From the above conditions it can be seen, that neither the arc nor the induction furnace is suitable for the purpose, and so an electrical resistance furnace had to be employed.

The furnace employed for determining the thermal data is shown in Figure 1. The casing was of mild steel $\frac{1}{4}$ ins. thick; the top and bottom plates were also made of mild steel but of $\frac{3}{8}$ ins. in thickness to minimise warping.

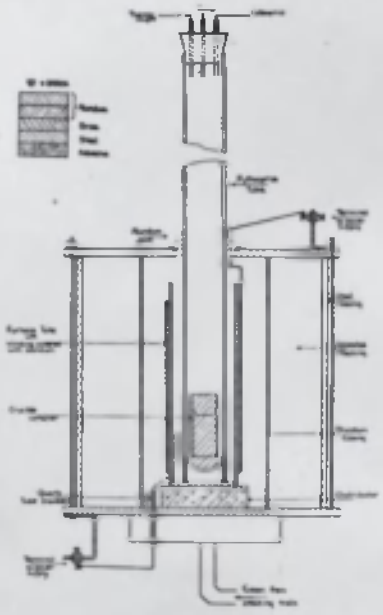

Fig. 1.

Spigot and faucet jointing was used both at top and bottom to ensure tightness. This was particularly important in the case of the bottom joint, as leakage of air into the furnace caused rapid deterioration of the winding, which was of molybdenum wire. A welded bottom joint has been used on some of the furnaces but as another type of plate was required for certain work, interchangeability was an advantage. However, it was possible to make a suitable joint without resorting to welding by using a cement of alundum and asbestos over the joints. Furnaces of this type have been in daily use to 1650° C. and have had lives of more than six months. The furnace winding was carried on an alundum tube of 3 ins. diameter. Such a tube was made by mixing together 90% of alundum of grade 563, and 10% of grade 562 of the same material, and moistening with a little water. An iron tube of an external diameter slightly less than the required internal diameter of the alundum tube was used as a former. Round the iron tube were wrapped three or four layers of damp brown paper. The alundum mixture was put round the wet paper and worked by hand until it was of uniform thickness of about $\frac{1}{4}$ in. The iron tube supported on a steel rod was slowly dried by placing it near a hot muffle. Slow drying was essential to avoid cracking. When thoroughly dry the tube was rubbed down with emery paper to uniform thickness. Thick string was wound round the tube

at the required spacing of the winding, which was usually five turns to the inch. The string was fixed in position by means of a very thin coating of alundum cement, the tube having been previously moistened to ensure complete union of the layer. The former with the alundum on it was now placed in a large furnace and slowly heated to 1100°C. The string and paper were burned so that after firing, the tube was easily removed from the former. It was finally dressed and the grooves for the wire cleaned.

About 45 feet of molybdenum wire of 0·04 ins. diameter were required to wind the furnace. The wire was first cleaned with emery to remove the graphite coating formed during drawing. The top and bottom of the winding were fixed in position by a binding wire consisting of a few turns of molybdenum wire. This same wire also served to fix the lead-in wires which were made of very heavy nichrome wire. It was found advisable to embed the molybdenum winding in a thin coating of alundum.

The tube carrying the winding fitted into a recessed groove in the bottom plate and was thus held in position.

Another alundum tube, made in exactly the same manner but of greater diameter, (about 4 inches) was slipped over the winding to prevent the asbestos insulation (see Fig. 1.) coming into contact with the hot tube, and causing slagging.

Into the annular space between the two tubes was passed

a stream of hydrogen and nitrogen, obtained by cracking ammonia gas. Strong ammonia solution (0·88 Sp. Gr.) was heated in a flask and the ammonia gas passed over iron turnings in a series of morganite tubes, heated to 700°C. in a nichrome wound furnace (Figure 2.). For very efficient cracking five morganite tubes of 1 inch internal diameter had to be used. The cracked gases were first bubbled through water, then through dilute and concentrated sulphuric acid in turn, and finally through calcium chloride, before passing into the furnace, whereby any uncracked ammonia gas was absorbed and the gases (N_2 and H_2) dried at the same time.

TEMPERATURE MEASUREMENT.

The temperature measurements were made by means of a tungsten-molybdenum thermocouple which can be used with precision up to temperatures beyond 1650°C. (error ± 5°C.). The tungsten-molybdenum thermocouple has a high melting point, but oxidises readily and must be used in an inert atmosphere or in vacuo. The electromotive force developed was small and was measured by means of a sensitive Tinsley Potentiometer graduated in millivolts. This was done by balancing the electromotive force set up in the thermocouple, against an oppositely directed electromotive force until a galvanometer needle showed zero current. Thus, when the

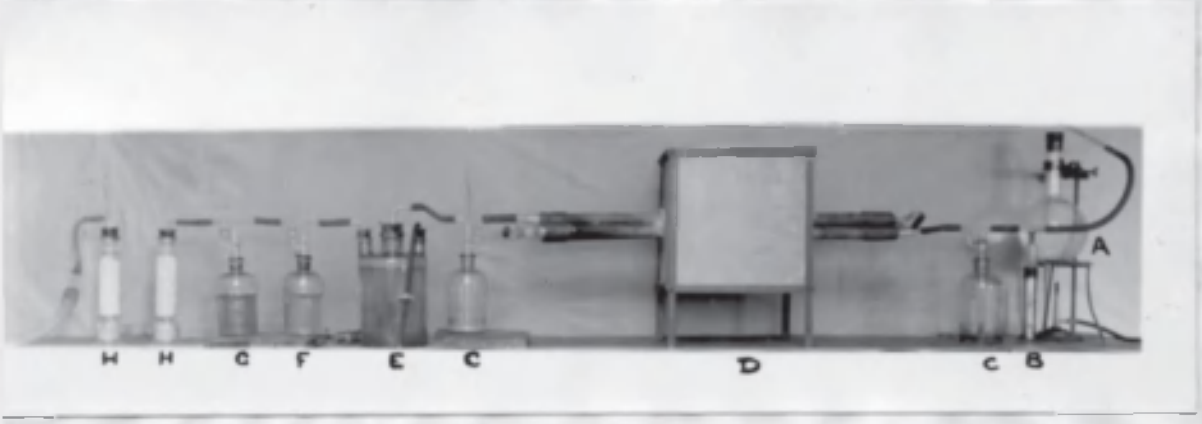

Figure 2.

A = Flask containing ammonia (Sp. Gr. 0·88).

B = Mercury blow-off valve.

C = Trap.

D = Nichrome-wound Furnace + Morganite Tubes.

E = Bottle filled with water.

F = Dilute sulphuric acid.

G = Concentrated sulphuric acid.

H = Calcium chloride.

potentiometer was balanced there was no current flowing in the thermocouple circuit and so the resistance of the thermocouple and the leads had no influence on the reading.

An ordinary lead accumulator was used for the balancing current and it was standardised daily against a standard Weston Cell.

Before use the thermocouple was carefully calibrated; for the lower temperatures (from zero up to 1,000°C.) against a standard chromel-alumel thermocouple, and at higher temperatures (from 900°C. to 1600°C.) reference points were obtained from the melting points of the pure metals, silver, gold, copper, nickel, iron and palladium. The melting points of the pure metals mentioned above were obtained by using short lengths of wire of each of the metals, to form a bridge between the tungsten molybdenum wires and so constitute the hot junction. The thermocouple was then slowly heated in the open furnace (i.e. in an atmosphere of hydrogen) and as soon as the wire melted the thermocouple went dead, and the millivolt reading corresponding to the melting point of the particular metal was read off from the potentiometer. The circuit and method of forming the bridge is shown in Figure 3.

A check on the values obtained for the metals mentioned above, was obtained by watching the chosen metal wires melt under conditions as near experimental conditions as possible.

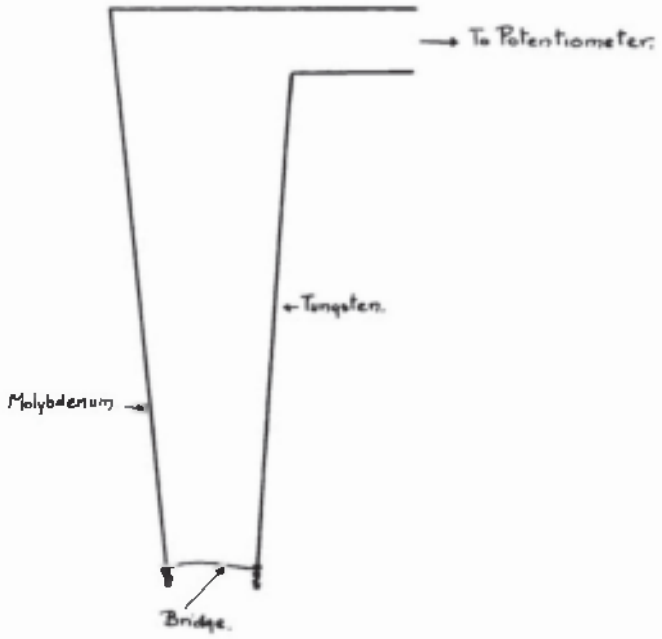

FIGURE 3.

Complete agreement was obtained in the millivolt reading for a particular wire, irrespective of the method used.

By plotting the millivolt reading corresponding to the melting temperature of the particular metal, against the melting point of the particular metal, a graph was obtained in the form of a parabola, from which the temperature corresponding to any particular millivolt reading could be read off directly.

Long lengths of molybdenum and tungsten wires (30 feet and 25 feet respectively) were used for the thermocouple, but frequent calibrations showed little variation in the electromotive force developed, as the length of the couple wires grew shorter.

HEATING AND COOLING CURVES.

There are several methods of thermal analysis the simplest of which consists in plotting the temperature of the specimen under investigation directly against the time. The temperature readings are taken at fixed intervals of time, and by plotting the results with temperature as ordinates and times as abscissae, a "time-temperature" curve is obtained which indicates the behaviour of the specimen in the most direct way. The only objection to this type of curve, is that the irregularities produced in it by comparatively small evolutions or absorptions of heat, are themselves extremely small, unless the curve is plotted to an

impracticably large scale. Consequently, a method of plotting is used which allows of the use of a very much more open scale, with the result that even minute thermal phenomena appear quite clearly. This result is obtained by the use of what is known as the "inverse rate" curve first adapted by Osmond[10] in 1887. Here the intervals of time, which are occupied by the specimen in falling or rising through successive equal differences of temperature are noted. The time occupied by successive rises are plotted as abscissae, against the actual temperature of the specimen at each observation, when a curve is obtained whose ordinates are θ (temperature), and whose abscissae are $\frac{\Delta t}{\Delta \theta}$ where t is time. With a uniform rate of heating or cooling, the curve becomes a vertical straight line: an evolution of heat during cooling or an absorption of heat during heating, caused the curve to deflect outwards to form a peak. If the rate of heating is uniform, the area of this peak is proportional to the quantity of heat evolved or absorbed.

There are still other types of heating and cooling curves, known as the "differential" and the "derived differential" which are obtained by a method devised by Roberts-Austen[11], which consists in comparing the rate of heating or cooling of the specimen, with a piece of metal placed in the same furnace, and heated and cooled along with the experimental specimen. The method has the advantage that no clock is required, and the results are capable of a high degree of

accuracy, even with no extremely sensitive galvanometer. This is obtained by the use of a "differential" thermocouple which consists of two thermocouple junctions arranged to oppose one another, and attached one to the experimental sample, and the other to a standard piece of metal, commonly known as the "blank." The readings of this couple simply indicate the difference of temperature between the specimen and the blank, and if these are plotted against the actual temperature of the specimen, as obtained from the readings of an independent thermocouple attached to the specimen, a "differential" curve is obtained. Since the heating and cooling of the blank which is the basis of this type of curve, is really proportional to the time which elapses between successive readings, the "differential" curve is practically identical with a time-temperature curve, the clock being replaced by the blank. Hence, to make the "differential" curves comparable with the "inverse-rate" curves the actual readings of the differential thermocouple at each temperature must not be plotted, but the change in its reading since the previous observation. If these are plotted against the temperature of the specimen, the "derived differential" first employed by Rosenhain[12] is obtained, which is very similar to the "inverse-rate" curve and is practically identical with it in physical meaning.

Examples of these various types of thermal curves are

shown in Figure 4. In curve A the values of θ (temperature) are plotted directly against t (time in seconds), and two developments of heat are indicated, the second one beginning immediately at the close of the first. B is the curve of a neutral body (blank) added for comparison. By reading off from the curve A the values of t at each successive 1°C. and tabulating, the differences between successive values of t, the time taken for the sample to cool through successive intervals of 1°C. (represented by $\frac{\Delta t}{\Delta \theta}$) are obtained. Plotting these differences against θ the curve C is obtained. The difference curve D constructed by plotting $(\theta - \theta_1)$ as recorded by the differential thermocouple against θ, shows the developments of heat with great clearness. Lastly, the curve E is obtained by measuring the change of $(\theta - \theta_1)$ for each 1°C. change of θ, or more strictly the slope of D at each point and plotting these values against θ.

Because of the smallness of the crucibles employed for the melts in this present work (see below), the amount of mixture which could be used was necessarily small (about 2 grammes). Besides, the failure to find a suitable refractory material to protect the tungsten-molybdenum thermocouple from the active substances ferrous oxide and manganous oxide, necessitated in having the thermocouple attached to the outside of the crucible. From the above conditions it is evident, that the heat changes developed

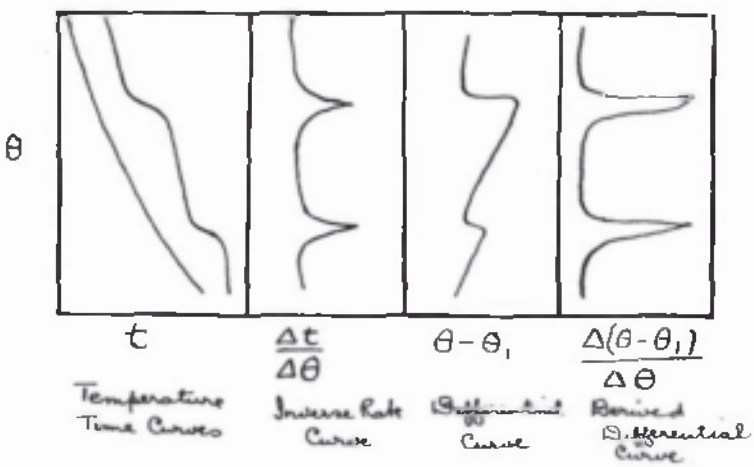
θ
t
Δt/Δθ
θ − θ1
Δ(θ − θ1)/Δθ
Temperature Time Curves
Inverse Rate Curve
Curve
Curve

Figure 4

must necessarily be small, and since the differential method of thermal analysis is particularly suited to demonstrating small heat reactions, that was the method mainly employed throughout the present investigation. The latter method as well as being the most sensitive method of plotting heating and cooling curves, has the advantage that if in addition the time Δt is measured by a chronograph then the "inverse-rate" curve may also be drawn. Thus, the method has the advantage of giving two independent lines based on different principles, their agreement affording assurance that there was no disturbing factor in the experiment. Further details concerning the differential method employed is discussed under the next sub-heading.

THE CRUCIBLES EMPLOYED AND THE DIFFERENTIAL SET-UP.

One of the chief difficulties in dealing with substances such as ferrous oxide (FeO), manganous oxide (MnO), and titanium dioxide ($Ti O_2$) was to find a suitable refractory material to withstand the attack of these active materials at temperatures up to 1,700° C. It was found that materials could be obtained which would retain these substances in the molten condition, but for the work proposed it was of the greatest importance that the molten material should not be contaminated by the refractory material, otherwise the composition of the mixture might be seriously affected. Many refractory substances, including fused alumina (Al_2O_3),

magnesia (MgO) and carborundum (S_iC) were tried, but all had to be rejected on account of either contamination of, or reaction with the melt. The greatest importance was placed upon the examination of the melts from this standpoint. A Higler spectrograph and various highly sensitive chemical tests were employed to detect any contamination of the melts. Furthermore, an analysis of the material was carried out after each fusion to ensure that no serious change in composition had occurred during melting.

For the investigation of the systems $FeO - T_iO_2$, $MnO - T_iO_2$ and $FeO - MnO - T_iO_2$, special molybdenum crucibles were employed since they were found to meet all the requirements. These crucibles were made by drilling out solid molybdenum rod, and a special plug of the same material was made to fit the top of the crucible. Owing to the size of the rod available the crucible was necessarily small. Fortunately, this did not interfere with the accuracy of the thermal curves, for it was found that the very smallness of the crucibles made it possible to consider the molybdenum crucible itself, as the hot junction of the thermocouple system. As stated above, a differential thermocouple was employed, and this greatly increased the sensitivity of measurement of heat changes. It was found that the couple wire could be bound to the outside of the crucible without any loss in accuracy. The system of the thermocouple connections and the alundum con-

tainer for the blank and the crucible are shown in Figure 5. The blank employed was a piece of molybdenum rod of approximately the same weight as the crucible and its contents.

The mixtures of FeO + Ti_2O_3, MnO + Ti_2O_3, and FeO + MnO + Ti_2O_3, respectively were made up by weighing the necessary quantities of the oxides to give the desired composition, and thoroughly mixed by grinding in an agate mortar. The appropriate melt was then transferred to a molybdenum crucible, which held roughly 2 grammes of the mixture. Each mixture investigated was packed as tightly as possible in the molybdenum crucible. The molybdenum crucibles normally employed were 1 inch long, with an internal diameter of 0·3 inches. Where difficulty was experienced with the melts boiling over and attacking the thermocouple point, (as in the case of melts with a high ferrous oxide content) the crucibles were made 1·5 inches long and the length of the stem of the plug increased correspondingly. When the above precautions proved insufficient, further protection of the thermocouple point was made by means of a small molybdenum sheath, which did not appreciably interfere with the sensitivity of the method.

The thermocouple and differential thermocouple were bound to the crucible and blank respectively, by means of thin molybdenum wire, and these inserted in the appropriate pockets of the alundum container. The top of the container

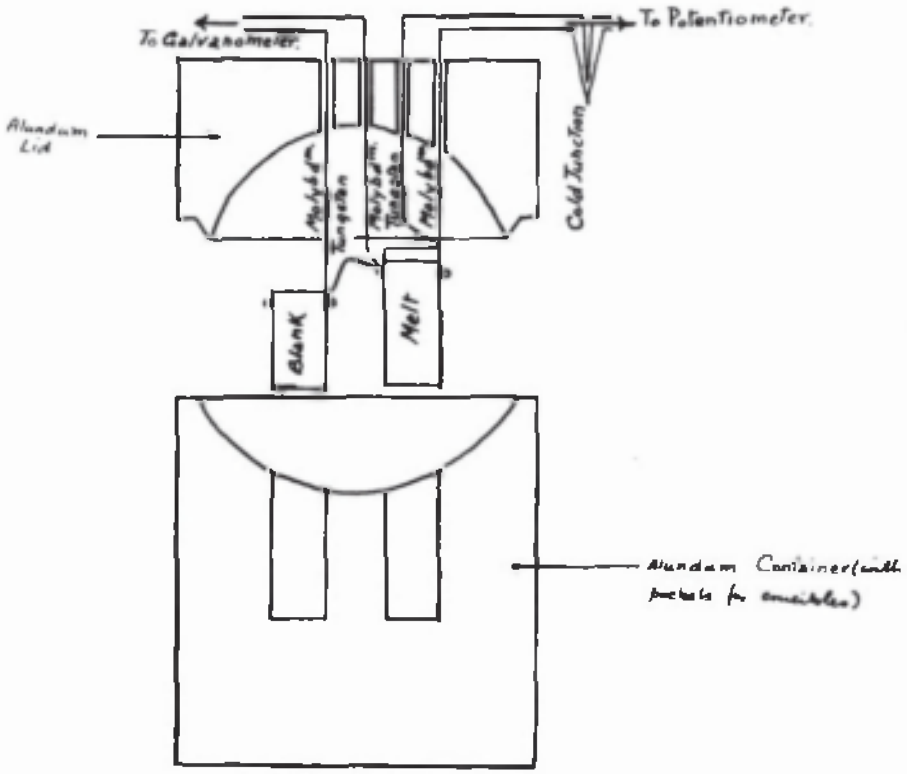
To Galvanometer
To Potentiometer
Alundum Lid
Molybdenum
Tungsten
Molybdenum
Tungsten
Molybdenum
Cold Junction
Blank
Melt
Alundum Container (with
holes for crucibles)

FIGURE 5.

was luted on with alundum and the whole inserted in the "Pythagoras" tube (see Figure 1.). The tube was evacuated by means of a Hyvac pump and then slowly heated. The "Pythagoras" tube (the inner refractory tube which was impervious to gases at the temperatures employed) 90 cms. long and 50 m.m. internal diameter, was found to hold a vacuum up to 1,470° C., but at temperatures above this it was liable to collapse. Thus, with mixtures having their melting-points above 1,470° C., it was necessary to admit nitrogen gas to prevent the collapse of the tube. If a nitrogen atmosphere had to be used, it was found that if enough of this gas (N_2) was allowed to enter the cold tube until a pressure of approximately half-an-atmosphere was obtained, then at the maximum temperatures employed this volume was just sufficient to give one atmosphere of pressure, and by this means collapsing and buckling of the tubes was greatly minimised. Generally, it was found that the heating and cooling curves taken in an atmosphere of nitrogen were irregular, whilst those obtained in vacuo were uniform and smooth.

It was found necessary to protect the tungsten-molybdenum thermocouple with a molybdenum grid attached to the outside of the "Pythagoras" tube. Failure to do this resulted in the tungsten-molybdenum thermocouple giving false temperature readings above 1,000° C. (probably the result of electronic disturbances). The grid simply consisted of a

piece of molybdenum sheet, 9 inches long and 0·01 inches thick, bound round the "Pythagoras" tube with molybdenum wire.

Generally, three heating and two cooling curves were determined for each mixture. The first heating curve was unreliable. This was particularly noticeable in the case of the two binary systems FeO - TiO_2 and MnO - TiO_2, due to the heats of formation of compounds. However, the second and third curves were usually in complete agreement. Time-temperature determinations were occasionally made in addition to the differential determinations.

INTERPRETATION OF DIFFERENTIAL CURVES.

The differential curve should be a vertical line so long as there is no difference in the rate of heat absorption or evolution between the crucible and the blank. Actually in practice, a slow drift of the zero took place chiefly due to small differences in mass and the relative positions in the furnace of the crucible and blank. When the contents of the crucible underwent phase changes e.g. in melting, heat was absorbed by the crucible at a greater rate than by the blank, so that the rate of heating of this portion of the system was reduced. This resulted in a deviation from the normal of the differential curve. The first deviation from the normal was taken as marking the commencement of melting. When the phase change was complete the temperature of the crucible started to gain on that of the blank and

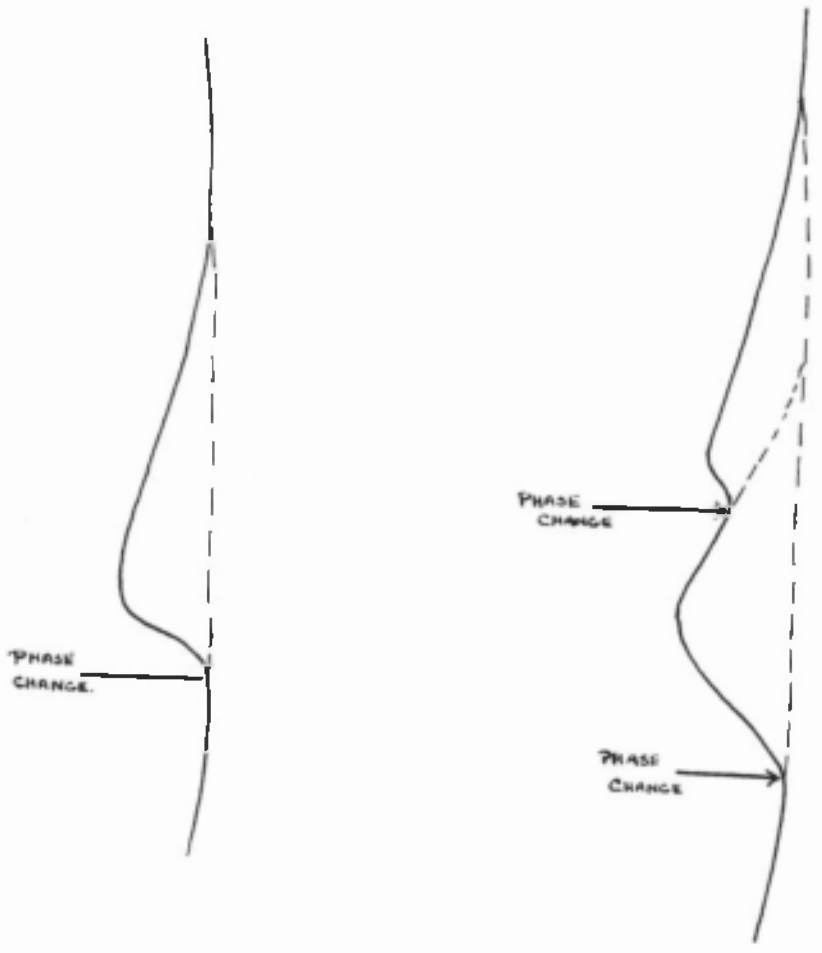

FIGURE 6.

the deviation decreased more or less asymptotically till the normal was again reached. Hence, the maximum deviation occurred at the conclusion of the heat absorption. This method of interpretation of the differential curves is shown diagrammatically in Figure 6.

CHAPTER 2.

THE PREPARATION AND EXAMINATION OF THE CONSTITUENTS - FERROUS OXIDE (FeO), MANGANOUS OXIDE (MnO) AND TITANIUM DIOXIDE (TiO_2).

It is of the highest importance that the components required for work of this type should be of the greatest purity attainable, for one or two per cent. of a foreign material may have a marked effect upon the physical properties of the mixture. So, before any elaborate physical researches of a high degree of accuracy are attempted, it is desirable that all the components to be used should be analysed and tested.

EXISTENCE AND PREPARATION OF FERROUS OXIDE (FeO).

Before proceeding to give an account of the method used for the preparation of ferrous oxide, it might be advisable to give a résumé of the literature concerning it (FeO), in view of the conflicting evidence regarding its existence.

According to R. Schenck and co-workers[18], who carried out investigations on the equilibrium between the oxides of iron and gaseous CO - CO_2 mixtures at various temperatures, pure ferrous oxide (i.e. oxide having a composition corresponding to the formula FeO) is incapable of existing. The ferrous oxide phase actually occurring in the system

Fe - O is a solid solution of magnetite (Fe_3O_4) in ferrous oxide (FeO), the homogeneity limits of which lie wholly to the oxygen-rich side of the composition of FeO (22·27% oxygen). To distinguish this phase from the hypothetical oxide FeO, Schenck suggested the name Wustite for it. His conclusions were at first strongly criticised by several writers, notably by Benedicks and Lofquist[14], who decided, on the evidence then available, that pure ferrous oxide could be and had been prepared. In their proposed form of the iron-oxygen diagram they, therefore, placed the homogeneity range of the ferrous phase to include the composition FeO. Mathewson, Spire and Milligan[15], however, accepted R. Schenck's findings on this point. H. Schenck and Hengler[16] also accept R. Schenck's data and claim to have confirmed the homogeneity limits given by him. In addition Pfeil[17], who investigated a considerable range of the iron-oxygen system by thermal and microscopical methods, and Jette and Foote[18], who investigated the lattice structure of the Wustite phase by X-rays, agree in placing the homogeneity limits of the Wustite phase entirely to the right of the composition FeO. There are however, appreciable differences in the actual solubility limits indicated by these various workers. Figure 7, shows the solubility limits as given by R. Schenck[13].

Below approximately 570°C. (the temperatures given by

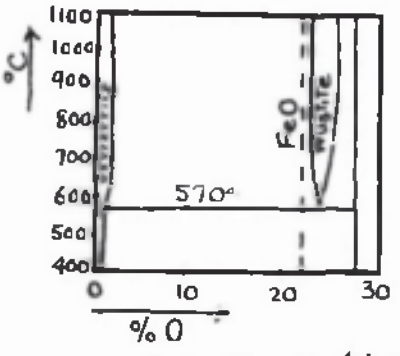

Iron - Oxygen (stable)

Figure 7.

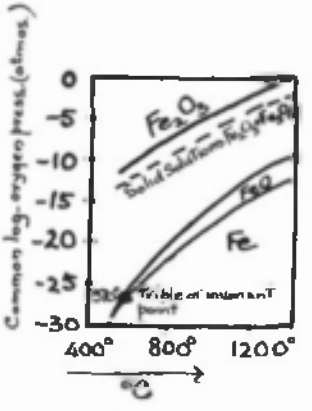

Figure 10.

the various workers vary but little) wustite is unstable and breaks down into a eutectoid mixture of metallic iron and magnetite. This is shown in the thermal equilibrium diagram by the fact that the two limiting solubility curves of the wustite phase intersect at 570° C. The composition of the point of intersection has been assigned various values eg. 23·3 per cent. of oxygen (Pfeil[17]), 23·55 per cent. of oxygen (Jette and Foote[18]) and 24·0 per cent. of oxygen (R. Schenck and co-workers[13]). The reaction involved in the breakdown can, presumably be represented by the equation:

$$4FeO \rightleftharpoons Fe + Fe_3O_4$$

This reaction has been studied by Kanz and Scheil[19], and by Chandron and Forestier[20]. The latter authors, who used magnetic means to measure the extent of the decomposition, found that the maximum rate of decomposition occurred at 480° C., when about 80 per cent. of the oxide was decomposed in 24 hours, while below 300° C virtually no decomposition occurred. It was found that the rate of decomposition of ferrous oxide is in accord with the equation:

$$\frac{dx}{dt} = k(100 - x)^4$$

where x denotes the decomposition in the time t and k is a constant. From this it would appear that wustite prepared above 570° C., can safely be cooled down to room temperature without appreciable decomposition, provided that it is rapidly cooled through the range 570° C. to 300° C. If the

product is slowly cooled, however, it will be contaminated with iron (Fe) and magnetite (Fe_3O_4), the amounts of these formed increasing as the cooling rate is decreased.

From the point of view of its behaviour in slags, the melting characteristics of wustite are of considerable importance. Benedicks and Lofquist[14] basing their conclusions on the findings of Tritton and Hanson[21], indicate that ferrous oxide (FeO) melts incongruently at 1370°C., with the separation of metallic iron (saturated with oxygen) and formation of a liquid oxide melt containing 23·4 per cent. of oxygen. Mathewson, Spire and Milligan[15] also concluded that wustite in contact with iron melts incongruently at 1370°C. They found that the oxygen content of molten iron and oxide in equilibrium with metallic iron at 1370°C., was 23·0 per cent. corresponding to the presence of 11.56 per cent. of ferric oxide (Fe_2O_3), and this figure has been confirmed by Bowen and Schairer[22]. The location of the point M in Figure 8, can thus be accepted with some certainty.

The slope CGM is of importance in that it gives an indication of the temperature at which the melting of wustite saturated with iron will be complete. Benedicks and Lofquist[14] fixed the point C to the left of the composition FeO, in agreement with Tritton and Hanson's findings[21]. Mathewson, Spire and Milligan[15], however, showed that, if the presence of silica (SiO_2) and other impurities were allowed

Iron – Oxygen Thermal Equilibrium Diagram.

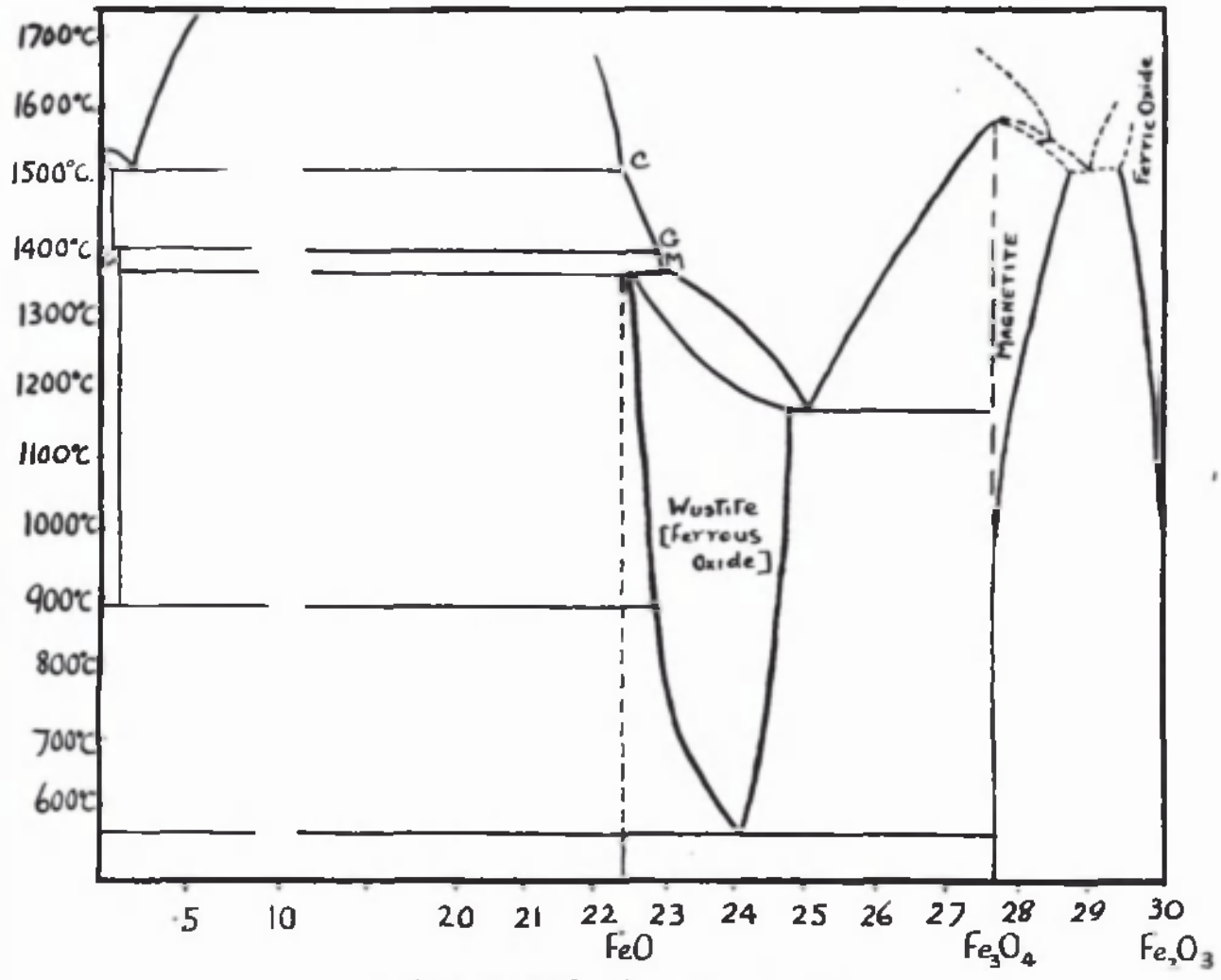

FIGURE 8.

for, C would be located (on Tritton and Hanson's data)[21] at 23·1 per cent. of oxygen. Their own redetermination of this point indicated an oxygen content of 22·25 per cent., this being the mean of two independent determinations. According to this figure Wustite saturated with iron would not melt completely till a temperature of 1500° C. had been reached. This is in fairly good agreement with evidence provided by thermal curves of Wustite obtained by Hay and co-workers[28].

It may be noted that neither Pfeil[17] nor H. Schenck and Hengler[16], agree with the melting relationships described above. The thermal equilibrium diagrams proposed by these workers, indicate normal congruent melting of Wustite without separation of iron. The bulk of the evidence available, however, supports the view that the relationships indicated by Mathewson, Spire and Mulligan[15], are substantially correct. Figure 8 is based essentially on the diagram proposed by these workers. That part of it relating to the partial system Fe_3O_4 - Fe_2O_3 has, however, been modified on the basis of data given by White, Graham and Hay[23], and by White[24]. These have enabled the limits of the solid solubility of Fe_2O_3 and Fe_3O_4 in one another to be fixed from 1200° C. to 1450° C. Their findings also indicate the existence of a eutectic between Fe_2O_3 and Fe_3O_4, instead of a peritectic as suggested by Mathewson, Spire and Milligan[15].

The relationships shown in Figure 8 take account of temperature and composition only. Actually, the stability of the phases in the system Fe - O, is as much dependent on the oxygen pressure as it is on the temperature. This aspect of the equilibrium between the oxides of iron has been discussed in some detail by Benedicks and Lofquist[14], and also by C.C. Ralston[25]. Figure 9 which is given by the former authors, shows diagrammatically the way in which the dissociation (oxygen) pressure varies with the composition of the solid oxide across the iron-oxygen diagram, at constant temperature, on the assumption (as indicated in Fig. 8) that each oxide forms a restricted range of solid solution at high temperatures. The horizontal sections of the curve, correspond to the composition ranges within which two separate oxide phases co-exist. When only one phase is present, the dissociation pressure is a function of the composition (oxygen content) of that phase. Thus, the sloping parts of the curve correspond to the solid solution ranges of the phases, metallic iron (with oxygen in solution), Wustite, magnetite and ferric oxide (Fe_2O_3). As the temperature is raised the dissociation pressures of the various oxides increase in approximately logarithmic fashion. This is clearly shown in Fig. 10, which is due to Ralston[25], the curves indicating the variation with temperature of the dissociation pressures of the various saturated phases, (i.e. phases in equilibrium with adjacent phases in the iron-

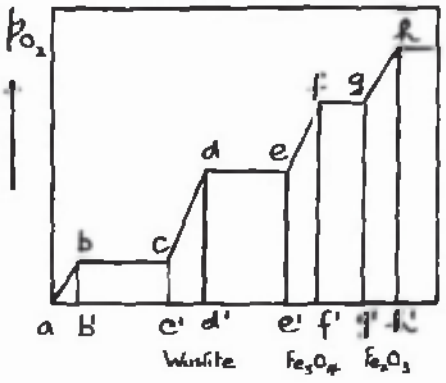

Relation between Oxygen Pressure and Oxygen Content (% O) of the different Iron Oxides (schematically.)

Figure 9.

oxygen diagram). Hence the curves represent the paths traced out, in terms of oxygen pressure and temperature, of the various horizontal sections of Figure 9.

It will be seen from Figure 10 that the oxygen pressures in equilibrium with iron-saturated wustite is, at all ordinarily obtainable temperatures, immeasurably small. Actually atmospheres in equilibrium with this phase can only be produced indirectly e.g., in mixtures of CO and CO_2 or of H_2 and H_2O. Work on the equilibrium between such mixtures and wustite has been carried out by Matsubara[86], Eastman and Evans[87], Schenck[13] and others.

Summing up the evidence discussed above, the position appears to be that no definite compound of the composition FeO exists, but that the "ferrous oxide" or wustite phase of the iron-oxygen system is a solid solution, stable only above 570° C., and extending over the range of approximately 23 to 24 per cent. of oxygen. It follows that this phase, even when it contains the minimum possible content of oxygen, has still appreciably more than corresponds to the formula FeO. (23·27 per cent. oxygen). Hence so-called pure "FeO" can not be prepared. Wustite saturated with iron, which is the nearest attainable approximation to FeO, can however, be prepared above 570° C., and can be preserved to room temperature if it is cooled fairly rapidly. Strictly speaking, as pointed out by Ralston[85], the preparation can

only be accurately carried out in a mixture of CO and CO_2 (or H_2 and H_2O) in the correct ratio, the value of this ratio being dependent on the temperature used. Given this ratio and assuming that it can be maintained constant, e.g., by passing a stream of the mixture over the sample, it should be possible to prepare iron-saturated wustite accurately, starting from either a higher or lower state of oxidation. According to Ralston[85], small amounts of wustite have, in fact, been prepared in this way. In practice however, such a method is difficult to carry out, and is only suitable for the preparation of small amounts of the oxide. The wustite for the present investigation was prepared by the method used by Hay and co-workers[88], which had been found capable of giving an oxide containing approximately 76·8 - 76·9 per cent. of iron (FeO - 77·27% Fe).

The method simply consisted in decomposing pure recrystallised ferrous oxalate in vacuo at 650° C., the complete set-up being shown in Figure 11. The ferrous oxalate was packed loosely in a porous alundum container, about 9 inches long and with an internal diameter of 1·5 inches approximately. The latter was completely closed at one end but stopped with a loose-fitting alundum stopper and a packing of asbestos at the other, which facilitated the escape of gases during the decomposition:

$$FeC_2O_4 \cdot 2H_2O = FeO + 2H_2O + CO_2 + CO.$$

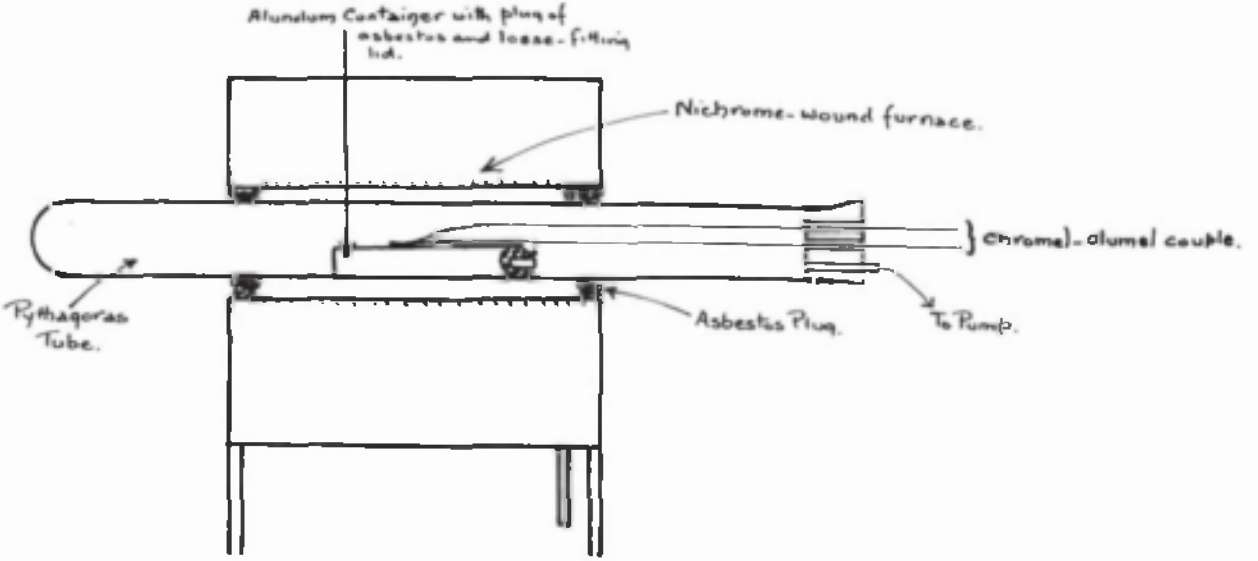
Alundum Container with plug of asbestos and loose-fitting lid.
Nichrome-wound furnace.
} chromel-alumel couple.
Pythagoras Tube.
Asbestos Plug.
To Pump.

FIGURE 11.

The container was placed in a "Pythagoras" tube fitted horizontally in a nichrome-wound furnace. The "Pythagoras" tube was closed at one end but was fitted with a three-holed rubber bung at the other, two of the holes bearing connections to a mercury manometer and a Cenco-Hyvac Pump respectively, while the third hole carried the chromel, alumel thermocouple for the temperature control. It was found desirable to heat the furnace slowly at first, and to remove the gases evolved as rapidly as possible, for the lower the temperature of decomposition of the oxalate the better the product. On completion of the decomposition, the temperature of the furnace was raised to 1,000° C., and held there for approximately one hour, when the ferrous oxide was then allowed to cool quickly (in vacuo). If the product of decomposition was not soaked at the high temperature, then the pyrophoric form of ferrous oxide was obtained.

It is interesting to note in the "Chemie Minerale", it is stated there are two modifications of ferrous oxide. The low-temperature modification is pyrophoric, and when it is heated in nitric acid, nitrous fumes are evolved. The high-temperature modification does not decompose nitric acid and is more stable in air. It is also stated, that the low-temperature modification can be converted into the high-temperature stable form by heating to above 1,000° C.

By keeping the ferrous oxide in well-stoppered air-tight bottles, it could be preserved for some time without decomposition taking place.

The purity of the ferrous oxide was determined from its chemical analysis, and the microscopic examination of a representative sample which had been melted in vacuo, under experimental conditions, using the special molybdenum crucibles. From the microscopic examination of the ferrous oxide melt, any magnetite present was easily spotted because of its characteristic hammer-head or spinel structure. Finally, the absence of magnetic properties in the prepared sample of ferrous oxide, was taken as a further criterion of its purity.

Analysis of the prepared sample by the method above, gave the percentage iron as 76·7. For analysis, a known weight of ferrous oxide was dissolved in hydrochloric acid, then stannous chloride was added until the solution was clear, the excess stannous chloride present was then precipitated by the addition of mercuric chloride. Without filtering off the precipitate, the solution of the ferrous salt was quickly titrated against standard dichromate solution, using potassium ferricyanide as the indicator.

Weight of crucible + FeO = 12·0864 gs.

Weight of crucible = 11·9190 gs.

Weight of FeO = 0·1674 gs.

Volume of K dichromate used = 14·8 c.cs.

But 1 c.c. K dichromate = 0·0088 gs. Fe

$$\% \text{ Fe} = \frac{0{\cdot}0088 \times 14{\cdot}8 \times 100}{0{\cdot}1674}$$

$$= \underline{77{\cdot}7}$$

The heating curves for pure FeO (Figure 12) showed a large deflection at 1370°C., indicating that at this temperature most of the material had become liquid. In all the curves however, there is a small but definite deflection at 1410°C., and another at 1480°C., and a very small arrest is noted at 1170°C. This agrees with the investigations of Hay and co-workers[88]. The latter found that the presence of this low-point at 1170°C., and in the increase in magnitude of this arrest when partially magnetic FeO is thermally investigated tends to confirm the work of Mathewson, Spire and Milligan[15], who found a eutectic between FeO and Fe_2O_3 with a melting point of 1175°C. It would presumably indicate that the oxide even after melting tended to be non-homogeneous. Thus, the ferrous oxide used in the following work, does not appear to have a definite melting point, but at 1370°C., undergoes a peritectic reaction resulting in the formation of a liquid phase and a very

FeO - 100% (non-magnetic).

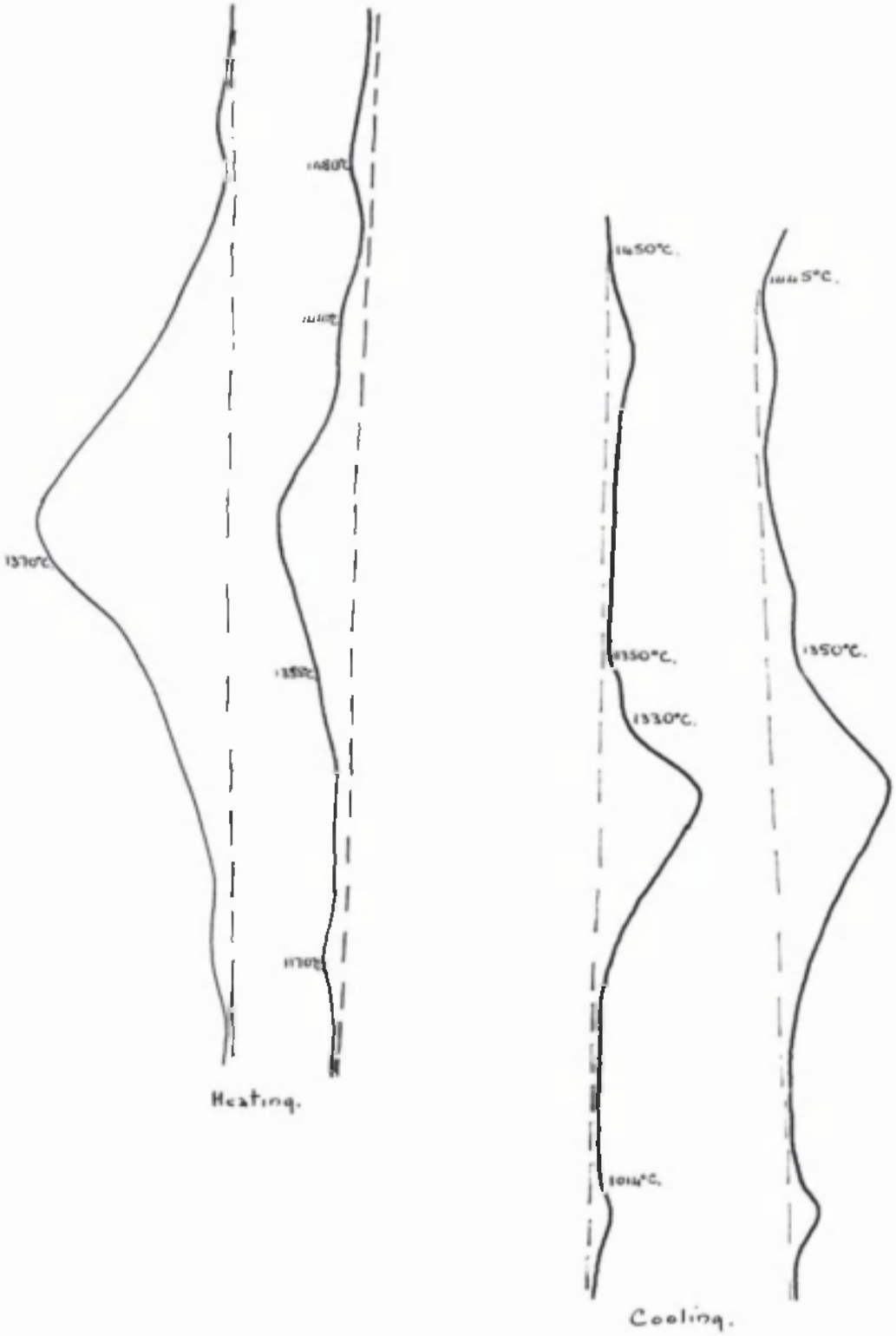

FIGURE 12.

small amount of a solid phase, the latter being a saturated solid solution of oxygen in iron. The small arrest at 1410° C., would then be due to the γ to δ change in the iron, and the point at 1480° C., to the final solution of the iron. The thermal changes are in good agreement with those found by Tritton and Hanson[31].

MANGANESE MONOXIDE.

Manganese monoxide can be prepared in a like manner to ferrous oxide, but differs from the latter in being more stable at ordinary temperatures. In fact, according to C.W. Blomstrand[30], emerald green cubic crystals of manganous or manganese monoxide (MnO) contaminated with approximately 1 per cent. iron, occur in the manganiferous dolomite of Langbau, Wermland, Sweden.

Part of the thermal equilibrium diagram of the system Mn - O, provisionally constructed by C. Benedicks and H. Lofquist[14], based on an analogy between manganous oxide and ferrous oxide is shown in Figure 13. The diagram shows a region of immiscibility between the liquid manganese-phase and the liquid manganous oxide-phase (curve C---D---E). A eutectic point B has been assumed quite close to Manganese (100%), so that the eutectic Mn - MnO consists almost entirely of pure manganese. The MnO liquidus curve BC continues on the other side of the region of immiscibility

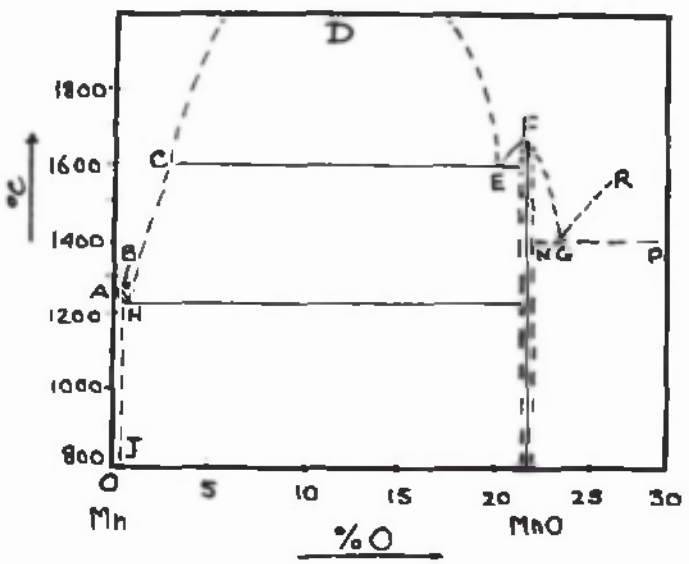

Equilibrium Diagram of the Partial System Mn – MnO.

Figure 13.

as the liquidus curve EF, starting from the assumed MnO - maximum F. At higher oxygen contents the presence of a eutectic corresponding to FGR is assumed, but the position of G and NP have not been fixed. The homogeneity range of manganese monoxide (MnO) extends down to low temperatures (along LM and NO) owing to the greater stability of this compound.

The melting point of MnO is given as 1650°C., as found by Tiede and Birnbrauer[31]. However, this value for the melting point was not directly determined, but from determinations on mixtures of manganese monoxide (MnO) and ferrous oxide (FeO), (Oberhoffer and von Keil)[38] by extrapolation, the melting point of MnO may be estimated at about 1700°C., according to Benedicks and Lofquist[14]. Investigations by Andrews and co-workers[37], give the melting point of MnO as 1585°C., but direct determinations by Hay and co-workers[32], found it to be 1785°C., a value much higher than had been anticipated, and a value which was used by the author throughout this work.

There are several ways in which manganese monoxide may be prepared. C.W. Scheele[33], prepared the latter by heating manganous carbonate to redness out of contact with air, E.G.L.Roberts, and E.A. Wraight[34], by fusing manganese dioxide (MnO_2) in a magnesia lined crucible, and J. von Liebig[35], and others by heating manganous oxalate. The

latter method of preparation was the one adopted and the apparatus used was identical with that used for the preparation of ferrous oxide (see Figure 11). The pure recrystallised manganous oxalate, was decomposed in vacuo at 750°C., and it was found advantageous to heat at 1,000°C., for about one hour, which rendered the product more stable in air. The manganese monoxide was cooled quickly in an atmosphere of hydrogen gas.

Manganous oxide so prepared is an olive green powder, which on chemical analysis shows a manganese (Mn) content of 77·4 per cent. X-ray analysis of the manganous oxide (prepared in the above method) by Hay and co-workers[38], showed that it had a cubic space lattice of the sodium chloride (NaCl) type, and that the elementary cube was found to be $4{\cdot}44_5$ Å.U., which is in good agreement with the generally accepted figure for this material. It is of interest to note, that the above workers found the refractive index of the manganous oxide after fusion, to be 2·16 and that the spectrographic analysis of the same sample showed no presence of any impurity.

Oberhoffer and d'Huart[36] established that manganese monoxide, in contradistinction to ferrous oxide, is not reduced by hydrogen at 900°C. On examining the sintered manganese monoxide under the microscope, it was found to consist of clear deep-green globules.

TITANIUM DIOXIDE.

The purest titania (TiO_2) that could be obtained commercially was used and its purity tested in various ways.

ANALYSIS.

The estimation of titanium was done by fusing the oxide with caustic soda, dissolving in hydrochloric acid, and reducing with metallic zinc to the titanous condition. The titanous solution in an atmosphere of carbon dioxide gas was titrated rapidly against standard iron alum solution using potassium thiocyanate as indicator.

Approximately 0·5 grammes of finely ground titanium dioxide was fused with about ten times its own weight of caustic soda in a platinum basin. The melt was cooled, acidified with hydrochloric acid and diluted accurately to 250 c.cs. capacity. 25 c.cs. of the above solution were transferred to a conical flask, 200 c.cs. capacity. The flask was fitted with a three-holed rubber bung, carrying a Bunsen valve, and two glass rod plugs which could be quickly replaced by an inlet and outlet tube respectively, for the carbon dioxide gas which must be used as soon as the reduction of the titanic salt is complete, for the titanous salt is unstable and readily oxidised under ordinary atmospheric conditions. The reduction of the titanic solution was carried out by dipping a rod of zinc into the acidified solution. On completion of the reduction, the rod

was lifted out by means of a wire to which it was attached. The titanous salt was then titrated rapidly against a standard iron alum solution in an atmosphere of CO_2, using potassium thiocyanate as indicator.

Many attempts were made before consistent results could be obtained, for there are many sources of error in an analysis of this type. The main sources of error were:

1. The instability of titanous salts in the presence of oxygen.
2. The trial and error method used in the reduction of the titanic salt.
3. The presence of small amounts of impurities in the zinc rod which interfere with the titration.

RESULTS.

Weight of bottle + iron alum = 22·7500 gs.
Weight of bottle = 18·7100 gs.
Weight of iron alum = 4·0400 gs.

The iron alum was dissolved in the usual manner and diluted to 500c.cs. in a standard flask.

Weight of bottle + Titania = 19·1860 gs.
Weight of bottle = 18·7100 gs.
Weight of Titania = 0·4760 gs.

The titania was treated as described above and diluted

to 1,000c.cs. in a standard flask and 25c.cs. of the solution were used for each titration.

Volume of titanous chloride solution used.	Volume of iron alum solution required.	Per cent. of titanium[a] in sample.
25 c.cs.	6·4	87·0%
25 c.cs.	7·2	98·4%
25 c.cs.	7·2	98·4%
25 c.cs.	7·2	98·4%

The results of the analysis obtained suggested that the titanium dioxide was pure enough for our purpose, but since the above analysis was rather troublesome to carry out accurately, it was thought advisable to carry out some further tests. So, the following additional experiments for the presence of impurities such as, soluble materials, alkalis, alumina, and iron were carried out.

The tests simply consisted in boiling a known weight of titanium dioxide in water and in acids respectively, filtering and finding the change in weight of the dried residue.

RESULTS.

Weight of titania used = 2·00 gs.

Weight of titania after washing and igniting. = 1·9945 gs.

Loss in weight = 0·0055 gs.

= 0·25%

Similar figures were obtained when acids were used.

The loss in weight under the above conditions is so small as to suggest the titanium dioxide is of a high degree of purity.

LOSS ON IGNITION.

A known weight of titanium dioxide was heated in air in a platinum crucible first, at 400° C., (approx.) and finally at a bright red heat. The heating was continued at each of the temperatures until the weight remained constant.

RESULTS.

Weight of crucible + titania at room temperature. = 17·42 gs.

Weight of crucible + titania after heating to 400° C. = 17·41 gs.

Weight of crucible. = 14·03 gs.

Weight of titania used. = 3·39 gs.

Loss in weight of titania after heating to 400° C. = 0·01 gs.

= 0·295%

Weight of same sample after heating to bright red heat. = 17·41 gs.

Loss in weight of titania between 400°C. and bright red heat. = 0·0 gs.

From the above, it is evident that there is no further loss in weight when the sample is heated from 400°C. to 600°C. Moreover, the loss in weight on heating the sample of titania to 400°C. is so small as to suggest it is due to combined or absorbed water.

LOSS AT HIGH TEMPERATURES.

The sample of titania above which had been heated in air to 600°C. (approx.) was now examined for changes in weight at higher temperatures, and the loss in weight of fresh samples was also noted both in vacuo and in an inert atmosphere of nitrogen gas.

RESULTS IN OXYGEN.

In oxygen using the sample which had been previously heated to 600°C.

Weight of crucible + titania after heating to 1580°C. = 17·59 gs.

Weight of crucible + titania after heating to 600°C. = 17·41 gs

Loss in weight of titania at 1580°C. = 0·02 gs.

= 0·59%

Total loss in weight on heating from room temperature up to 1580° C. = 0·295% + 0·59%

= 0·885%

RESULTS IN VACUO.

Fresh sample of titania used.

Weight of titania used.	= 2·00 gs.
Weight of platinum crucible + titania at room temperature.	= 16·4775 gs.
Weight of platinum crucible + titania after heating to 1300°C.	= 16·4678 gs.
Loss in weight after heating to 1300°C.	= 0·0097 gs.
	= 0·49%

RESULTS IN NITROGEN ATMOSPHERE.

Fresh sample of titania used.

Weight of titania used.	= 2·00 gs.
Weight of platinum crucible + titania at room temperature.	= 16·2361 gs.
Weight of platinum crucible + titania after heating to 1600°C.	= 16·2235 gs.
Loss in weight of titania after heating to 1600°C.	= 0·0076 gs.
	= 0·3%

It is interesting to note that all samples underwent considerable shrinkage during the above tests, and were strongly sintered. They became dark grey in colour, and after prolonged heating in air and nitrogen, traces of an orange-yellow colouration were frequently noticed on the surface of the sample exposed to the atmosphere, and more especially where the sample had been in contact with the

platinum crucible.

Examination of the titania sample which had been heated in vacuo, showed no evidence of the orange-yellow colouration, but the whiteness of the original sample had been replaced by the dark grey colour, common to the other samples which had been heated in nitrogen and oxygen.

At this stage it was thought that dissociation or association, or even both, were taking place on heating the titania, with the formation of higher and lower oxides of titanium (Ti). Such reactions would account for the colour changes and the weight changes at the high temperatures.

The dissociation of titania was now investigated using the high-temperature balance previously developed by J. White[24] for the study of the high-temperature dissociation of ferric oxide (Fe_2O_3).

A sketch of the apparatus used is given in Figure 14, which is largely self-explanatory. The experiments simply consisted in weighing the samples of titania while they were actually at high temperatures. The balance employed was a sensitive assay balance, placed on a shelf above the furnace, the platinum crucible used being suspended in the hot zone of the molybdenum furnace by means of a platinum wire attached to one pan as shown.

A sample of titania (which had previously been heated to 1600°C., in an atmosphere of nitrogen) was now heated in an atmosphere of oxygen, and its change in weight after

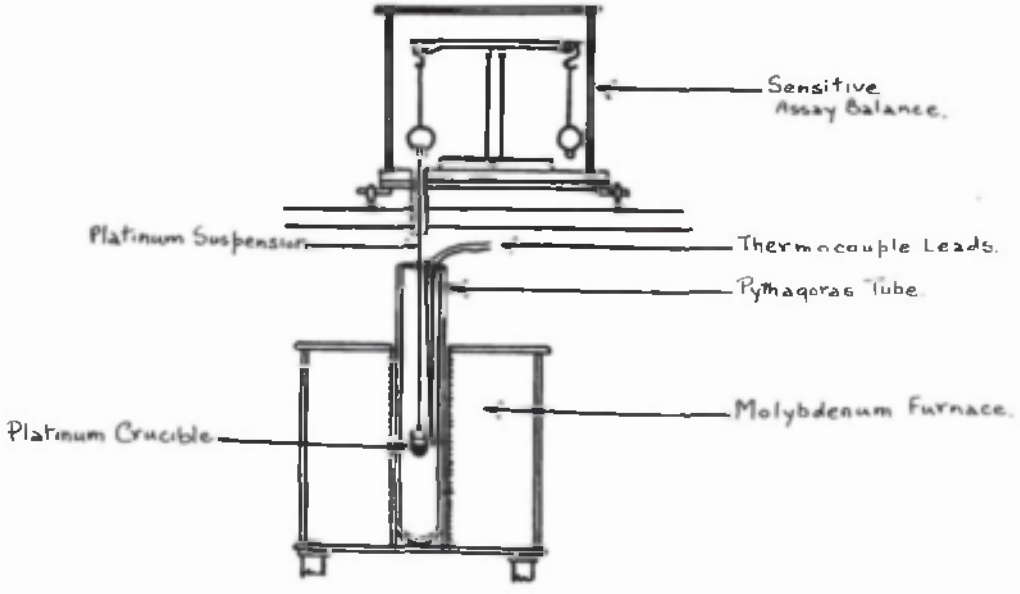

HIGH-TEMPERATURE BALANCE.

FIGURE 14.

definite intervals of time was noted, both on heating and cooling. The experimental results are given in Table 1, +, being used to denote an increase in weight, and -, a decrease in weight.

Table 1 shows that the titanium dioxide lost weight steadily with rise in temperature, whilst on cooling there was an initial loss in weight followed by an increase in weight on cooling over-night. However, the increase in weight on cooling is much less than the loss in weight on heating. It is evident from the results obtained above, that it is very unlikely that the titanium dioxide undergoes dissociation, but the experiment was repeated using a fresh sample of titania. Here, the sample was held for greater lengths of time at the chosen temperatures, since there was a possibility that the dissociation, (if taking place) was a very sluggish reaction. The results of the investigation are given in Table 2, and it can be seen that once again the sample lost weight progressively on heating. Even after soaking the titania, at 1500°C., for 3·5 hours the loss in weight showed no signs of reaching a limit. But, on cooling the sample gains in weight for a short period only, and at room-temperature it is lighter than it was at 1500°C. The behaviour of the same sample at still higher temperatures is shown in Table 3, and once again the sample kept losing weight regularly on heating at 1600°C. for approximately

TABLE 1.

Time in minutes.	Temperature in °C.	Weight in grams.	Change in weight in grams.	
-	Room	40·2850	- -	HEATING.
-	-	40·2810	- 0·0040	
-	1290° C.	40·2810	None	
-	1440° C.	40·2783	- 0·0027	
-	1450° C.	40·2761	- 0·0022	
15	1560° C.	40·2688	- 0·0073	
15	1560° C.	40·2658	- 0·0030	
15	1560° C.	40·2640	- 0·0018	
15	1560° C.	40·2620	- 0·0020	
15	1600° C.	40·2600	- 0·0020	
45	1600° C.	40·2544	- 0·0056	
		Total Loss	= - 0·0306	
15	1540° C.	40.2544	-	COOLING.
15	1450° C.	40·2500	- 0·0044	
15	1450° C.	40·2500	None	
15	1450° C.	40·2500	None	
Overnight	Room	40·2534	+ 0·0034	
		Total change =	- 0·0010	

TABLE 2.

Time in Minutes.	Temperature in °C.	Weight in Grams.	Change in Weight in Grams.	
-	1000	42·6180	None	HEATING.
15	1000	42·6120	- 0·0060	
15	1000	42·6090	- 0·0030	
15	1000	42·6090	None	
15	1260	42·6054	- 0·0046	
15	1260	42·6052	- 0·0002	
15	1500	42.6034	- 0·0018	
15	1500	42·6000	- 0·0034	
15	1500	42·5974	- 0·0026	
15	1500	42·5960	- 0·0014	
15	1500	42·5946	- 0·0014	
15	1500	42·5934	- 0·0012	
15	1500	42·5920	- 0·0014	
15	1500	42·5910	- 0·0010	
15	1500	42·5900	- 0·0010	
15	1500	42·5822	- 0·0018	
15	1500	42·5876	- 0·0006	
15	1500	42·5868	- 0·0008	
15	1500	42·5858	- 0·0010	
15	1500	42·5851	- 0·0017	
		Total Loss =	- 0·0329	
15	1260	42·5851	None	COOLING.
15	1260	42·5856	+ 0·0005	
15	1260	42·5856	None	
Overnight	Room Temperature	42·5837	- 0·0019	
		Total Change=	- 0·0014	

TABLE 3.

Time in Minutes	Temperature in °C.	Weight in Grams.	Change in Weight in grams.	
75	1260	42·5790	-	HEATING.
5	1450	42·5776	- 0·0024	
10	1600	42·5764	- 0·0012	
15	1600	42·5740	- 0·0024	
15	1600	42·5720	- 0·0020	
15	1600	42·5702	- 0·0018	
15	1600	42·5784	- 0·0018	
15	1600	42·5680	- 0·0004	
15	1600	42·5671	- 0·0009	
		Total Loss =	- 0·0119	
15	1450	42·5680	-	COOLING.
15	1450	42·5677	- 0·0003	
15	1450	42·5677	None	
15	1450	42·5680	+ 0·0003	
15	1450	42·5676	- 0·0004	
15	1450	42·5676	None	
15	1450	42·5676	None	
15	1450	42·5676	None	
		Total Change =	- 0·0004	

$1\frac{3}{4}$ hours as well as showing a slight loss in weight on cooling.

Summing up the experimental data above, it is seen that even after heating the titania for several hours at high temperatures, the loss usually amounted to only 0·5 to 0·8 per cent. by weight, and did not appear to be reaching a limit. Further, from the cooling investigations no evidence of reversibility could be obtained. Thus, it is improbable therefore that dissociation to a lower oxide was taking place (see also discussion below). A more probable explanation is that titanium dioxide is slightly volatile at high temperatures. It was noticed after one experiment, that there were traces of a white deposit on the upper part of the platinum wire used to suspend the crucible in the furnace.

All the samples underwent considerable shrinkage during the tests, and were strongly sintered. They also became dark grey in colour and after prolonged heating in air, traces of an orange-yellow colouration were often noticable, especially on the exposed surface and round the outside of the sample, where it had been in contact with the platinum crucible. This effect was never noticed during the normal heating of titania in molybdenum crucibles under non-oxidising conditions.

An orange-yellow trioxide of titanium (T_iO_3) is known to exist. Presumably, in air, oxidation to this higher

oxide was taking place, possibly promoted by the ability of platinum to absorb and re-emit oxygen.

REFRACTIVE INDEX ANALYSIS OF THE SINTERED TITANIA.

A refractive index analysis of the sintered titania by the Becke immersion method was made in an attempt to find out if there was more than one phase present (impurities). The finely powdered sintered titania was mixed in turn with liquids of increasing refractive index, and viewed under the microscope by means of transmitted light. If the powdered particles have a refractive index value widely different from that of the liquid in which they are immersed, there is a bright border separating each particle from the liquid. On focussing the microscope up (away from the object) the bright line of demarcation between solid and liquid moves into the material possessing the greater refractive index. The opposite effect takes place when the microscope is put out of focus in the opposition direction.

For the lower refractive index comparisons the following liquids were used:

	μ	μ
Turpentine and clove oil.	= 1·475	- 1·540
Clove oil and α- monochlornaphthalene	= 1·540	- 1·635
α- monochlornaphthalene and α- monobromnaphthalene	= 1·655	- 1·740

It was found that the sintered titania powder was completely opaque in the liquids used above, which suggested

that its refractive index might be considerably higher than that of the highest liquid used. So, for the still higher refractive index determinations use was made of the sulphur, selenium glasses, as prepared and used by H.E. Merwin and E.S. Larsen[89].

THE PREPARATION OF VITREOUS MIXTURES.

The required weight of pure selenium was heated in a test-tube until it was properly fused, when it was allowed to cool and the proper amount of sulphur added. The mixture was then heated over a low flame just sufficiently hot to allow thorough mixing with a glass rod. As the material cools it is gathered on a glass rod, cut into small fragments and kept in a stoppered bottle.

For use with the microscope, a small piece of the vitreous mixture and a little of the powdered titania were heated on a glass slide under a cover-glass, over a small flame until the mixture was fluid. The powder and mixture were then mixed and pressed into a thin film. The film was then heated for 15 to 30 seconds until bubbles began to appear, when the cover-glass was again pressed firmly down and cooling allowed to take place. The table below gives the composition of the vitreous mixtures prepared, along with their refractive index values, using monochromatic light of the sodium and lithium flames respectively.

% Se	μ_{Na}	μ_{Li}
9·0	1·978	1·998
37·5	2·100	2·134
57·0	2·200	2·248
70·0	2·300	2·365
80·0	2·400	2·490
87·7	2·500	2·624
93·8	2·600	2·755
99·2	2·700	2·900

Monochromatic light was not employed since comparable figures were sufficient for our purpose. Moreover, the mixtures probably did not retain their initial composition owing to the volatility of the sulphur, but this was not considered a serious drawback, since the method was intended merely to distinguish between different phases, and not to measure refractive indices as such. Trouble was, however, encountered with vitreous mixtures containing less than 50 per cent. selenium by weight, which tended to crystallise instead of giving glasses.

This method of examination gave little information however, for with every vitreous mixture used the titania particles appeared opaque.

X-RAY ANALYSIS OF THE SINTERED TITANIA.

X-ray analysis of the sintered titania were carried out

using the powder method of crystal analysis as devised independently by A.W. Hull[40], and by P. Debeye and P. Scherrer[41]. By this method a large number of small crystal particles forming a narrow cylinder are irradiated by monochromatic X-rays, so as to produce all the possible spectra simultaneously on a cylindrical film concentric with the specimen. Consequently, several spectra overlap and the occurrence or otherwise of many lines is open to some doubt. This makes the analysis of the structure only possible in the case of crystals with comparatively high symmetry. When the symmetry of the crystal is low, the line pattern on the film is very complex and it may be impossible to work out the structure from the powder photograph alone.

In the present work the X-ray tube was of the "gas discharge" type with a cobalt target. The camera employed is shown in Fig. 15. A holder P, at the centre of the camera, carried the cylindrically shaped specimen about 0·5 - 0·6 mms. diameter and about 1 - 2 cms. long. The specimen was made by mixing the very finely powdered material with a small amount of vaseline, to form a very thick paste. A thick-walled glass capillary tube of 0·5 - 0·6 mm. bore was filled with the paste, which was compressed by inserting wire into both ends of the capillary when a reasonably stable solid rod was obtained. It was then partially pushed out of the capillary as a cylindrical rod. The rod obtained, if straight enough, was accurately centred in the

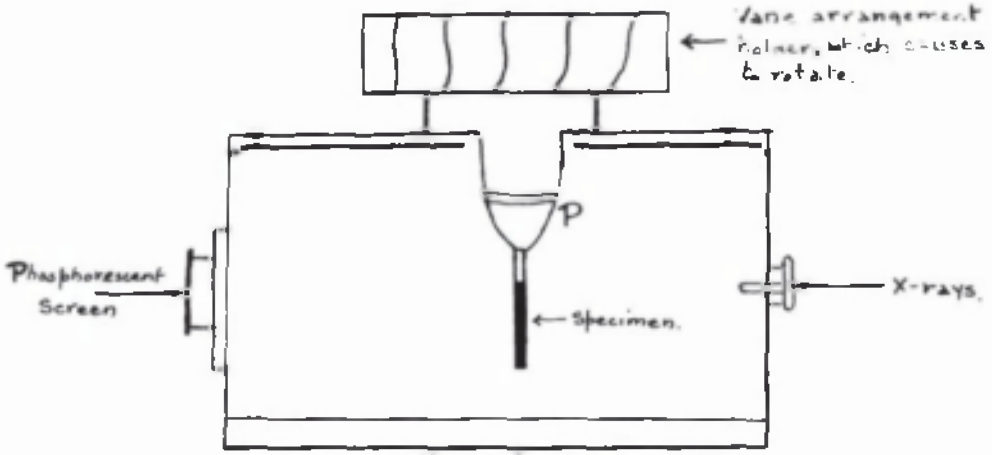

X-ray Camera.

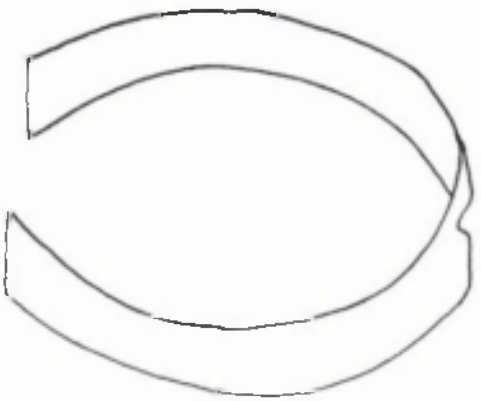

Arrangement of film inside the camera.

FIGURE 15.

camera, being securely held in the chuck by the glass capillary A finer adjustment of the specimen could be obtained when it was illuminated by the X-ray beam, and its shadow cast on a phosphorescent screen at the point where the beam left the camera. Use was also made of bristles from a brush, to mount the powdered specimens. The bristle was soaked in collodion, and then rotated in the fine powder, sufficient of the latter adhering to form a fairly homogeneous cylindrical layer. The bristle was mounted in the camera in the usual way after the collodion had dried. Before use, the bristle with the film of collodion was X-rayed, but no lines showed up on the film.

Even, when the specimen to be examined was finely ground, if the specimen was not rotated the coarseness of the powder resulted in a series of spots which appear in place of lines, because all the possible orientations of the crystalline particles did not occur. The random distribution of the particles was increased by continuously rotating the specimen. This resulted in very smooth lines.

The intensity and breadth of the lines in an X-ray photograph vary with the size of the crystallites in the specimen under examination, small particles giving rise to more diffuse and broader lines, due to the smaller resolving power of the three-dimensional grating in small crystallites. This is exactly the same phenomenon as occurs with a line grating, where the sharpness of the interference maxima is

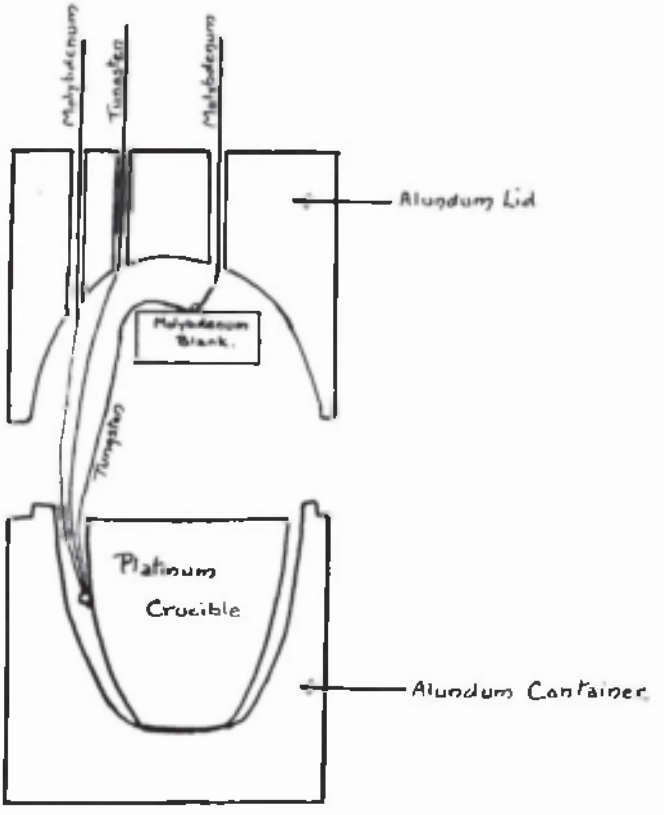
Molybdenum
Tungsten
Molybdenum
Aluminum Lid
Molybdenum Blank
Tungsten
Platinum Crucible
Aluminum Container

Figure 16.

a function of the total number of lines ruled on the grating and not their distance apart. The line broadening is due to incomplete cancelling of waves, diffracted at angles other than the Bragg angles due to the small number of cells.

The X-ray photographs for the different coloured powders obtained on heating the titania above 1200°C. (in platinum) were found to be identical in all respects. Calculation of the spectrum for the sintered titania gave that of Rutile, (tetragonal system) and corresponds to values of the lattice parameters, a = 5·36 Å, c = 2·94 Å, (see Appendix I for the calculation).

THERMAL CURVES FOR TITANIA (TiO_2).

Heating and cooling curves were finally taken of the titania, using a platinum crucible as a container, a molybdenum crucible as the blank and the differential tungsten-molybdenum thermocouple. The size of the platinum crucible prevented the blank from being placed along side it. The blank was accomodated in the roof of the lid (see Figure 16).

The heating and cooling curves for the titania are shown in Figure 17 and it can be seen there is no evidence of a point of any kind, which tends to show that the titania does not undergo an allotropic change of any kind.

TiO_2 (100%)

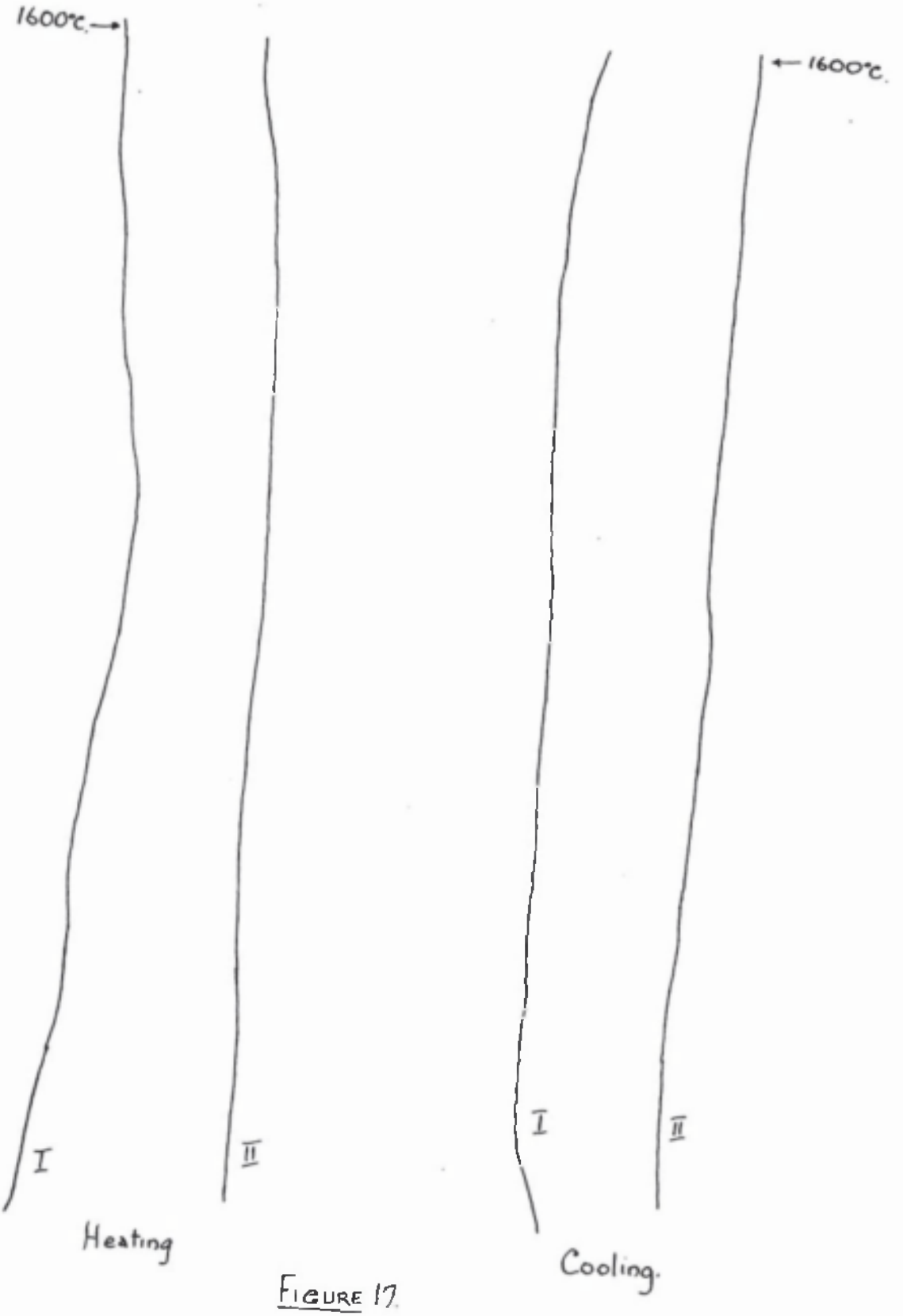

FIGURE 17

STABILITY OF TITANIA (TiO_2) AT HIGH TEMPERATURES.

A compressed sample of powdered titania in contact with a similar sample of ferrous oxide (FeO) was heated in a platinum basin to approximately 1300° C., in vacuo (i.e. below the fusion point of ferrous oxide). This was done by making a pellet of ferrous oxide and embedding it in a matrix of titania. The heating was carried out in a "Pythagoras" tube using the molybdenum furnace previously described. No evidence of oxidation of the ferrous oxide, or reduction of the titania at the surfaces of contact could be found from the microscopical examination of the polished surfaces. Systematic examination of the FeO - TiO_2 melts made later in molybdenum also failed to reveal any such reaction. Further, the molybdenum of the crucibles appears to be without effect upon titania, since in some of the melts primary crystals of this constituent showing no traces of alternation, could often be found in direct contact with the crucible wall. In some of the melts, minute metallic dendrites were observed under the microscope in the vicinity of the crucible wall. A similar effect has also been noted in certain silicate melts, and they appear to be very similar to those occurring in ground-coat enamels as reported by King[48]. Probably the mechanism of their formation is similar, but, their effect on the composition of the melt would be negligible. From the point of view of

contamination of the melts, molybdenum is much superior to ordinary refractories as a crucible material, whilst platinum picks up appreciable quantities of iron from melts containing ferrous oxide.

There is little quantitative thermo-chemical data on the stability of titania at elevated temperatures. N. Nasu[43] studied the reaction:-

$$2TiO_2 + H_2 = Ti_2O_3 + H_2O$$

up to 1009°C., at which temperature he found the equilibrium constant (P_{H_2O}/P_{H_2}) had the value 0·595. For the reaction:-

$$FeO + H_2 = Fe + H_2O$$

Emmett and Shultz[44], found the value of the constant to be 0·678 at 1,000°C. Hence, at this temperature titania is more stable than ferrous oxide, a conclusion which was confirmed experimentally by Nasu.

Data on titania applicable to higher temperatures can only be obtained by extrapolation. Extrapolation of Nasu's results to 1600°C., gives a value for the above constant of 2·74. This would correspond to a dissociation pressure of titania of the order of $1{\cdot}21 \times 10^{-7}$ atmospheres, assuming the expression given by Mc'Cance[45], for the dissociation constant of water at high temperatures to be correct (for calculations see Appendix II). This would indicate a high degree of stability for titania at 1600°C. Mc'Cance's data for ferrous oxide (FeO) and magnetite (Fe_3O_4) indicate dissociation pressures for these oxides of 7.27×10^{-8} and

$8{\cdot}14 \times 10^{-5}$ atmospheres respectively. Hence, the dissociation pressure of ferrous oxide (FeO) is only slightly lower than that of titania at this temperature, whilst that of magnetite (Fe_3O_4) is considerably higher. From that it is probably safe to conclude, that the oxygen content of an iron oxide melt in equilibrium with titania, would be little, if any, in excess of that contained in ferrous oxide (FeO). The results of the microscopic study of the melts in the present instance appear to confirm this.

CHAPTER 3.

THE SYSTEM FeO - TiO_2.

From what has been said earlier, it should be clear that the system FeO - TiO_2 (or, to be more exact, wustite - FeO) cannot with complete accuracy be considered as a binary system, since, on melting wustite dissociates to form metallic iron and a liquid melt richer in oxygen than the original oxide phase. (Similarly below 570° C., wustite forms metallic iron and magnetite, but this need not, of course, be considered in dealing with high temperature relationships.) Hence phases are formed whose composition cannot be represented on a binary FeO - TiO_2 diagram. Strictly speaking, therefore, wustite cannot be considered as a single component, and complete representation of the relationships shown by mixtures of ferrous oxide (FeO) and titania (TiO_2) is only possible on a ternary diagram viz. on the ternary diagram of the system Iron - Oxygen - Titania. It will be obvious that strict observance of these requirements considerably complicates the investigation, and graphical representation of systems containing ferrous oxide, for "binary" systems become ternary, "ternary" systems become quaternary, and so on. For most purposes, however, it is sufficiently accurate to neglect the decomposition of ferrous oxide and to treat it as a single stable

component with a melting point at 1370°C. The separation of iron at this temperature is thus ignored, as is the fact, that the liquid oxide phase first formed contains more oxygen than the original ferrous oxide. The amount of iron formed is in any case small, being less than three per cent. of the weight of the initial ferrous oxide, while the liquid oxide phase contains only about 0·75 per cent. more oxygen than the original oxide. Further investigations on similar systems e.g. (the system FeO - SiO_2 by Bowen and Schairer[46]) have shown that only melts whose composition lies near the ferrous oxide (FeO) end of the diagram are appreciably effected by this behaviour of ferrous oxide. Hence, no serious loss of accuracy is to be expected from the treatment of the system FeO - TiO_2, as a two component system. This simplified method of treatment has in the past been adopted by many workers in dealing with systems containing ferrous oxide (FeO).

The thermal equilibrium diagram of the system FeO - TiO_2 was investigated by the thermal methods previously described (see Chapter 2) aided by microscopic examination of the various melts by reflected light after sectioning, polishing and, where necessary, etching. Considerable difficulties were at first encountered in studying this system since the thermal curves tended to be very irregular, and difficult to interpret. Further, the melts proved very

difficult to polish satisfactorily owing to their brittleness (see below). Hence, it was found necessary to repeat the investigation of some of the mixtures several times.

The procedure adopted in the thermal study was to take, whenever possible, three heating and two cooling curves of each composition chosen. The first heating curve with the mixture of oxides in the crucible was usually abnormal, but not without value in elucidating the changes undergone by the system at high temperatures. The heating was done in a "Pythagoras" tube either in vacuo or in an atmosphere of nitrogen. Under ideal conditions the differential curve should be a vertical line, as long as there is no difference in the rate of heat absorption or evolution between the crucible and the blank. In actual practice, however, a slow drift of the zero takes place chiefly due to small differences in mass, and relative positions in the furnace of crucible and blank. The method of interpretation of ideal differential thermal curves has already been described in Chaper 2.

The thermal curves obtained for the various compositions of FeO + Ti_2O_3 studied are shown in Figures 18 to 42, the temperatures of the various arrests being indicated. The data thus obtained are summarised in the table below (Table 4).

It was found that the melting point of titania could not

TABLE 4.

Composition Weight per cent. FeO	TiO_2	Temperature of separants °C.	Etchant.
97·5	2·5	1305 and 1370	Dilute HCl.
90	10	1305 and 1350	Dilute HCl.
80	20	1305 and 1408	Dilute HCl.
70	30	1305 and 1440	HF.
64·3	35·7	1470	HF.
60	40	1320 and 1408	HF.
55	45	1320 and 1410	HF.
53	47	1320 and 1430	HF.
50	50	1320 and 1460	HF.
47·4	52·6	1470	HF.
40	60	1332 and 1400	HF.
30	70	1330 and 1355	HF.
20	80	1330 and 1426	HF.
10	90	1330 and 1450	HF.

FeO 97·5%.
TiO_2 2·5%.

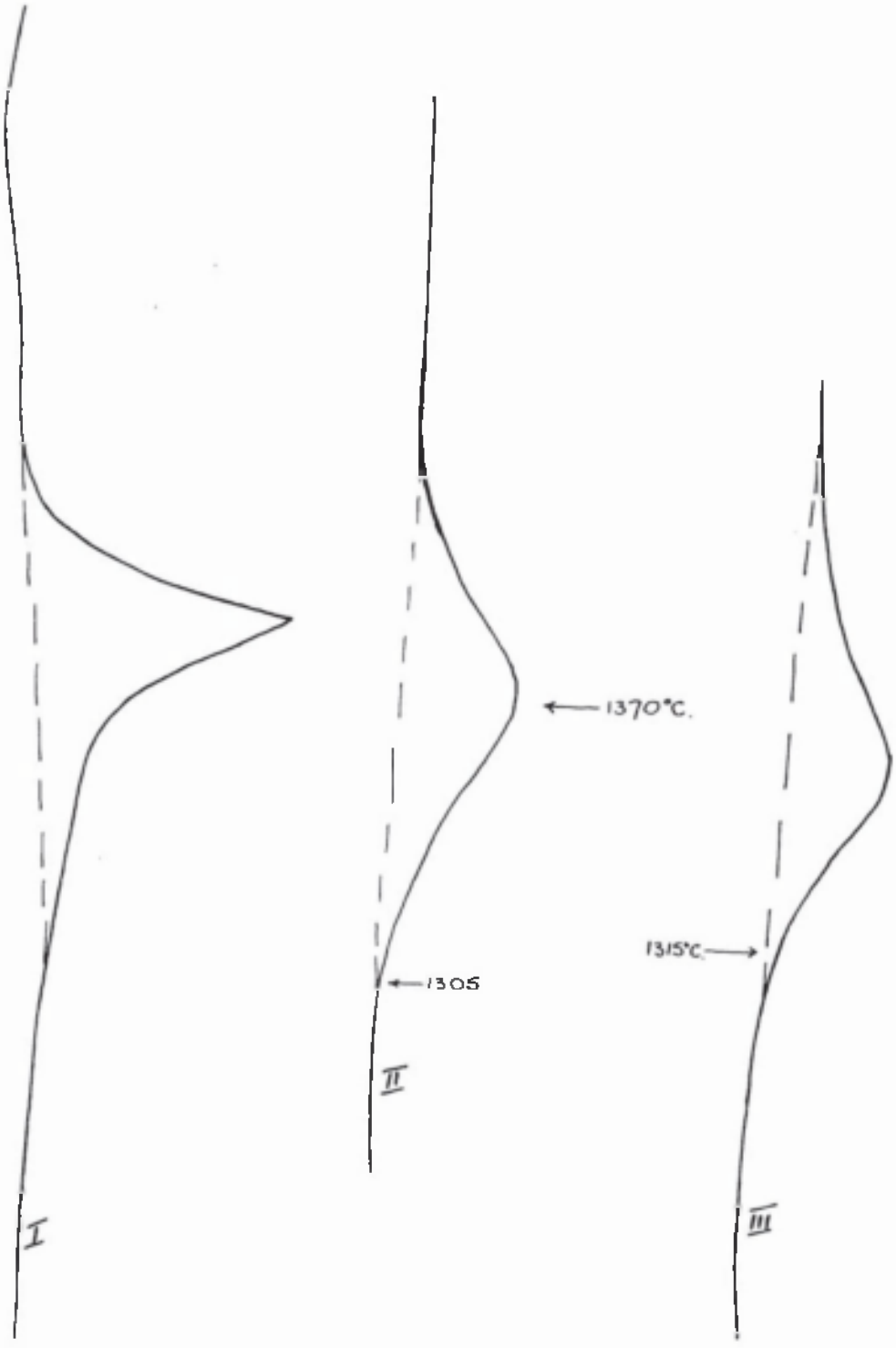

Heating (in vacuo.)

Figure 18.

FeO 97·5%
TiO_2 2·5%

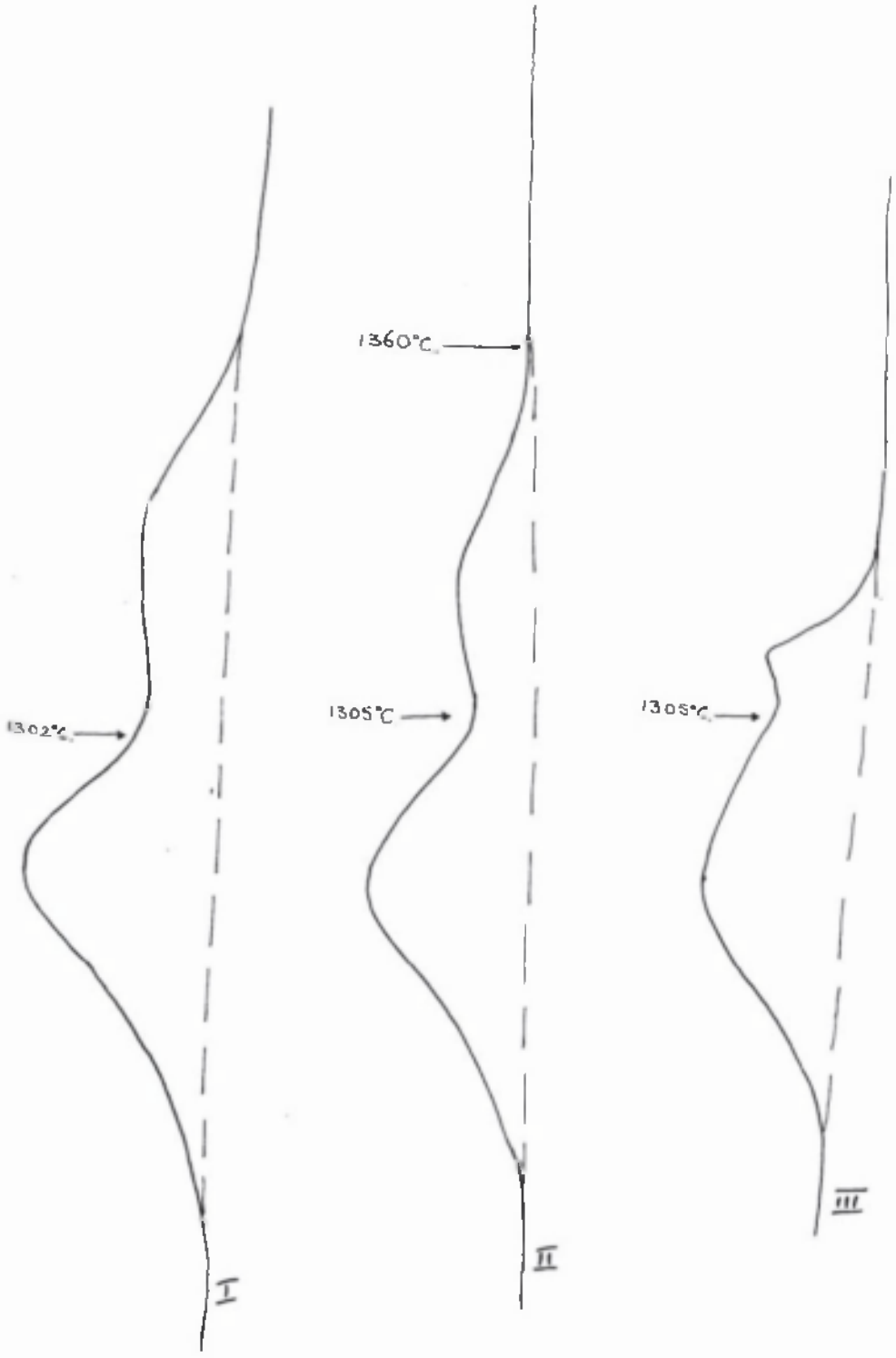

Cooling (in vacuo).

Figure 19.

FeO 90%.
TiO_2 10%.

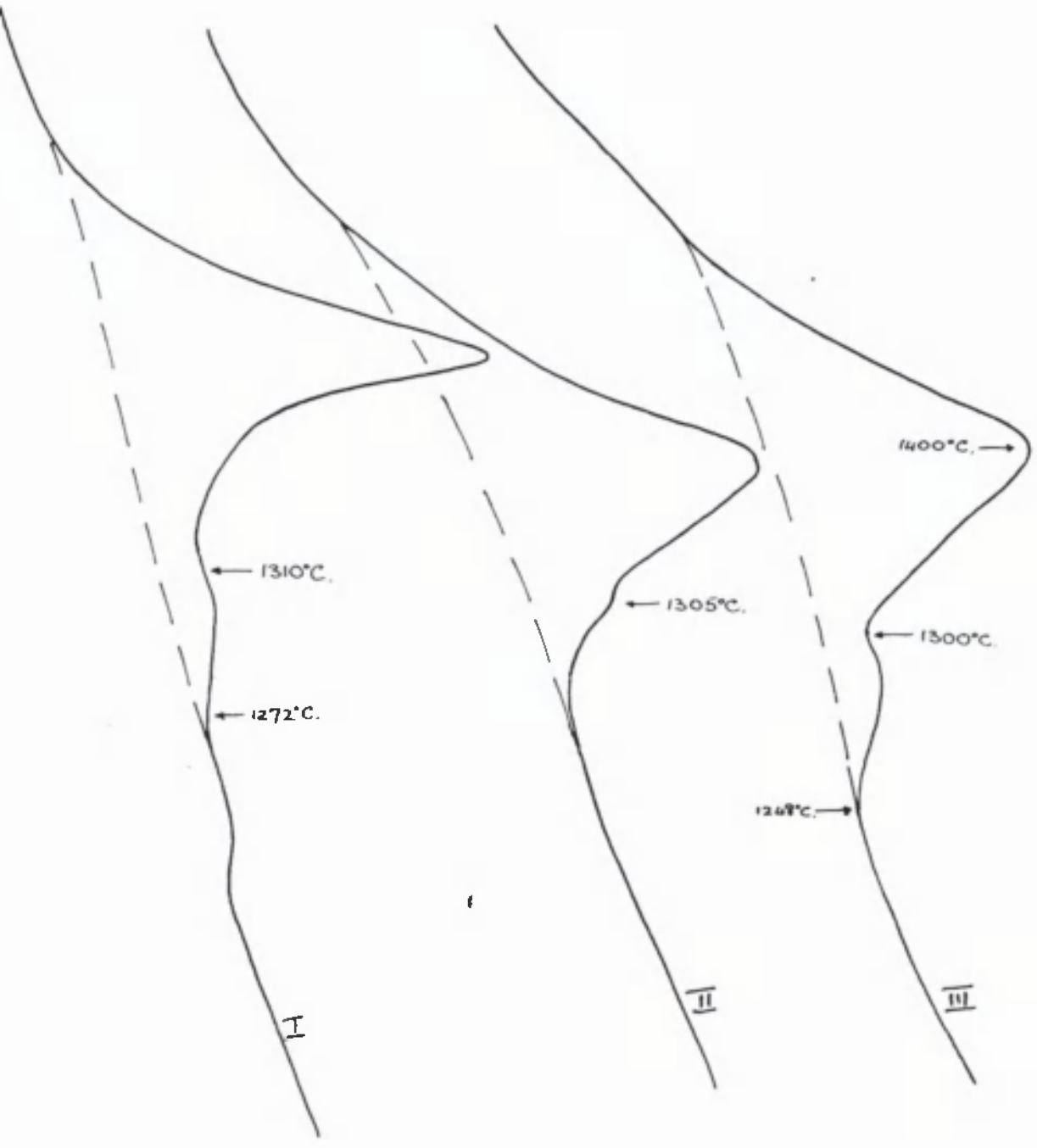

Heating (in vacuo).

Figure 20.

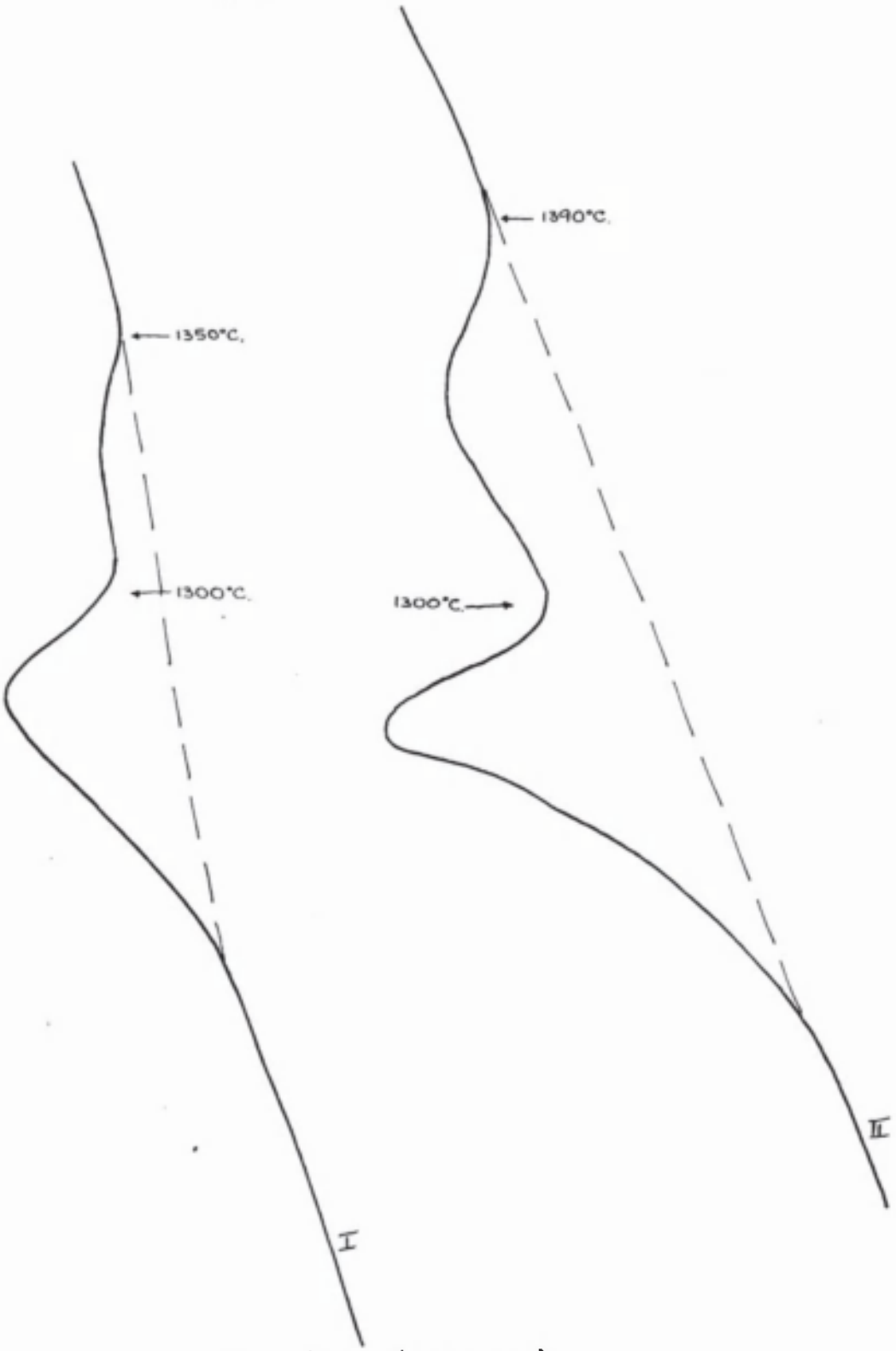

Cooling (in vacuo).

Figure 21.

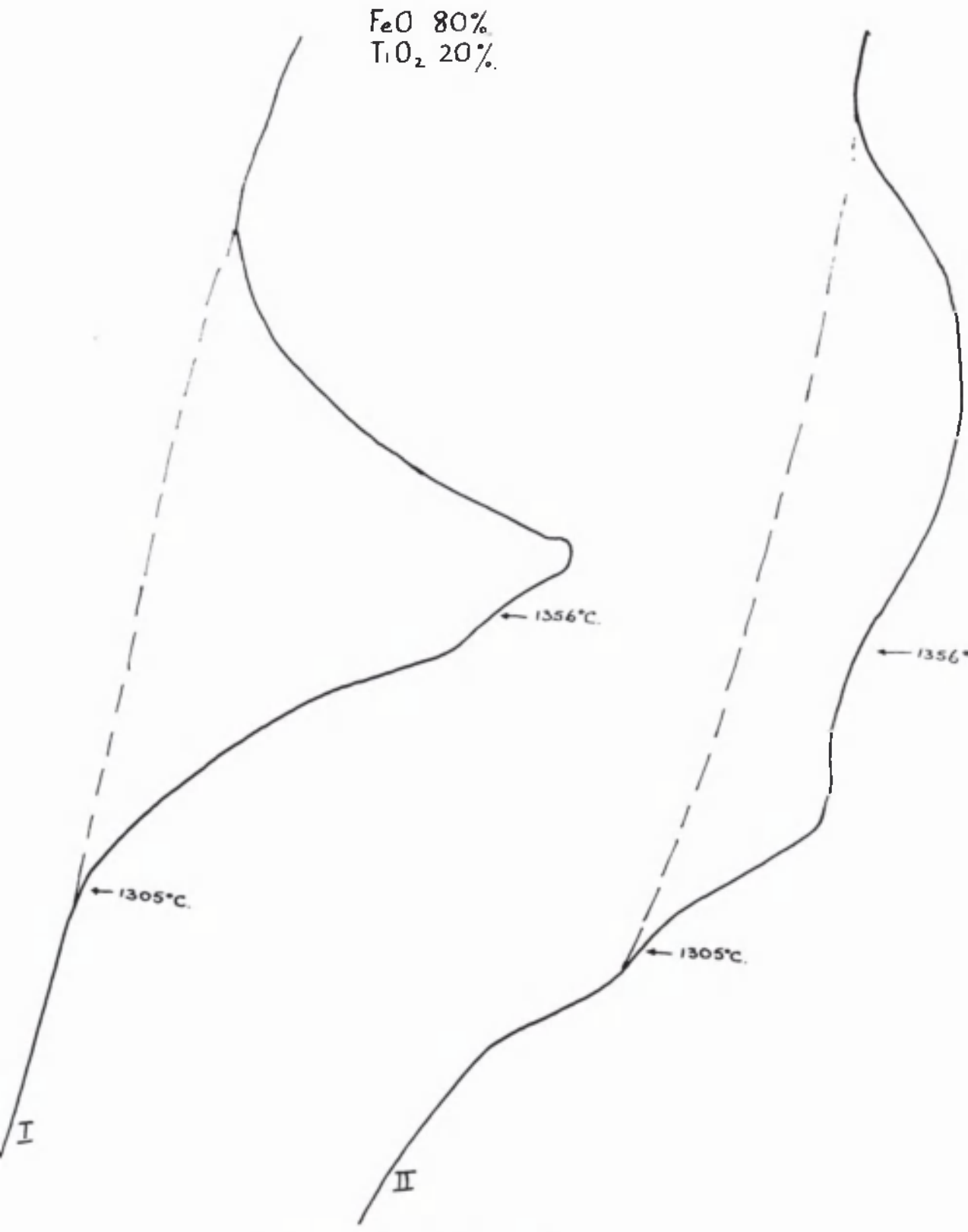

Heating (in nitrogen).

Figure 22.

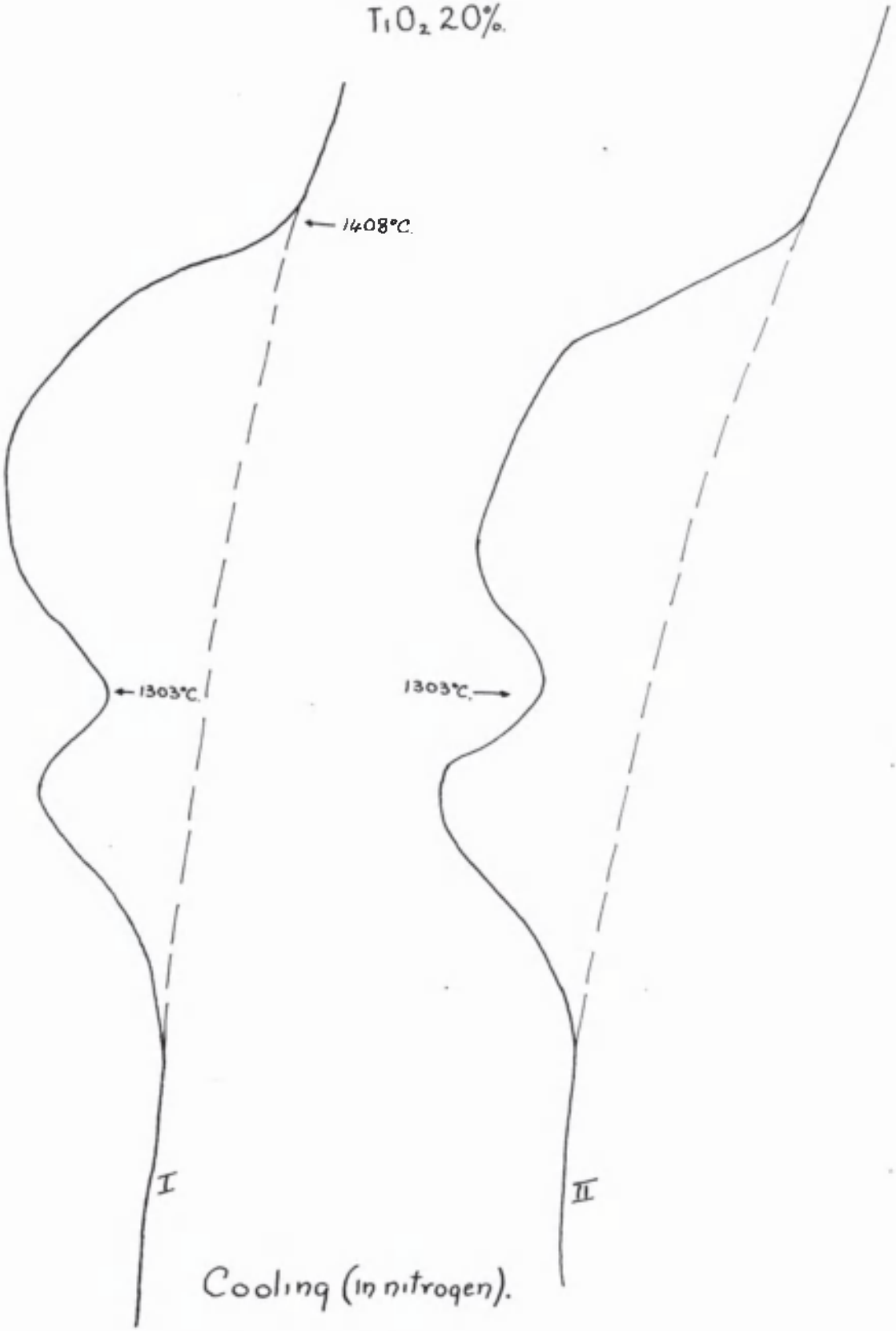

Figure 23.

Heating (in nitrogen).

Figure 24.

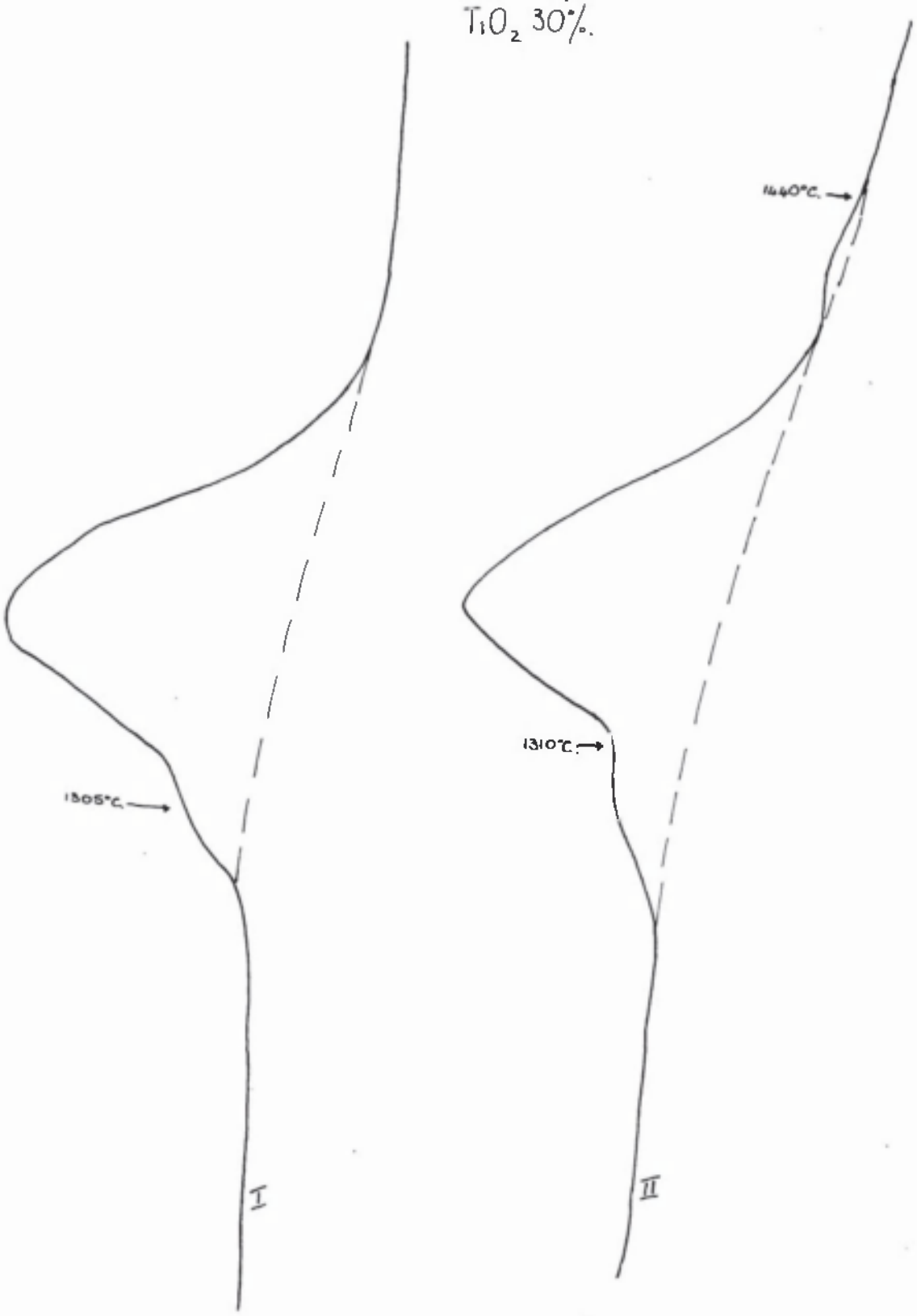

Cooling (in nitrogen).

Figure 25.

FeO 64·3%.
TiO_2 35·7%.

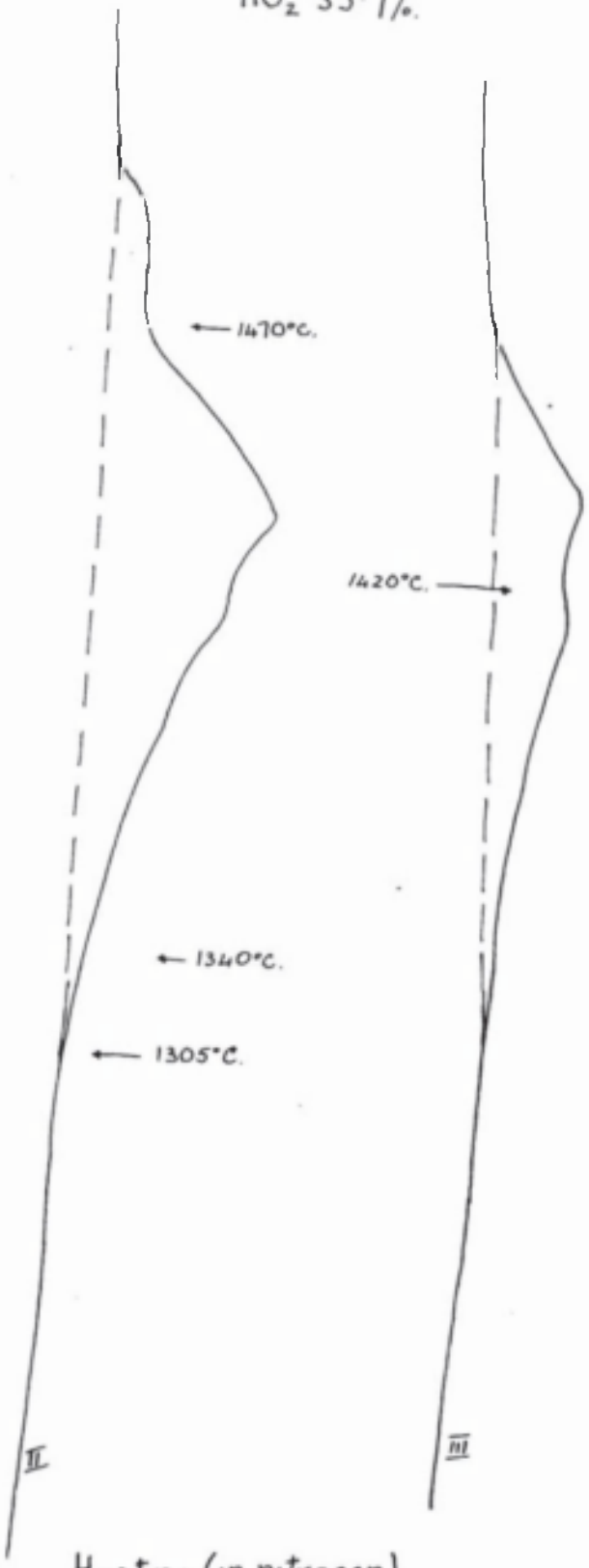

Heating (in nitrogen).

Figure 26.

FeO 64·3%.
TiO_2 35·7%.

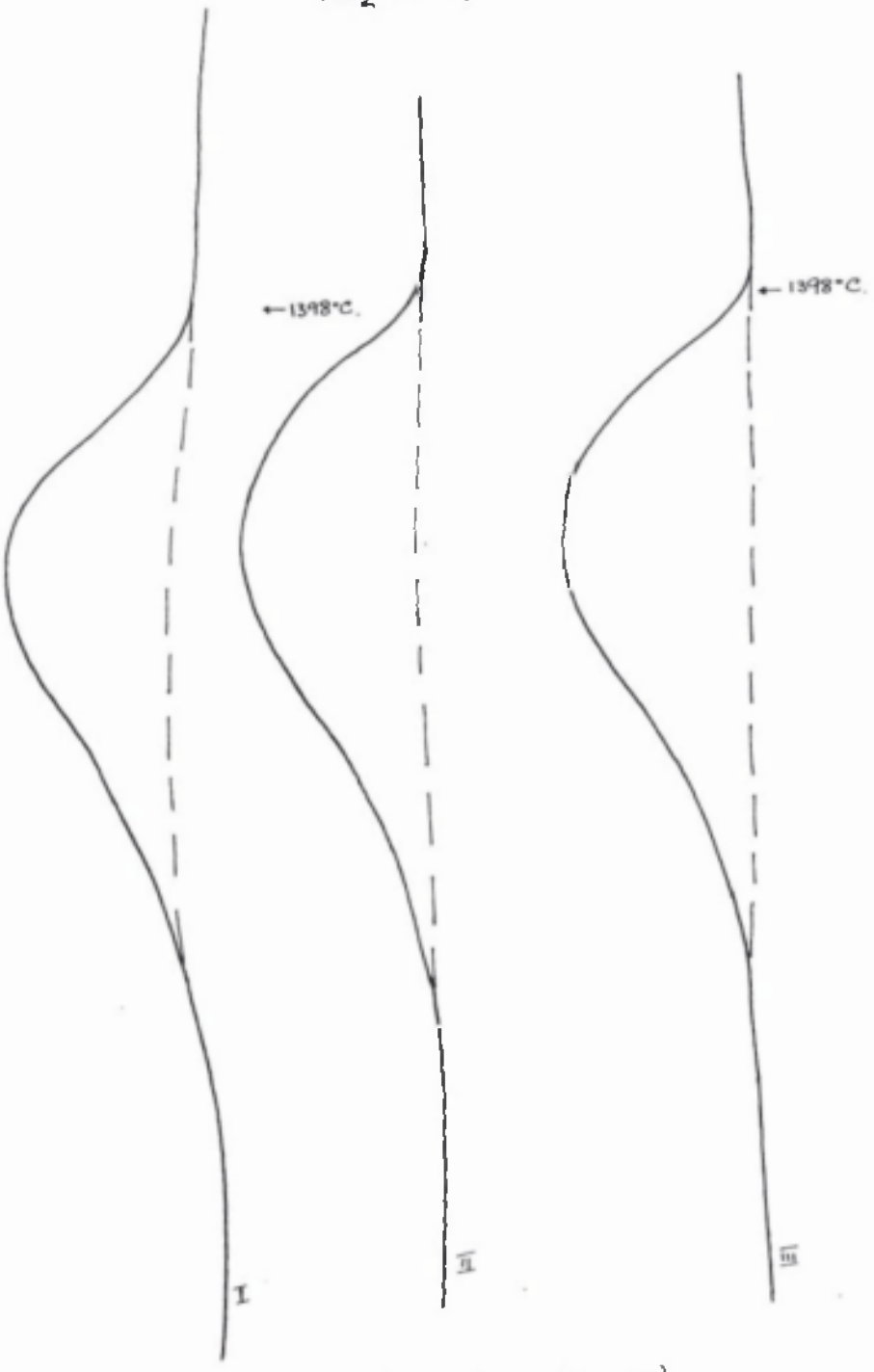

Cooling (in nitrogen).

Figure 27.

FeO 60%.
TiO_2 40%.

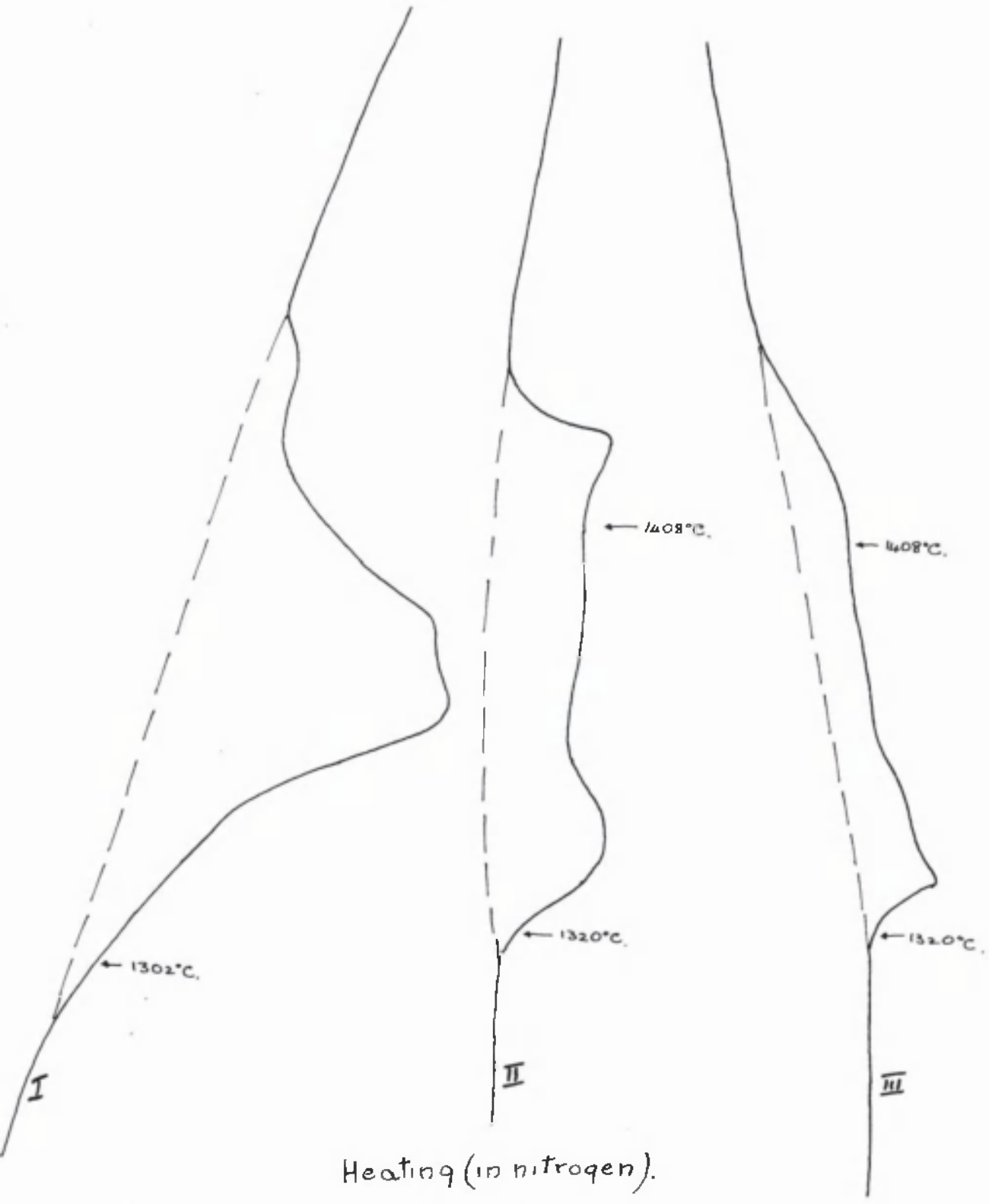

Heating (in nitrogen).

Figure 28.

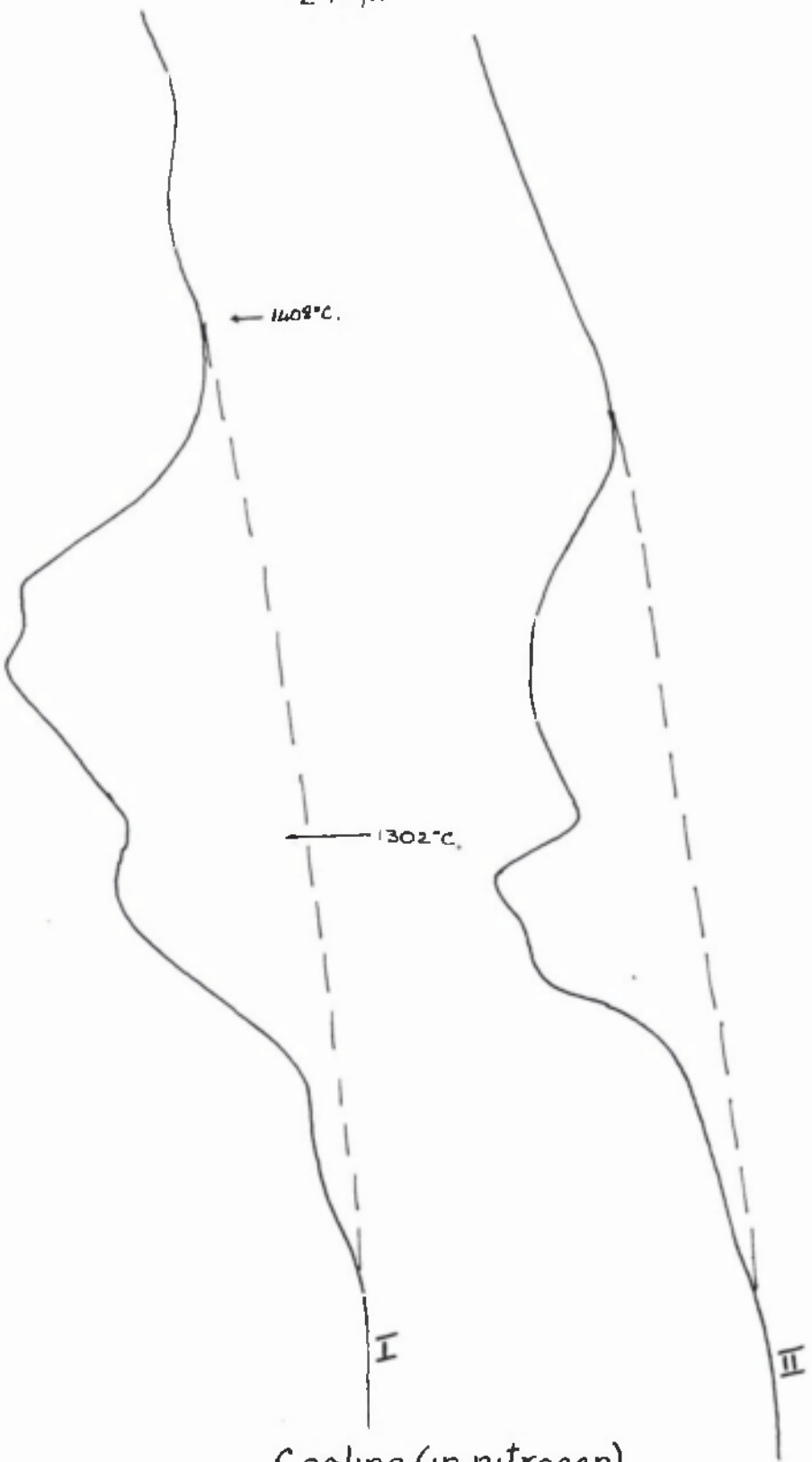

Figure 29.

FeO 55%.
TiO_2 45%.

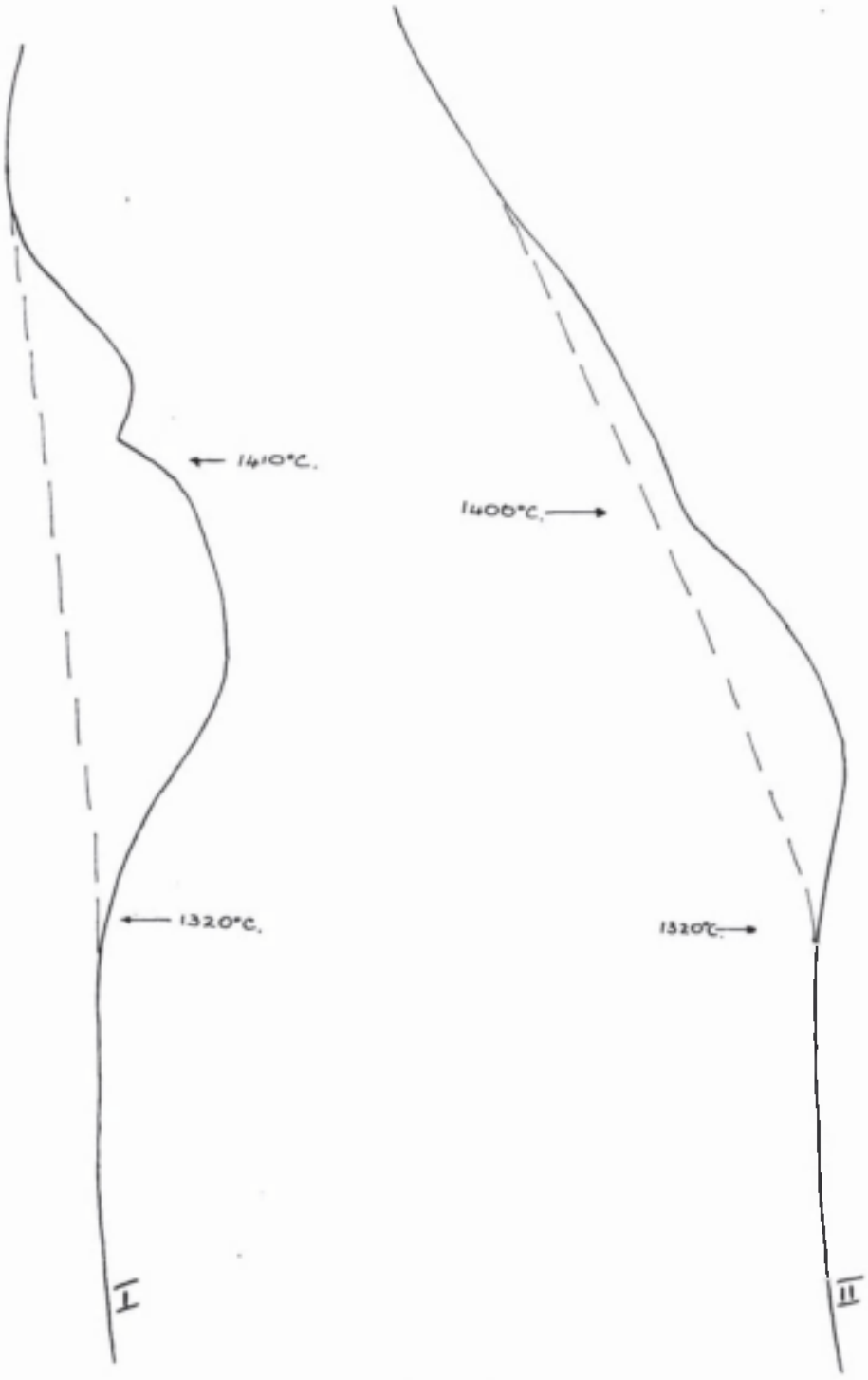

Heating (in nitrogen).

Figure 30

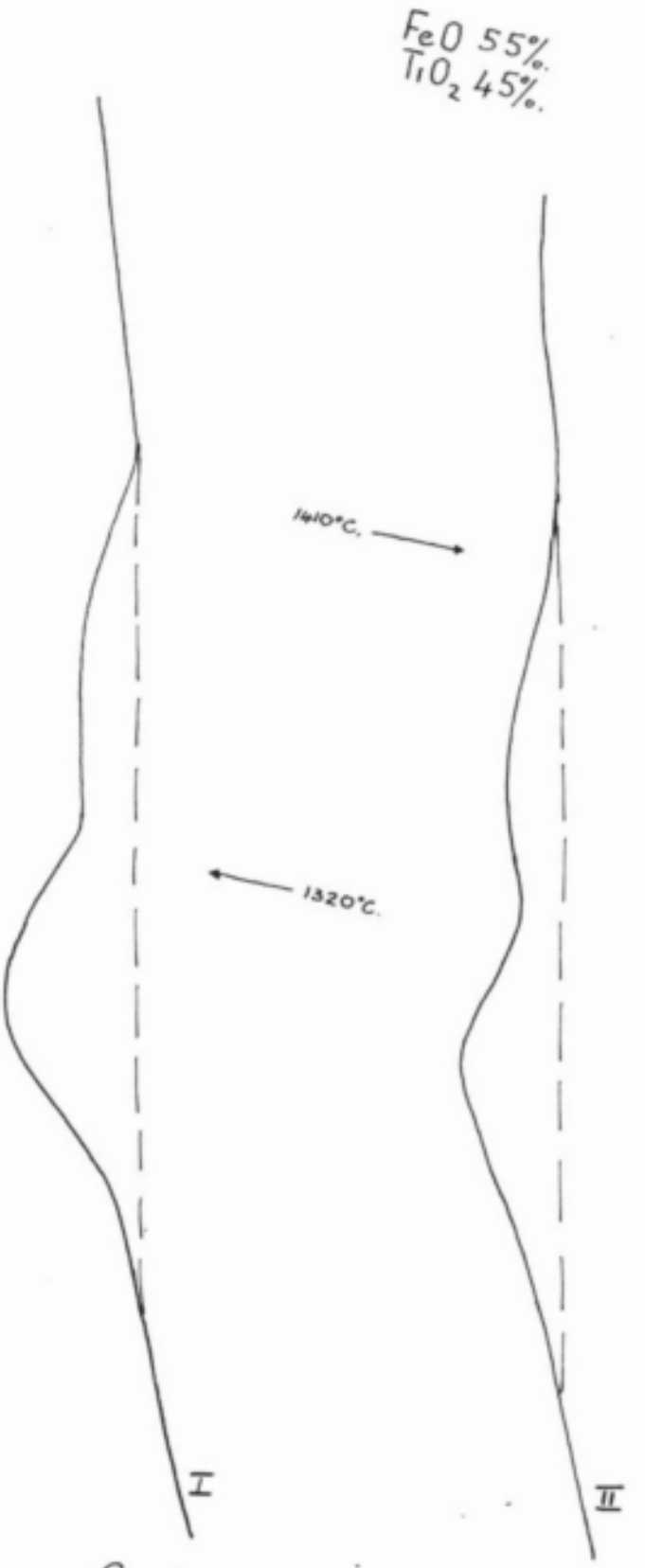

Cooling (in nitrogen).

Figure 31.

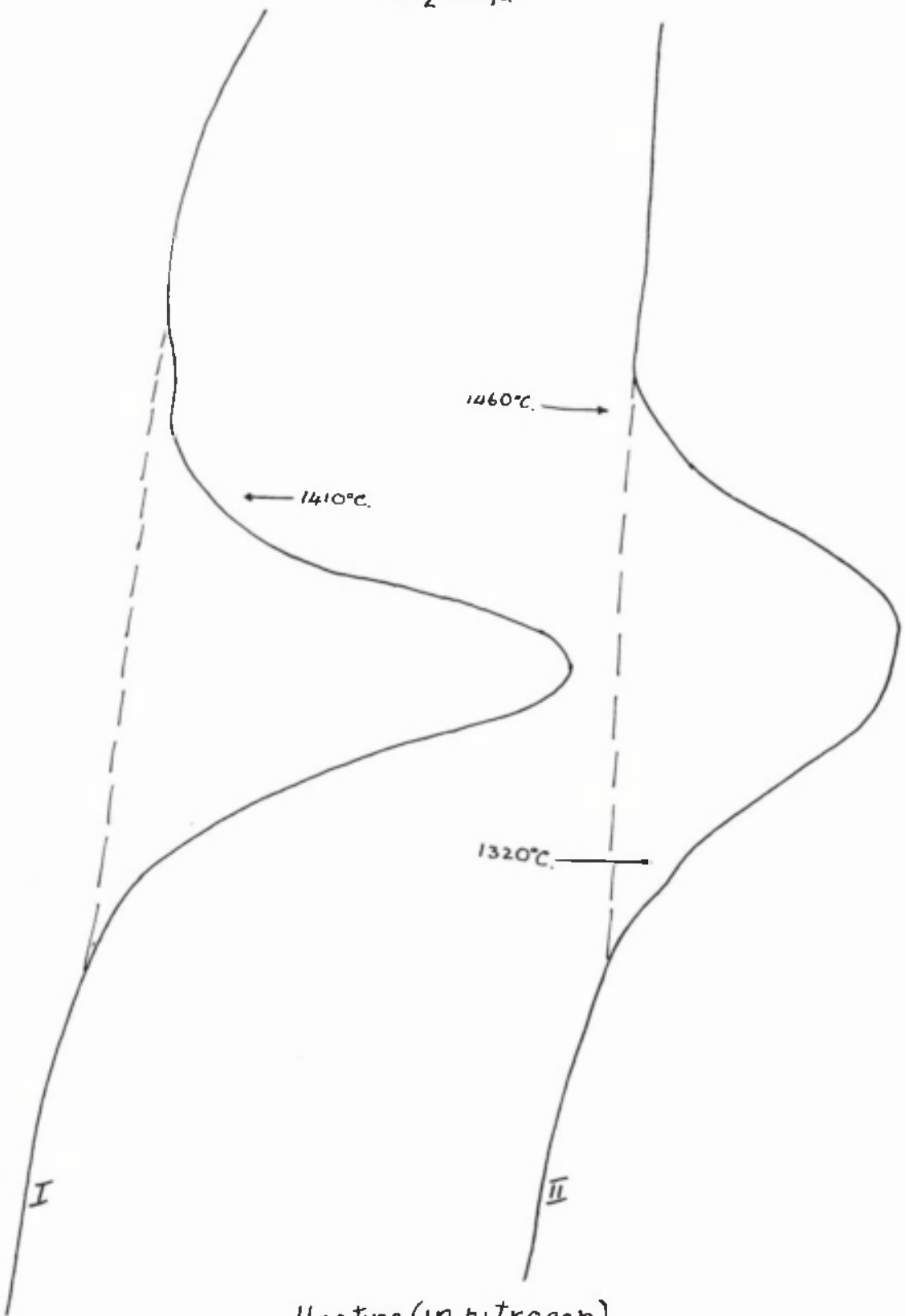

Figure 32.

FeO 50%.
TiO_2 50%.

Cooling (in nitrogen).

Figure 33.

FeO 47·4%.
TiO_2 52·6%.

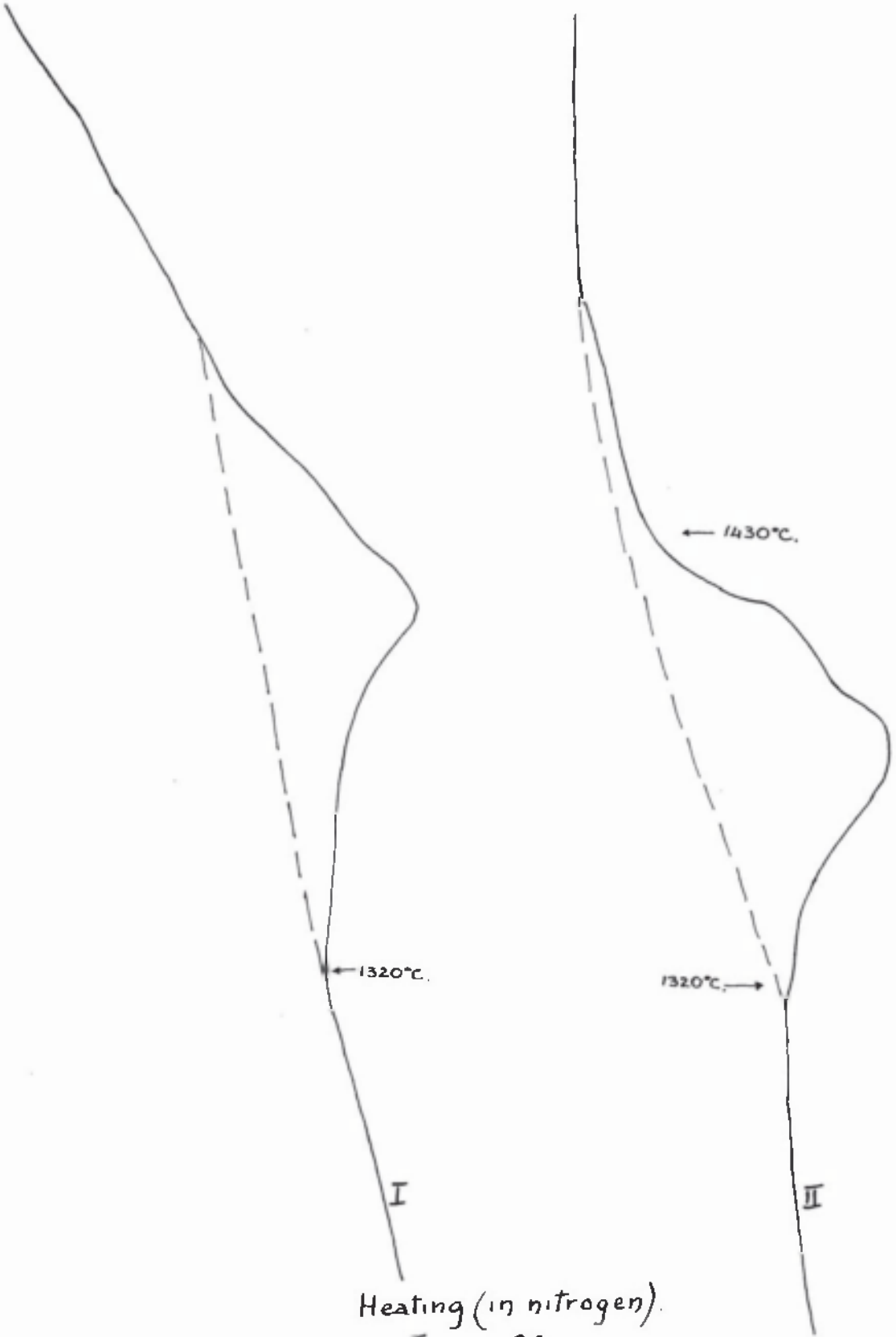

Heating (in nitrogen).

Figure 34.

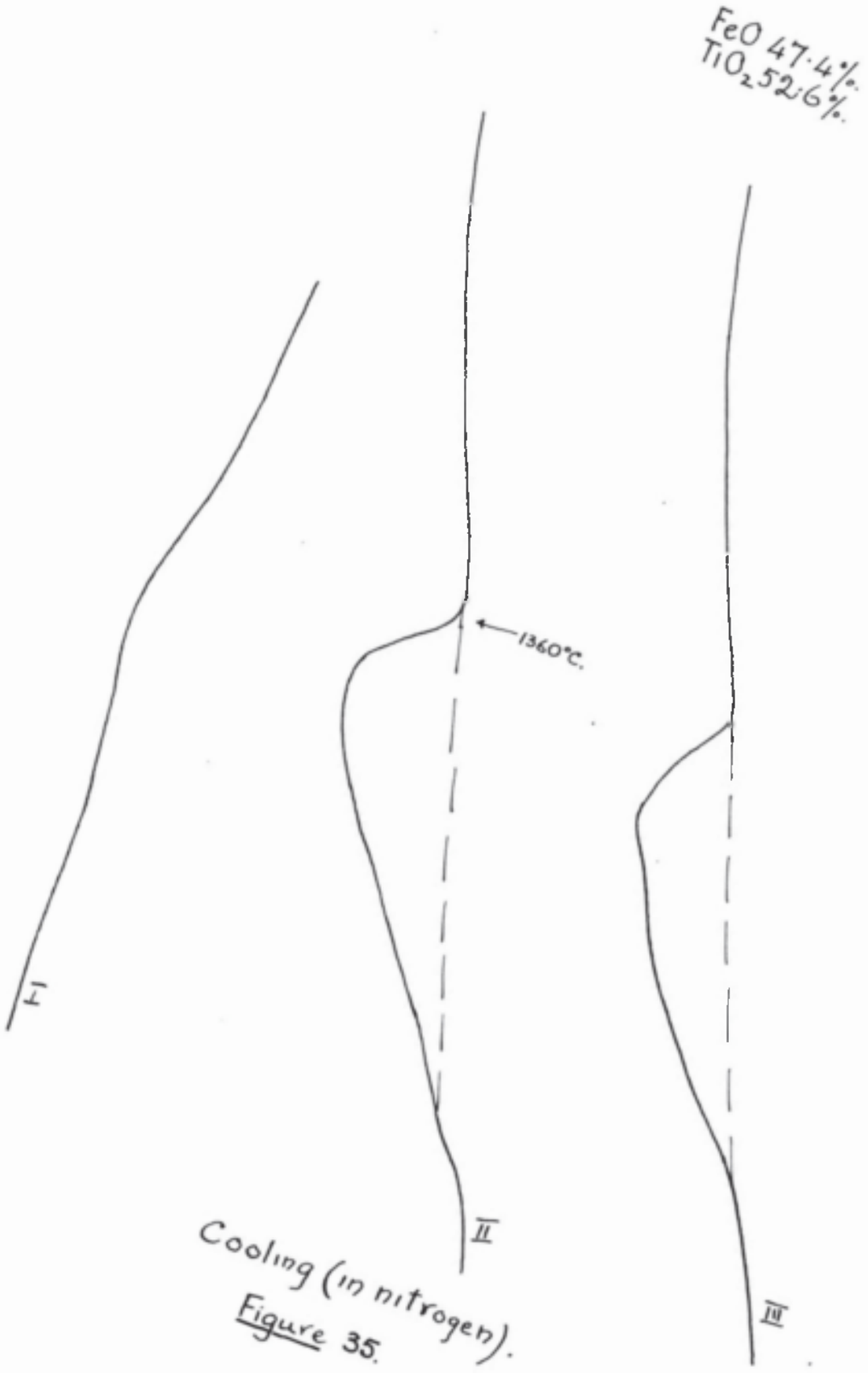

Cooling (in nitrogen).

Figure 35.

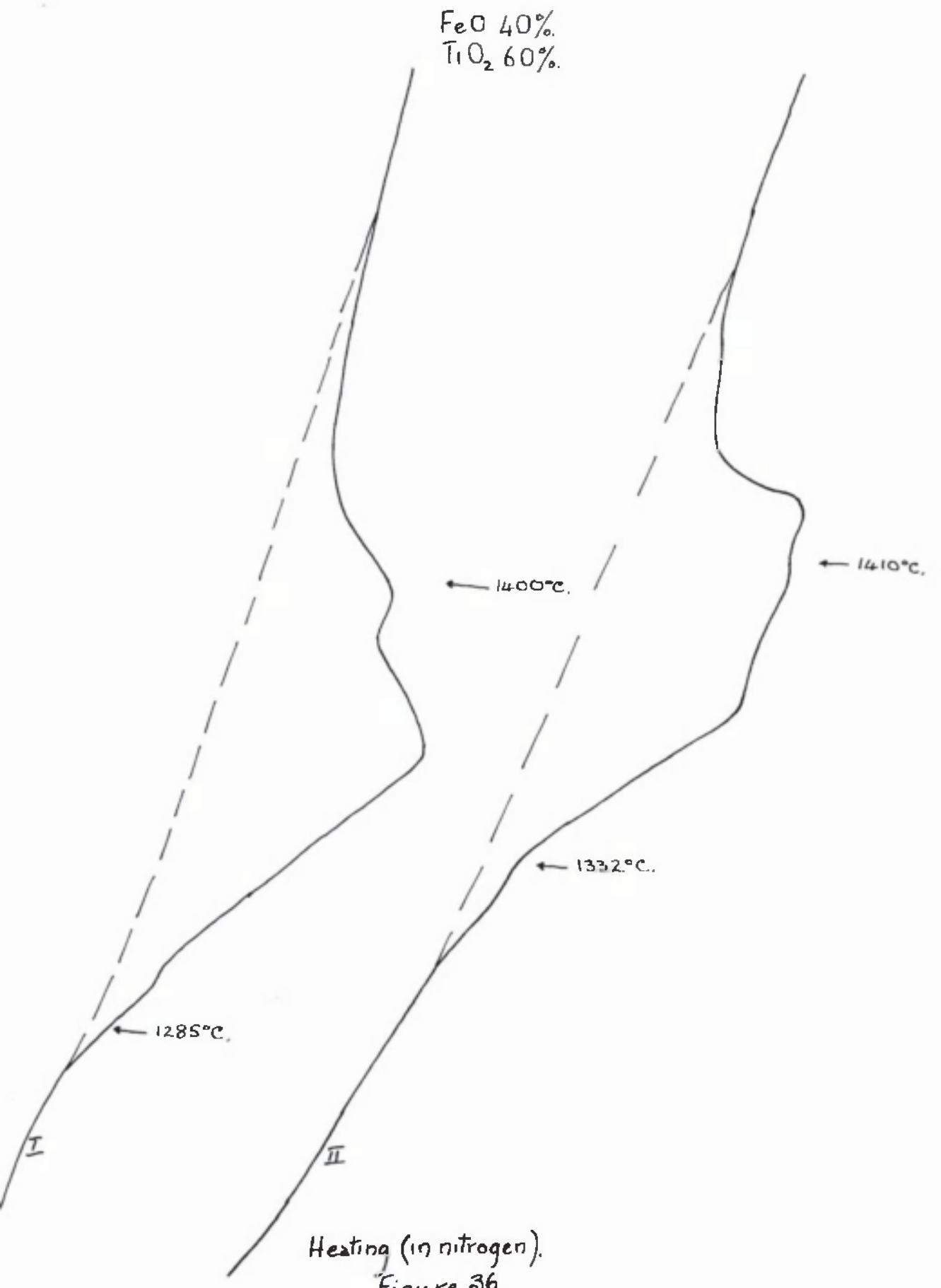

Heating (in nitrogen).

Figure 36.

FeO 40%
TiO_2 60%

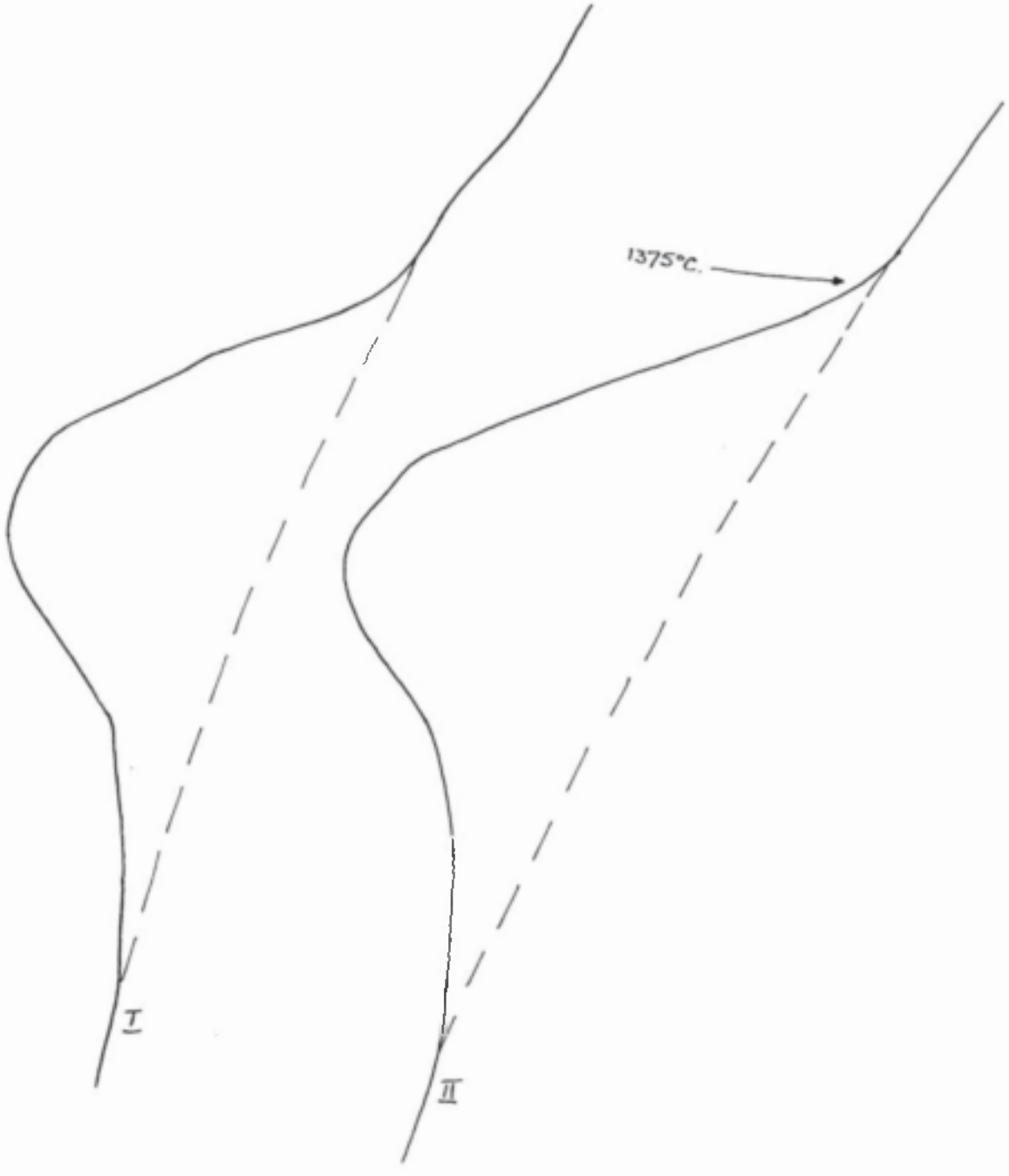

Cooling (in nitrogen).

Figure 37.

FeO 30%.
TiO_2 70%.

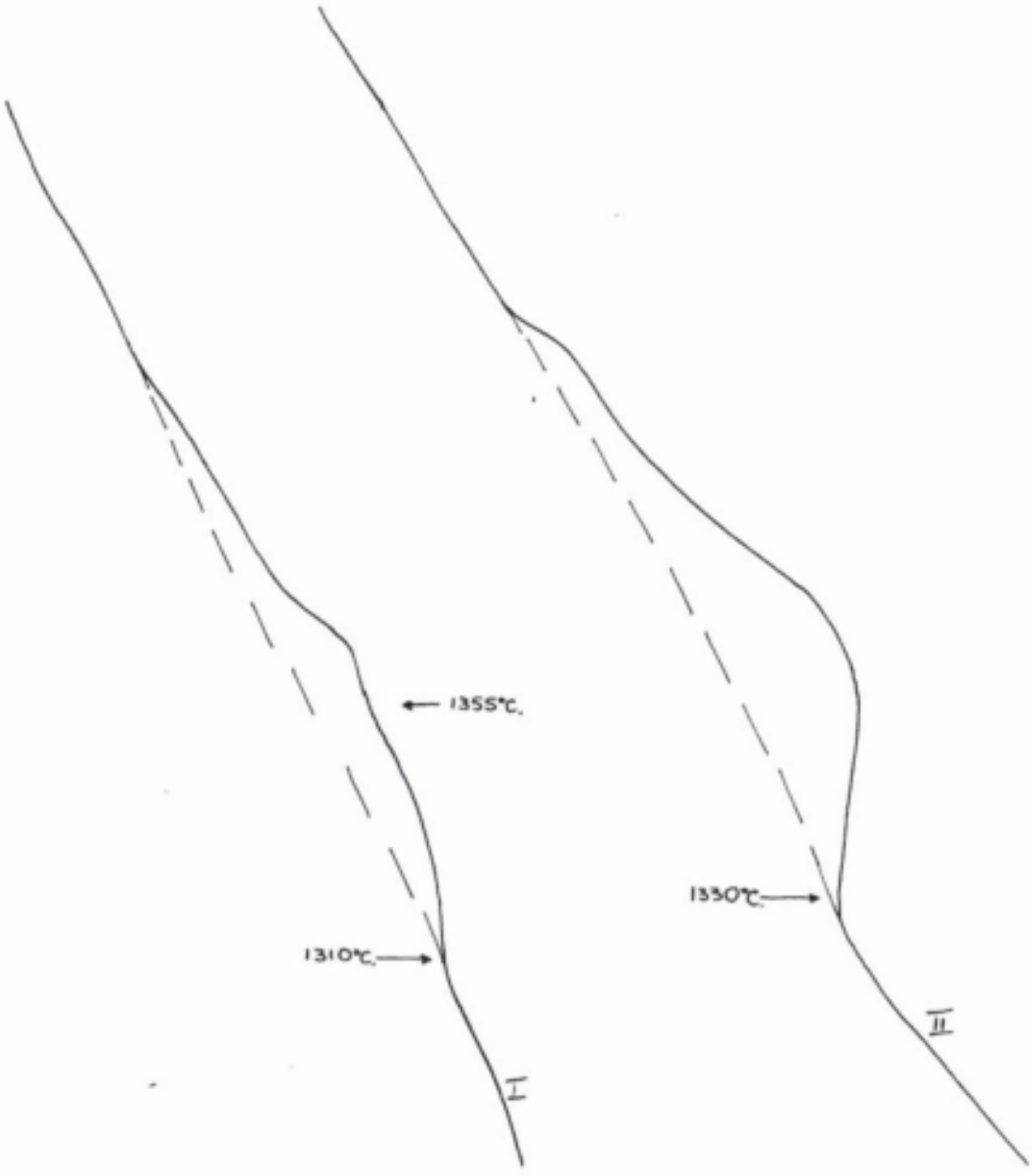

Heating (in nitrogen).

Figure 38

FeO 30%.
TiO_2 70%.

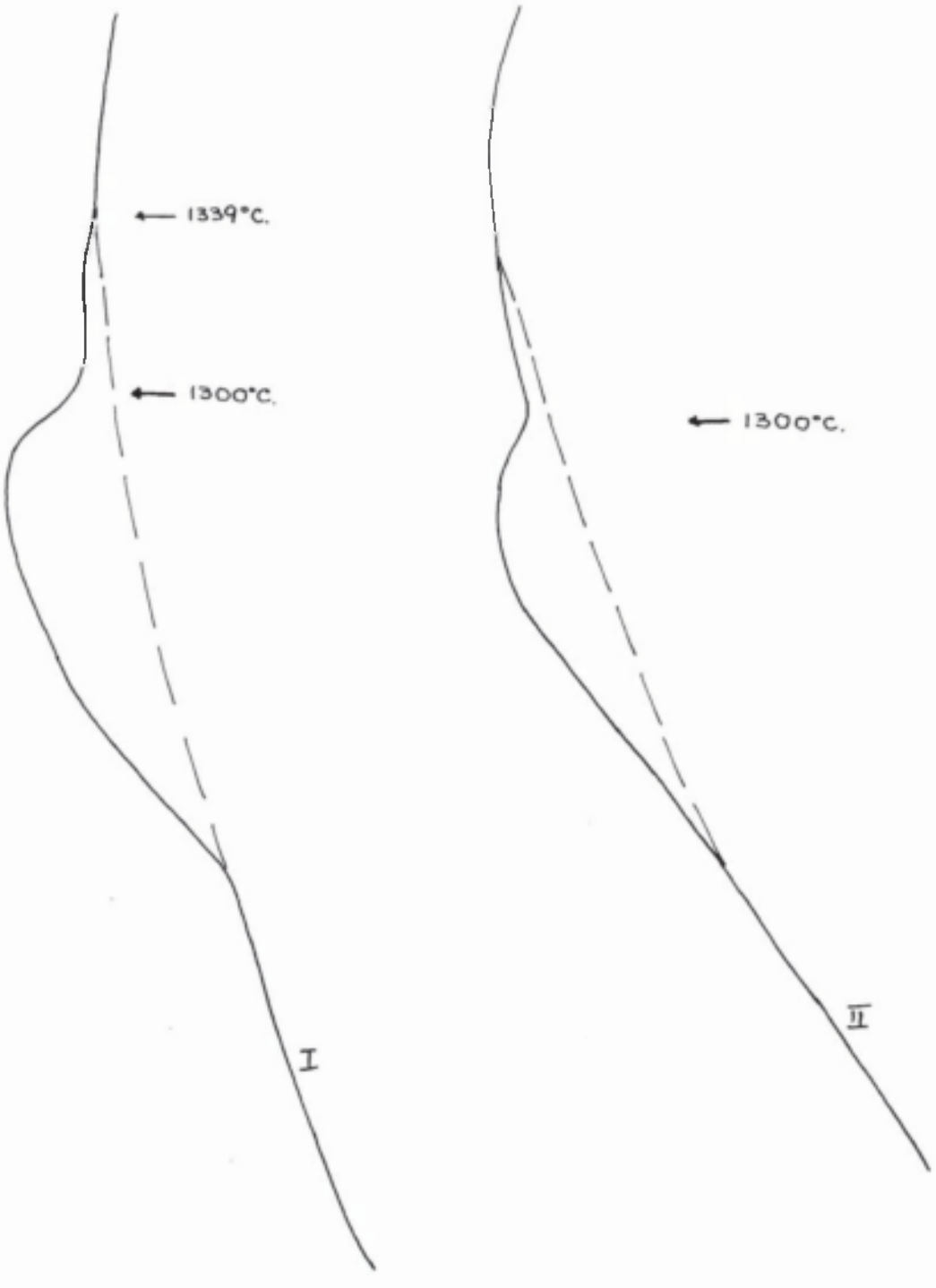

Cooling (in nitrogen).

Figure 39.

FeO 20%.
TiO_2 80%.

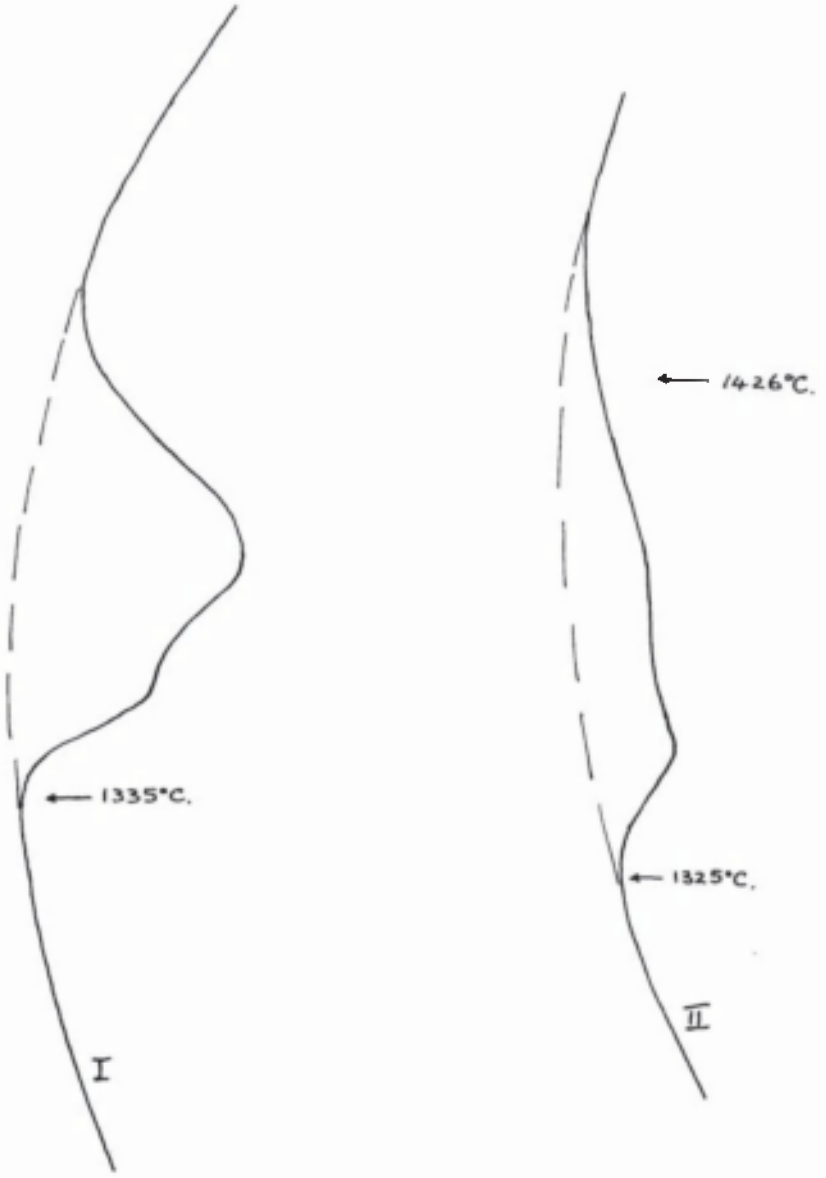

Heating (in nitrogen).

Figure 40.

FeO 20%.
TiO_2 80%.

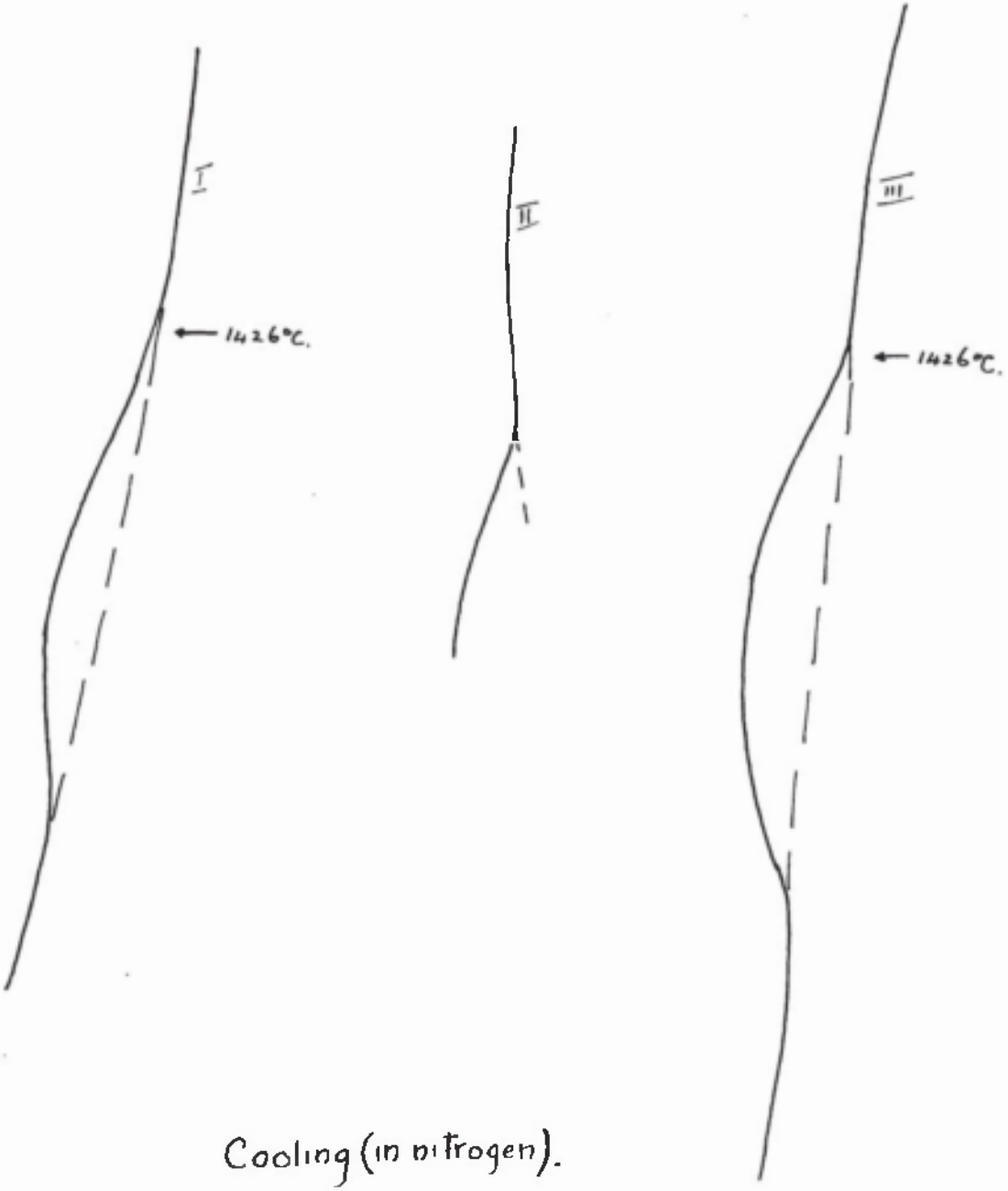

Cooling (in nitrogen).

Figure 41.

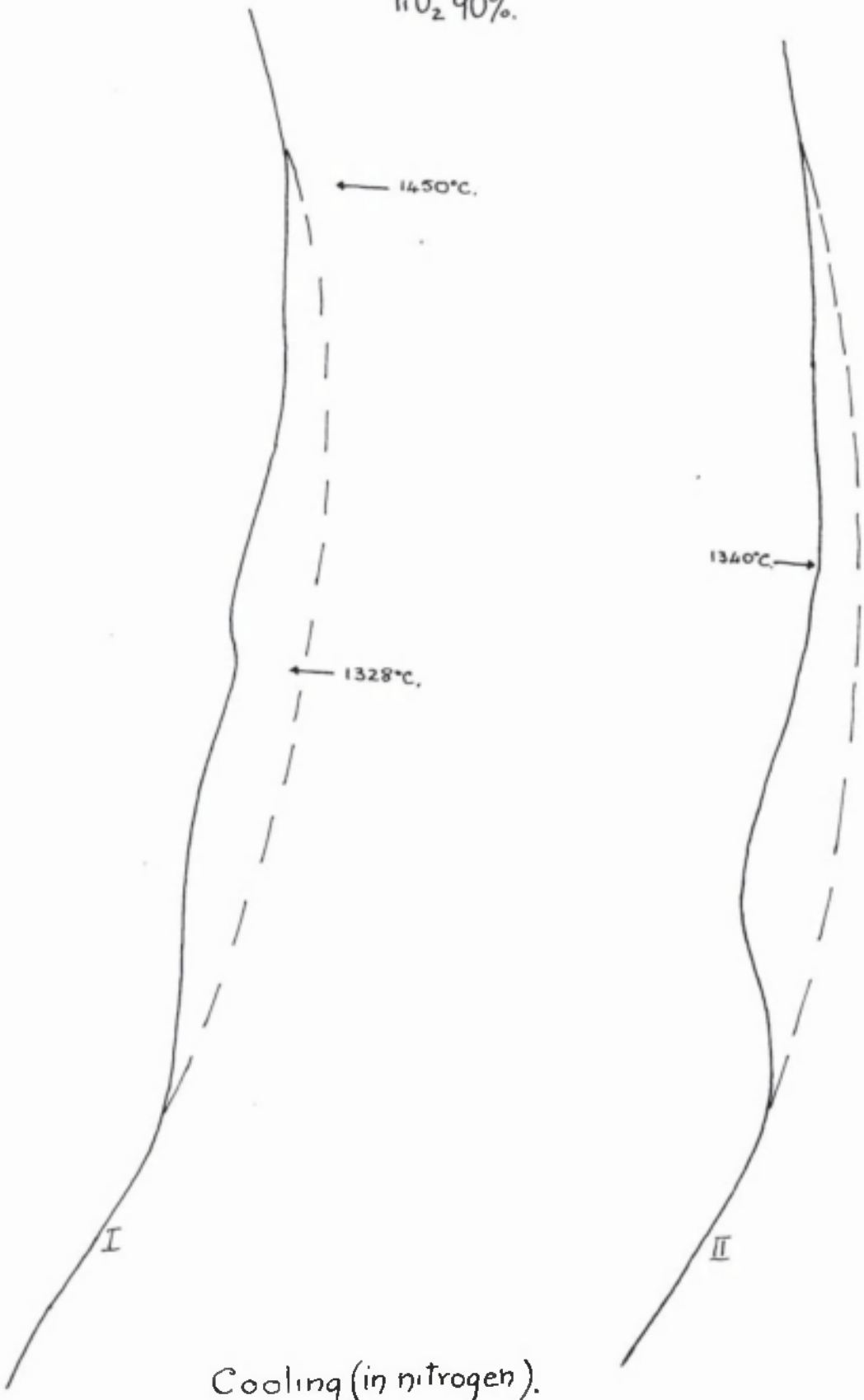

Cooling (in nitrogen).

Figure 42.

be fixed with any certainty. No arrests were found on the heating and cooling curves of a pure sample. Besides, samples heated to 1650°C., appeared to the eye to have melted, but under the microscope they were found to be very porous and the outlines of many of the grains could be distinguished. It was difficult to decide whether a simple sintering process had taken place,(feasible with a substance of appreciable vapour pressure) or whether melting to give an exceedingly viscous liquid had occurred. The melting point is most probably in excess of 1600°C., and was accepted as such in the present investigation.

After thermal study, each melt was sectioned longitudinally and examined microscopically by reflected light.

Great difficulty was experienced in polishing the melts. Ordinary hand-polishing using the usual grades of emery paper could not be used,owing to the friable and brittle nature of the melts. Machine polishing using oil and graded carborundum powders resulted in even worse surfaces being obtained. The use of paraffin oil as a lubricant with the emery papers resulted in no improvement. In an effort to fill in the holes in the surfaces, the specimens were immersed in Canada Balsam and placed in a Bell-jar, which was evacuated for several hours by means of a Hyvac pump. The surface holes having been freed from air and filled with Canada Balsam, the latter was prepared in the

usual manner by heating gently. Polishing the specimens treated in the above manner resulted in a marked improvement in their surfaces. Thus, the method proved quite satisfactory for those melts which could be etched with dilute hydrochloric acid, (melts with a high ferrous oxide content) but unsatisfactory for the melts which could only be etched with pure re-distilled hydrofluoric acid; the latter dissolved out the Canada Balsam very readily. Mounting the specimens in Wood's Metal and Bakelite in turn produced no better results in the surfaces.

The most successful method of polishing the extremely brittle specimens was found to be by hand on emery papers, using only the finer grades when the tearing of the surface was cut down to a minimum. This, of course, was rather a laborious and lengthy process which required much patience.

Since thin sections of minerals are usually capable of yielding more information than polished sections, attempts were made at preparing thin sections of several of the melts. However, even the thinnest sections prepared by the author, appeared opaque when viewed in transmitted light.

Figure 43, shows the thermal equilibrium diagram of the system FeO - TiO_2, as derived from the thermal and microscopic data. Two compounds, $2FeO,TiO_2$ (pseudo-brookite) and FeO,TiO_2 (ilmenite) are formed between the components and there are three eutectic points. The phase

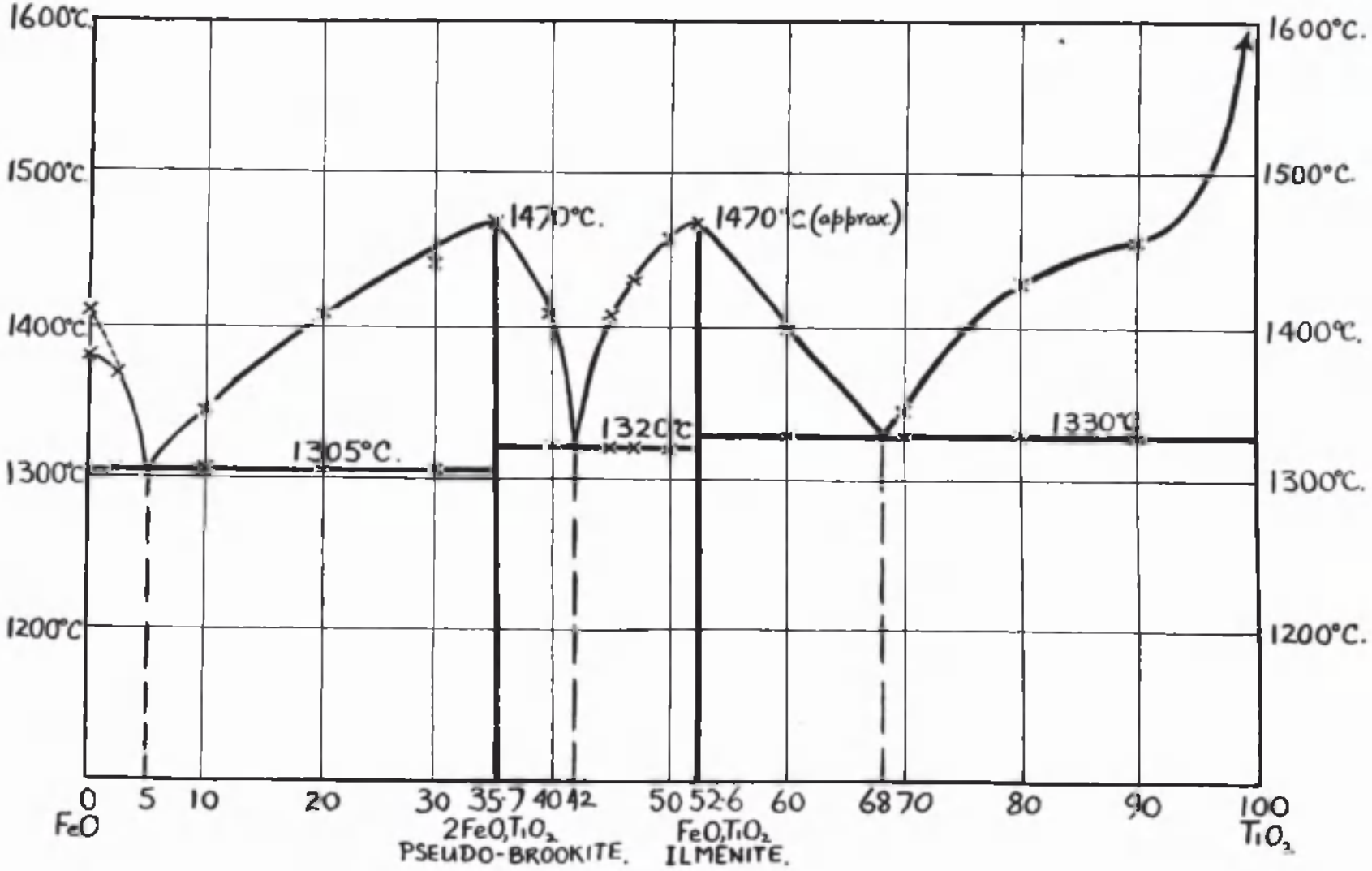
1600°C.
1500°C.
1400°C.
1300°C.
1200°C.
1470°C.
1470°C (approx.)
1320°C
1305°C.
1330°C
0
FeO
5
10
20
30
35·7
40
42
50
52·6
60
68
70
80
90
100
TiO2
2FeO,TiO2
PSEUDO-BROOKITE.
FeO,TiO2
ILMENITE.
WEIGHT % TiO2.

Figure 43.

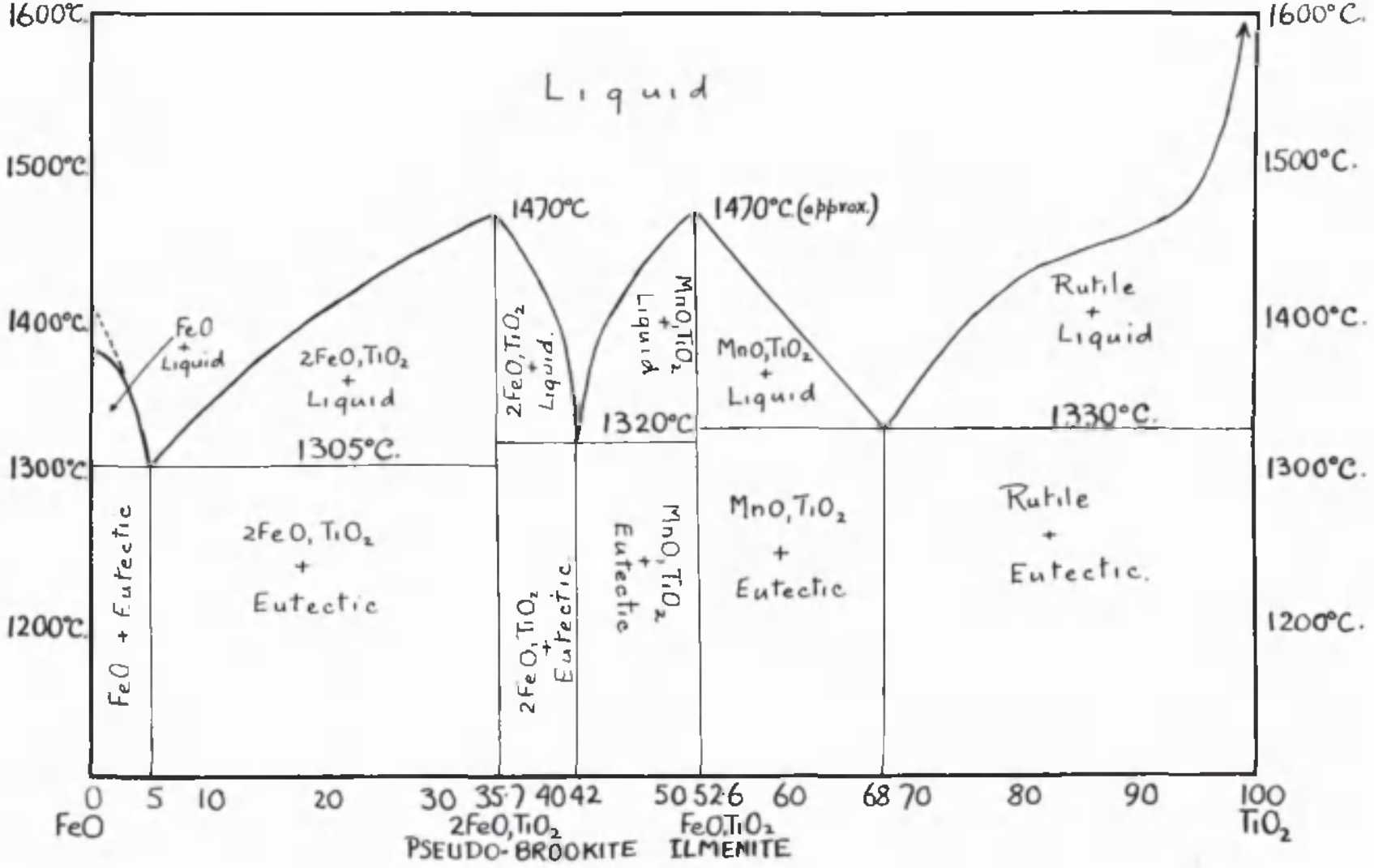
1600°C.
1500°C.
1400°C.
1300°C.
1200°C.
Liquid
1470°C
1470°C (approx.)
1320°C
1330°C.
1305°C.
FeO + Liquid
2FeO,TiO2 + Liquid
2FeO,TiO2 + Liquid.
MnO,TiO2 + Liquid
MnO,TiO2 + Liquid
Rutile + Liquid
FeO + Eutectic
2FeO, TiO2 + Eutectic
2FeO,TiO2 + Eutectic
MnO,TiO2 + Eutectic
MnO,TiO2 + Eutectic
Rutile + Eutectic.
0 5 10 20 30 35·7 40 42 50 52·6 60 68 70 80 90 100
FeO
2FeO,TiO2
PSEUDO-BROOKITE
FeO.TiO2
ILMENITE
TiO2
WEIGHT % TiO2

Figure 44.

distribution is shown in Figure 44.

From thermo-dynamic principles it has been proven, that, mutual insolubility between two chemical species is highly improbable. However, there are frequent cases where the solid solubility is so small that for most purposes it is sufficiently accurate to call the substances insoluble. Since, no evidence of changes in the solid state was obtained from the thermal curves of the FeO - T_iO_2 system, and since examination of the melts microscopically showed no evidence of solid solubility, (except maybe at the high titania end of the diagram) it can be inferred that the solid solubility is so small as to be negligible.

Figure 43, shows no peritectic dissociation of the compounds, but the rounded maxima indicates some dissociation in the liquid state. However, the degree of dissociation is inappreciable, the two compounds appearing to melt and freeze congruently.

Figures 45 to 50, show micrographs of representative melts and these indicate the relationships indicated in Figure 44. A short description of the micrographs is given below.

Figure 45. - x 125. 95% FeO: 5% T_iO_2.
Etchant dilute hydrochloric acid. Shows eutectic of ferrous oxide (FeO) and pseudo-brookite ($2FeO,T_1O_2$). The pseudo-brookite

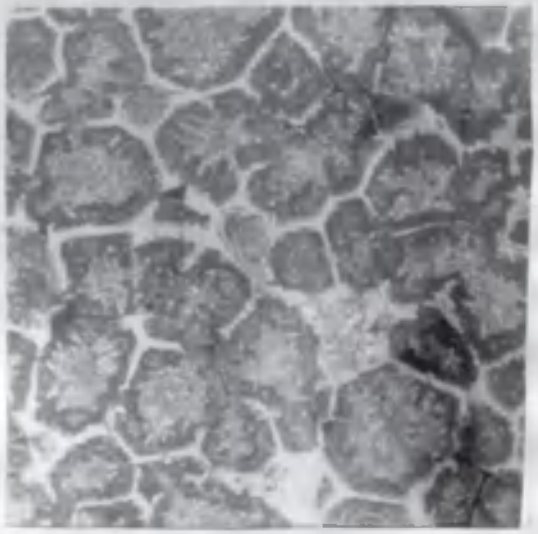

Figure 45.

Figure 46.

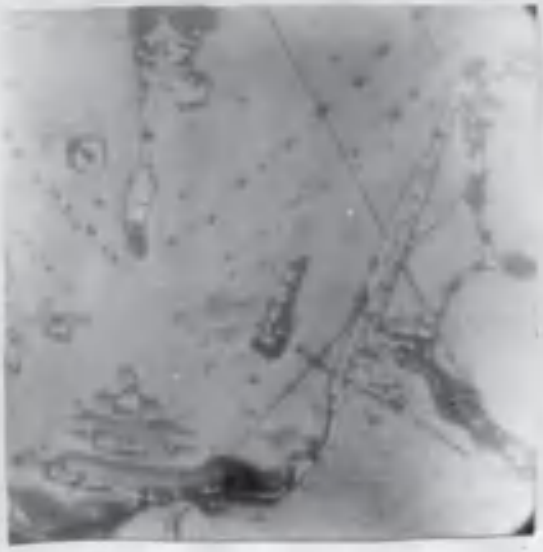

Figure 47.

Figure 48.

shows a tendency to coalesce to form a continuous network round the ferrous oxide, which tends to assume a globular form.

Figure 46. - x 250. 90% FeO: 10% TiO_2.

Etchant dilute hydrochloric acid. Primary pseudo-brookite, in eutectic of ferrous oxide and pseudo-brookite. The pseudo-brookite tends to separate as very large dendrites, a part of one of which is seen on the right of the micrograph.

Figure 47. - x 70. 64% FeO: 36% TiO_2.

Etchant hydrofluoric acid. Consists mainly of pseudo-brookite with a small amount of eutectic of pseudo-brookite and ilmenite. (FeO,Ti_2O_2). The pseudo-brookite separates in the form of large dendrites part of one of which is seen on the left of the micrograph.

Figure 48. - x 250. 50% FeO: 50% TiO_2.

Etchant hydrofluoric acid. The micrograph shows equiaxed crystals of ilmenite with the boundary material (pseudo-brookite) mostly removed by etchant.

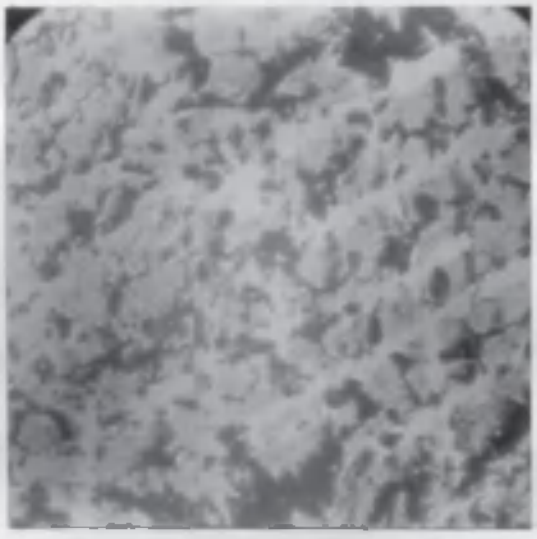

Figure 49

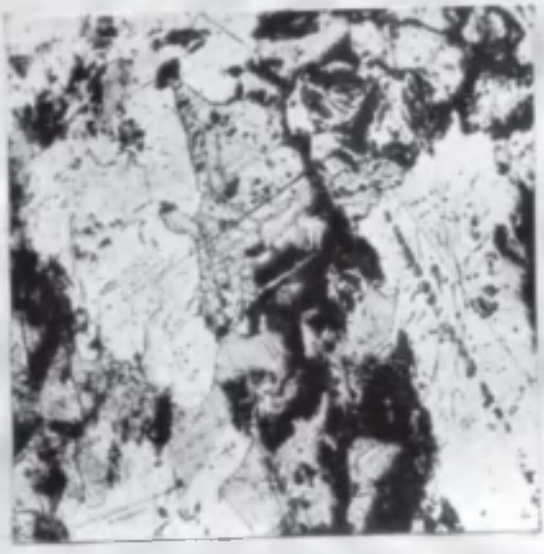

Figure 50

Figure 49. - x 70. 30% FeO: 70% TiO_2.

Etchant hydrofluoric acid. Consists of rutile (TiO_2, the light constituent mainly dendritic) in a background of equiaxed ilmenite, the dark areas are holes due to the tearing out of brittle material during polishing.

Figure 50. -x 250. 20% FeO: 80% TiO_2.

Etchant hydrofluoric acid. The micrograph shows primary rutile (light constituent) in a background of ilmenite, which shows a banded structure at this magnification. This is probably the result of partial solubility of rutile (TiO_2) in ilmenite (FeO,TiO_2) at high temperatures.

Attempts made to identify the phases present in the melts by the Becke immersion method were not successful due to the opacity of the various constituents.

The Debeye and Scherrer[41], method of X-ray analysis as described earlier on (see Chapter 2) was finally used to identify the phase distribution. The X-ray photographs (Figures 51 to 57) confirm the phase distribution proposed in the thermal equilibrium diagram. A short description of the X-ray photographs is given below.

Figure 51. - Ferrous Oxide (FeO, melted in platinum in vacuo).
The lines for FeO indicate the value of the lattice parameter, a = 4·30 Å. Additional lines are due to Magnetite (Fe_3O_4).

Figure 52. - 80% FeO: 20% TiO_2.
Lines due to pseudo-brookite ($2FeO,TiO_2$) appear in addition to spectrum of ferrous oxide (FeO).

Figure 53. - 70% FeO: 30% TiO_2.
Lines as in previous photograph.

Figure 54. - 60% FeO: 40% TiO_2.
Presence of a new phase indicated. Spectrum of ilmenite (FeO,TiO_2) together with that of pseudo-brookite. ($2FeO,TiO_2$).

Figure 55. - 30% FeO: 70% TiO_2.
Stronger lines in spectrum of Rutile (TiO_2), along side spectrum of ilmenite.

Figure 56. - 10% FeO: 90% TiO_2.
Spectra of rutile (TiO_2) and ilmenite.

Figure 57. - Titania (TiO_2, heated to 1600° C., in platinum).
Spectrum is that of rutile (tetragonal system) and corresponds to the values of the lattice parameters, a = 5·36 Å, and c = 2·94 Å.

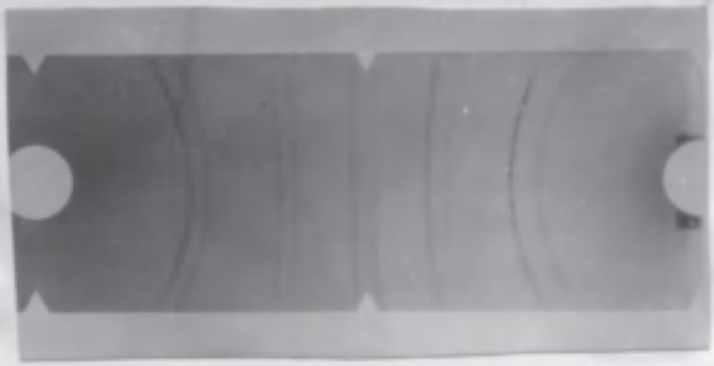

Figure 51.

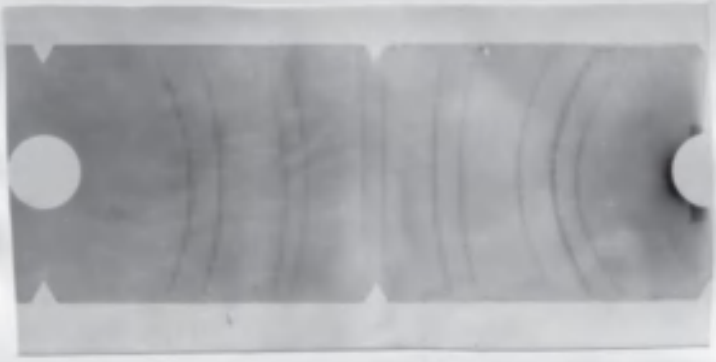

Figure 52.

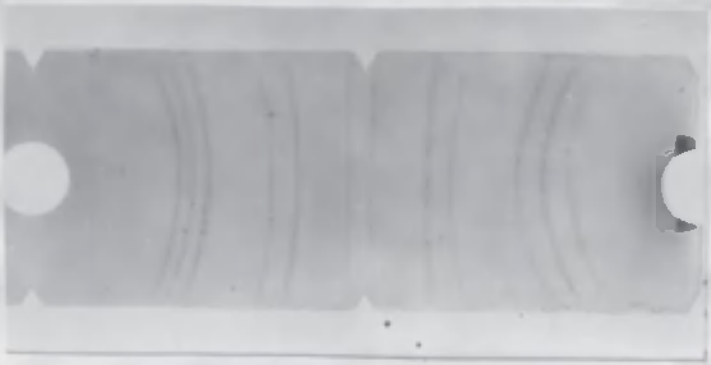

Figure 53.

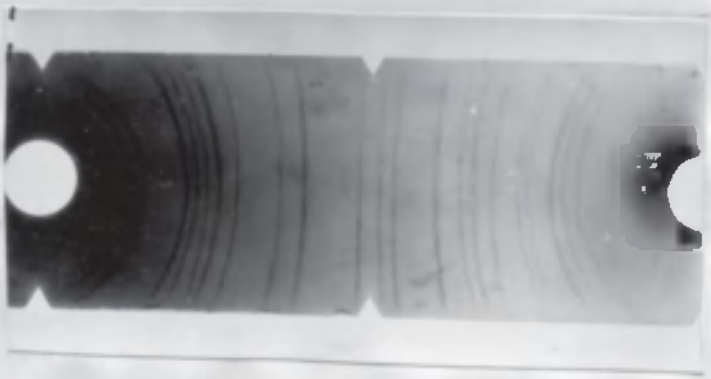

Figure 54.

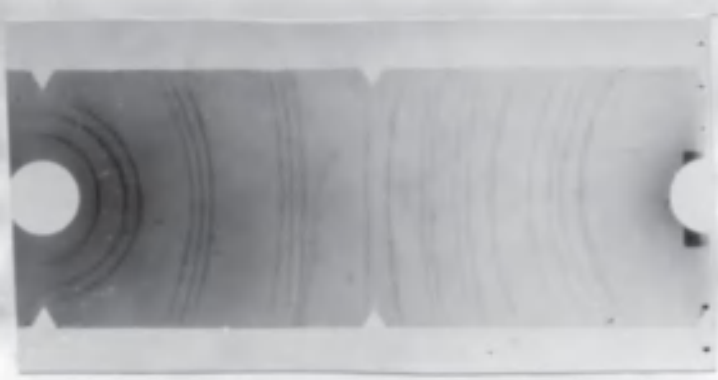

Figure 55.

Figure 56.

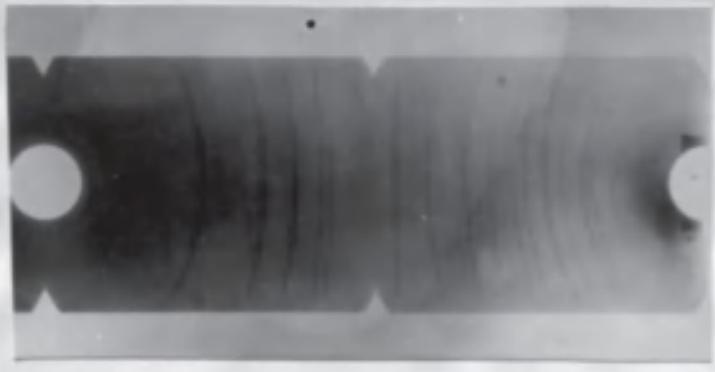

Figure 57.

CHAPTER 4.

THE BINARY SYSTEM MnO - TiO_2.

The binary system MnO - TiO_2 was investigated by methods similar to those used in the FeO - TiO_2 binary system, to which it is complementary. The finely ground two gramme melts were packed closely into the small molybdenum crucibles, and the heating was carried out in a "Pythagoras" tube in an atmosphere of nitrogen or in vacuo. A differential tungsten-molybdenum thermocouple was again used for the thermal analysis. The usual three heating and two cooling curves were determined for each melt, but the first heating curve was unreliable due to heats of formation of compounds.

After thermal analysis each melt was sectioned longitudinally and microscopically examined in reflected light. As in the case of the FeO - TiO_2 melts, the most satisfactory surfaces were obtained by hand polishing using only the finer grades of emery papers, since the coarser grades of paper caused tearing of the surface. However, the polished surfaces of the MnO - TiO_2 melts were superior to those obtained with the corresponding melts of the FeO - TiO_2 binary system. Melts having the compositions of the compounds MnO,TiO_2 and 2MnO,TiO_2 respectively, were exceedingly brittle and tended to break down into small fragments on sectioning. Melts intermediate in composition

to the two compounds had a marked metallic lustre.

The purity and preparation of the constituents used have been described elsewhere (see Chapter 2).

The thermal curves of the various compositions studied are shown in Figures 58 to 69, with the temperatures of the various thermal arrests indicated. A summary of the thermal data thus obtained is given in Table 5 below.

Figure 70 shows the thermal equilibrium diagram as derived from the thermal and microscopical data. It will be noted that manganous oxide like ferrous oxide forms two compounds with titania, these being manganous metatitanate ($2MnO,TiO_2$), and manganous orthotitanate or pyrophanite (MnO,TiO_2). The thermal equilibrium diagram shows the presence of two eutectic points as well as a peritectic reaction. Coincident or congruent melting takes place in the eutectics MnO: $2MnO,TiO_2$ (m.p. 1330°C.) and MnO,TiO_2 : TiO_2 (m.p. 1290°C.), in the pure components MnO (m.p. 1785°C.) and TiO_2 (m.p. above 1600°C.), and in the pure compound $2MnO,TiO_2$ (m.p. 1460°C. approx.). On the other hand, the compound MnO,TiO_2 melts incongruently, as can be seen from an examination of the thermal curves (see Figures 60 to 66), and before becoming completely molten is decomposed into a liquid and a solid phase. The orthotitanate (MnO,TiO_2) can exist only to a maximum temperature of 1360°C., when decomposition takes place into

TABLE 5.

Composition Weight %.		Temperature of Separants °C.	Etchant.
MnO	TiO_2		
80	20	1330 and 1500	Dil. HCl.
70	30	1330 and 1385	Dil. HCl.
63	37	1330 and 1450	HF.
60	40	1360 and 1445	HF.
57	43	1360 and 1430	HF.
53	47	1360 and 1418	HF.
50	50	1360 and 1400	HF.
47	53	1360 and 1388	HF.
40	60	1290 and 1358	HF.
30	70	1290 and 1392	HF.
20	80	1290 and 1475	HF.
10	90	1290 and 1532	HF.

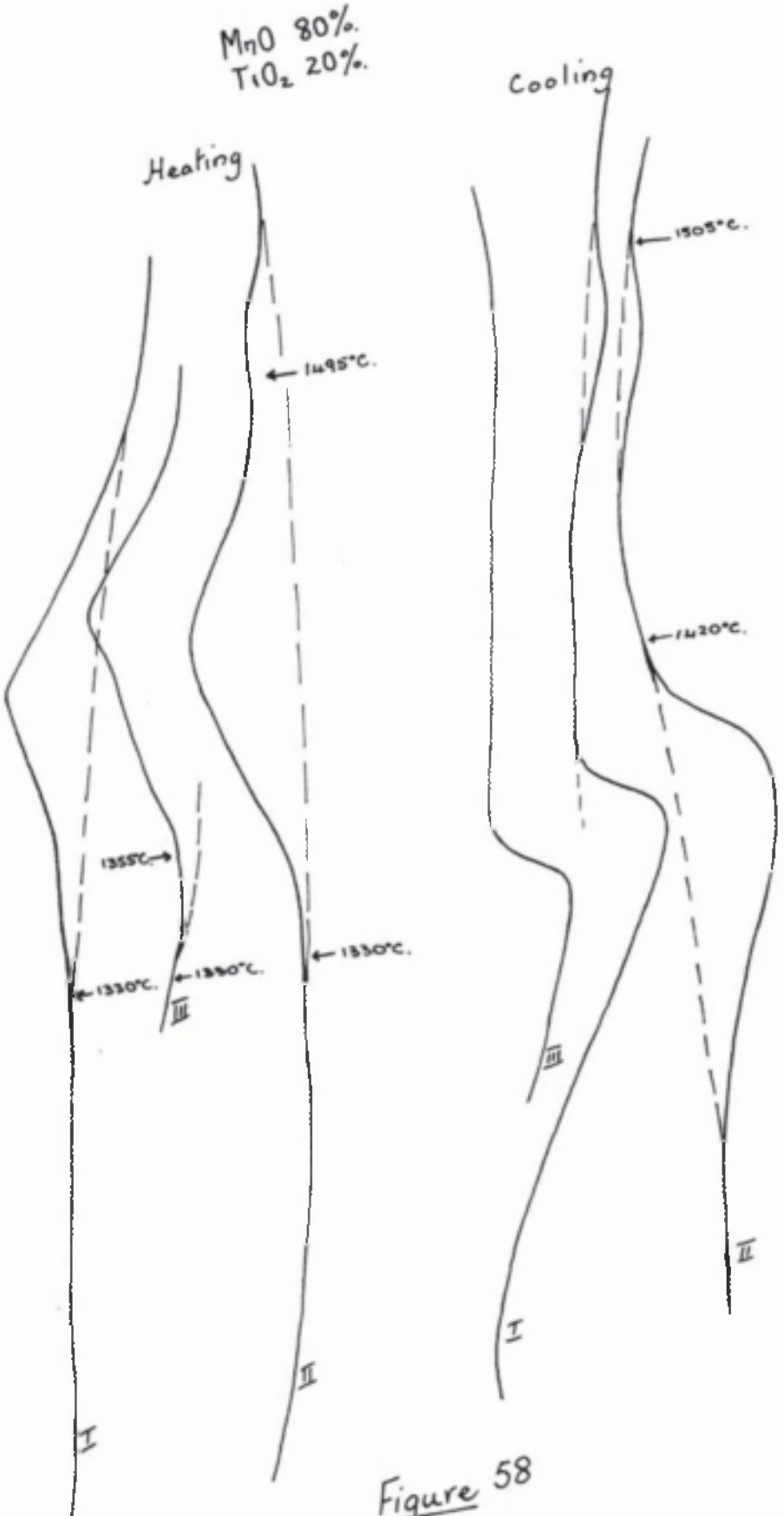
MnO 80%.
TiO2 20%.
Heating
Cooling
1495°C.
1505°C.
1420°C.
1355°C.
1330°C.
1330°C.
1330°C.
III
III
II
II
I
I

Figure 58

MnO 70%.
TiO_2 30%.

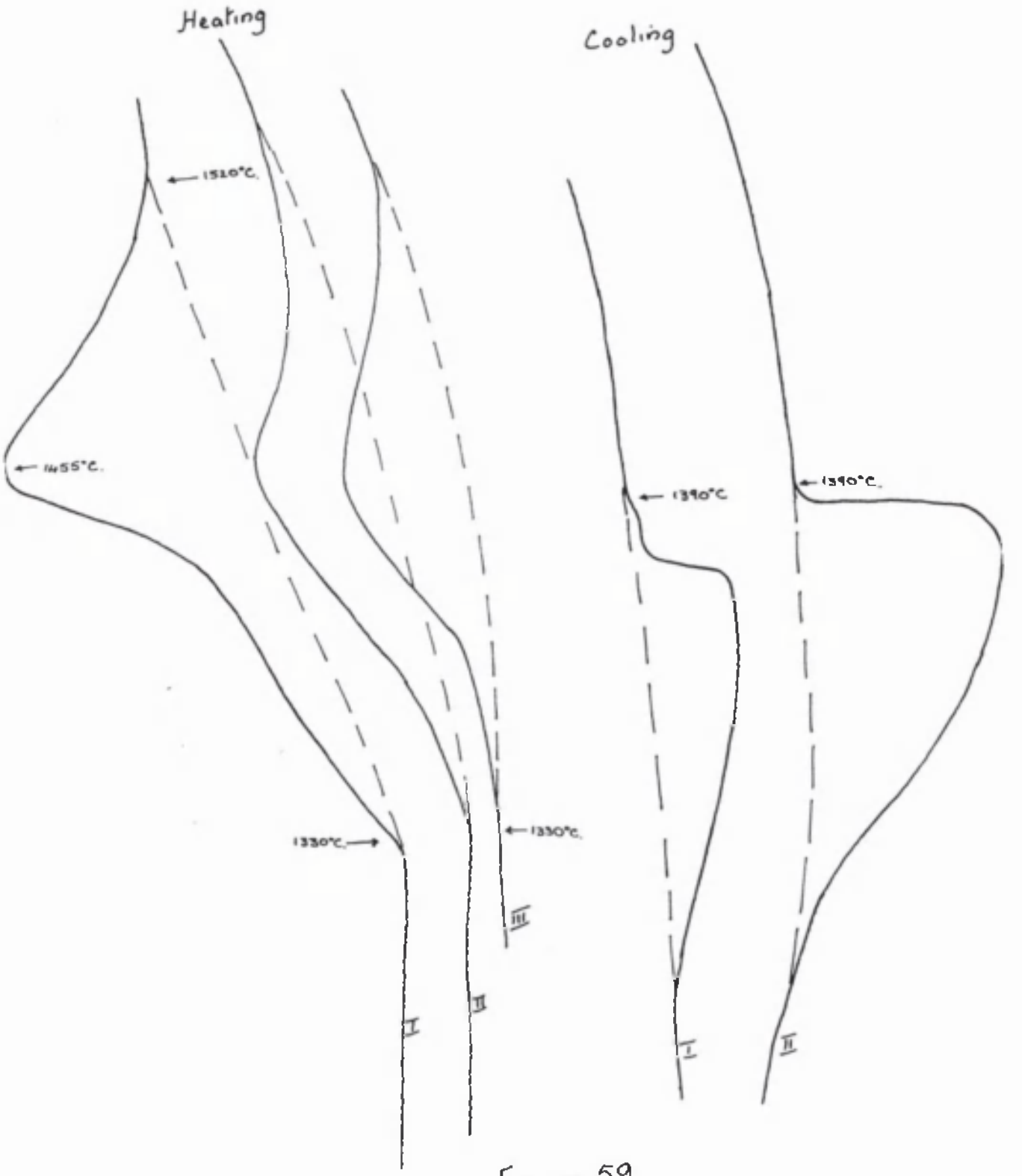

Figure 59.

MnO 63%.
TiO_2 37%.

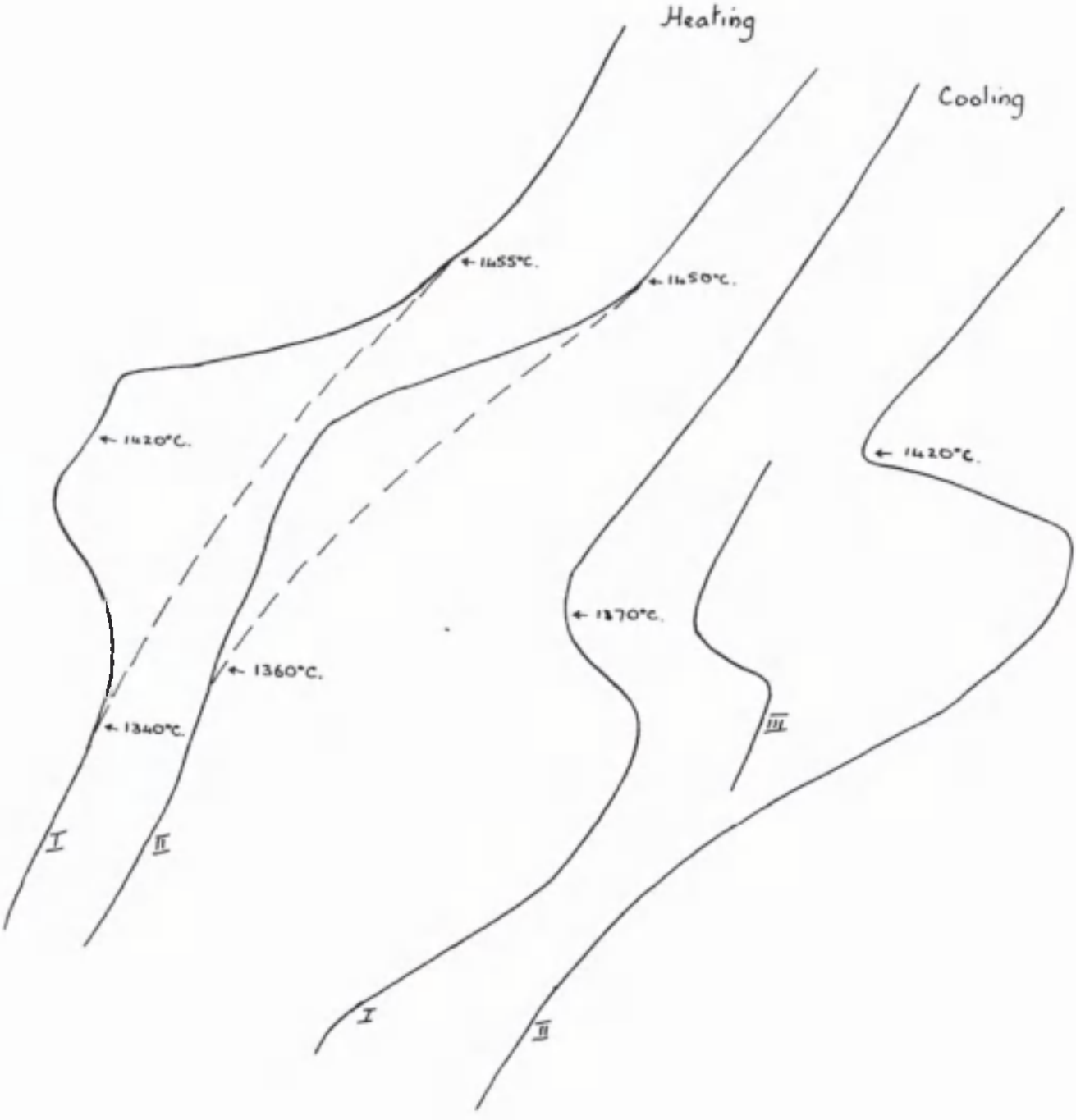

Figure 60

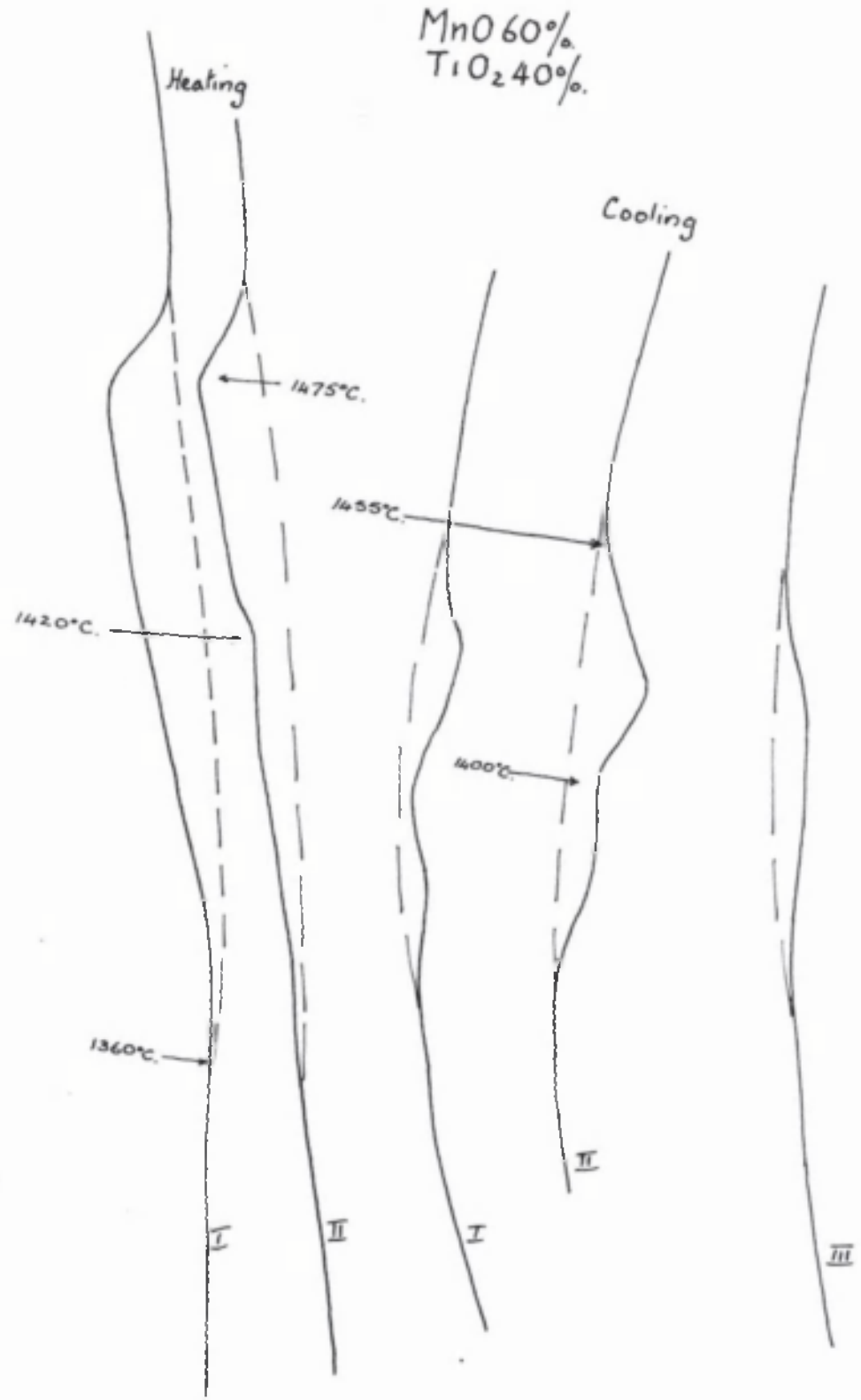
MnO 60%
TiO2 40%.
Heating
Cooling
1475°C.
1455°C.
1420°C.
1400°C.
1360°C.
I
II
I
II
III

Figure 61

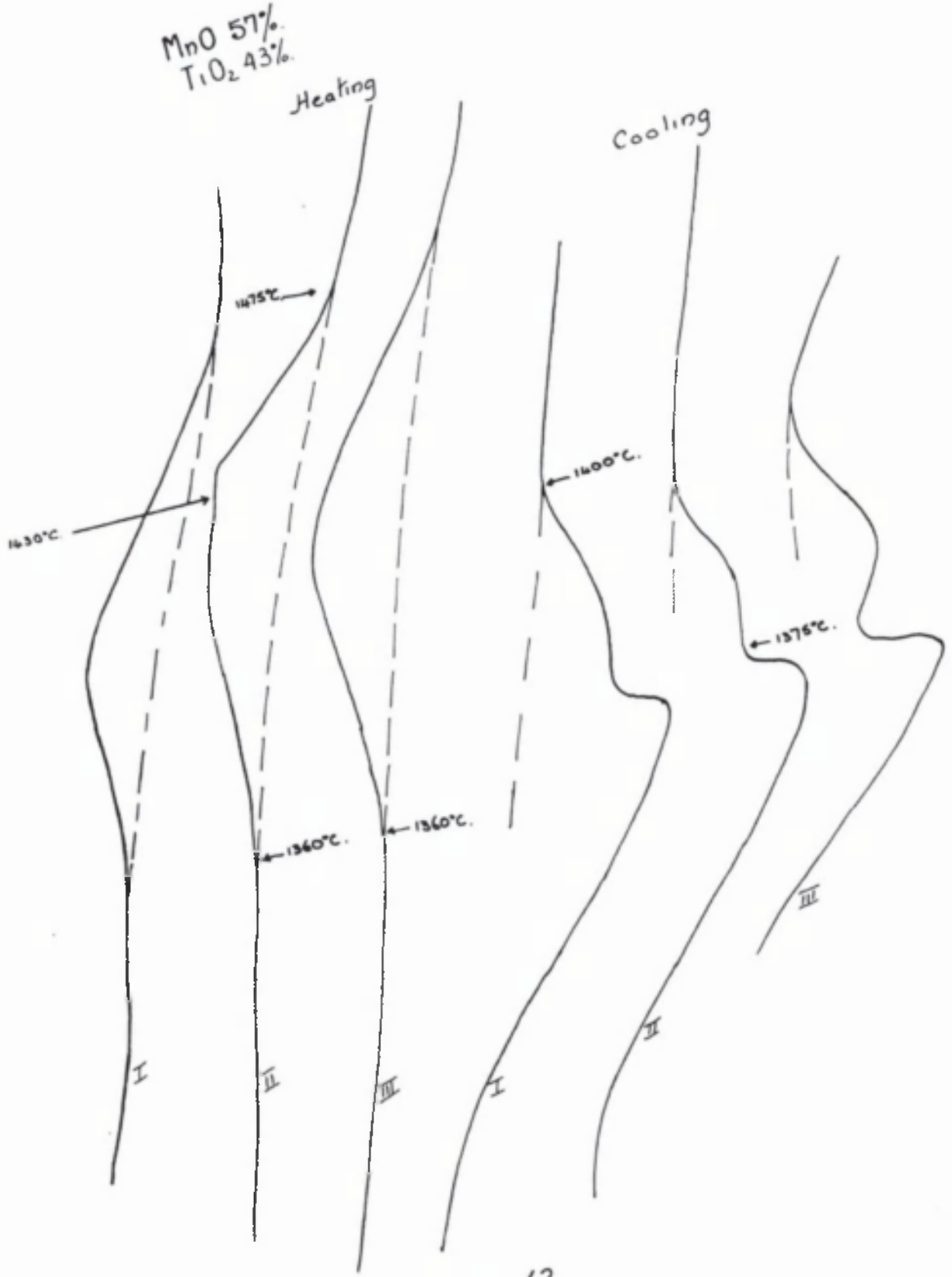
MnO 57%
TiO2 43%
Heating
Cooling
1475°C
1430°C
1360°C
1360°C
1400°C
1375°C
I
II
III
I
II
III

Figure 62

MnO 53%
TiO_2 47%

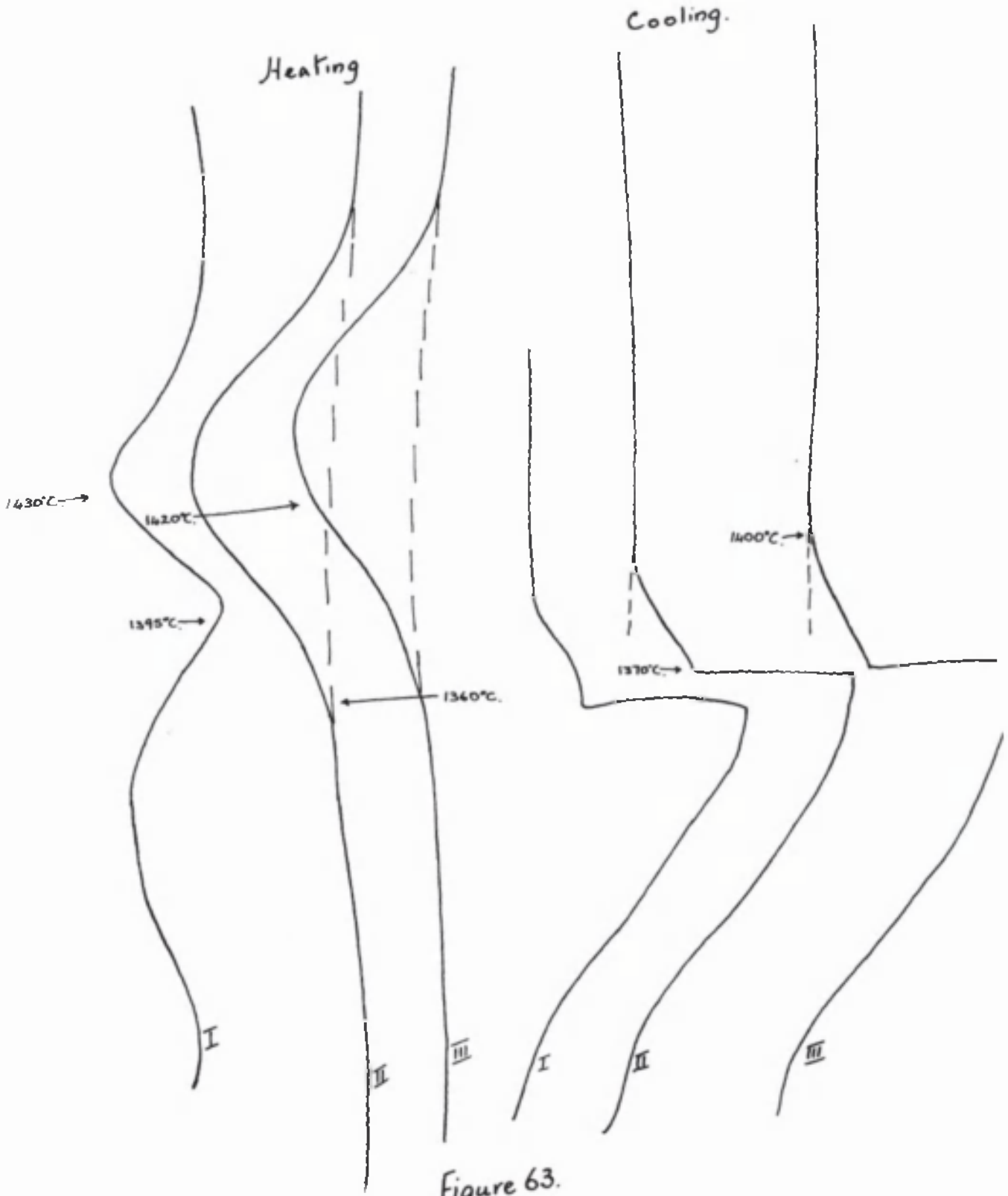

Figure 63.

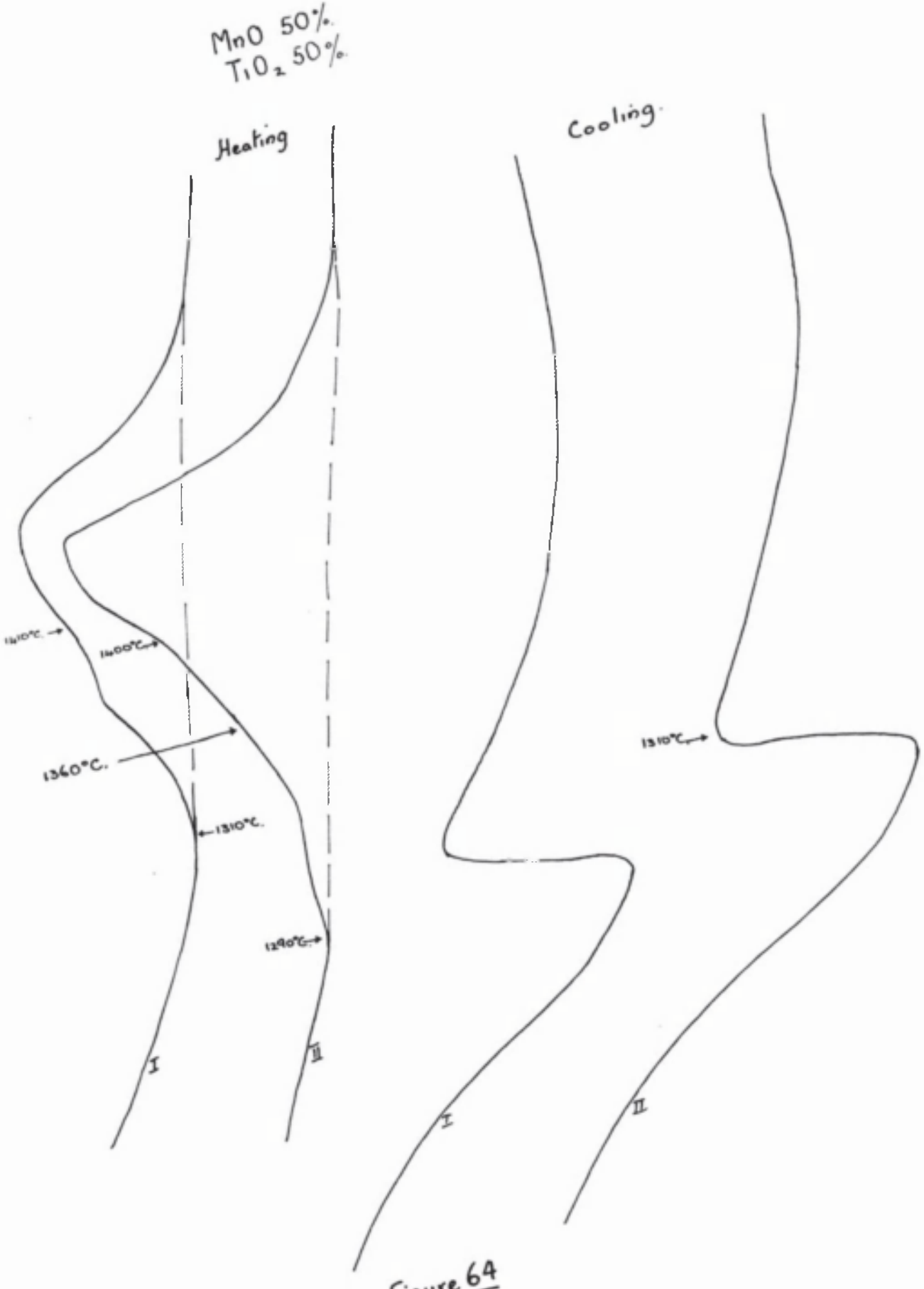
MnO 50%
TiO2 50%
Heating
Cooling
1410°C.
1400°C.
1360°C.
1310°C.
1290°C.
1310°C.
I
II
I
II

Figure 64

MnO 40%
TiO_2 60%

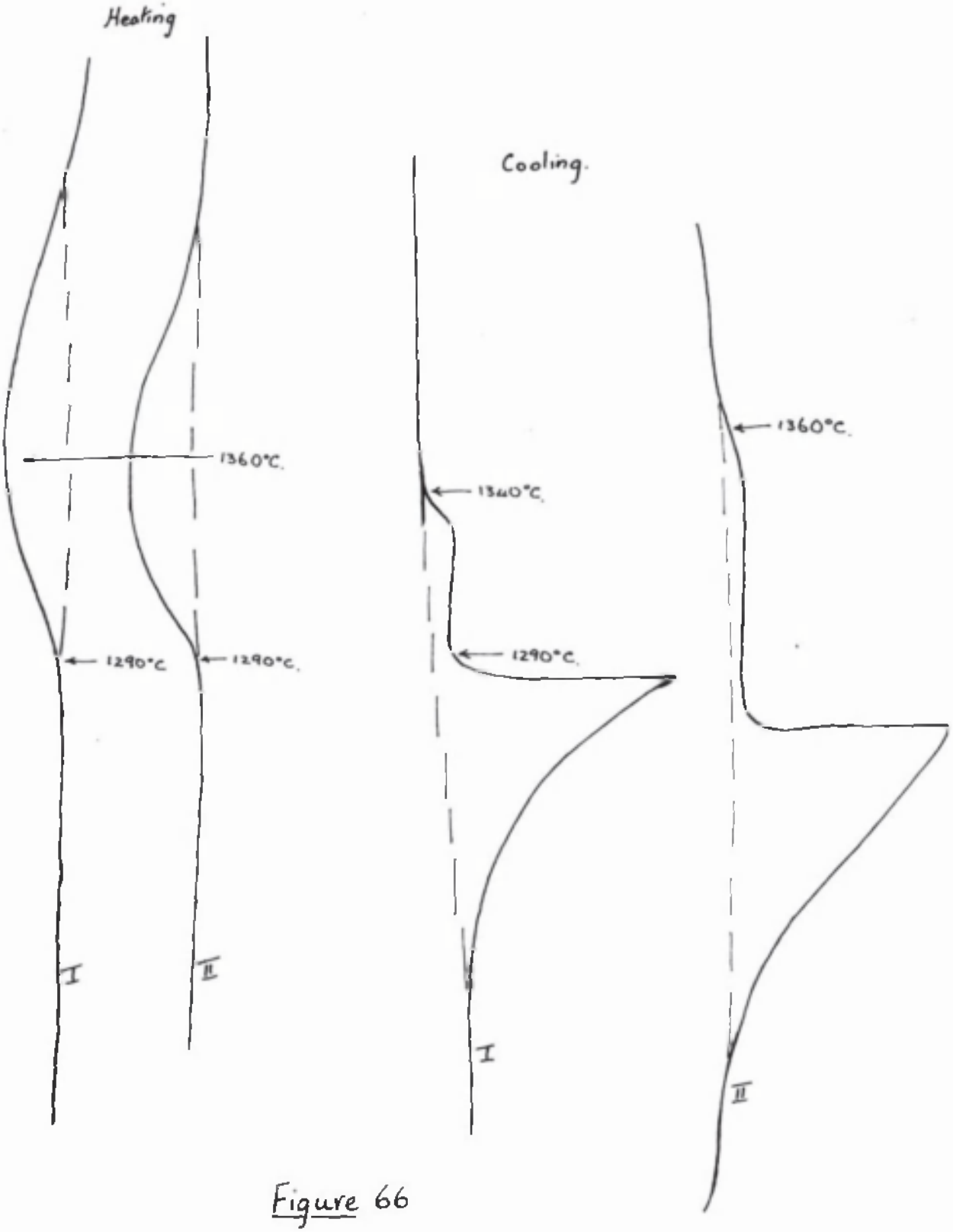

Figure 66

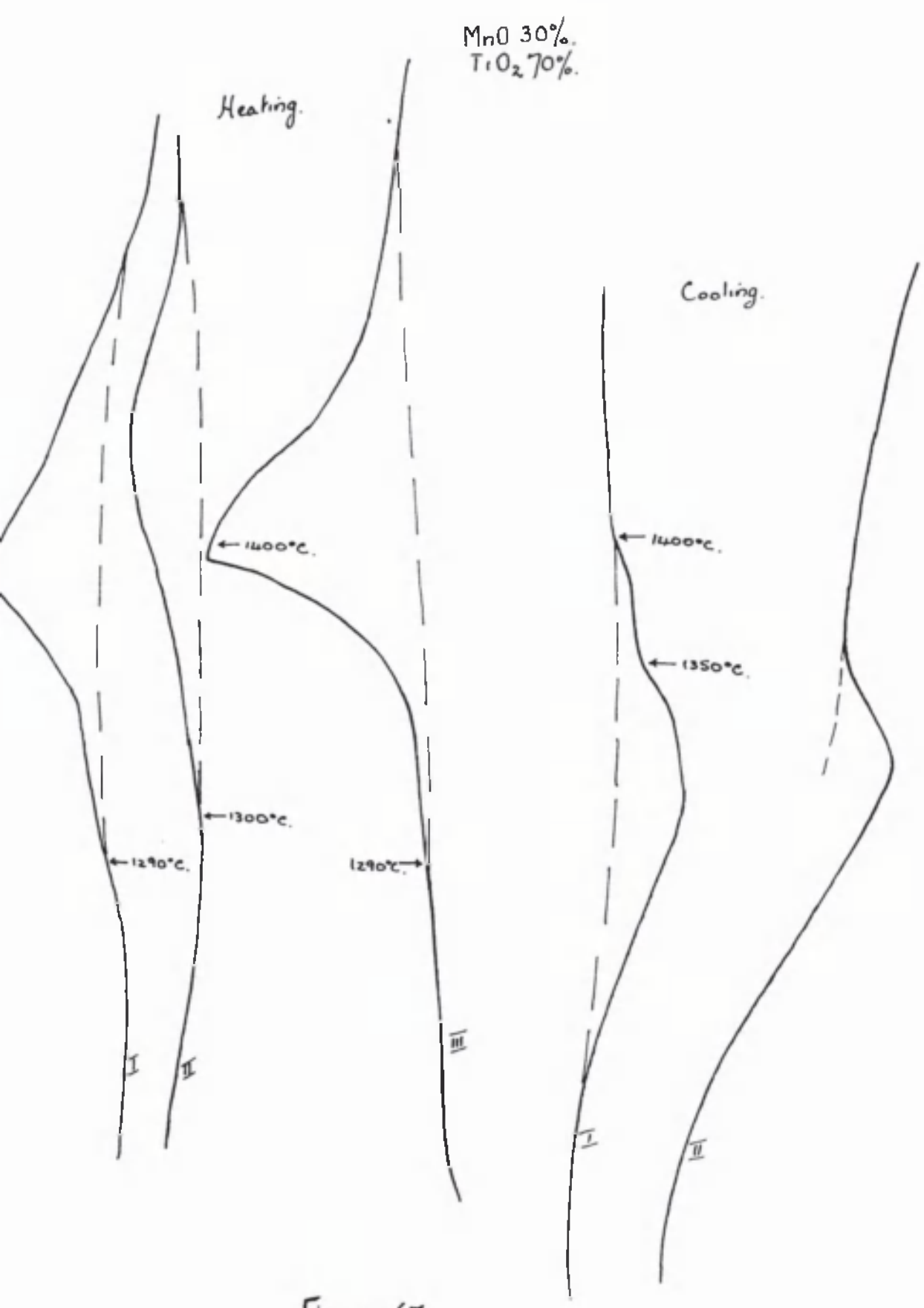
MnO 30%.
TiO_2 70%.
Heating.
Cooling.
1400°C.
1300°C.
1290°C.
1290°C.
1400°C.
1350°C.
I
II
III
I
II

Figure 67

MnO 20%.
TiO_2 80%.

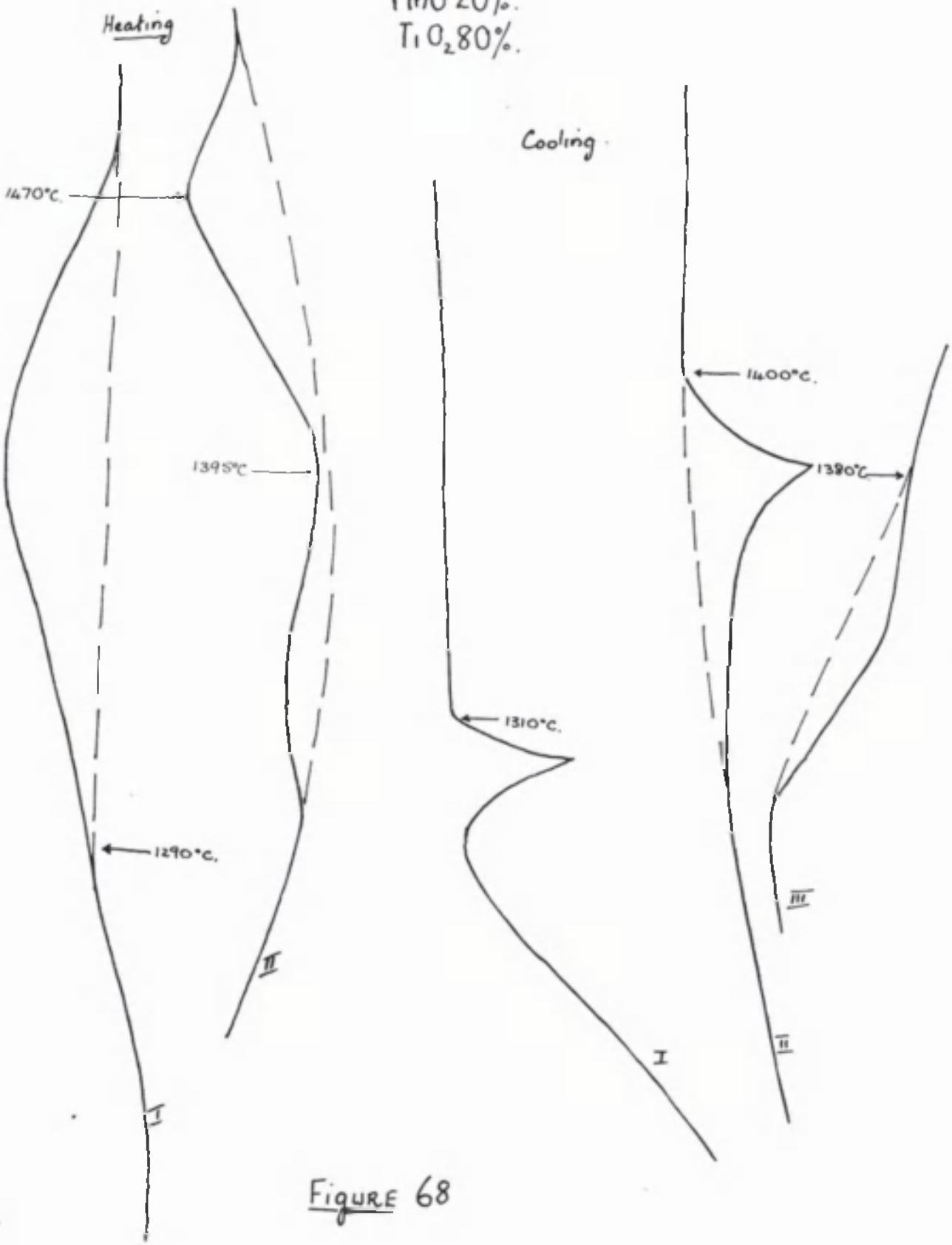

FIGURE 68

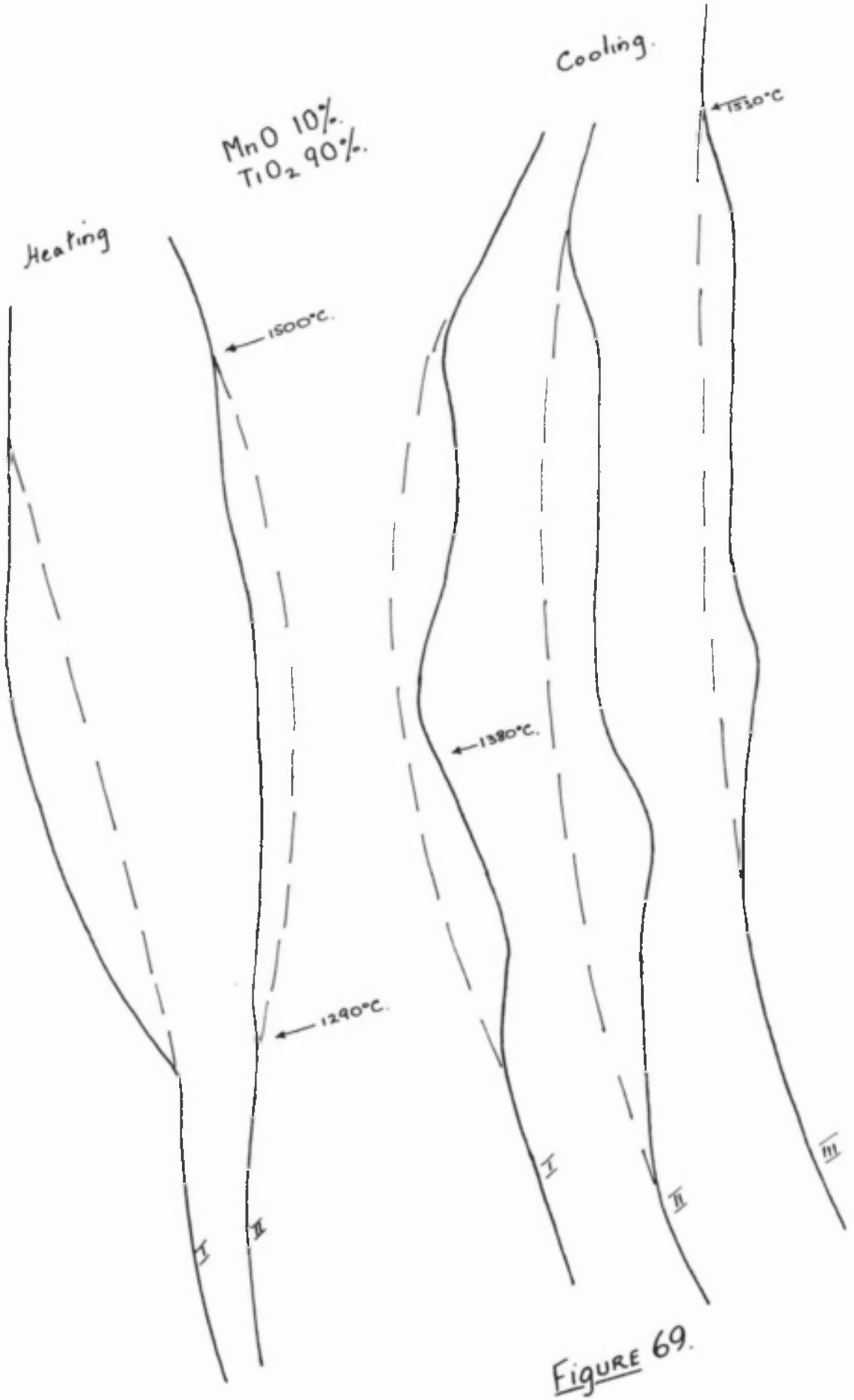
MnO 10%.
TiO2 90%.
Heating
1500°C.
1290°C.
I
II
Cooling.
1520°C
1380°C.
I
II
III

Figure 69.

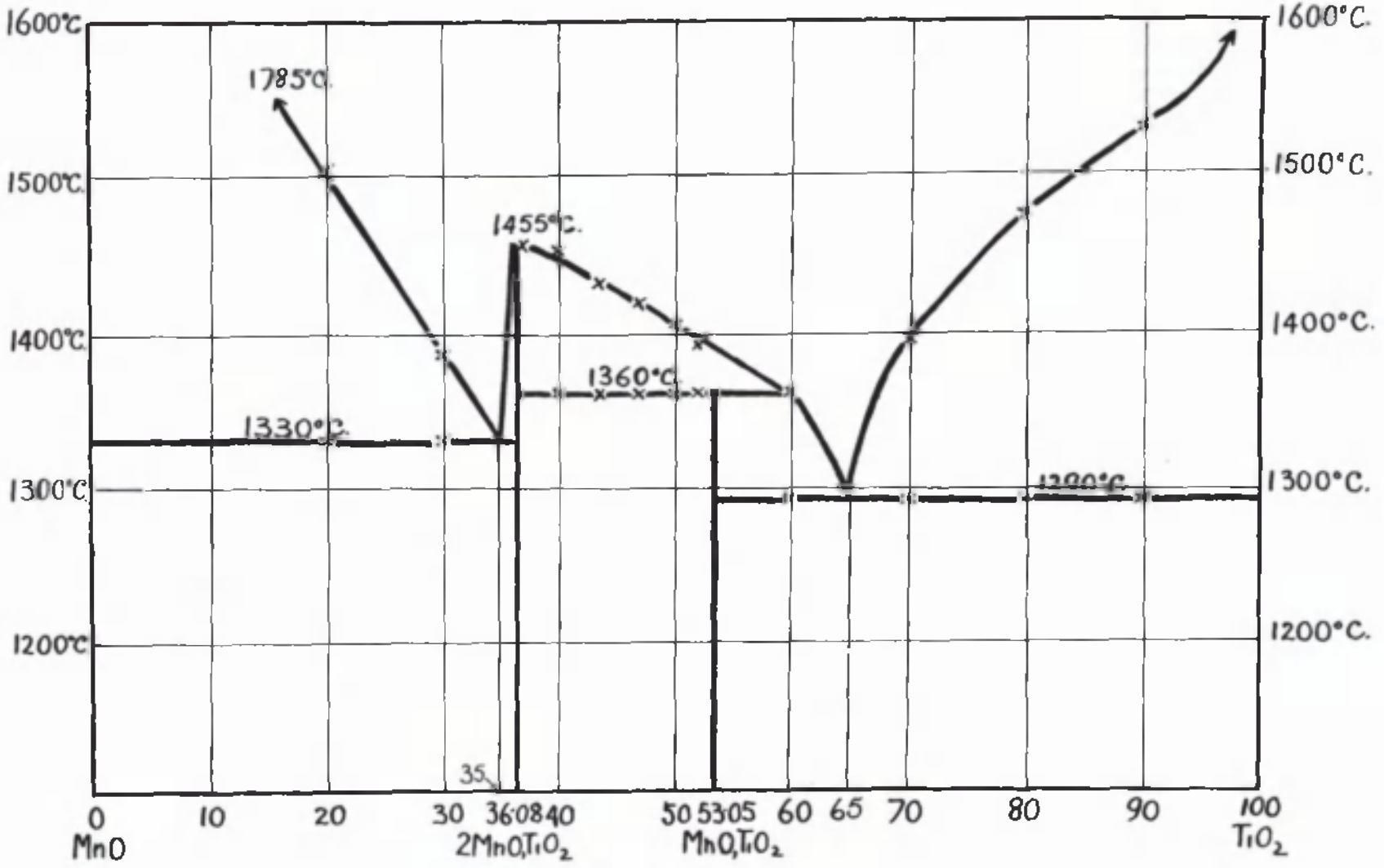
1600°C
1500°C
1400°C
1300°C
1200°C
1785°C
1455°C
1360°C
1330°C
1290°C
35
0
10
20
30
36
40
50
53
05
60
65
70
80
90
100
MnO
2MnO,TiO2
MnO,TiO2
TiO2
WEIGHT % TiO2.

Figure 70.

the metatitanate ($2MnO,TiO_2$) and the corresponding liquid phase. Hence at 1360°C. there must be three phases in equilibrium: undecomposed orthotitanate (MnO,TiO_2), solid metatitanate ($2MnO,TiO_2$), and the appropriate liquid phase. Applying the Phase Rule:

$$P + F = C + 1$$

$$3 + F = 2 + 1$$

$$F = 0$$

where P = no. phases; F = degrees freedom and C = no. of components. We find there is no other variable at our disposal for a binary system. Thus, the equilibrium can exist only at a single temperature and among three phases of definite composition.

The Phase-distribution diagram is shown in Figure 71.

As can be seen from the thermal equilibrium diagram melts with more than 80% MnO by weight, are not molten below 1600°C., and could not be investigated by the apparatus used. The melting point of MnO was taken as 1785°C., as found by Hay, Howat and White[88].

The melting point of TiO_2 was taken as greater than 1600°C. This being so, the liquidus curve marking equilibrium between primary TiO_2 and the liquid phase will be of an S- type as shown. The point is of some theoretical interest, since the S- type of liquidus curve can be

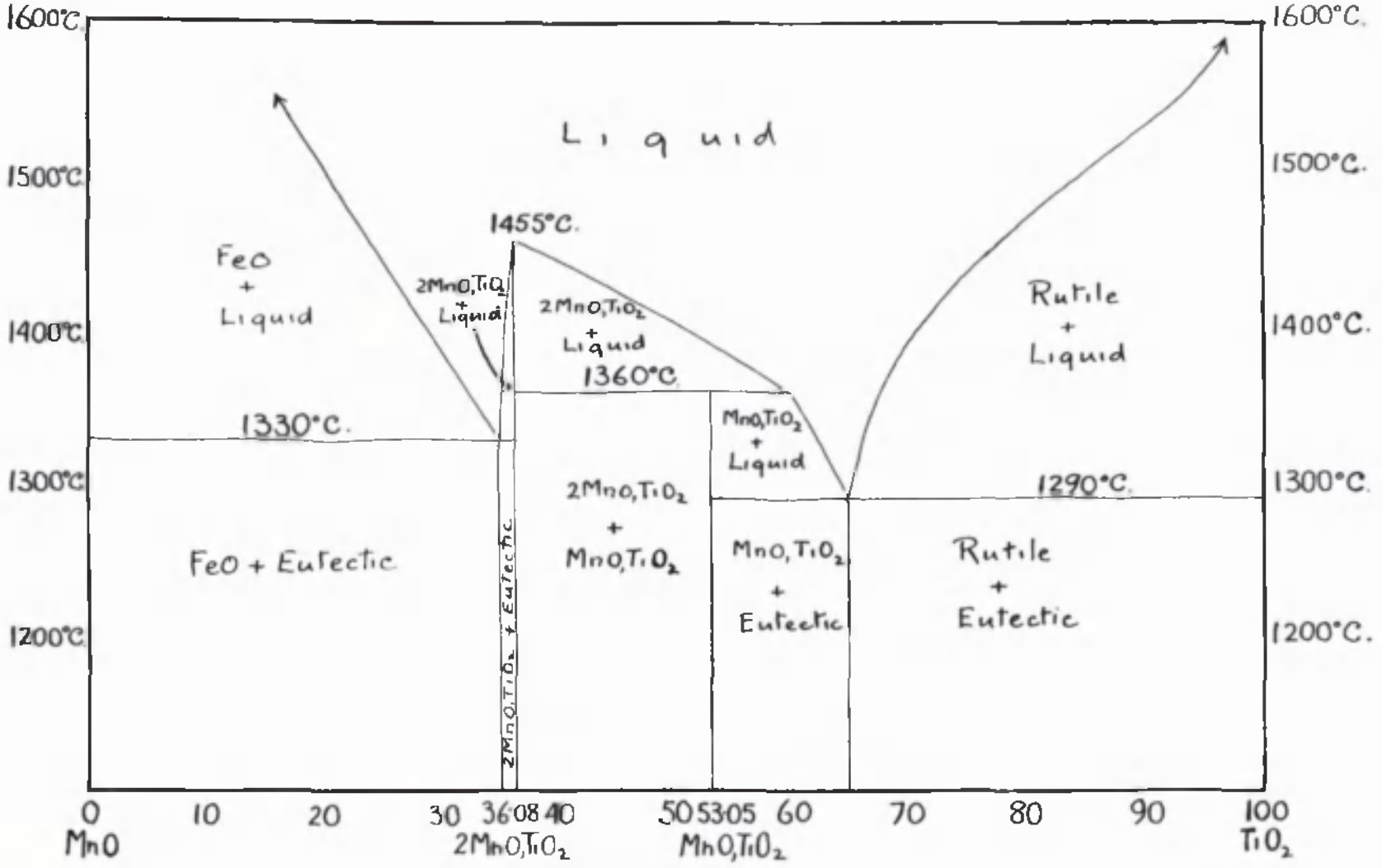
1600°C.
1500°C.
1400°C.
1300°C.
1200°C.
Liquid
1455°C.
FeO
+
Liquid
2MnO,TiO2
+
Liquid
2MnO,TiO2
+
Liquid
1360°C.
1330°C.
MnO,TiO2
+
Liquid
Rutile
+
Liquid
1290°C.
2MnO,TiO2
+
MnO,TiO2
MnO,TiO2
+
Eutectic
Rutile
+
Eutectic
FeO + Eutectic
2MnO,TiO2 + Eutectic
0
MnO
10
20
30
36
08
40
50
53
05
60
70
80
90
100
TiO2
2MnO,TiO2
MnO,TiO2
WEIGHT % TiO2.

Figure 11

regarded as being intermediate to the normal smooth type of curve, and the type in which an actual horizontal section occurs due to the formation of two immiscible liquids on melting. Silica (SiO_2) which is closely related chemically to titania (TiO_2) gives liquidus curves of the latter type with both FeO and MnO. With titania (TiO_2) no actual separation into two liquid phases occurs, but the fact that the liquidus curves, in both the MnO and FeO binary systems, have this "S" form is an indication that influences tending to produce such a separation exist in the liquid state. Such influences will, presumably take the form of attractive forces tending to the formation of aggregates in the liquid phase, with the result that the normal relationships between composition and freezing point is upset, though at the same time, the extent of the attraction is not sufficient to cause separation into two phases. Incidentally, it has been stated in the literature that titaniferous slags are "plastic" in nature due to their colloidal structure.

Examination of the polished melts under the microscope using reflected light agrees with the thermal diagram Fig. 70. Representative micrographs are reproduced in Figs. 72 - 78.

The position of the eutectics explain the absence of eutectic structure. No evidence is obtained from the thermal curves of any changes in the solid state, but from the microscopic examination of the melts, it would appear as

if there was solid solubility between the metatitanate ($2MnO,TiO_2$) and the orthotitanate (MnO,TiO_2), also the orthotitanate and rutile (TiO_2). No evidence of solubility was found between MnO and the metatitanate.

DESCRIPTION OF THE MICROGRAPHS.

Fig. 72 - MnO 80% : TiO_2 20%. × 120.
Etchant dilute HCl.
The micrograph shows primary dendrites of MnO in a background of titanate ($2MnO,TiO_2$) representing eutectic. The position of the eutectic explains the absence of eutectic structure. The holes are due to the tearing out of MnO globules.

Fig. 73 - MnO 63% : TiO_2 37%. × 250.
Etchant HF.
The melt is composed almost entirely of the compound $2MnO,TiO_2$ and a few globules of MnO,TiO_2 (Pyrophanite) as the micrograph shows. The cracks are probably due to contraction on cooling, but there is also a possibility that some of the furrows have been formed by the tearing out of material.

Fig. 74 - MnO 60% : TiO_2 40%. × 250.
Etchant HF.
This micrograph consists of grey $2MnO,TiO_2$ with

Figure 72.

Figure 73

Figure 74

Figure 75

light etching globules of MnO,TiO_2 (Pyrophanite). The banded structure of $2MnO,TiO_2$ is probably evidence of solid solubility (MnO,TiO_2 in $2MnO,TiO_2$) decreasing on cooling.

Fig. 75 - MnO 53% : TiO_2 47%. × 250.
Etchant HF.
The dark etching phase is $2MnO,TiO_2$ and the light etching phase MnO,TiO_2.

Fig. 76 - MnO 48% : TiO_2 52%. × 250.
Etchant HF.
It can be seen from the micrograph that the melt is composed of a small amount of grey $2MnO,TiO_2$ and coarse laths of light etching MnO,TiO_2.

Fig. 77 - MnO 40% : TiO_2 60%. × 250.
Etchant HF.
Shows primary laths of MnO,TiO_2, partly torn out, in a eutectic of MnO,TiO_2 and TiO_2 (the light etching phase). Traces of banded structure may be due to solid solubility of TiO_2.

Fig. 78 - MnO 20% : TiO_2 80%. × 250.
The micrograph shows primary dendrite of TiO_2 (Rutile) in eutectic of MnO,TiO_2. Melt contained

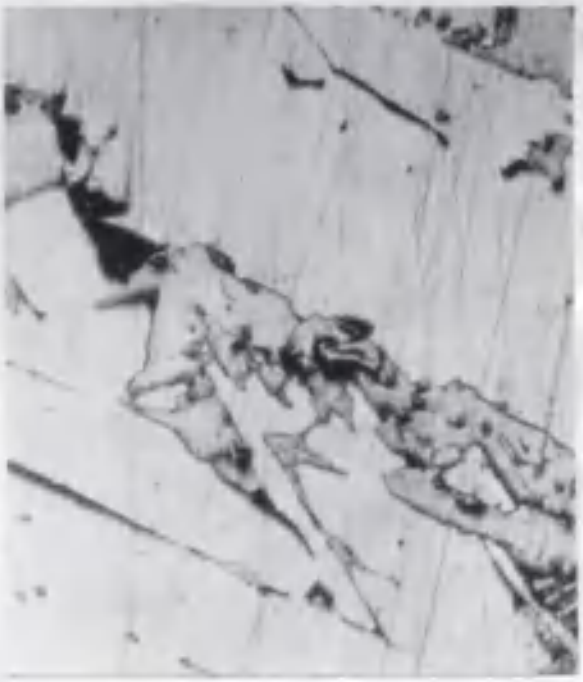

Figure 76

Figure 77

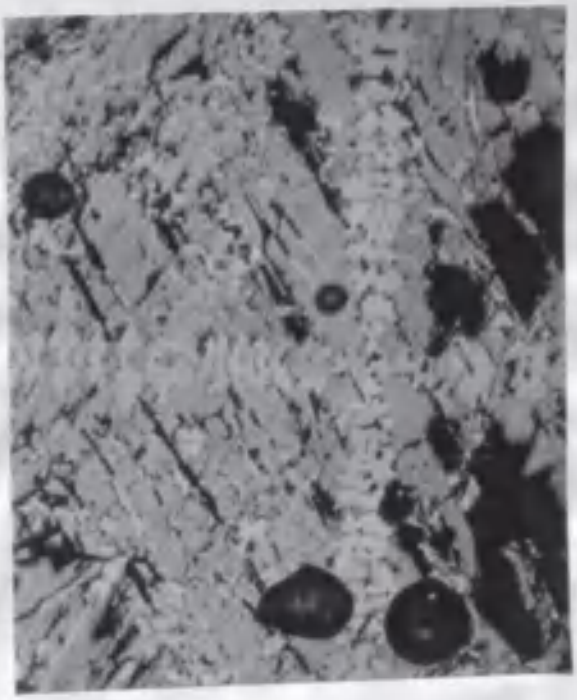

Figure 78

numerous gas cavities.

An X-ray analysis of chosen melts, using the powder method of Debeye, Scherrer and Hull[41], confirmed the phase distribution.

CHAPTER 5.

THE TERNARY SYSTEM FeO - MnO - Ti_2O_3.

PRELIMINARY.

The composition of any member of a ternary system is indicated by a point in an equilateral triangle, and the third dimension is then used to indicate temperature. A ternary system is therefore only truly represented by a space model, although the liquidus and solidus surfaces can be indicated by projecting upon the equilateral base the isothermals drawn upon them. However, the methods of representing the ternary system graphically are sufficiently different to warrant more explanation than was necessary for binary systems.

THE PHASE-RULE STATEMENT.

The phase-rule statement of the equilibria which may exist in a ternary system is summarised in the subjoined table:

The Ternary System.

$$f = 3 + 2 - p = 5 - p$$

Where f = degrees of freedom.

p = phases present.

p	f	Spatial representation
1	4	A four-dimensional solid.
2	3	A three-dimensional solid.
3	2	A surface.
4	1	A space curve.
5	0	A point; a quintuple point.

The Isobaric Ternary System.

p	f	Spatial representation.
1	3	A three-dimensional solid.
2	2	A surface.
3	1	A space curve.
4	0	A point (a quadruple point).

This demonstrates that the dimensions of any one phase increase by one as the components of the system are increased by one.

When we are dealing with oxide phases which are stable in vacuo or in nitrogen at the high temperatures employed, it is usual to neglect the vapour pressure, and to adopt the Isobaric Ternary System.

GRAPHIC REPRESENTATION. - Four variables - pressure, temperature and two concentrations - are involved, and there is no simple way to represent a ternary system graphically;

even an isobaric section of a ternary system is three-dimensional. By sectioning the isobaric section at constant concentration of one component, at a constant ratio of two components, or at constant temperature, this difficulty is got over.

Various methods have been suggested to represent the composition of ternary-isobaric systems based on the triangle, but only two have been used with any success. The first method proposed by Gibbs[47], makes use of an equilateral triangle of unit altitude, as shown in Fig. 79. The quantities of the components are expressed as fractional parts of the whole, thus the sum of the fractional parts is therefore equal to unity.

The pure components are represented by the corners of the triangle. A point on the side of the triangle represents the composition of a binary system, and a point within the triangle represents the composition of a ternary system. It is the property of any point within the triangle that the sum of the perpendiculars to the three sides which pass through that point is equal to unity, and it is evident that the composition of any ternary system can be represented by a point within the triangle located so that the perpendiculars from that point are equal in length to the fractional amounts of the three components. The fractional amounts of A, B, and C are represented by the perpendicular

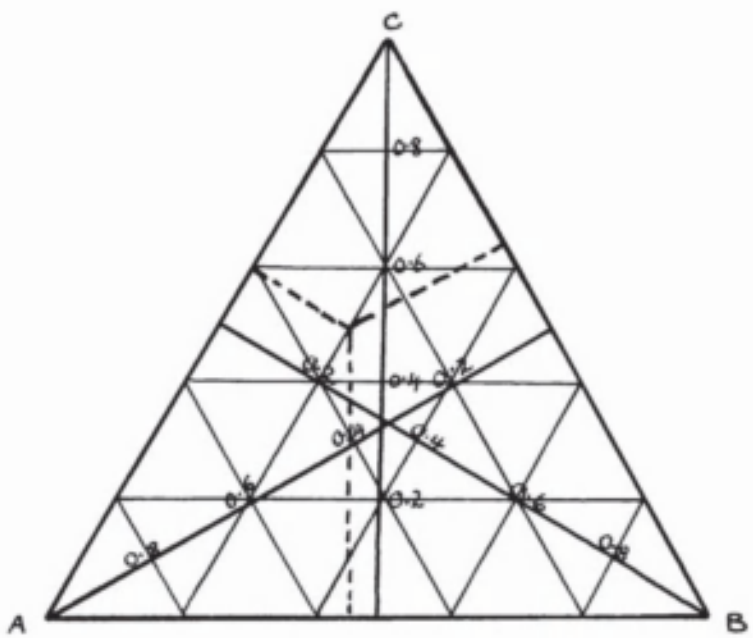

The Gibbs Triangle.

Figure 79

distances from the sides opposite the A, B, and C corners.

If the perpendiculars from the vertices, as A, B, and C of Figure 79, are subdivided as shown, the position of any point can be determined in virtually the same manner as with rectangular co-ordinates. Point x represents a composition of 0·3 A, 0·2 B, and 0·5 C, or 30, 20, and 50 per cent. respectively.

The second method, due to Roozeboom[48], has found greater usage here.

An equilateral triangle is also used, but the length of the side is made equal to unity, or 100. Thus, the composition of a ternary system is determined by this method by the distances to the sides in a direction parallel to the sides, as shown in Figure 80. So, the composition represented by a point x is A = Aa, B = Bb and C = Cc, or A = 0·45, B = 0·30, and C = 0·25. Here it is evident that only two distances need be determined, since the concentration of the third component may be obtained by difference (from unity in the terms of parts, or from 100 in terms of per cent.).

Any line drawn from a vertex of the composition triangle to the opposite side, represents the compositions of all mixtures in which the relative concentrations of the components represented by the remaining two vertices remains unchanged. Thus in Fig. 81, if component C is

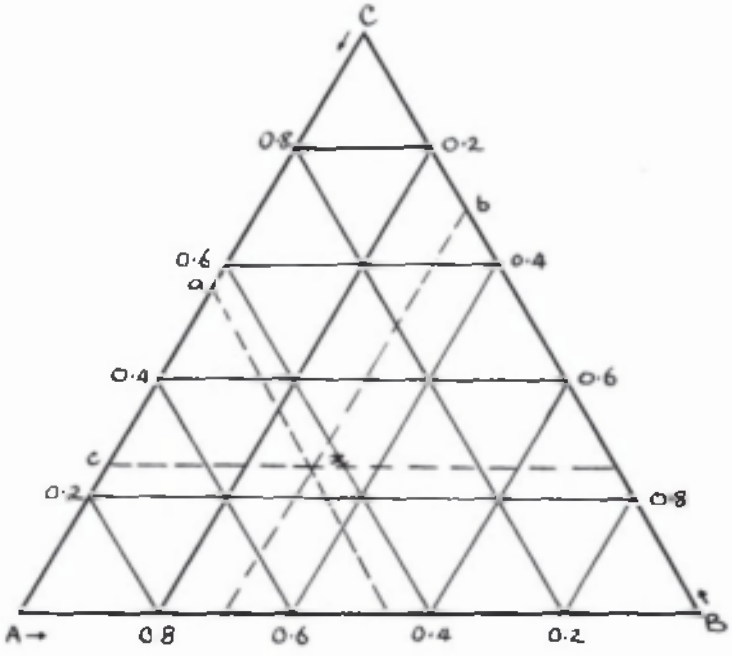

Figure 80 – The Roozeboom Triangle.

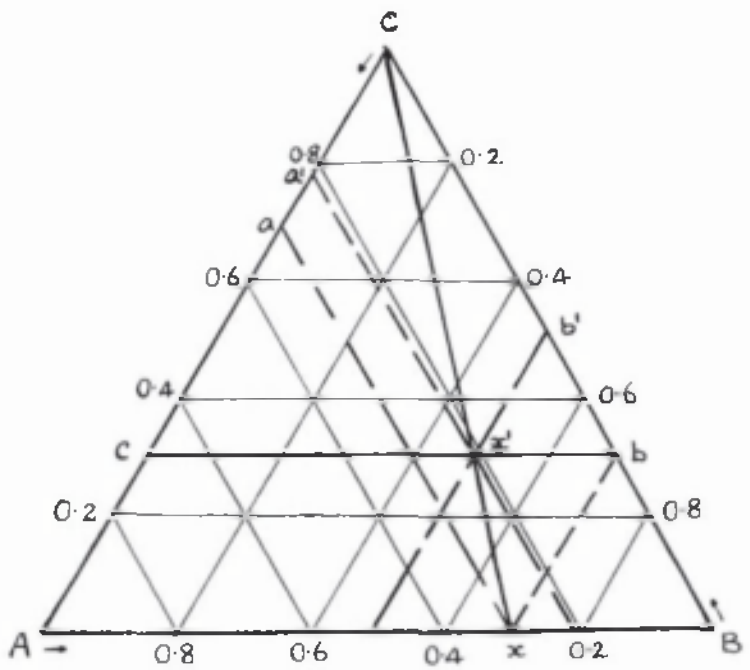

Figure 81 Demonstration of a useful property of the triangle.

added to a solution of composition x, in which A and B are represented in the proportion Ax: xB, until the composition x^1 is attained, the proportion of A and B remains the same. This can be shown by simple geometry.

Another method, making use of the isosceles triangle, is desirable if the effect of one component is much greater than the others, such as carbon in alloy steels, and if the composition triangle is not to be completed.

Within certain limits, a right-angled triangle may be used, with the advantage that the diagram may be plotted on regular rectangular- co-ordinate paper. However, throughout this work the method adopted by Roozeboom[48] was used, being more convenient to work with.

Temperature is usually plotted in the direction perpendicular to the composition triangle, as shown in Fig. 82, when a prism is formed. It follows that the composition triangle is an isothermic section of a ternary isobaric section, and that all isothermic sections of such sections are horizontal. Sections at constant concentration of one component or a constant ratio of two components are vertical.

THE TERNARY SYSTEM MnO - FeO - TiO_2.

The ternary system MnO - FeO - TiO_2 was investigated by methods similar to those employed for the binary systems

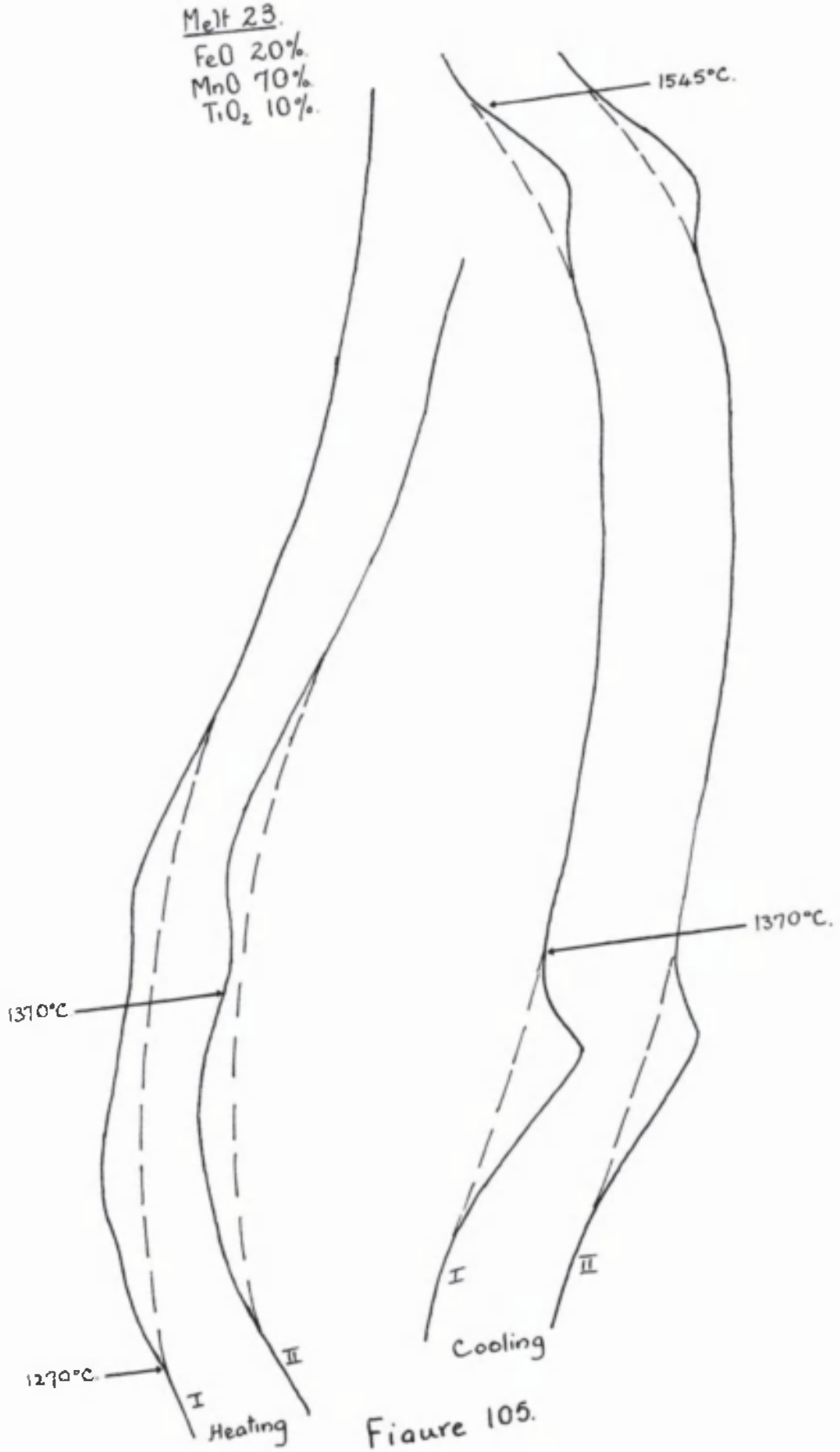
Melt 23.
FeO 20%
MnO 70%
TiO_2 10%
1545°C.
1370°C.
1370°C
1270°C.
I
II
Heating
I
II
Cooling

Fiaure 105.

Melt 24.
FeO 20%.
MnO 60%.
TiO_2 20%.

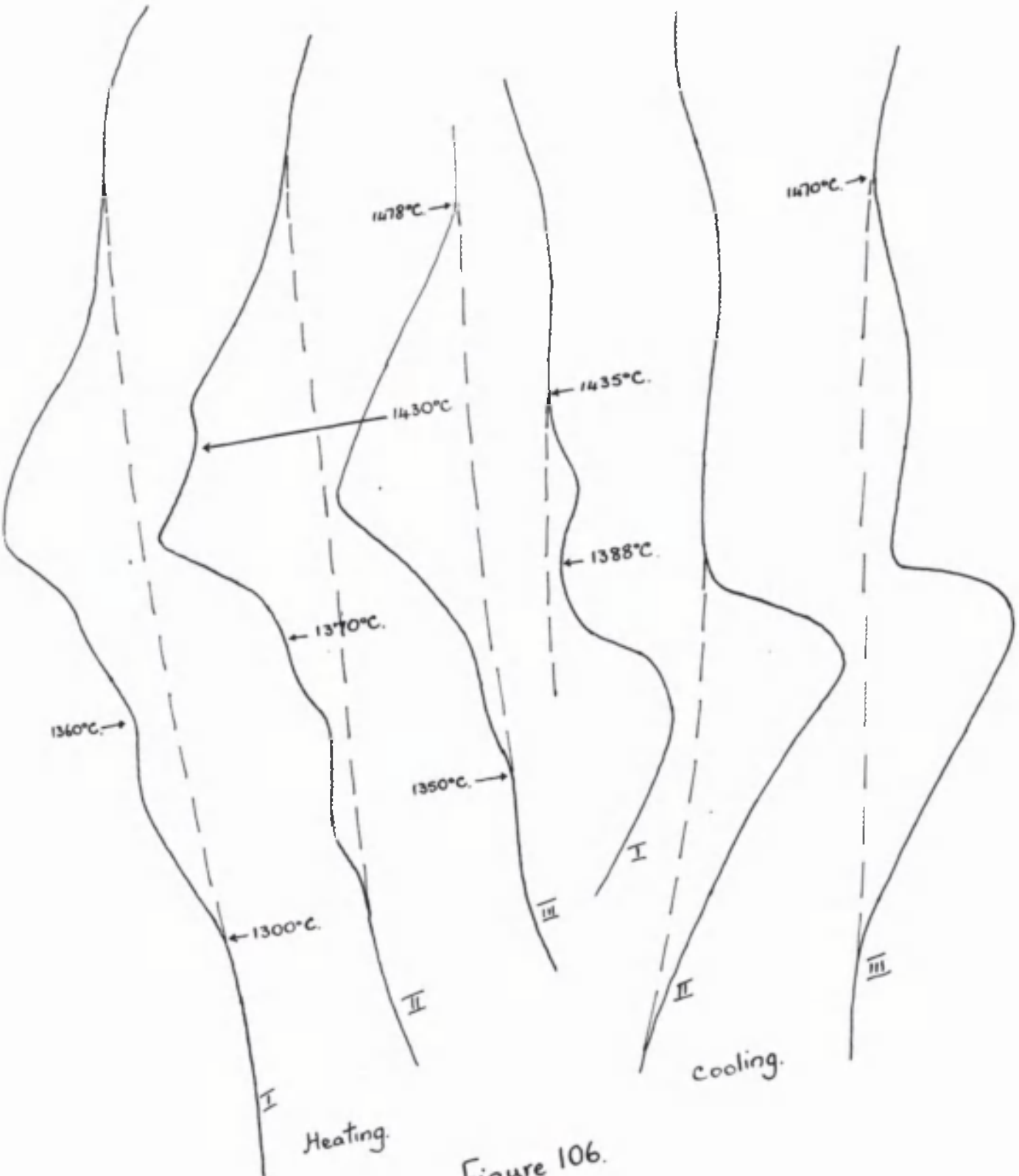

Figure 106.

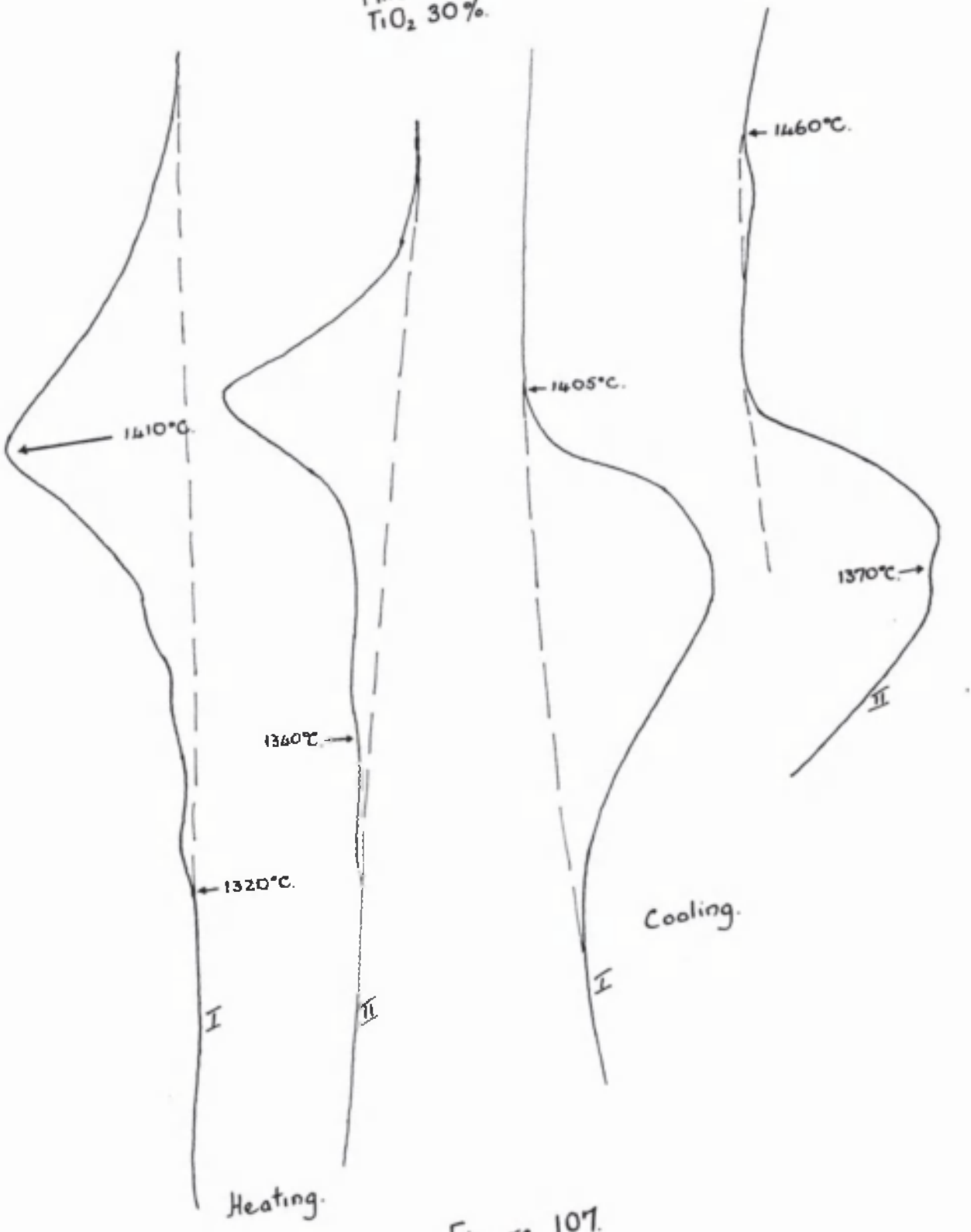
Melt 25
FeO 20%.
MnO 50%.
TiO_2 30%.
1410°C.
1320°C.
I
1360°C.
II
Heating.
1405°C.
I
1460°C.
1370°C.
II
Cooling.

Figure 107.

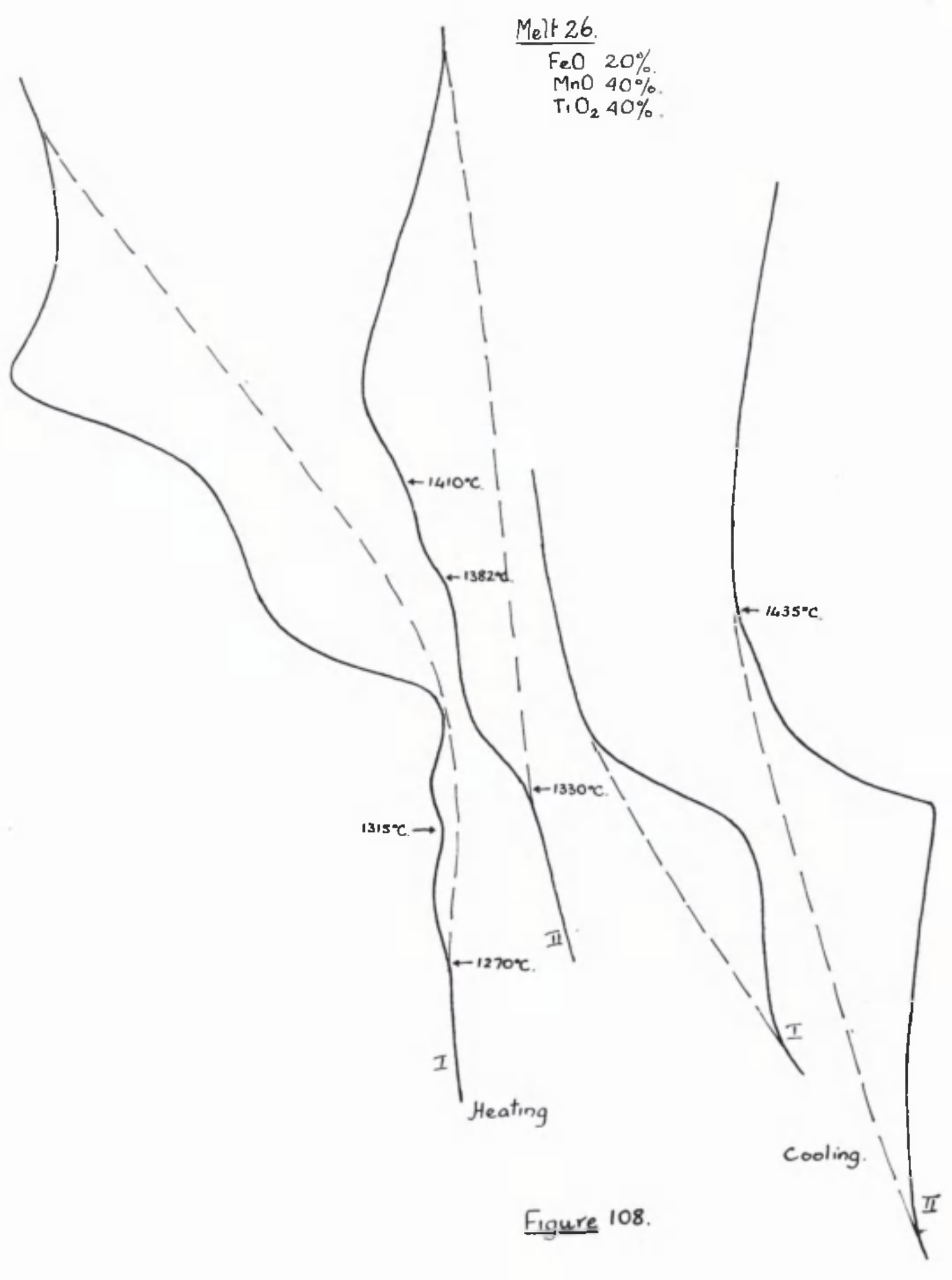
Melt 26.
FeO 20%.
MnO 40%.
Ti_2O_3 40%.
1410°C.
1382°C.
1330°C.
1315°C.
1270°C.
I
II
Heating
1435°C.
I
II
Cooling.

Figure 108.

Melt 27.

FeO 20%
MnO 30%
TiO_2 50%

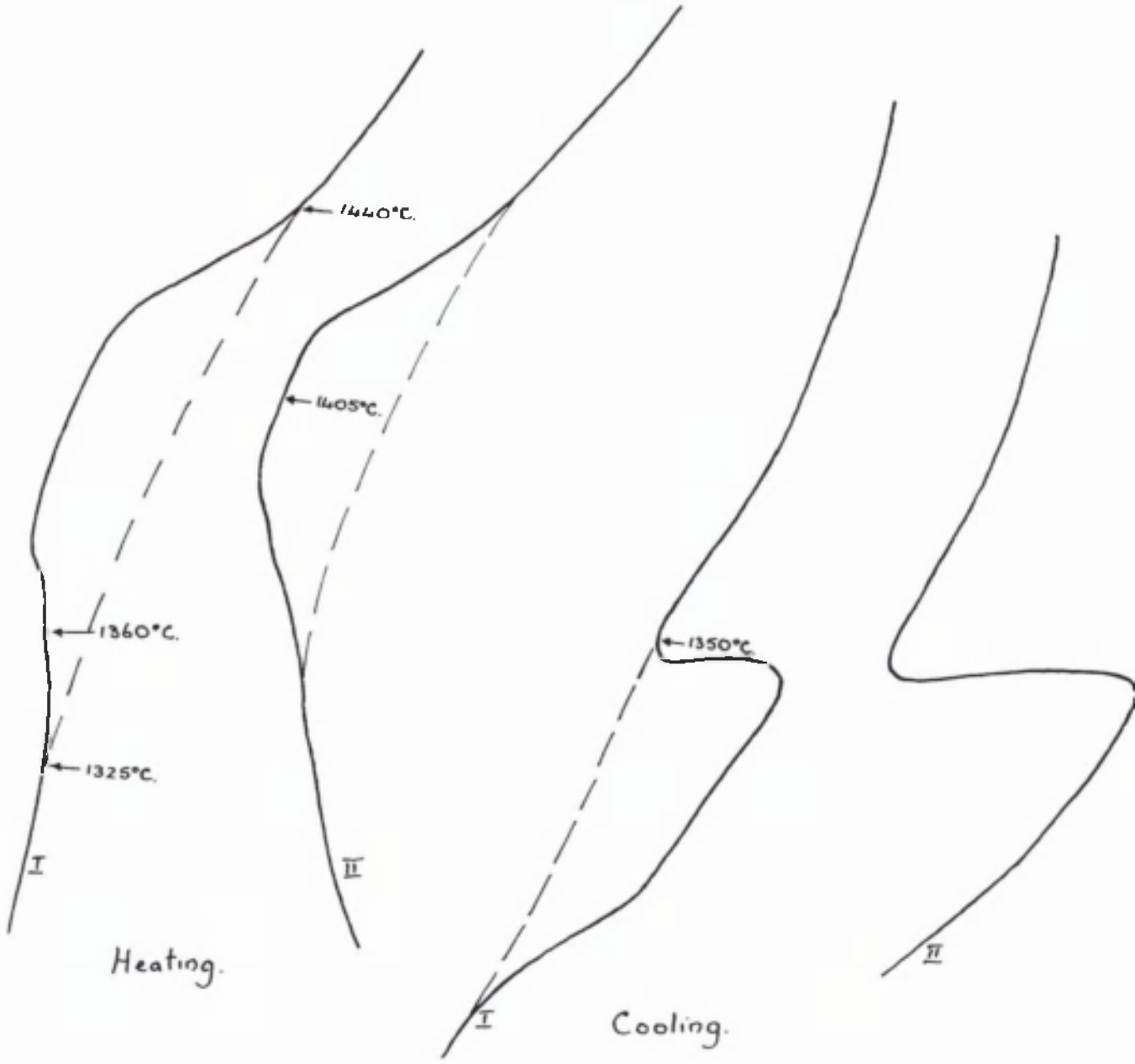

Figure 109.

Melt 28.

FeO 20%.
MnO 60%.
TiO_2 20%.

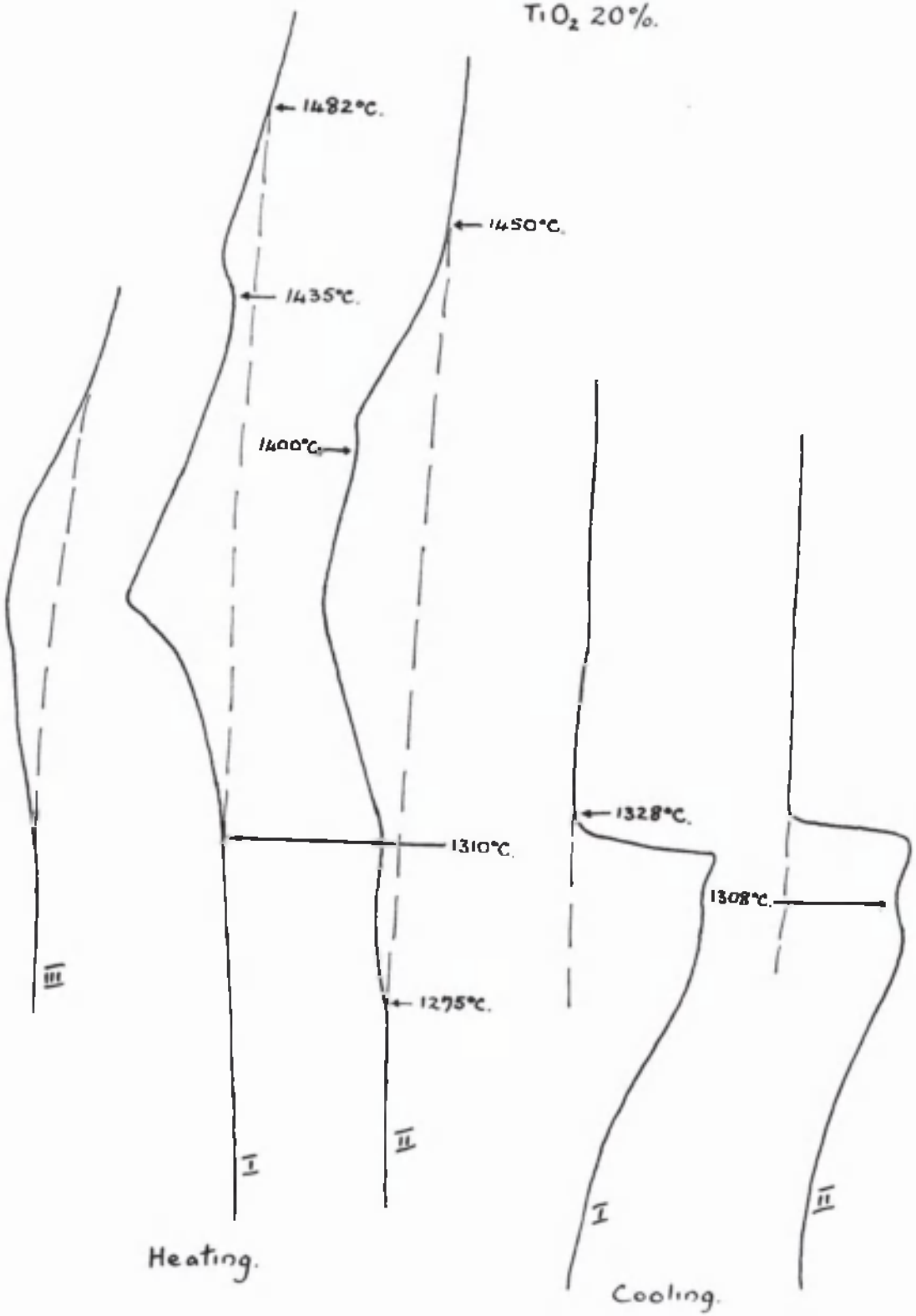

Figure 110.

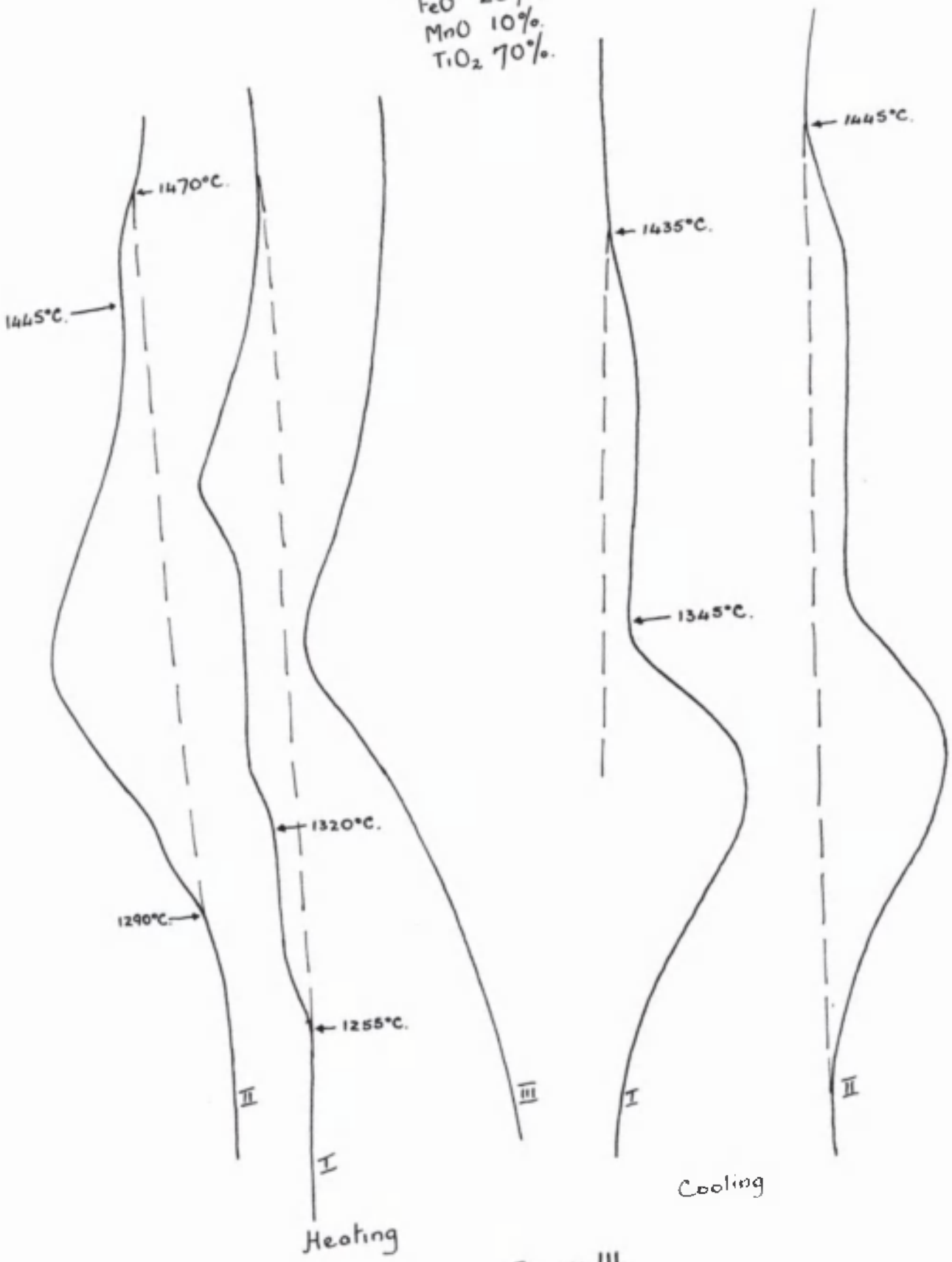
Melt 29.
FeO 20%.
MnO 10%.
TiO2 70%.
1470°C.
1445°C.
1320°C.
1290°C.
1255°C.
II
III
I
Heating
1445°C.
1435°C.
1345°C.
I
II
Cooling

Figure III.

Melt 30

FeO 10%
MnO 80%
TiO_2 10%

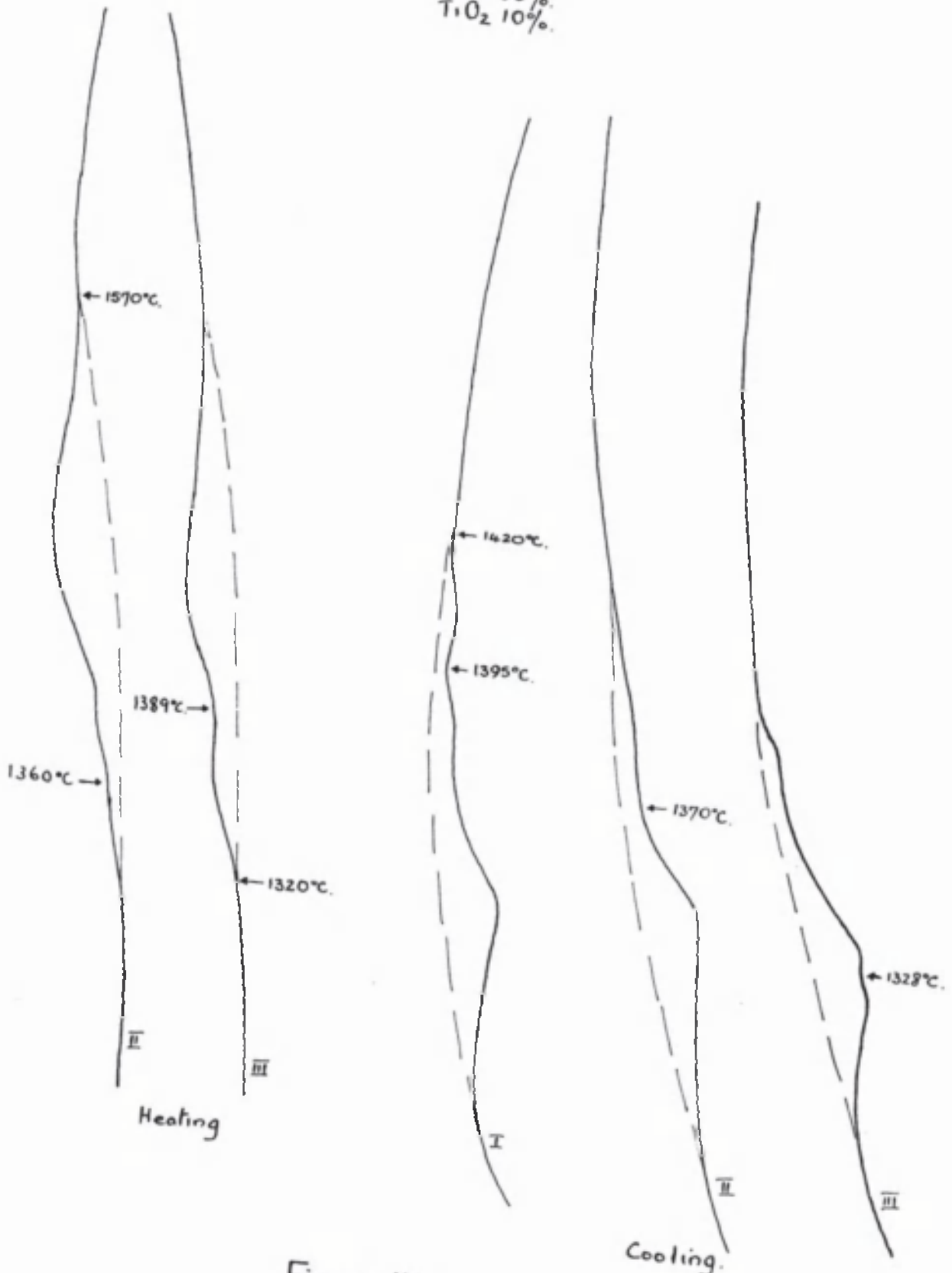

Figure 112.

occurs. Continuous series of solid solutions are formed between the pairs of isomorphous compounds $2MnO,TiO_2$ and $2FeO,TiO_2$. In addition, as mentioned above MnO and FeO are soluble in one another to a considerable extent, giving two series of solid solutions separated by a single range of immiscibility.

As a result of the occurrence of these solid solution formations the form of the thermal equilibrium diagram is relatively simple. In Fig. 114, AB is a binary eutectic trough between TiO_2 and the metatitanate solid solution series. From C to D line CDE indicates a binary eutectic trough between the metatitanate and the orthotitanate series. At D, however, it crosses the metatitanate join, this being necessitated by the fact that, MnO,TiO_2 (and hence also solid solutions of the metatitanate approaching MnO,TiO_2 in composition) melts incongruently. DE then represents the intersection between the surface of peritectic dissociation of this latter range of the metatitanate series and the liquidus surface, D being an invariant point but not a quintuple point. The metatitanate join is thus not a true binary join since D presumably is a minimum in the solid solution series. The orthotitanate join on the other hand, is a true binary section through the system, and is represented by a continuous ridge on the liquidus surface as indicated by the isothermals of Fig. 113. FGH is a

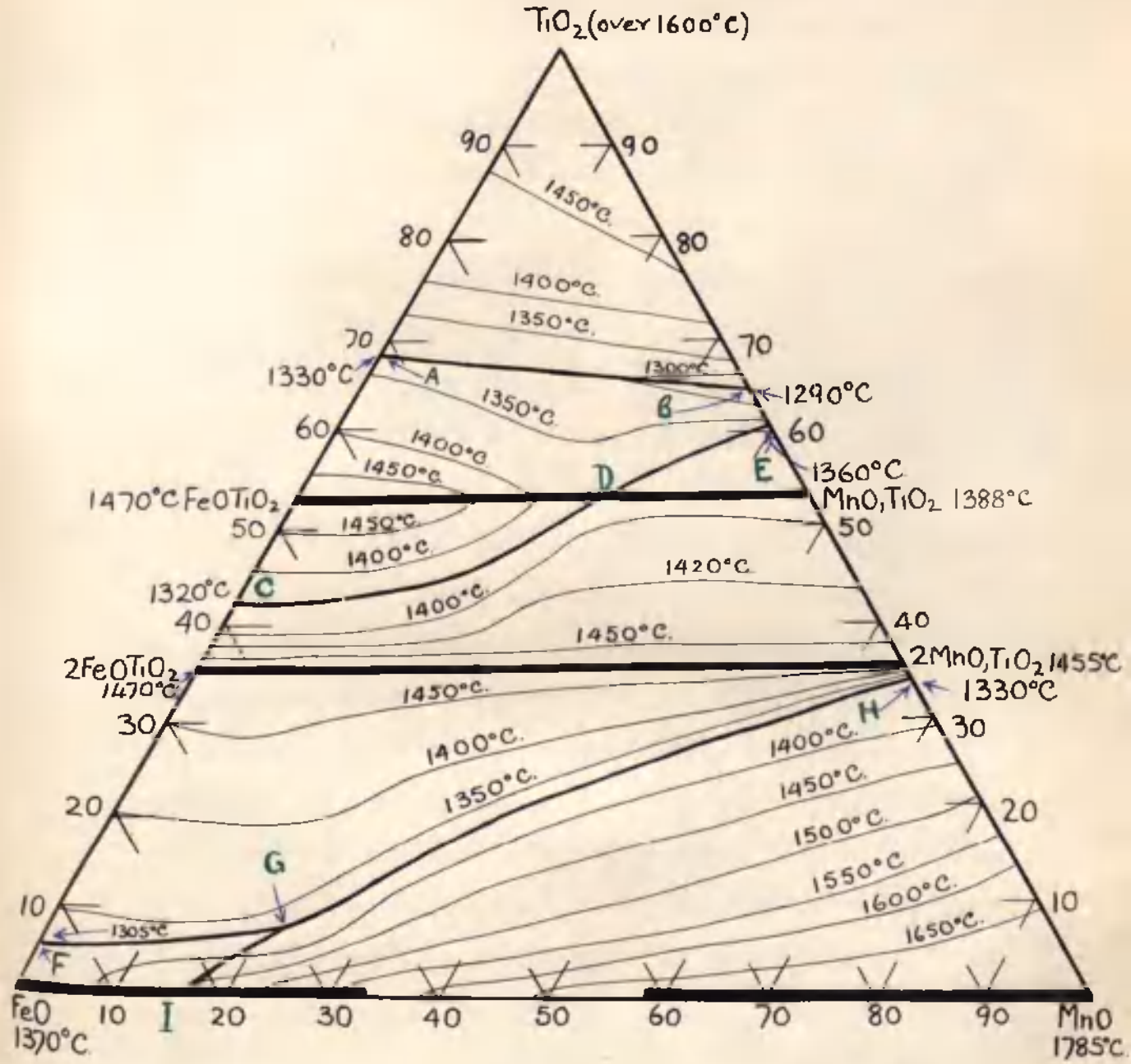
TiO2 (over 1600°C)
90
80
70
60
50
40
30
20
10
1450°C.
1400°C.
1350°C.
1330°C
A
1300°C
1290°C
B
1360°C
D
E
1470°C FeOTiO2
MnO,TiO2 1388°C
1420°C.
1320°C
C
2FeOTiO2
1470°C.
2MnO,TiO2 1455°C
1330°C
H
G
1305°C
F
FeO
1370°C.
I
MnO
1785°C.

Figure 113

eutectic trough, made up of two distinct parts, FG, which is a binary eutectic between the orthotitanate solid solutions rich in FeO and the FeO - rich solid solutions of the FeO - MnO series, and GH which is a binary eutectic between the orthotitanate solid solutions richer in MnO and the MnO - rich solid solutions of the MnO - FeO series. The intermediate point G is an invariant (quintuple) point, where three solid phases are in equilibrium with the liquid phase. Thus, G, the position of which is only approximate, is a reaction point, not a ternary eutectic. It represents the point at which the plane of the MnO - FeO peritectic reaction intersects the planes of the binary eutectics EG and GH. IG is the intersection between the former plane and the liquidus surface. It will be noted, that no minima occur in the latter.

The micrographs confirm the phase distribution indicated by the diagrams. As might be expected most of the melts studied contained only two phases at room temperatures. Only over a restricted range of compositions will three phases be present in the solidified melts, namely, over the range in which a member of the orthotitanate solid solution series will co-exist with both the FeO-rich and MnO - rich solid solutions of the MnO - FeO series. The existence of such a range of compositions in the ternary system is necessitated by the immiscibility gap in the MnO - FeO

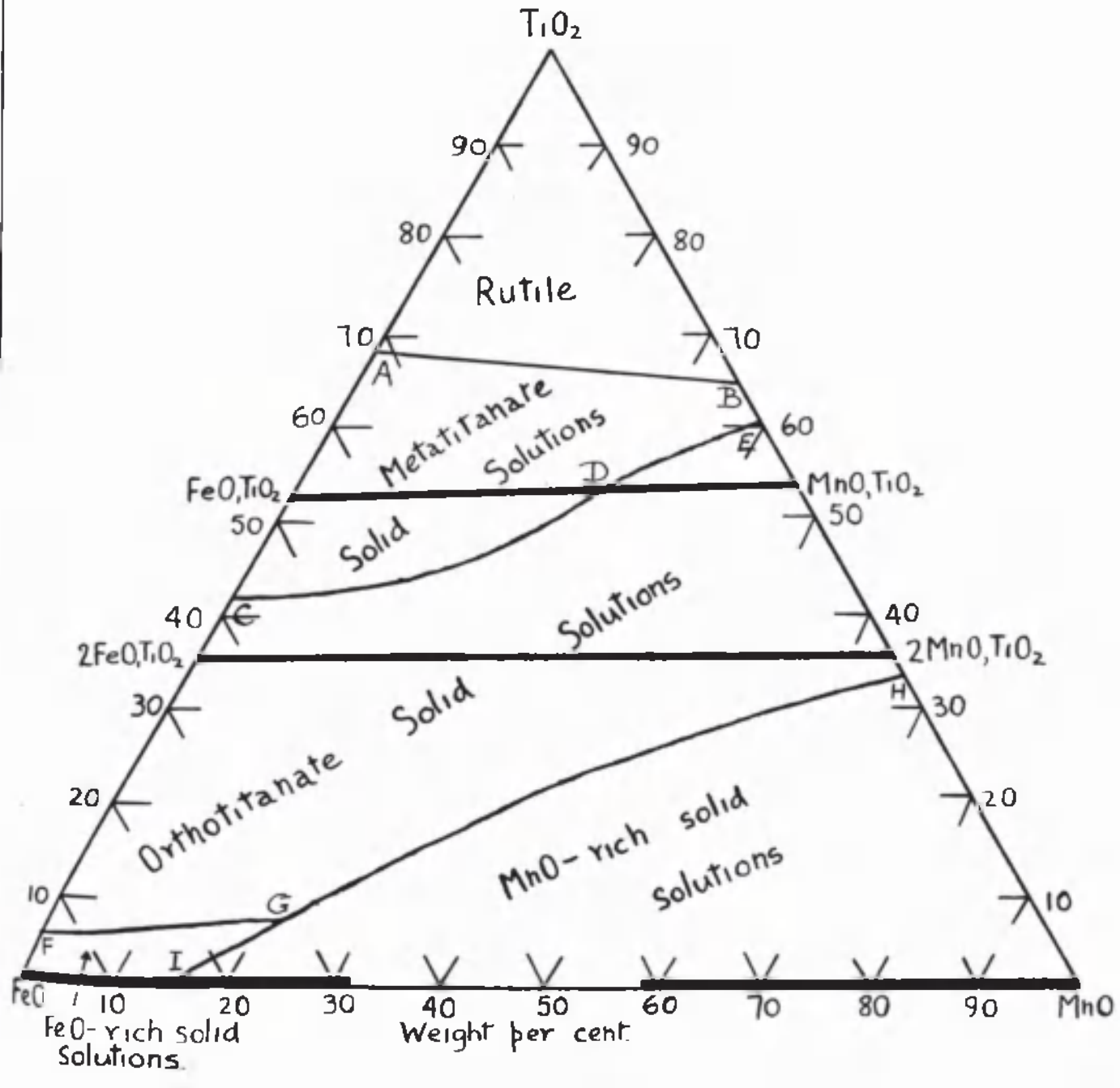
TiO2
90
90
80
80
Rutile
70
70
A
B
60
60
Metatitanate
Solutions
E
D
FeO,TiO2
MnO,TiO2
50
50
Solid
Solutions
40
40
C
2FeO,TiO2
2MnO,TiO2
30
30
H
Solid
Orthotitanate
20
20
MnO-rich solid
Solutions
10
10
G
F
I
FeO
10
20
30
40
50
60
70
80
90
MnO
FeO-rich solid
Solutions
Weight per cent

Figure 114

binary series, but, in actual practice it was found difficult to identify three phases in any of the melts with certainty, due to the difficulty of distinguishing between MnO and FeO when examined by reflected light. It was found possible, however, to fix the course of the curve FGH fairly accurately from the nature of the primary phase in appropriate melts, for which purpose it was not necessary to distinguish between MnO and FeO. The point G, however, has only been approximately fixed just like the point D.

MICROGRAPHS.

Fig. 115 - MnO 50% : FeO 20% : TiO_2 30% × 180
Etchant dil. HCl.
Primary orthotitanate phase plus small amount of eutectic.

Fig. 116 - MnO 10% : FeO 50% : TiO_2 40%. × 90
Etchant HF.
Primary dendrites of orthotitanate phase (dark etching) in eutectic of orthotitanate phase and metatitanate phase (light etching). The dark areas are holes due to the tearing out of eutectic constituents.

Fig. 117 - MnO 30% : FeO 30% : TiO_2 40%. × 104
Etchant HF.

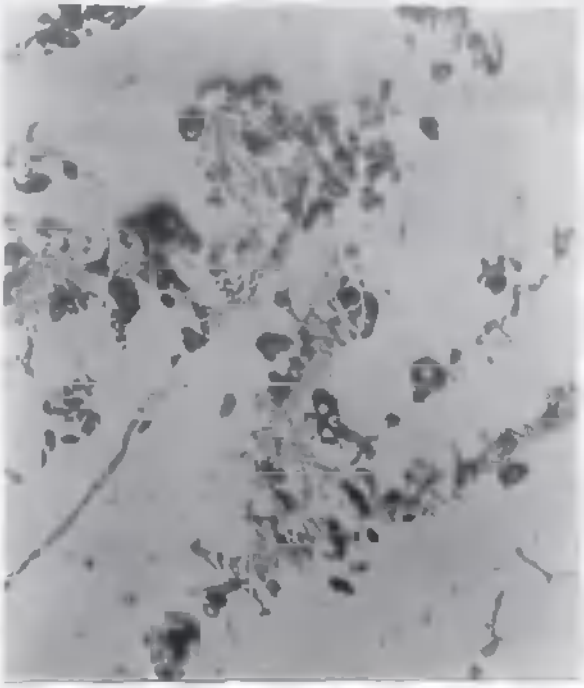

Figure 115

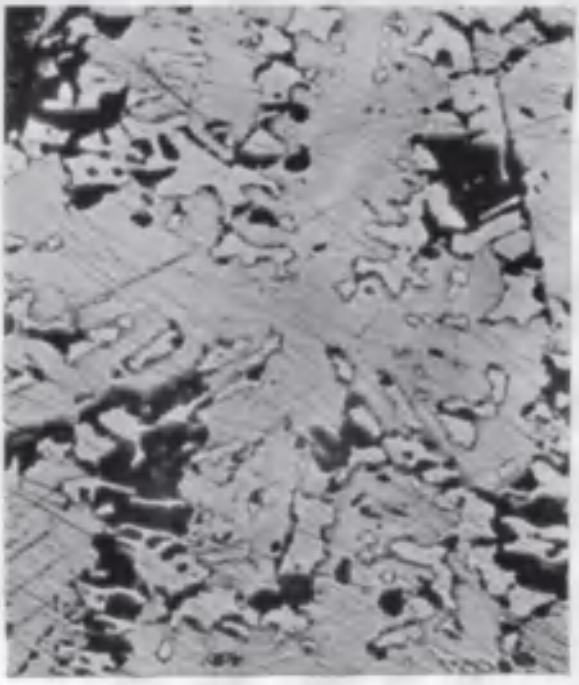

Figure 116

Figure 117

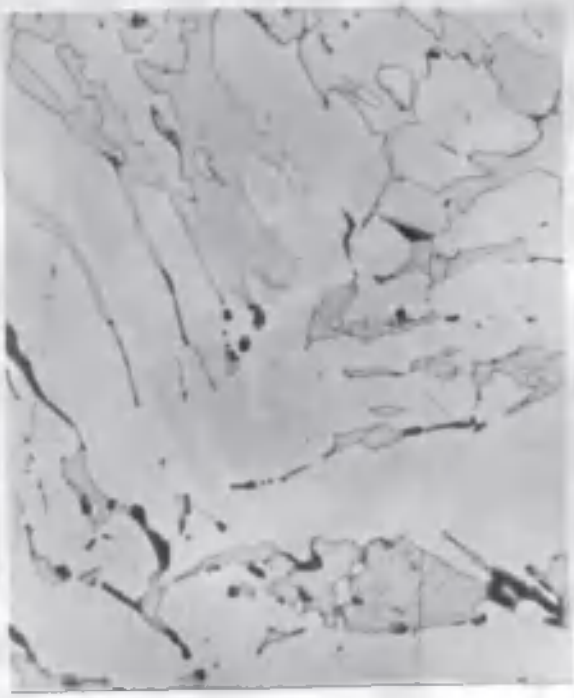

Figure 118

Mainly primary orthotitanate phase (part of a very large dendrite occupies most of the field) in lighter etching metatitanate phase.

Fig. 118 - MnO 20% : FeO 30% : TiO_2 50%. × 104
Etchant HF.
Primary metatitanate phase (part of a large dendrite shown) in darker etching orthotitanate.

Fig. 119 - MnO 30% : FeO 20% : TiO_2 50%. × 104
Etchant HF.
Mainly metatitanate phase (containing gas cavities) with darker etching orthotitanate phase. Dark material at boundaries appears to be residue from incomplete peritectic reaction. A similar effect was noticed in some of the binary MnO - TiO_2 melts in the vicinity of the compound MnO,TiO_2.

Fig. 120 - MnO 10% : FeO 80% : TiO_2 10%. × 90
Etchant dil. HCl.
Shows primary dendrites of orthotitanate phase in eutectic of orthotitanate and FeO - rich phase.

Fig. 121 - MnO 10% : FeO 70% : TiO_2 20%. × 90
Etchant dil. HCl.

Figure 119

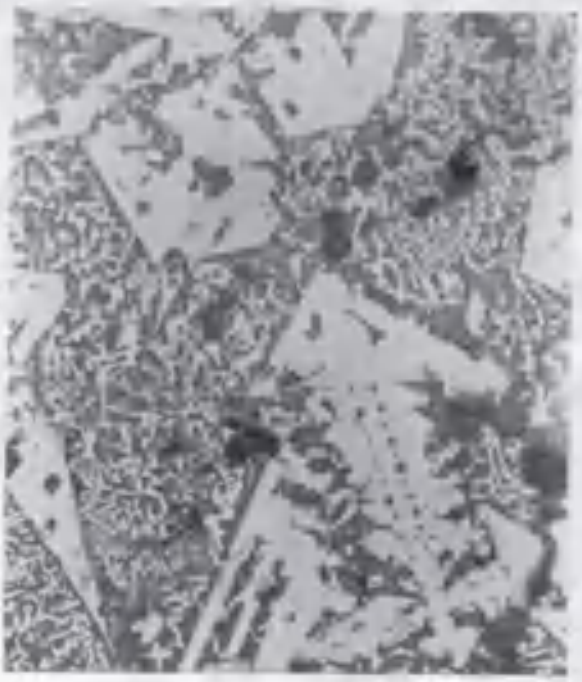

Figure 120.

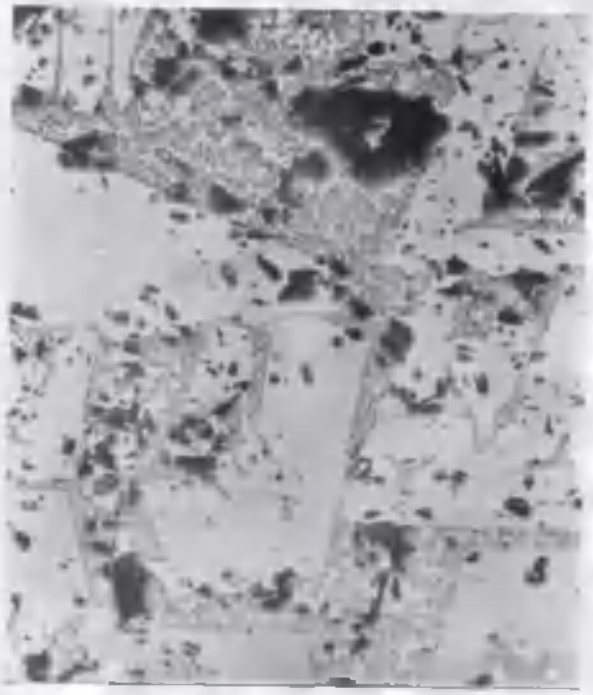

Figure 121

Figure 122

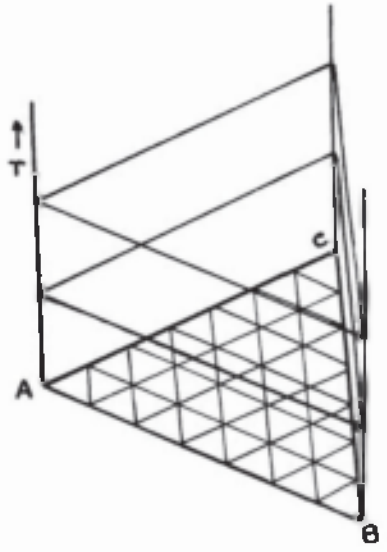

Figure 82 – The Isobaric Prism.

$MnO - Ti_2O_3$ and $FeO - Ti_2O_3$. As previously, the 2 gramme melts, in the fine powdered condition, were held in molybdenum crucibles, and heating was carried out in a "Pythagoras" tube in an atmosphere of nitrogen or in vacuo. Thermal analysis was by means of a tungsten-molybdenum differential thermocouple.

As was stated above, the Roozeboom triangle was chosen for graphical representation.

After thermal investigations each melt was sectioned, and microscopically examined in reflected light. As in the case of the two binary systems hand polishing was employed throughout and on the whole, the polished surfaces of the ternary melts were superior to those obtained in the $MnO - Ti_2O_3$ and $FeO - Ti_2O_3$ systems.

The system MnO - FeO which forms the third of the component systems of the ternary system $MnO - FeO - Ti_2O_3$ had been previously determined by Hay, Howat and White[88], who found partial solid solubility between MnO and FeO with a peritectic reaction between the two phases at 1430°C.

The $MnO - FeO - Ti_2O_3$ system can be considered as a ternary system only if the effects of the peritectic dissociation of FeO on melting are neglected. As is now well established this oxide melts incongruently at 1370°C. with the liberation of metallic iron and the formation of a liquid oxide phase containing approximately 11·5 per cent.

of ferric oxide. The liberated metal is only taken into solution at temperatures of over 1450°C. In dealing with slag systems containing FeO, however, it has become an accepted device to neglect this high temperature separation of metallic iron, and to take the melting point of FeO as 1370°C. This simplification has been adopted in the present case, since it is conducive to a simple presentation of the relationships established. In any case, the effects of this dissociation are appreciable only over a small range of compositions high in FeO.

The thermal arrests for the various compositions investigated are given in the table below, while the heating and cooling curves are reproduced in Figures 83 to 112.

Details of the thermal and phase relationships in the ternary system MnO - FeO - TiO_2 are shown in Figures 113 and 114. Figure 113 shows the form of the liquidus surface, melting temperatures being indicated by isothermals. Figure 114 shows the phase distribution, the primary phases in equilibrium with liquid at the liquidus temperatures being indicated.

The micrographs of Figs. 115 to 128 show the mineralogical structure of representative melts.

A noteworthy feature of the ternary system and one that has a determinative influence on the relationships within the system, is the extent to which solid solution formation

TABLE 6.

Composition - Weight %			Temperature of Separants °C.
MnO	FeO	TiO_2	
5	90	5	1310 and 1400
10	80	10	1315 and 1390
10	70	20	1315 and 1395
10	60	30	1315 and 1455
10	50	40	1320 and 1430
10	40	50	1320 and 1420
10	30	60	1310 and 1362
10	20	70	1310 and 1445
20	70	10	1300 and 1390
20	60	20	1315 and 1400
20	50	30	1320 and 1440
20	40	40	1320 and 1410
20	30	50	1325 and 1430
20	20	60	1310 and 1400
30	60	10	1330, 1370 and 1417
30	50	20	1320 and 1385
30	40	30	1310 and 1440
30	30	40	1325 and 1425
30	20	50	1335 and 1410
40	50	10	1325, 1385 and 1485
40	40	20	1340, 1360 and 1400
40	30	30	1315 and 1420
40	20	40	1330 and 1435
50	40	10	1320, 1395 and 1495
50	30	20	1315, 1350 and 1412
50	20	30	1320 and 1410
60	30	10	1310, 1385 and 1510
60	20	20	1320, 1370 and 1430
70	20	10	1370 and 1545
80	10	10	1320 and 1560

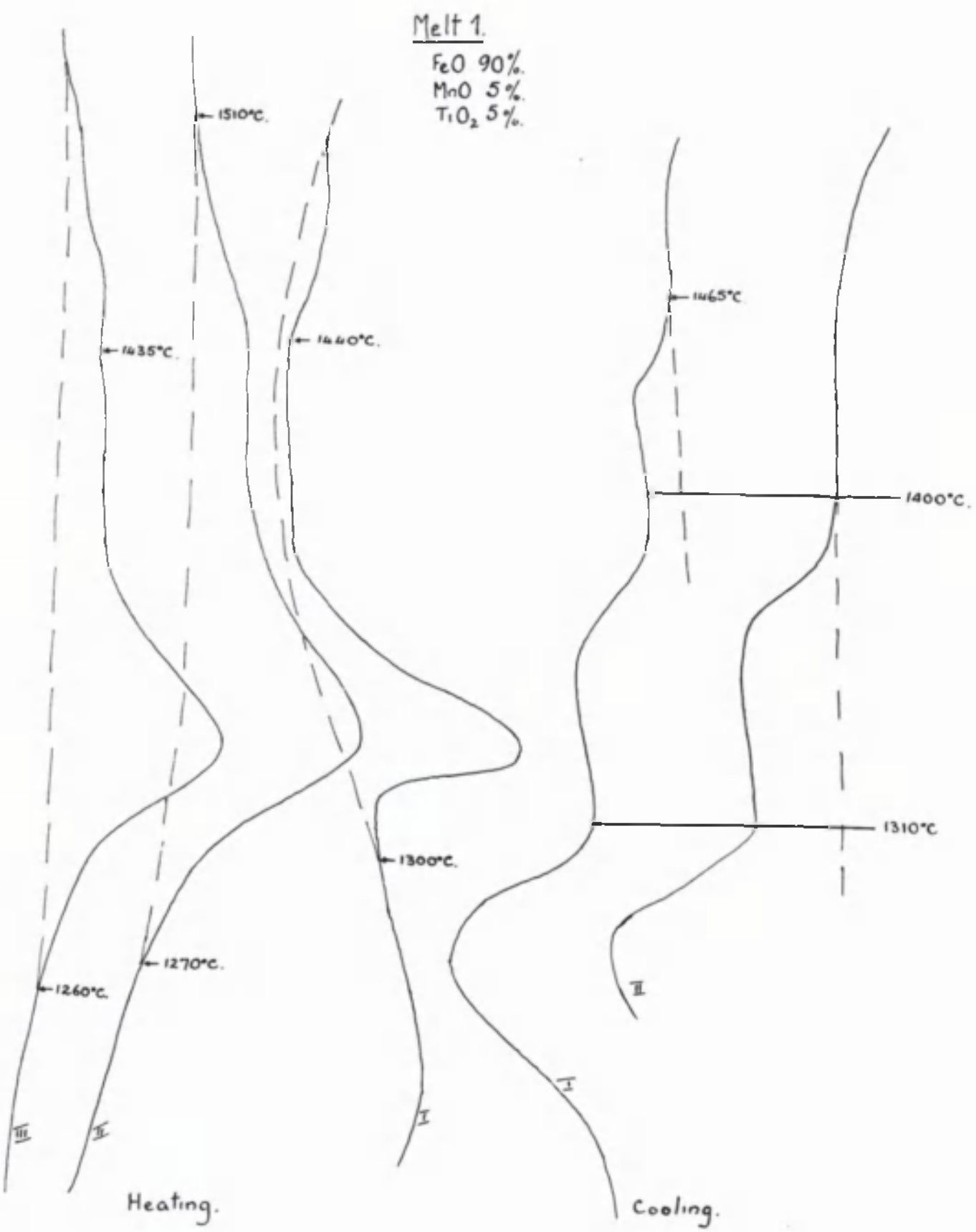
Melt 1.
FeO 90%.
MnO 5%.
TiO_2 5%.
1510°C.
1435°C.
1440°C.
1300°C.
1270°C.
1260°C.
III
II
I
Heating.
1465°C.
1400°C.
1310°C.
II
I
Cooling.

Figure 83.

Melt 2.
FeO 80%.
MnO 10%.
TiO_2 10%.

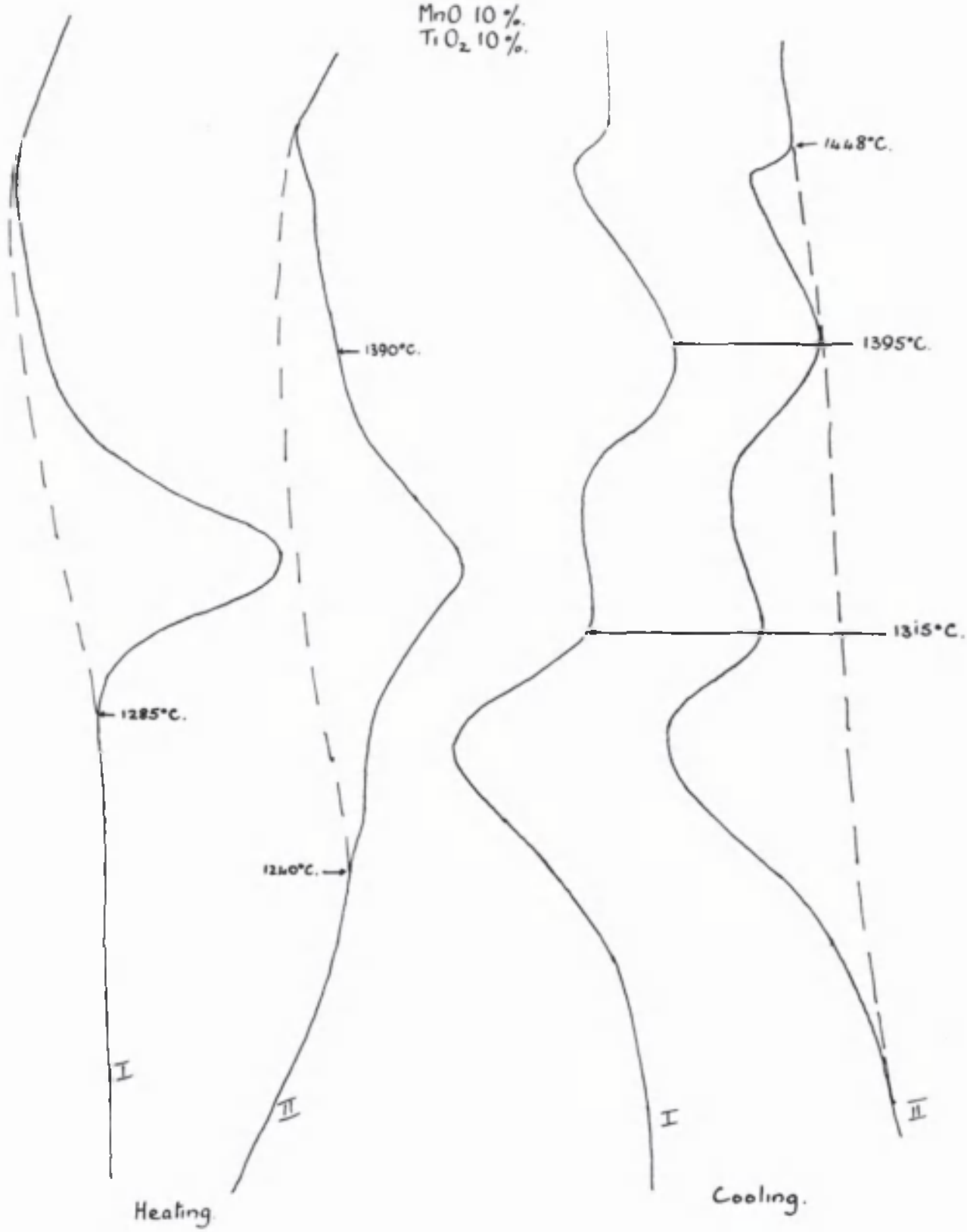

Figure 84.

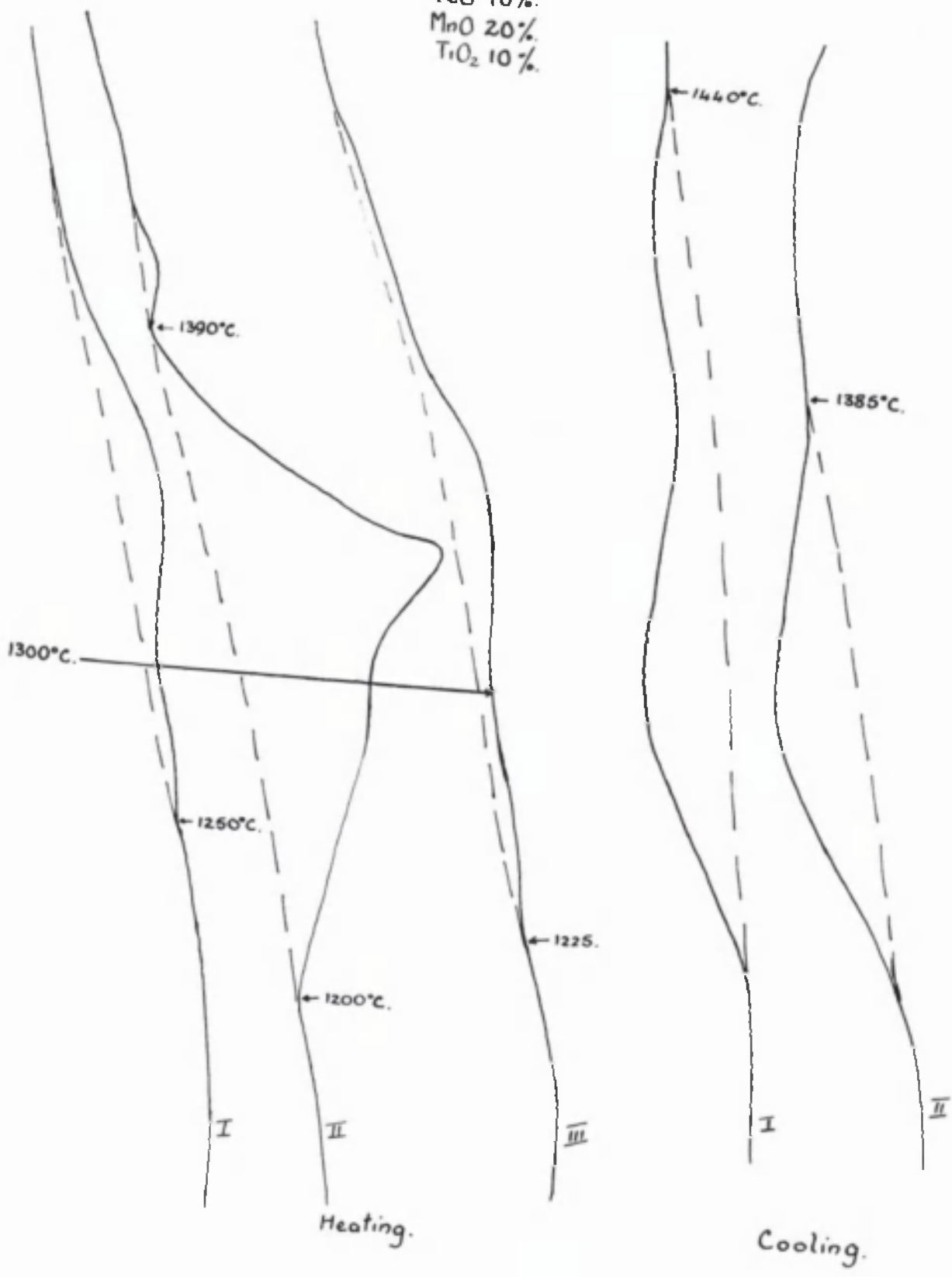
Melt 3
FeO 70%.
MnO 20%.
TiO2 10%.
1390°C.
1300°C.
1260°C.
1225.
1200°C.
I
II
III
Heating.
1440°C.
1385°C.
I
II
Cooling.

Figure 85.

Melt 4.

FeO 70%
MnO 10%
TiO_2 20%

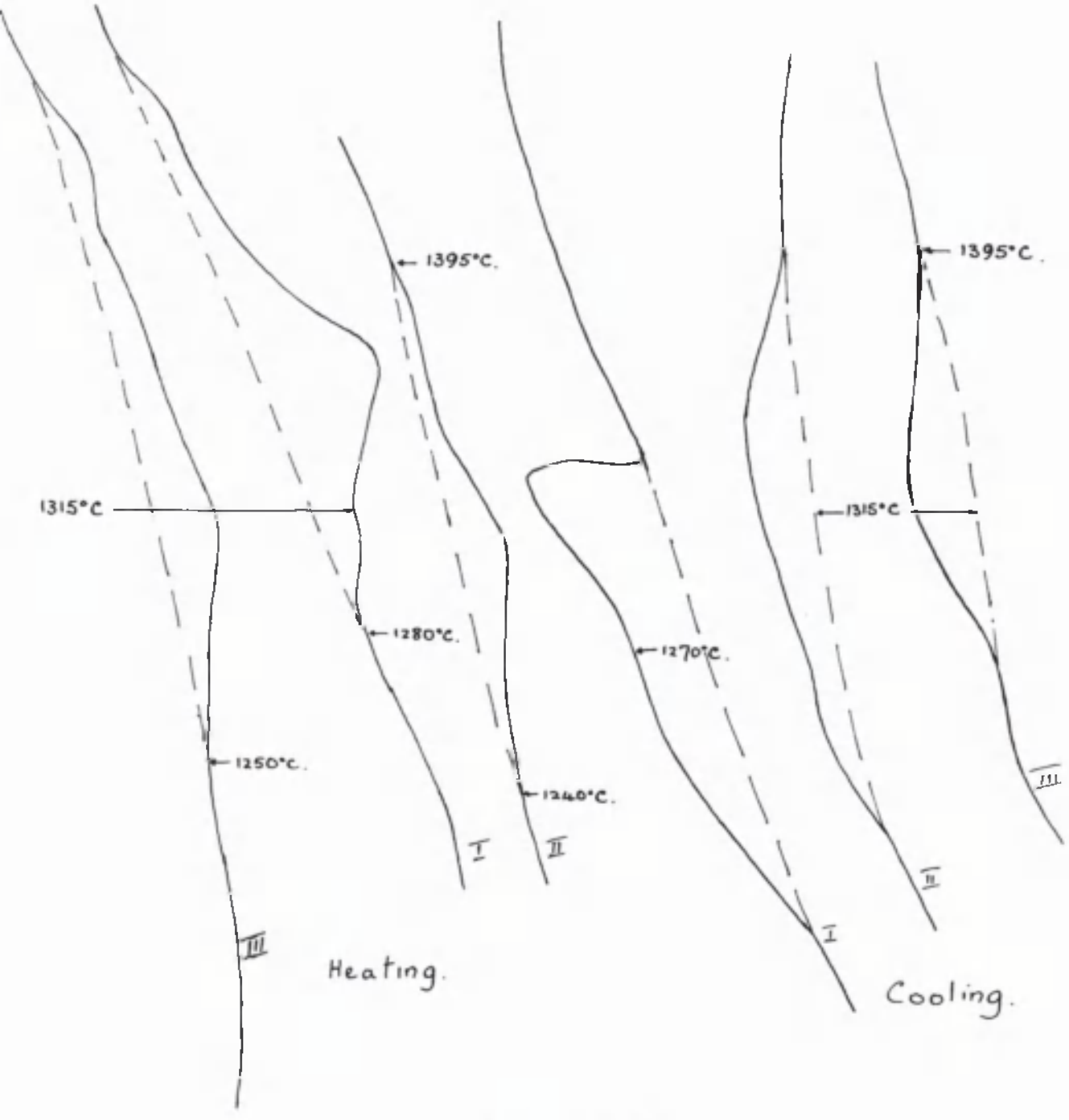

Figure 86

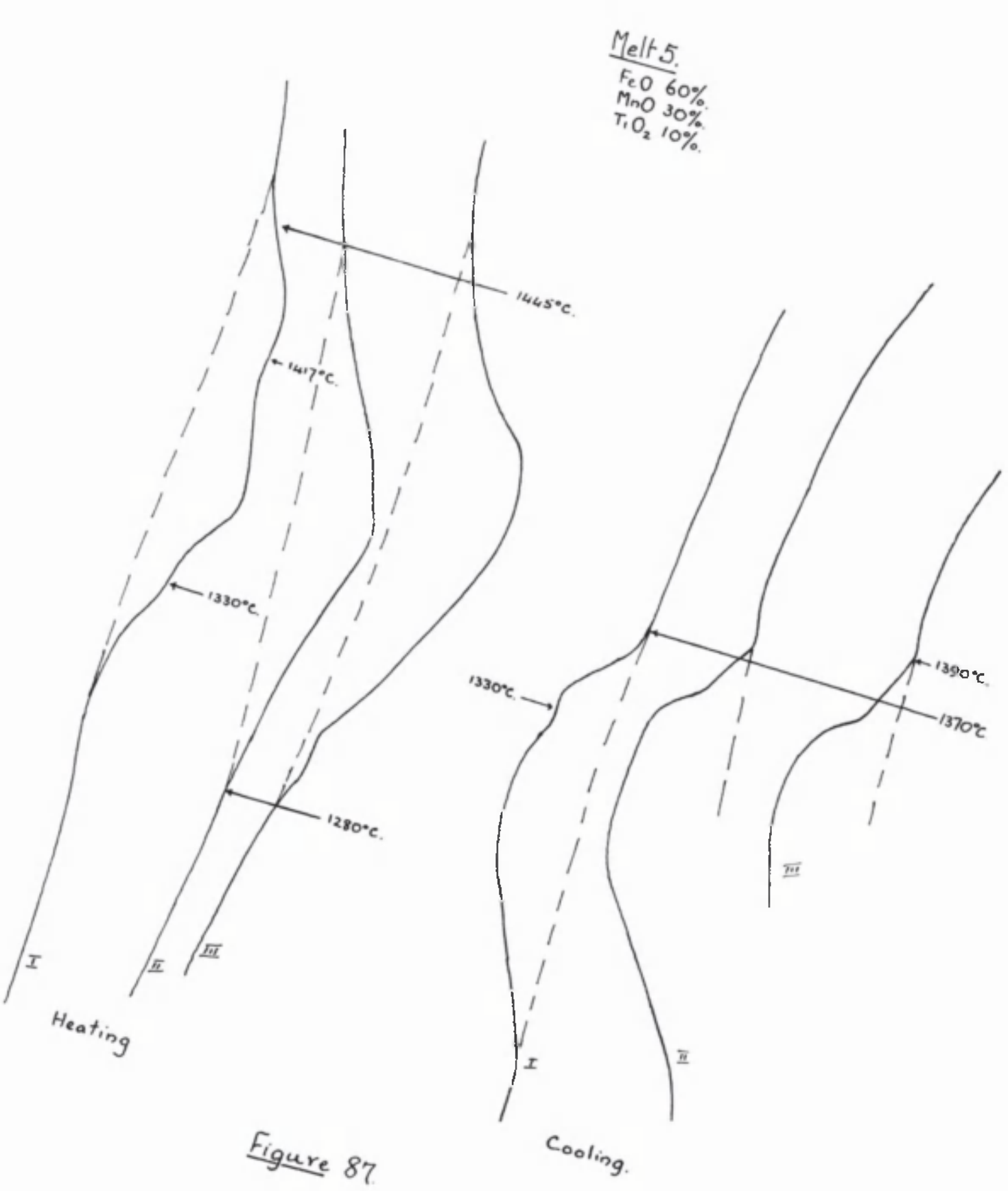
Melt 5.
FeO 60%
MnO 30%
Ti_2O_2 10%
1445°C.
1417°C.
1330°C.
1280°C.
I
II
III
Heating
1330°C.
1390°C.
1370°C
III
I
II
Cooling.

Figure 87.

Melt 6.
FeO 60%
MnO 20%
TiO_2 20%

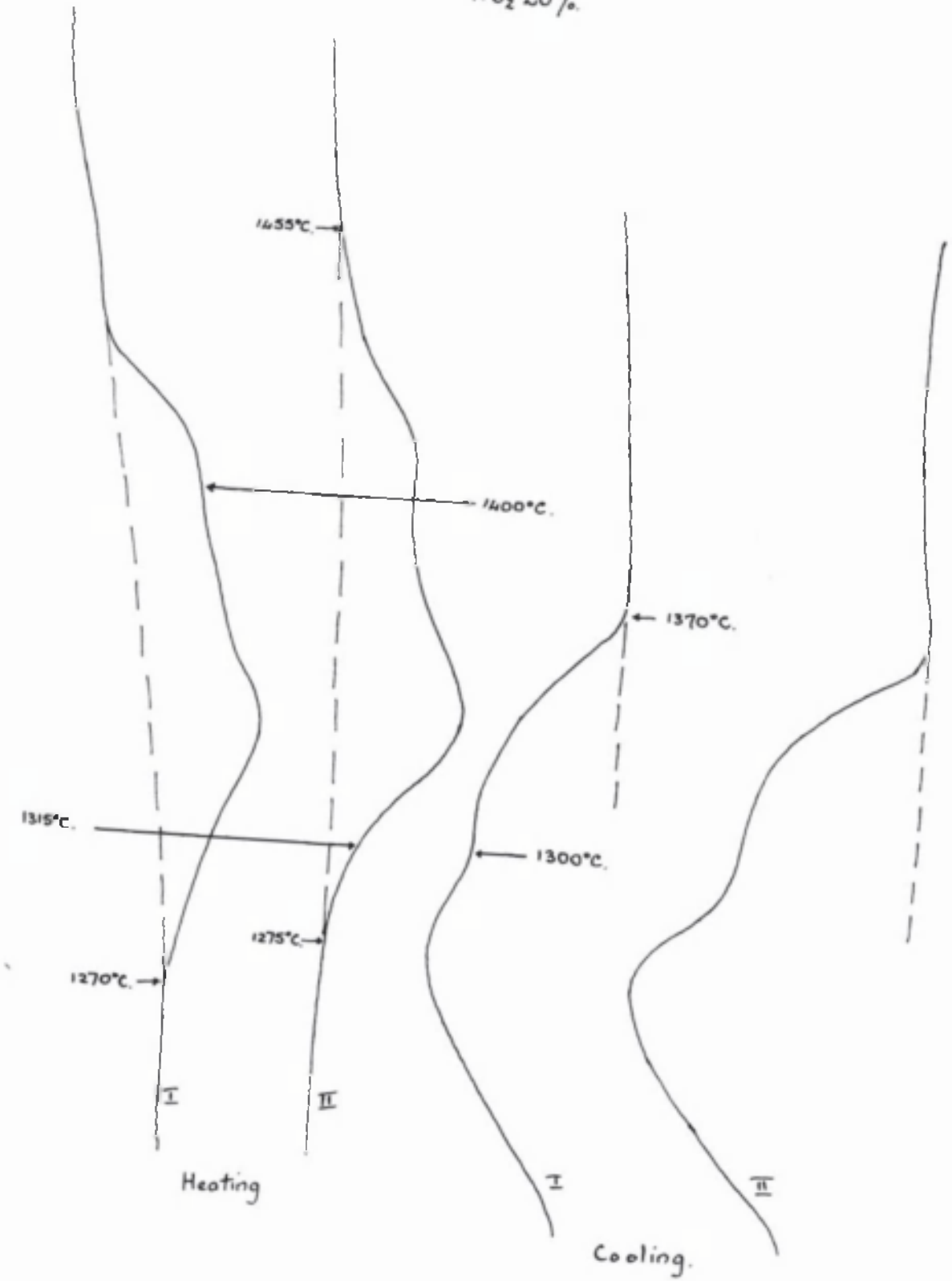

Figure 88.

Melt 7.

FeO 60%.
MnO 10%.
TiO_2 30%.

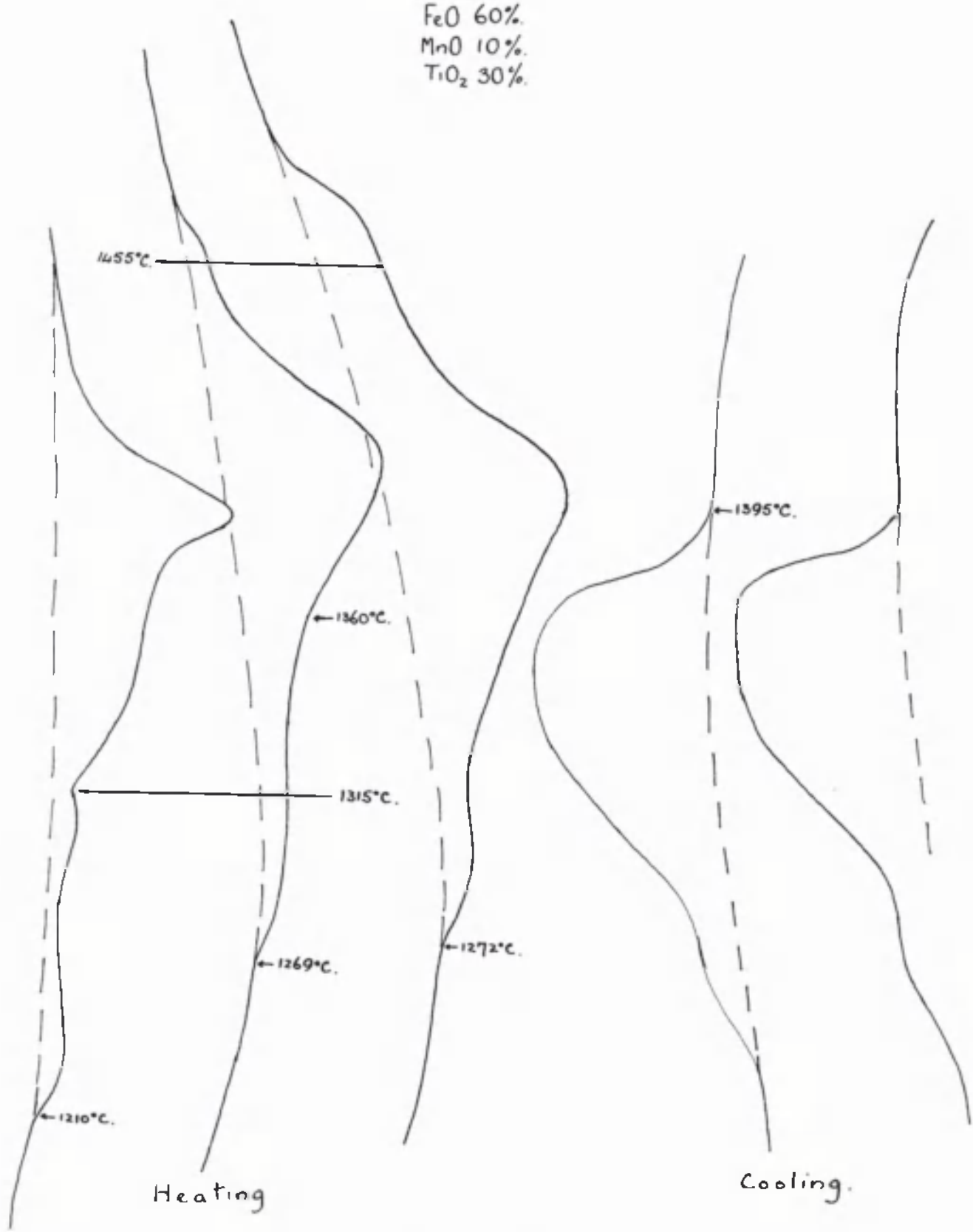

Figure 89

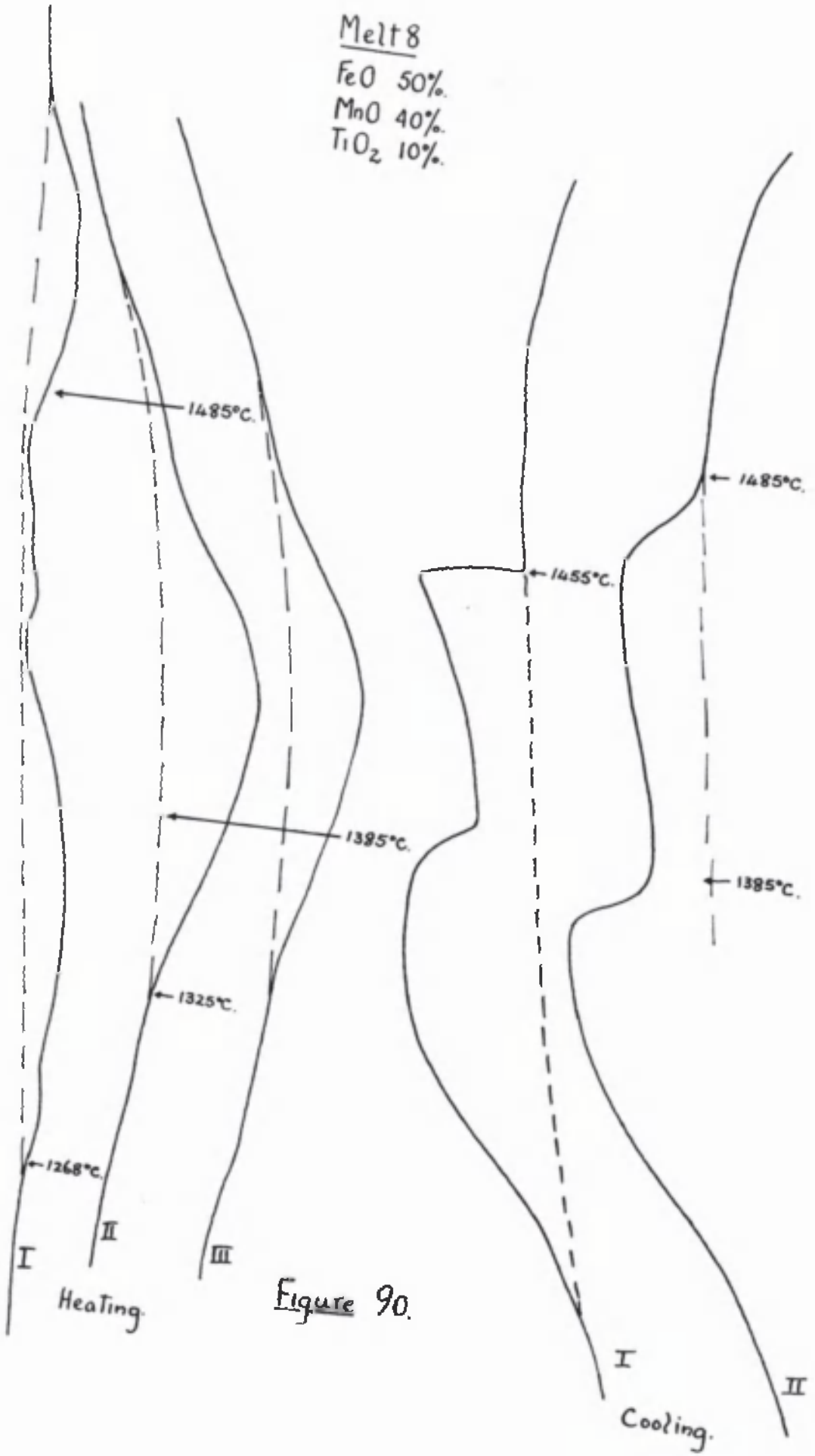
Melt 8
FeO 50%
MnO 40%
TiO2 10%
1485°C.
1385°C.
1325°C.
1268°C.
I
II
III
Heating.
1485°C.
1455°C.
1385°C.
I
II
Cooling.

Figure 90.

Melt 9

FeO 50%.

MnO 30%.

$Ti O_2$ 20%.

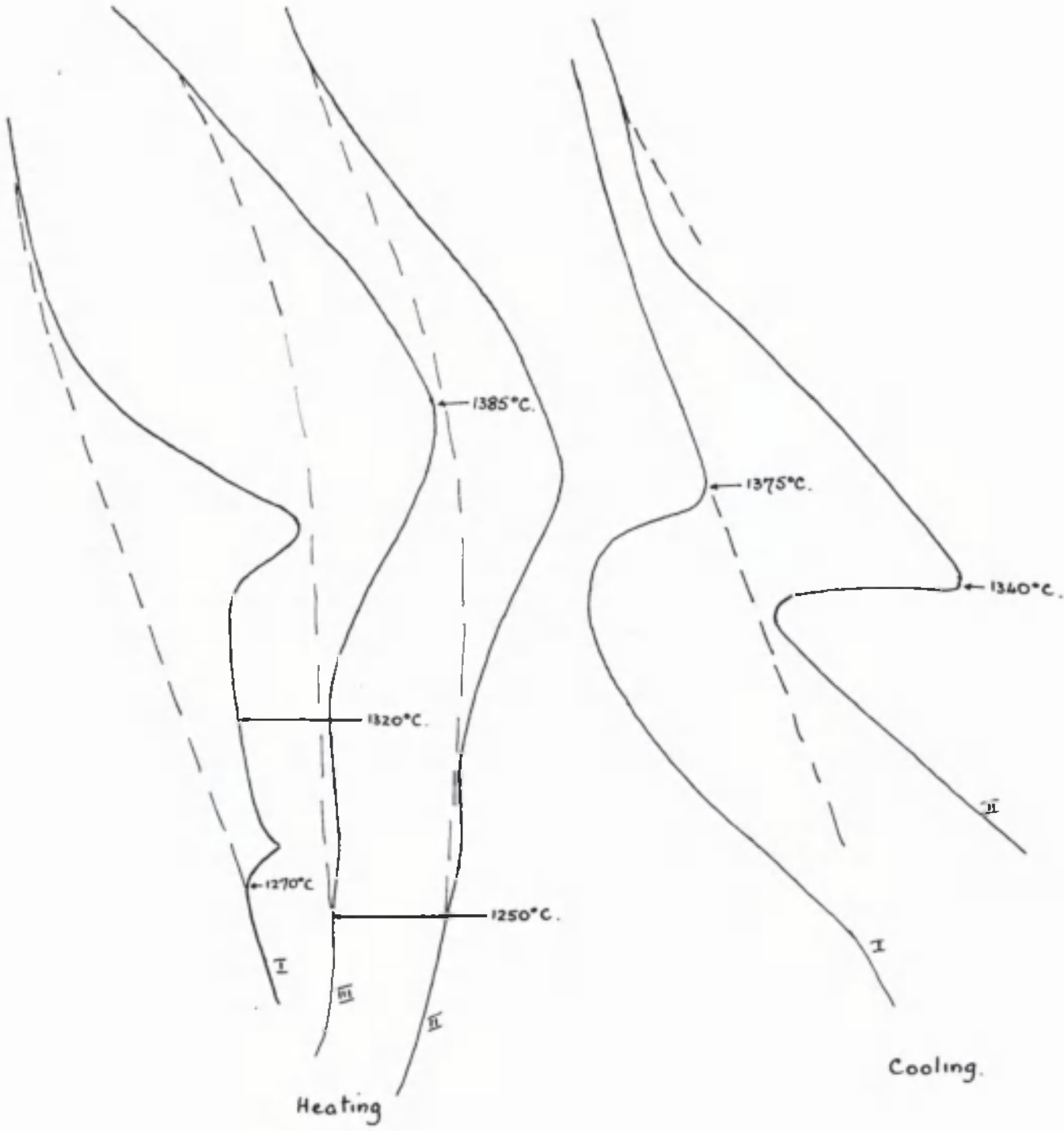

Figure 91.

Melt 10.

FeO 50%.

MnO 20%.

TiO_2 30%.

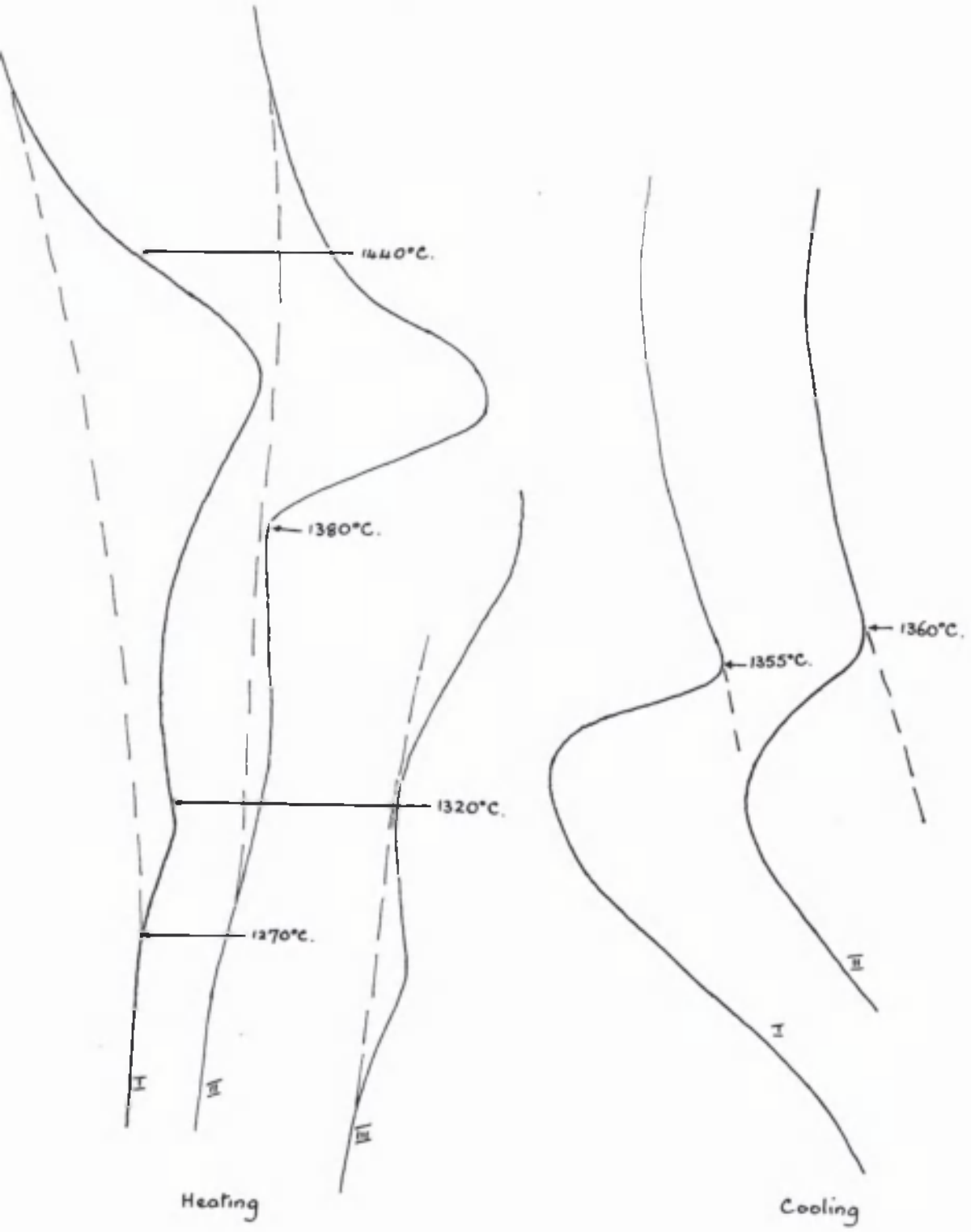

Figure 92.

Melt II

FeO 50%.
MnO 10%.
Ti_2O_2 40%.

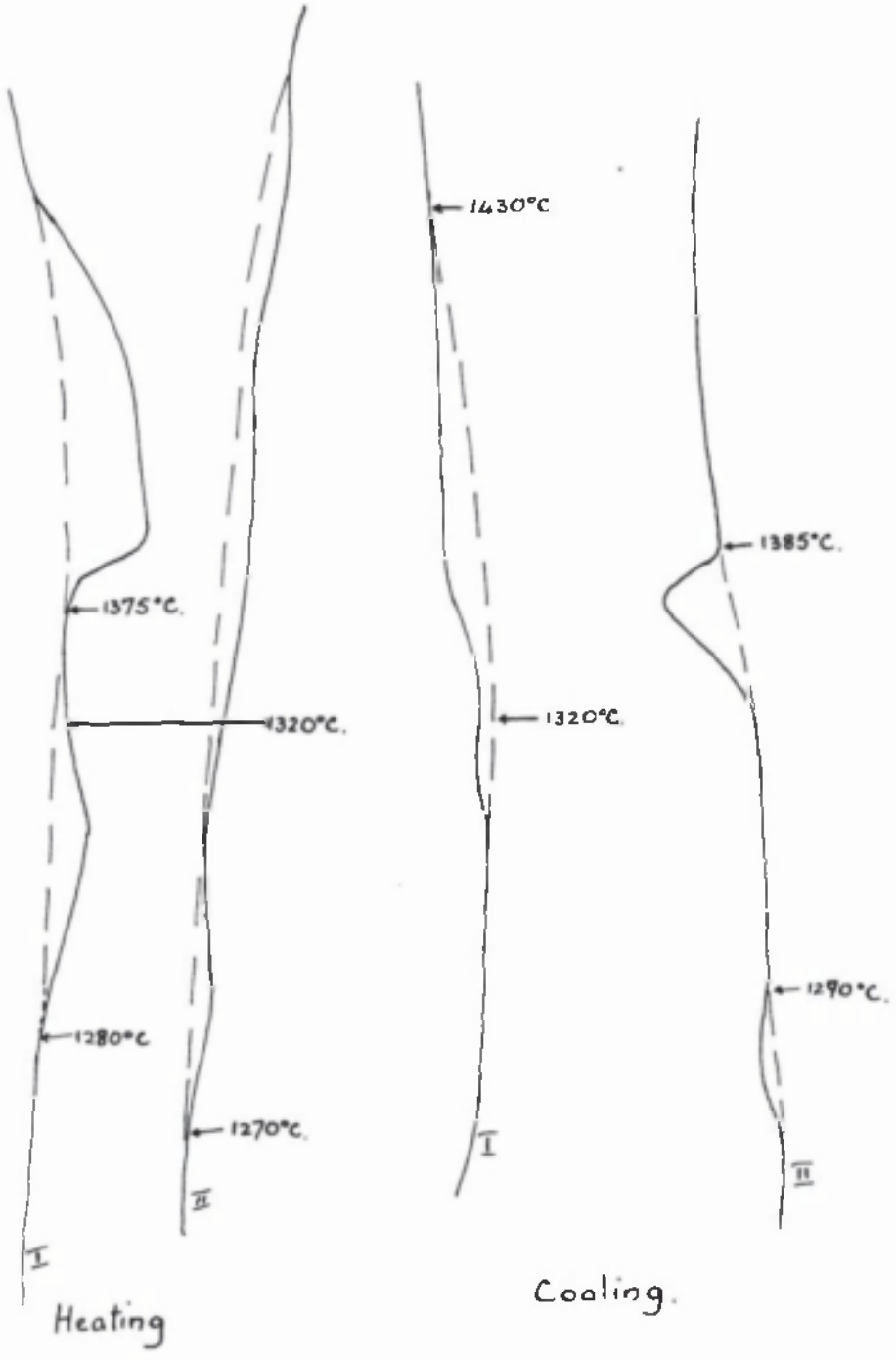

Figure 93

Melt 12.

FeO 40%

MnO 50%

TiO_2 10%

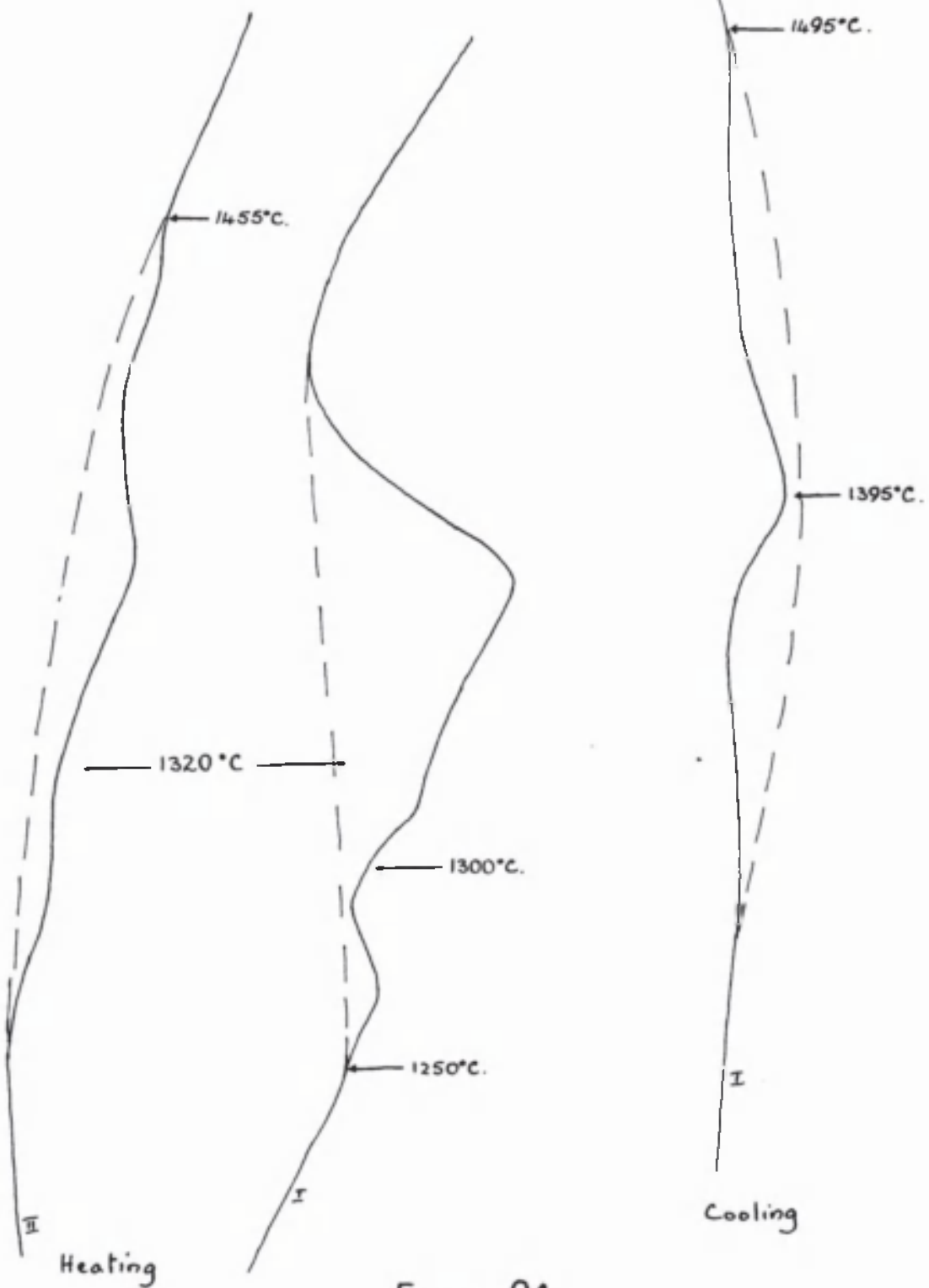

Figure 94.

Melt 13

FeO 40%

MnO 40%

TiO_2 20%

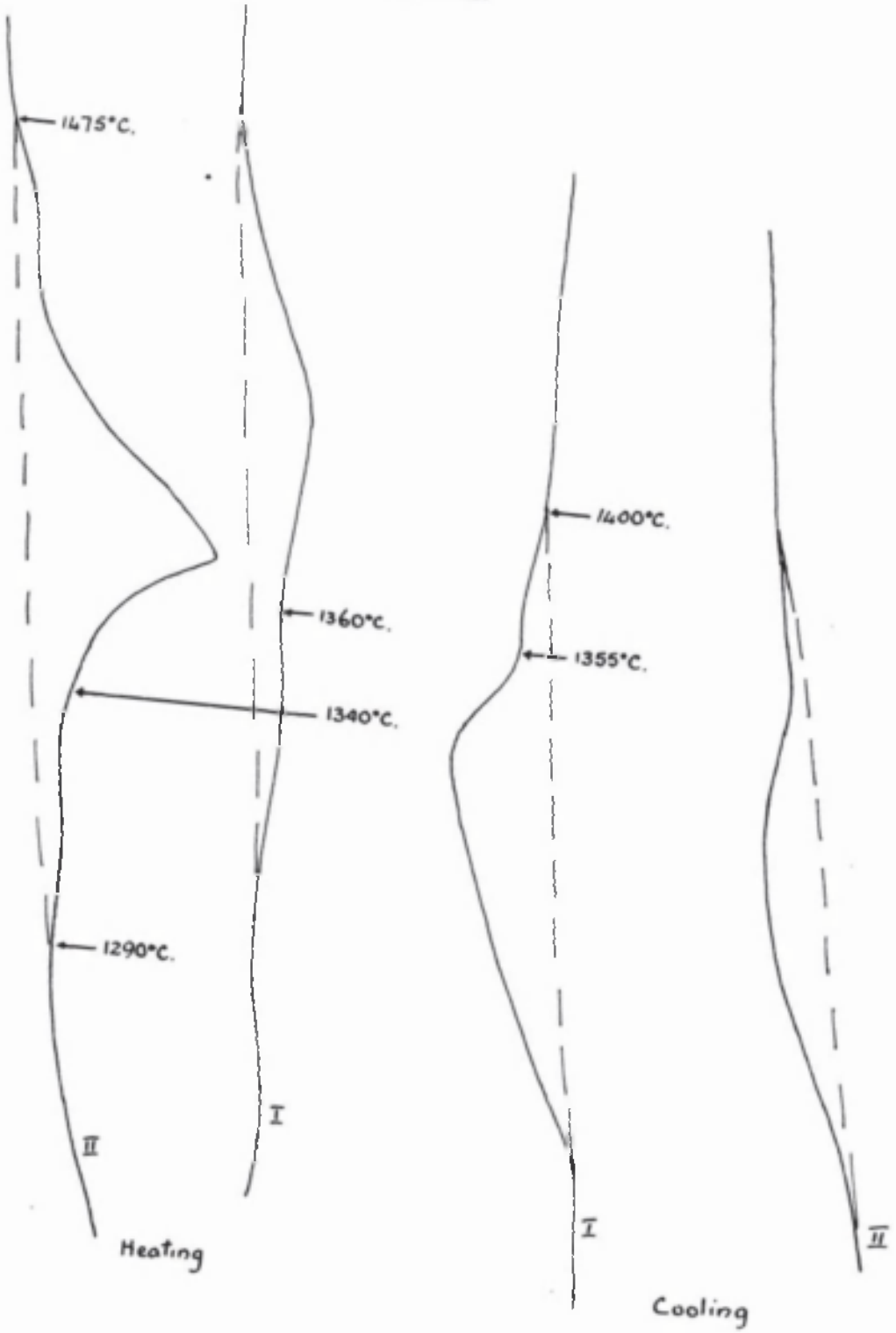

Figure 95.

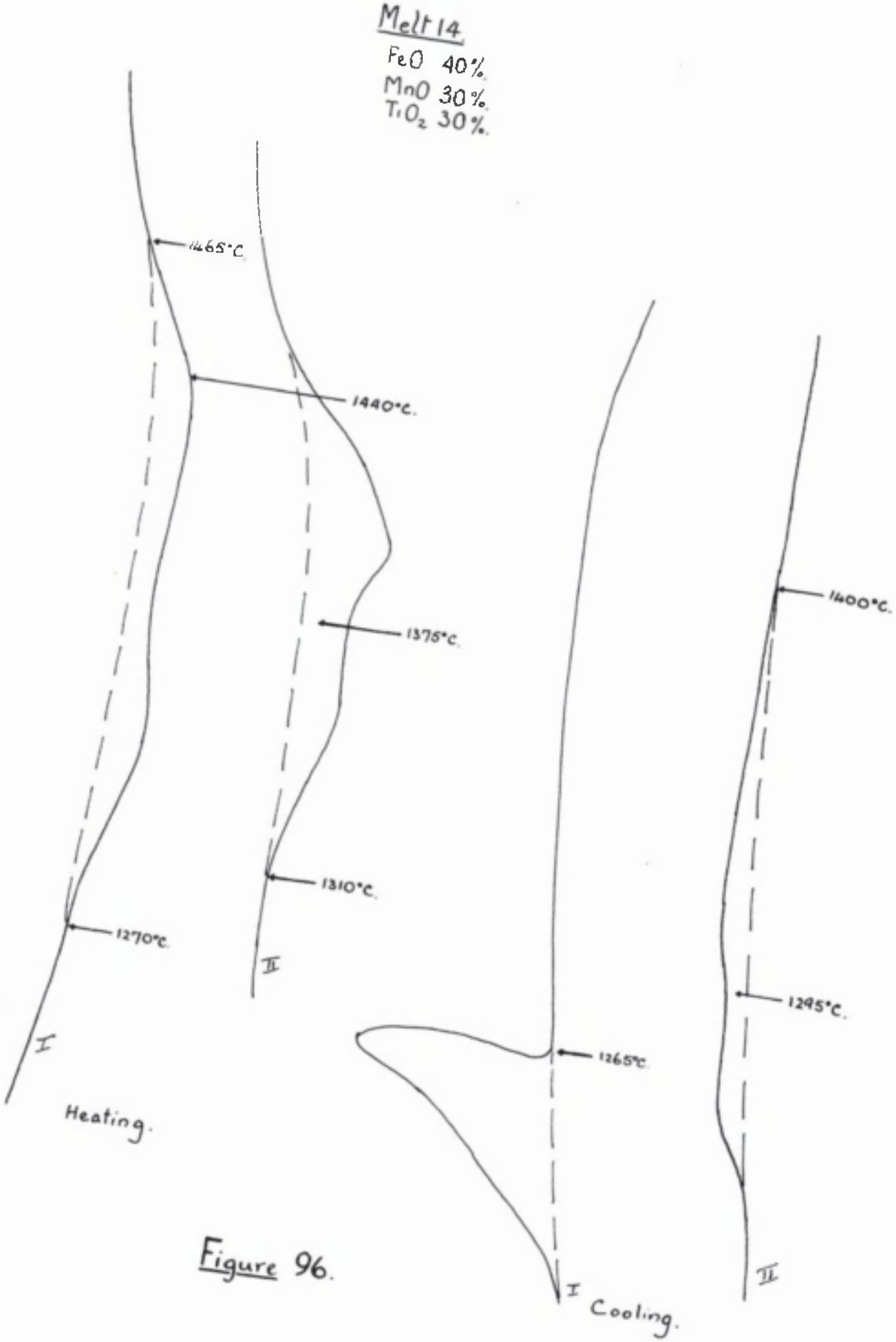
Melt 14
FeO 40%
MnO 30%
TiO_2 30%
1465°C.
1440°C.
1375°C.
1310°C.
1270°C.
I
II
Heating.
1400°C.
1295°C.
1265°C.
I
II
Cooling.

Figure 96.


Melt 15
FeO 40%
MnO 20%
TiO2 40%
1470°C.
1430°C.
1410°C.
1375°C.
1320°C.
1285°C.
1400°C.
1310°C.
I
II
Heating
I
II
Cooling

Figure 97

Melt 16.

FeO 40%.

MnO 10%

TiO_2 50%

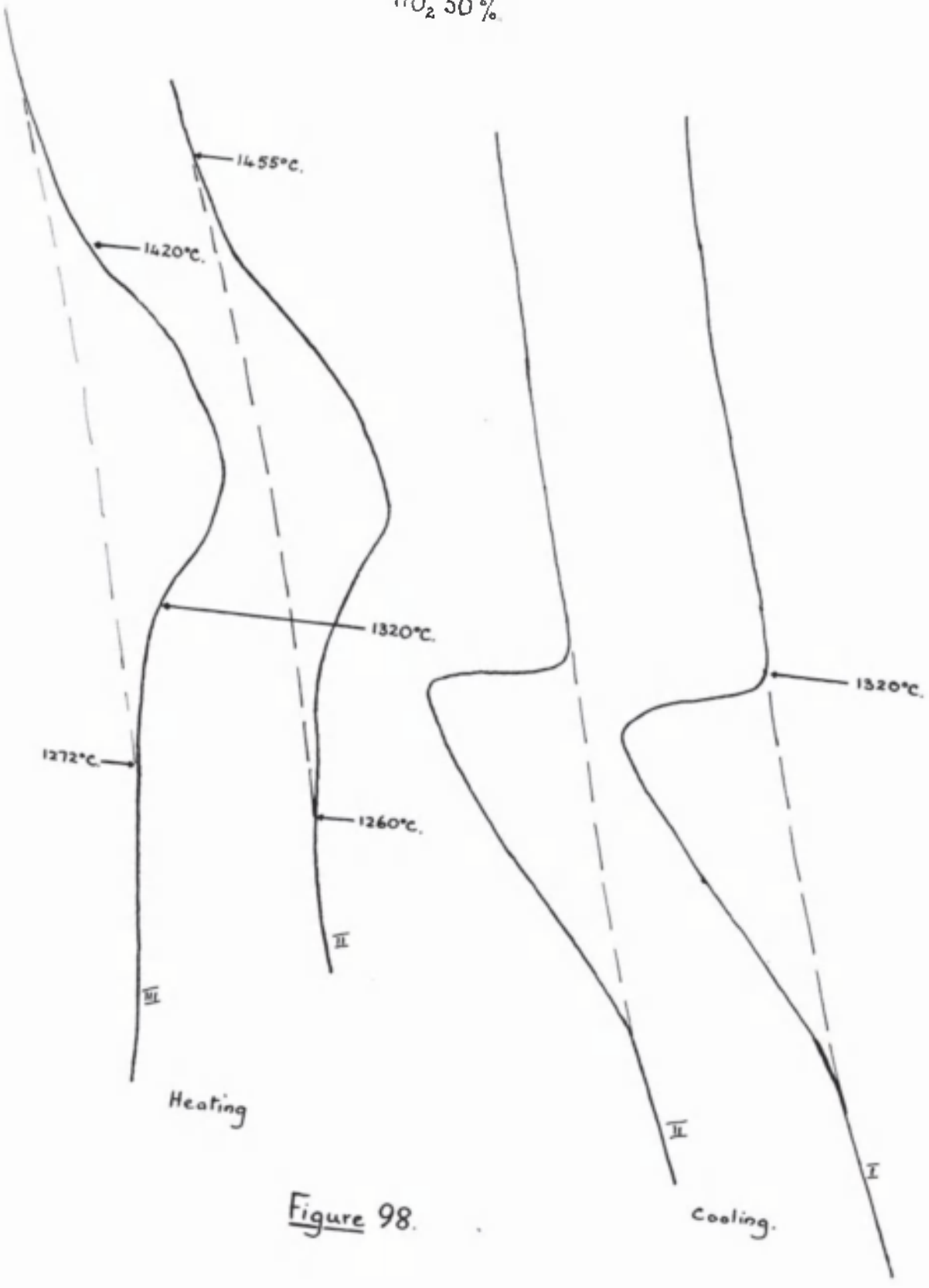

Figure 98.

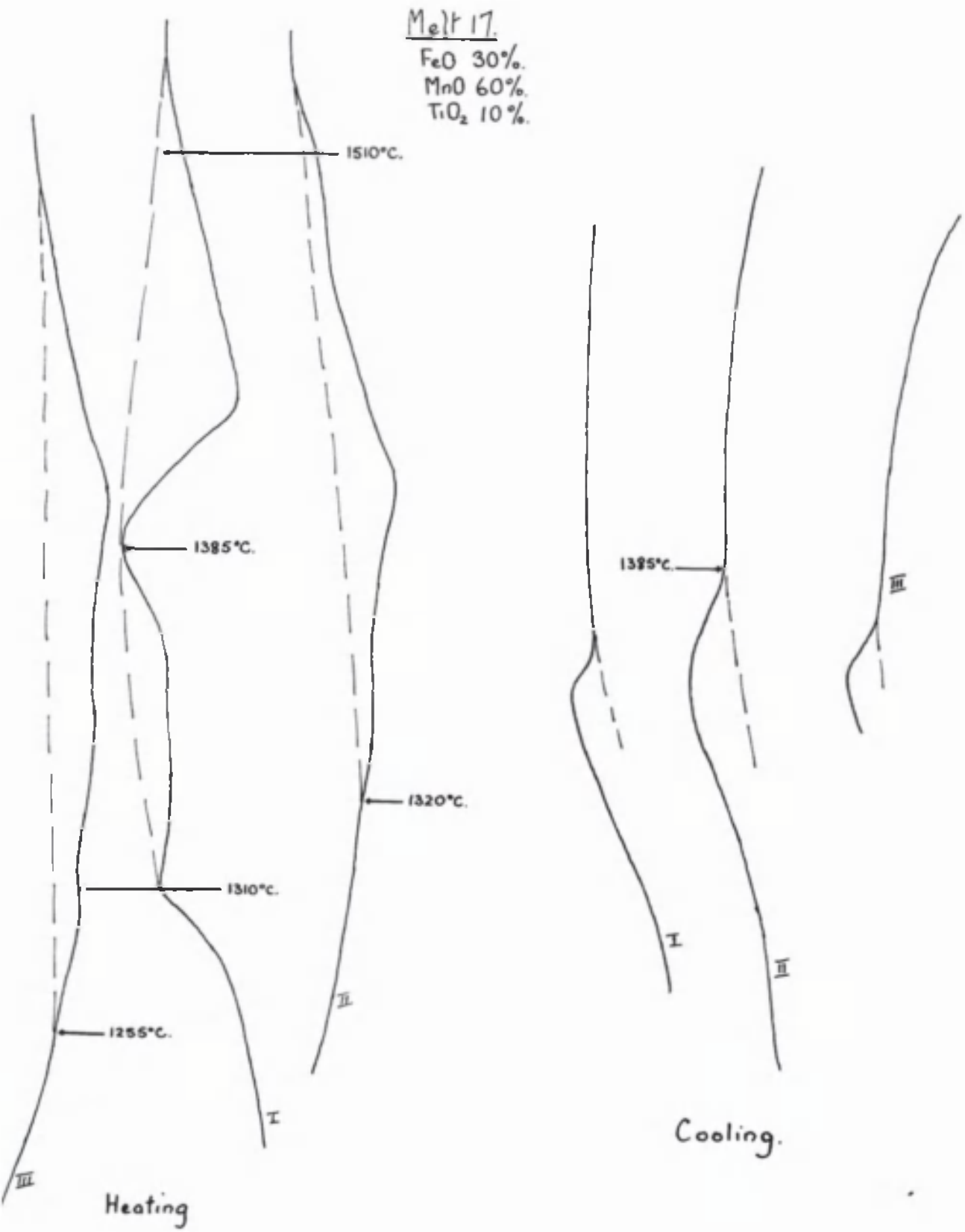
Melt 17.
FeO 30%.
MnO 60%.
TiO2 10%.
1510°C.
1385°C.
1320°C.
1310°C.
1255°C.
I
II
III
Heating
1385°C.
I
II
III
Cooling.

Figure 100

Melt 18.

FeO 30%.
MnO 50%.
TiO_2 20%.

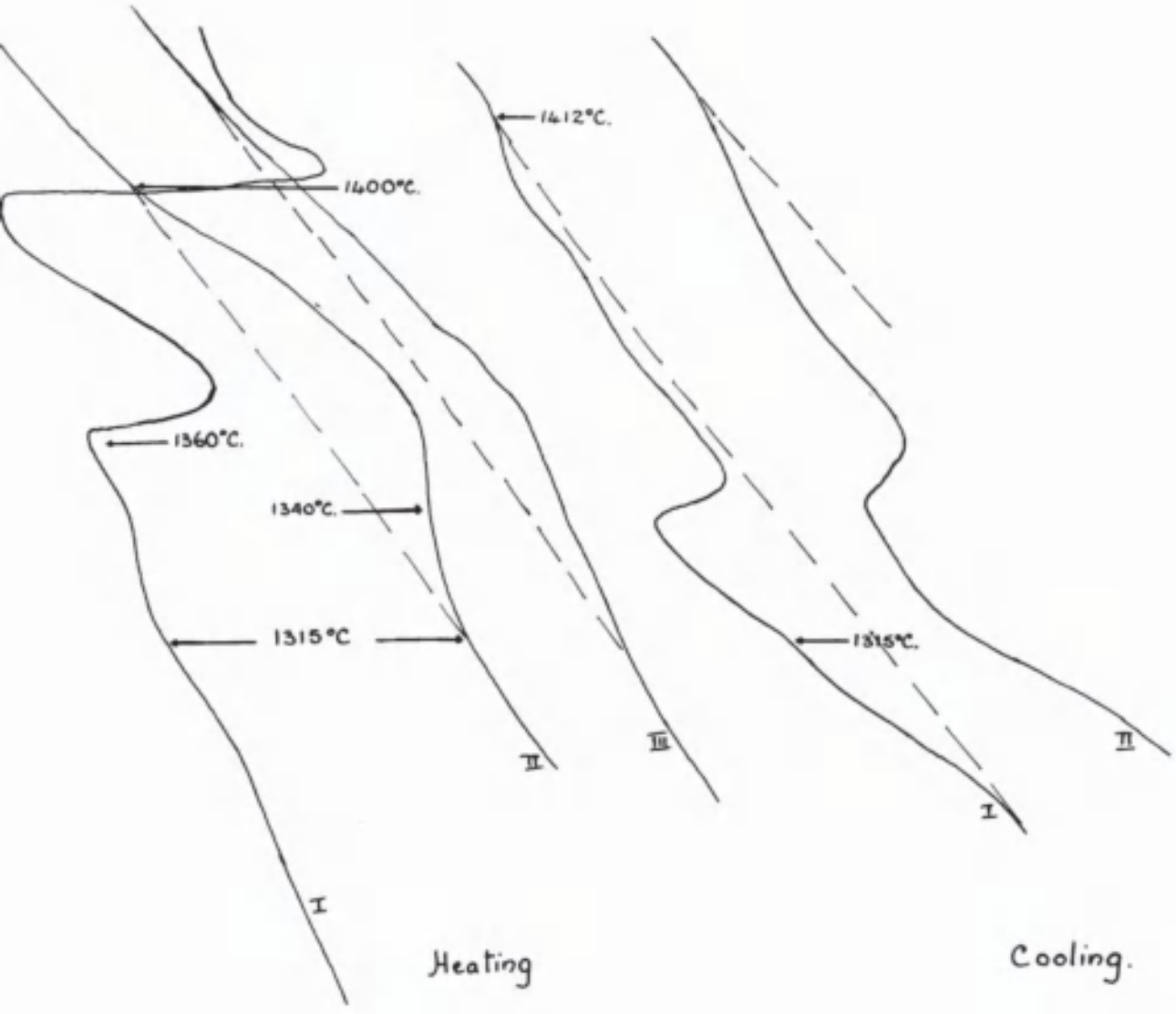

Figure 101

Melt 20

FeO 30%
MnO 30%
TiO_2 40%

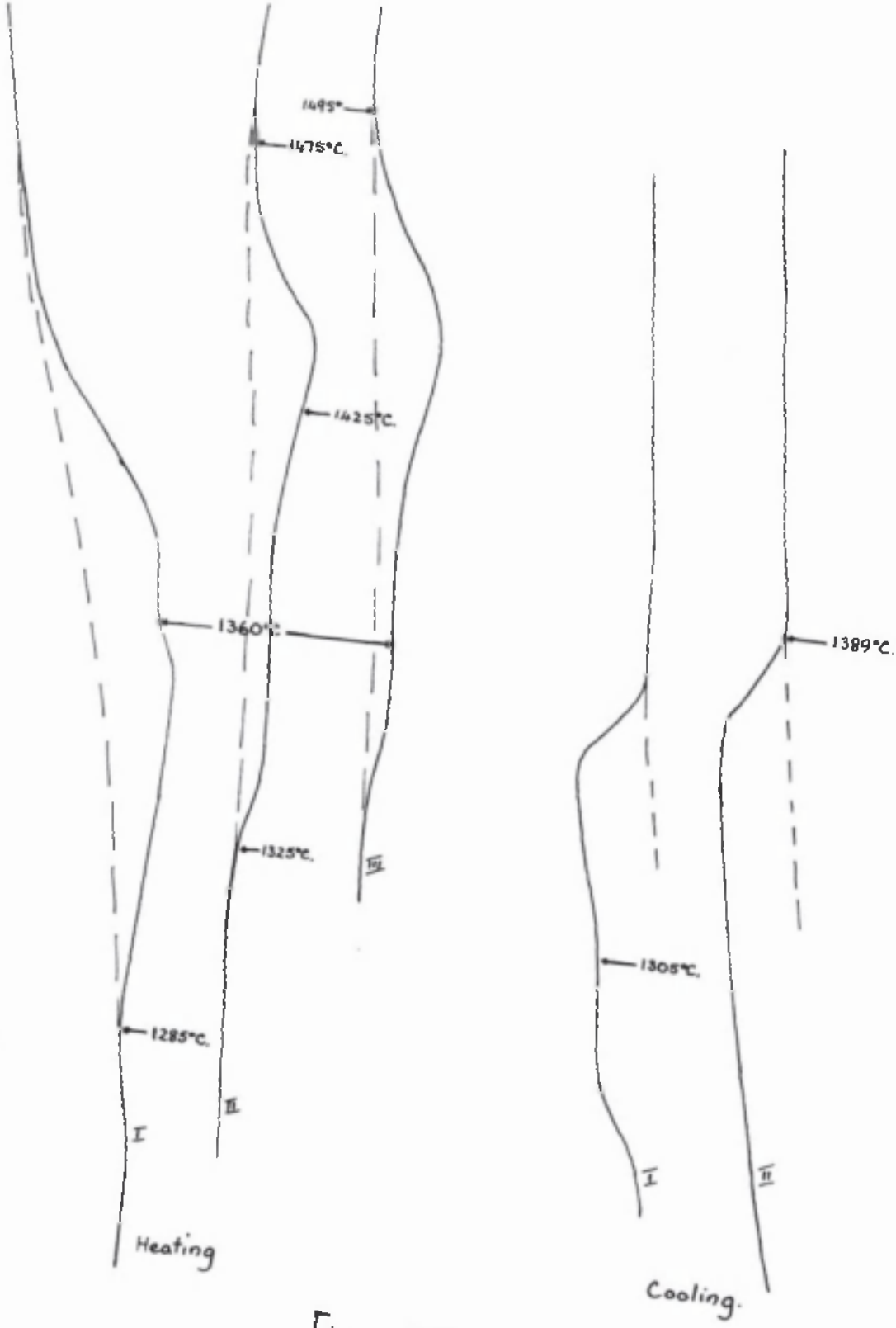

Figure 102.

Melt 21.
FeO 30%.
MnO 20%.
TiO_2 50%.

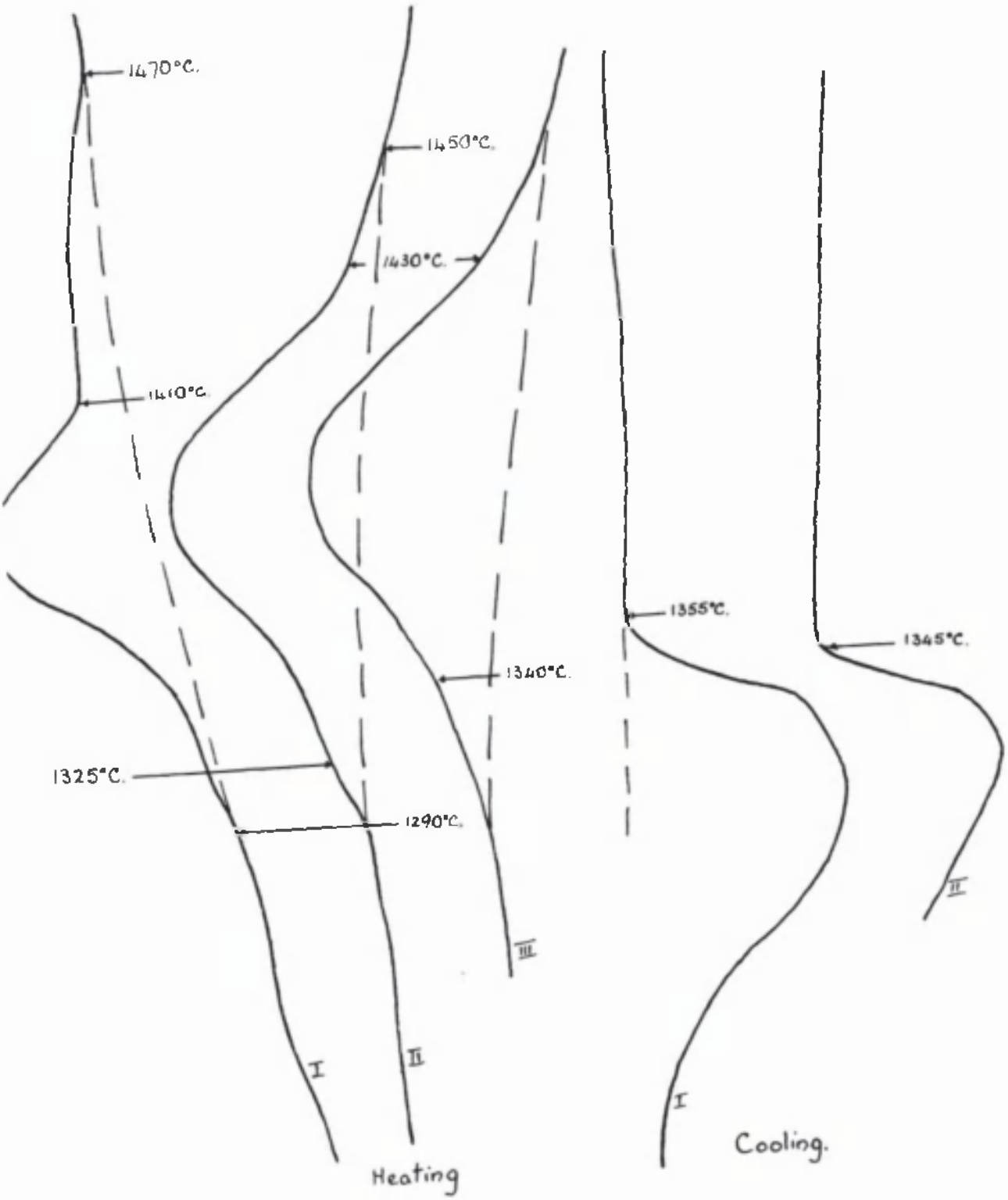

Figure 103.

Melt 22.

FeO 30%.
MnO 10%.
TiO_2 60%.

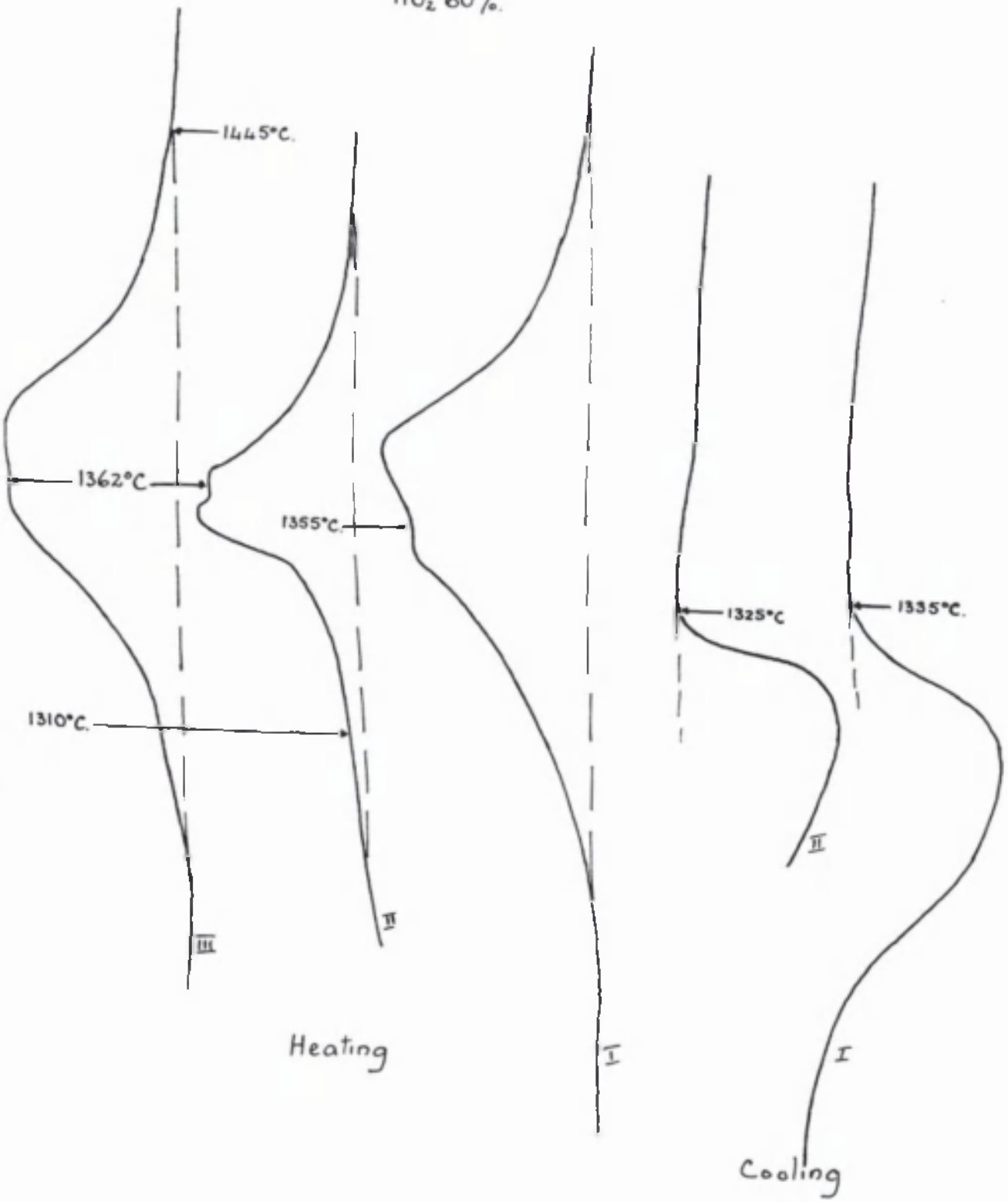

Figure 104.

As in previous figure, but greater amount of orthotitanate phase.

Fig. 122 - MnO 30% : FeO 60% : TiO_2 10%. ×180

Etchant dil. HCl.

Shows primary FeO - rich phase (dark etching) in eutectic of FeO phase and orthotitanate phase.

Fig. 123 - MnO 40% : FeO 50% : TiO_2 20%. ×90

Etchant dil. HCl.

Primary orthotitanate phase in eutectic background.

Fig. 124 - MnO 50% : FeO 40% : TiO_2 10%. ×180

Etchant HCl.

Primary dendrites and globules of MnO - rich phase in eutectic background.

Fig. 125 - MnO 50% : FeO 30% : TiO_2 20%. ×180

Etchant HCl.

As in previous figure but less primary phase.

Fig. 126 - MnO 70% : FeO 20% : TiO_2 10%. ×180

Etchant HCl.

Primary globules of MnO - rich phase in eutectic that is mainly orthotitanate phase.

Fig. 127 - MnO 10% : FeO 30% : TiO_2 60%. ×104

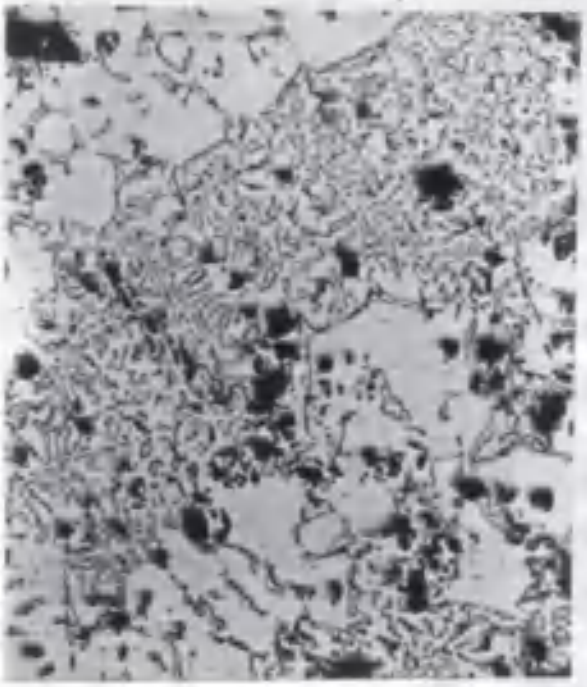

Figure 123

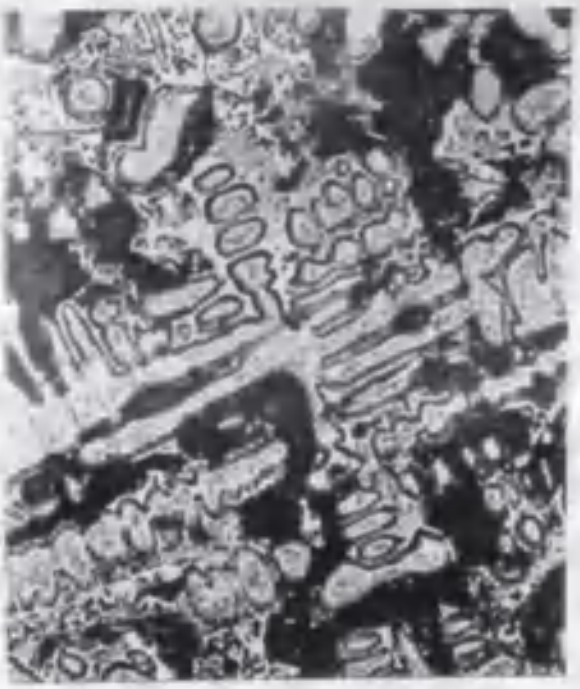

Figure 124

Figure 125

Figure 126

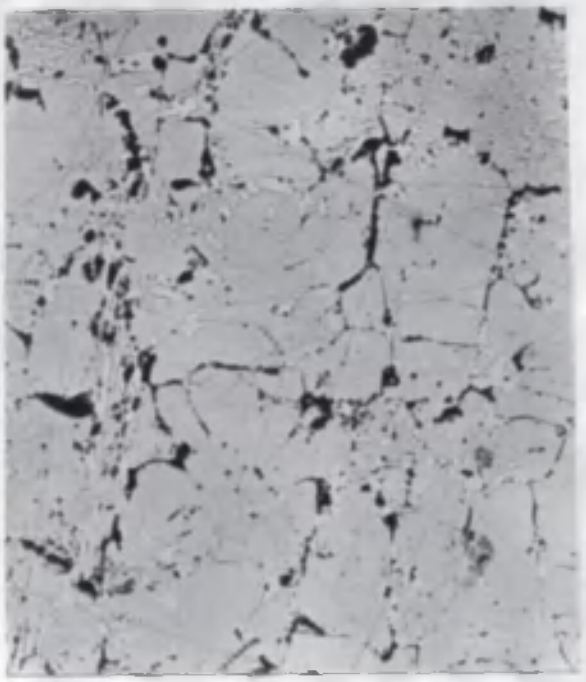

Figure 127

Figure 128.

Etchant HF.

Primary metatitanate phase in eutectic of metatitanate phase and rutile (bright etching).

Fig. 128 - MnO 10% : FeO 20% : TiO_2 70%. ×304

Etchant HF.

Primary rutile in background of metatitanate phase.

Figures 129 and 130 respectively show the liquidus temperatures and the solidus temperatures of the melts investigated. A more detailed examination of the ternary system FeO - MnO - TiO_2 was rendered impossible, since on the outbreak of war it was found impossible to obtain Pythagoras tubes with which to continue the research.

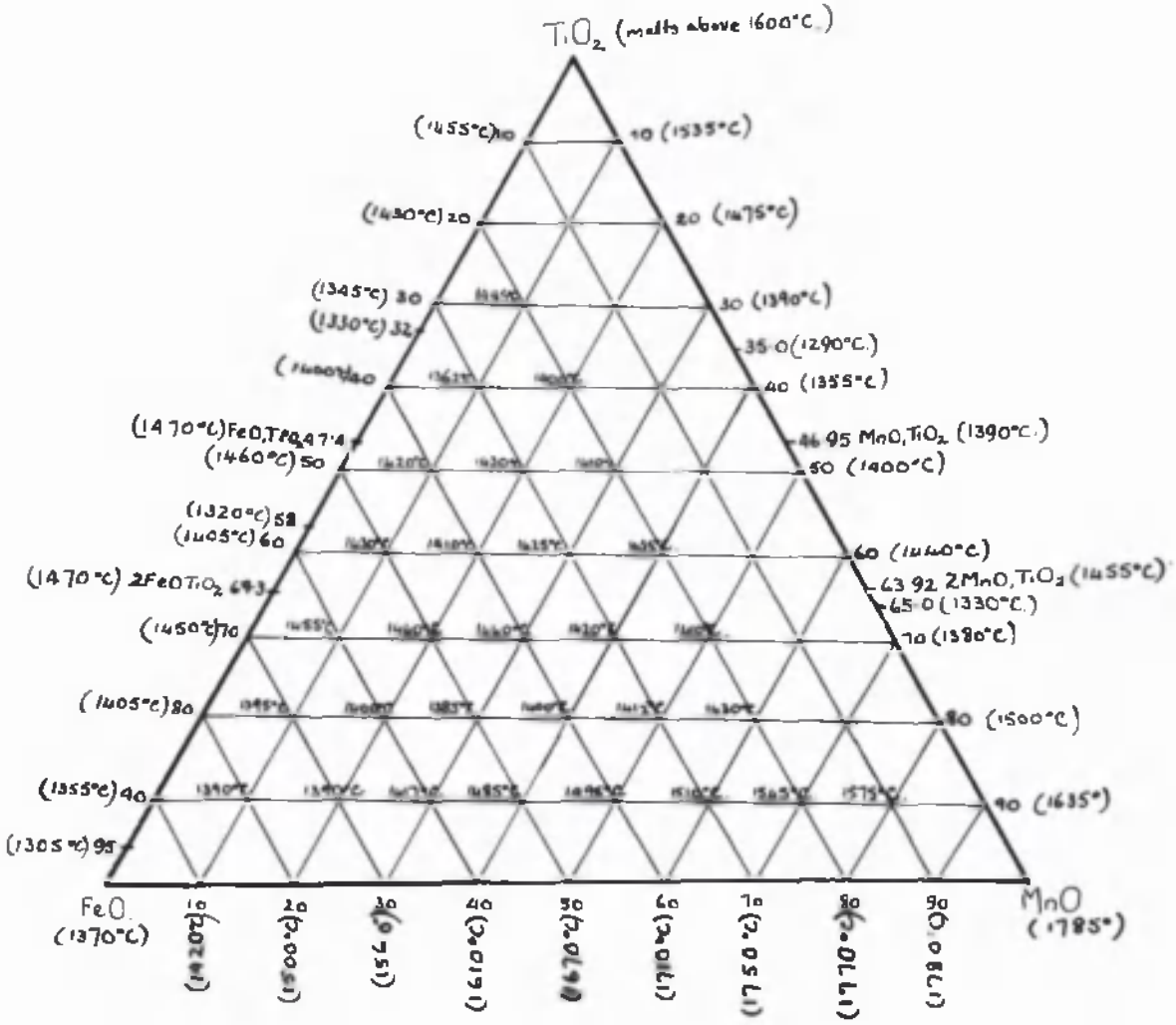
TiO2 (melts above 1600°C.)
(1455°C)10
10 (1535°C)
(1430°C) 20
20 (1475°C)
(1345°C) 30
30 (1390°C)
(1330°C) 32
35·0 (1290°C.)
40 (1355°C)
(1470°C) FeO,TiO2 47·4
46·95 MnO,TiO2 (1390°C.)
(1460°C) 50
50 (1400°C)
(1320°C) 58
(1405°C) 60
60 (1440°C)
(1470°C) 2FeO,TiO2 64·3
63·92 2MnO,TiO2 (1455°C)
65·0 (1330°C.)
(1450°C) 70
70 (1380°C)
(1405°C) 80
80 (1500°C)
(1355°C) 40
90 (1635°)
(1305°C) 95
FeO (1370°C)
MnO (1785°)
10
20
30
40
50
60
70
80
90
(1420°C)
(1500°C)
(1540°C)
(1610°C)
(1670°C)
(1710°C)
(1750°C)
(1770°C)
(1780°C)

FIGURE 129

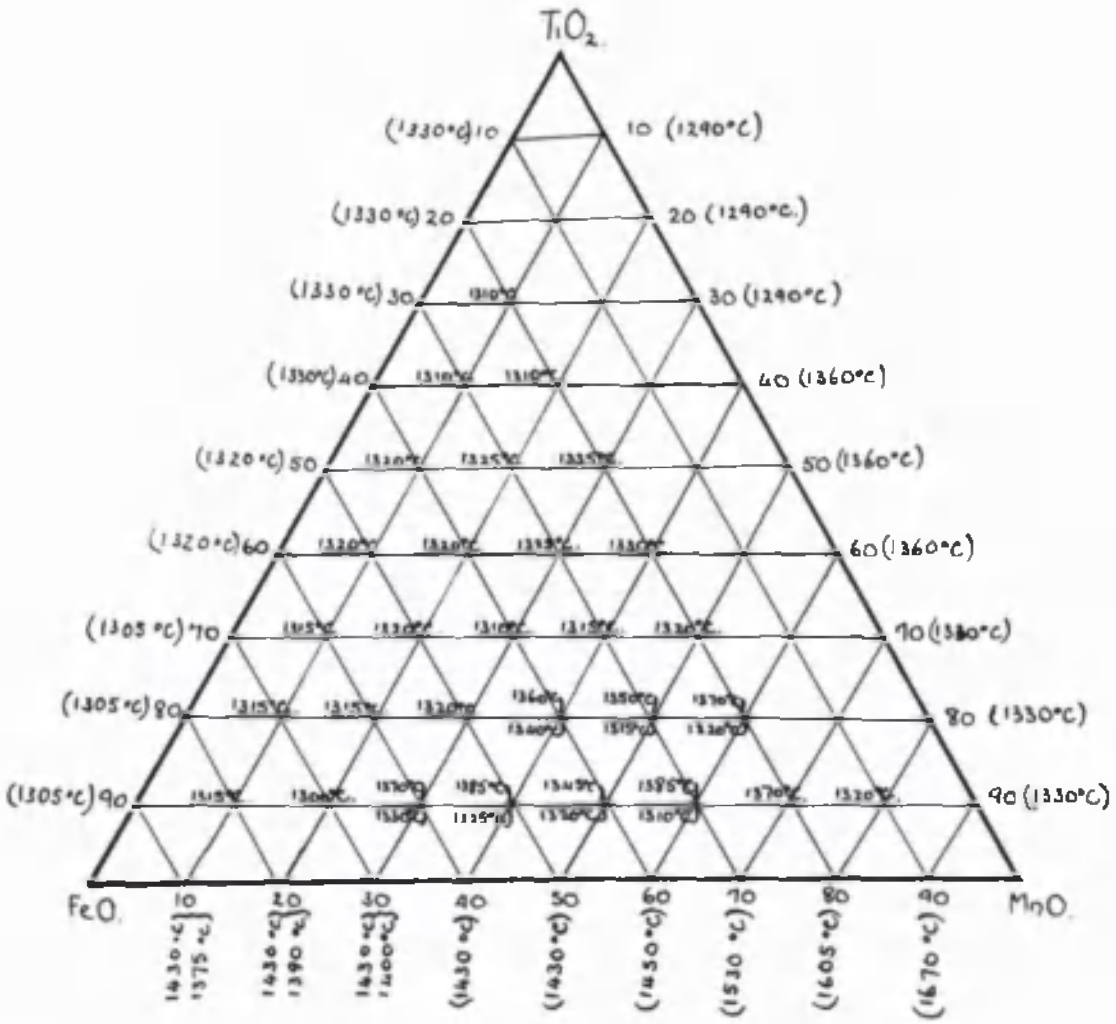
TiO2
(1330°C) 10
10 (1290°C)
(1330°C) 20
20 (1290°C)
(1330°C) 30
30 (1290°C)
(1330°C) 40
40 (1360°C)
(1320°C) 50
50 (1360°C)
(1320°C) 60
60 (1360°C)
(1305°C) 70
70 (1330°C)
(1305°C) 80
80 (1330°C)
(1305°C) 90
90 (1330°C)
FeO
MnO
10
20
30
40
50
60
70
80
90
(1430°C) 1375°C
(1430°C) 1390°C
(1430°C) 1400°C
(1430°C)
(1430°C)
(1430°C)
(1510°C)
(1605°C)
(1670°C)

FIGURE 130

APPENDIX I.

REDUCIBILITY OF TITANIA (TiO_2).

The reducibility of titania was studied by Nobuyuki Nasu[43]. He investigated the equilibrium constant of the reaction:-

$$2TiO_2 + H_2 = Ti_2O_3 + H_2O.$$

which can be represented by :-

$$Kp = \frac{P_{H_2O}}{P_{H_2}},$$ where Kp represents the equilibrium constant in terms of pressure, P_{H_2O} and P_{H_2}, being the partial pressures of H_2O and H_2 at equilibrium respectively.

The curve of log. Kp against $\frac{1}{T^\circ A}$ is shown in Figure (131) Up to 1009°C. it approximates closely to a straight line, hence by extrapolation the value of Kp at 1600°C. can be got fairly accurately (assuming linearity to hold over the range of the extrapolation).

Extrapolation to 1600°C. = 1873°A.

Hence $\frac{1}{T^\circ A} = 5{\cdot}339 \times 10^{-4}$ gives log. Kp = 0·437 and

Kp = 2·735.

DISSOCIATION OF H_2O AT 1600°C. (1873°A.).

According to Mc'Cance[45] :-

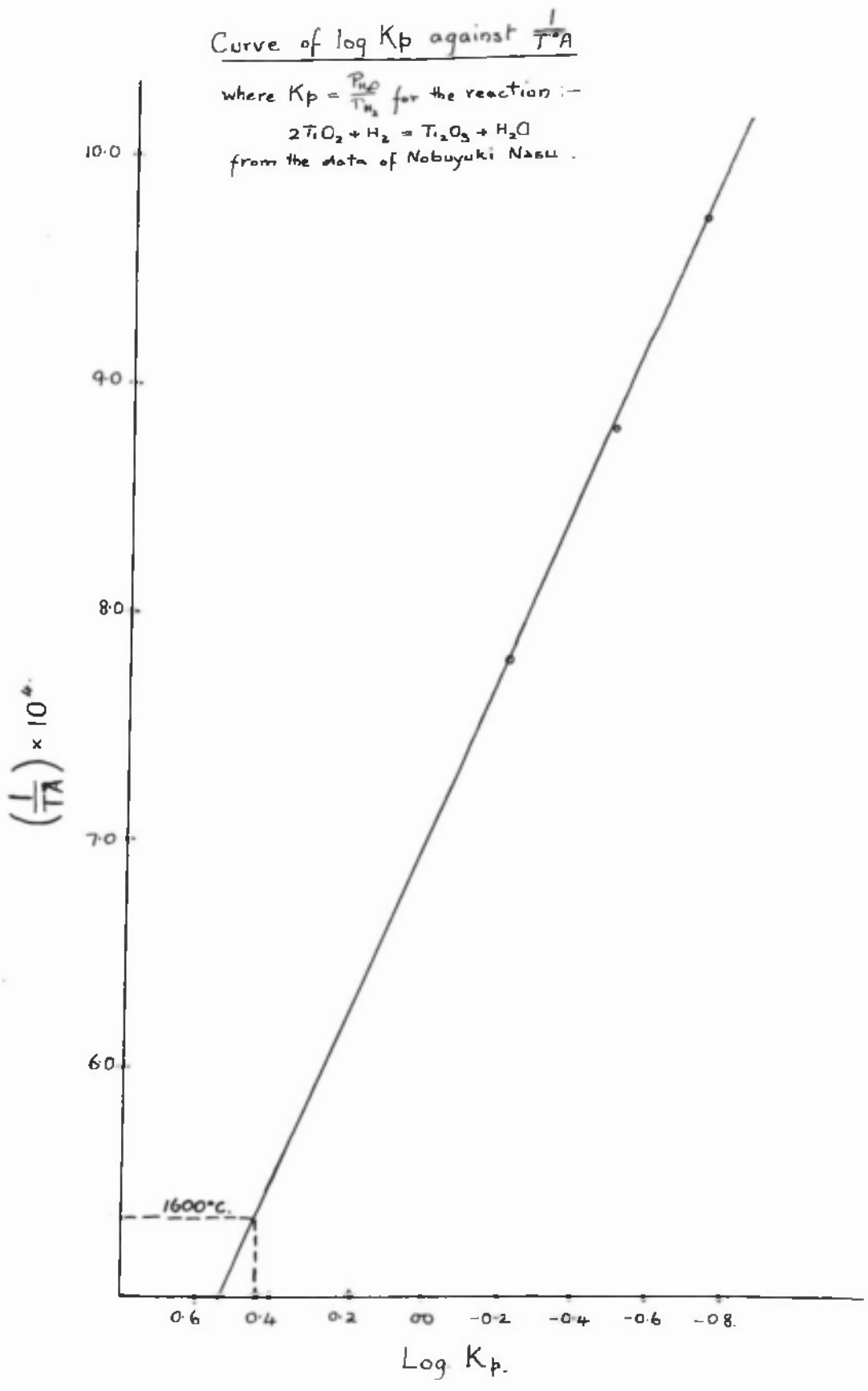
Curve of log Kp against $\frac{1}{T°A}$
where $K_p = \frac{P_{H_2O}}{P_{H_2}}$ for the reaction :-
$2TiO_2 + H_2 = Ti_2O_3 + H_2O$
from the data of Nobuyuki Nasu .
10·0
9·0
8·0
7·0
6·0
$\left(\frac{1}{T°A}\right) \times 10^4$
1600°C.
0·6
0·4
0·2
00
-0·2
-0·4
-0·6
-0·8
Log K_p.

FIGURE 131

$$\log K_p = \log K_1 - \frac{Q}{2.303RT}$$

$$= -\frac{[illegible]}{[illegible]} - [illegible]$$

$$= -[illegible] = [illegible]$$

$$K_p = 1.022 \times 10^{-6} = \frac{[illegible]}{[illegible]}$$

$$\text{Now } K_p = \frac{P_{H_2O}}{P_{H_2}} = 2.735$$

$$\therefore (K_p)^2 = 2.735^2$$

$$\text{And } K_7 \times (K_p)^2 = O_2$$

$$\therefore O_2 = 1.622 \times 10^{-8} \times 2.735^2$$

$$= 1.215 \times 10^{-7}$$

$$= 12.15 \times 10^{-8}$$

Thus, the dissociation pressure of T_1O_2 at $1600^{\circ}C.$ = 12.15×10^{-8} atmospheres, assuming the expression given by Mc'Cance[45], for the dissociation constant of water to be correct.

DISSOCIATION OF FeO.

According to Mc'Cance:-

$$FeO + H_2 = H_2O + Fe \text{----------} (4)$$

At $1600^{\circ}C$:-

$$\text{Log. } K_4 = -\frac{1300}{T} + 1.02$$

$$= -\frac{1300}{1873} + 1.02$$

$$= -6.94 + 1.02$$

$$= 0.326 \text{ (at } 1600^{\circ}\text{C.)}$$

$$\therefore K_4 = \frac{H_2O}{H_2} = 2.118$$

Thus, the dissociation pressure of FeO at 1600°C. is given by:-

$$P_{FeO} = \frac{(H_2)^2 \times O_2}{(H_2O)^2} \times \left(\frac{H_2O}{H_2}\right)^2 = O_2$$

$$= K_7 \times (K_4)^2$$

$$= 1.622 \times 10^{-8} \times 2.118^2$$

$$= 7.27 \times 10^{-8} \text{ atmospheres.}$$

DISSOCIATION OF MAGNETITE (Fe_3O_4) AT 1600°C. (1873°A.)

$$Fe_3O_4 + H_2 = 3FeO + H_2O \quad \text{----------(5)}$$

$$\text{Log. } K_5 = -\frac{3300}{1873} + 3.61$$

$$= -1.76 + 3.61$$

$$= 1.85$$

$$\therefore K_5 = \frac{H_2O}{H_2} = 70.79$$

$\therefore$ Dissociation pressure of $Fe_3O_4 = 1.622 \times 10^{-8} \times 70.79^2$

$$= 8.14 \times 10^{-5} \text{ atmospheres.}$$

DISSOCIATION OF FERROUS OXIDE (FeO) AT 1000°C. (1273°A.)

According to Mc'Cance:-

$$FeO + H_2 = H_2O + Fe \quad \text{---------- (4)}$$

$$\therefore \text{Log. } K_4 = -\frac{1300}{1273} + 1.02$$

$$= -1{\cdot}02 + 1{\cdot}02$$

$$= 0$$

$$\therefore K_4 = \frac{H_2O}{H_2}$$

$$= 1{,}000$$

Now at 1,000° C.

$$\text{Log. } K_7 = -\frac{25500}{1273} + 1{\cdot}75 \text{ log. } 1273 + 0{\cdot}11$$

$$\therefore P_{O_2} = 2{\cdot}6 \times 10^{-16} \text{ (value of } K_7 \text{ at 1,000° C.)}$$

Emmett and Shultz[44] got $0{\cdot}678 \times 10^{-16}$ for K_7 at 1,000° C.

DISSOCIATION OF T_1O_2 AT 1,000° C. - Can be read off directly from the curve (Fig. 131) and has the value 0·595 approximately

The equation numbers (7), (5) and (4) are those used by Mc'Cance[45].

APPENDIX II.

CALCULATION OF THE CRYSTAL STRUCTURE OF SINTERED TITANIA.

Rutile is tetragonal with:

$$a = 4{\cdot}58 \text{ Å}.$$

$$c = 2{\cdot}95 \text{ Å}.$$

$$\text{and } \frac{c}{a} = 0{\cdot}644$$

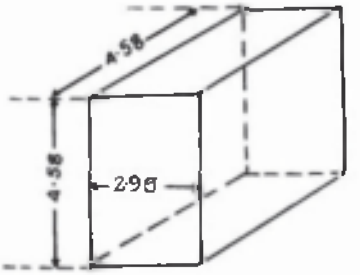

DETAILS OF CAMERA.

1 cm. on film represents $20{\cdot}3^{\circ}$ deviation.

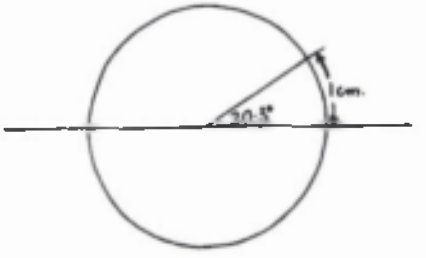

BRAGGS LAW states:

$$n\lambda = 2d \sin\theta$$

where θ is $\frac{1}{2}$ the angle of refraction or deviation

n = frequency

λ = wave-length

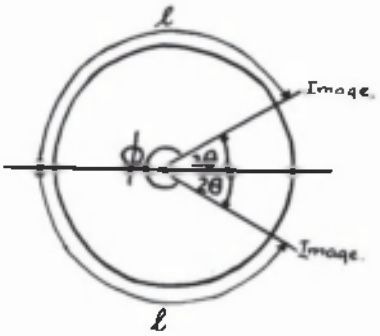

d = space between the atomic planes.

$$\therefore d = \frac{n\lambda}{2\sin\theta}$$

Also $d = \dfrac{a}{\sqrt{h^2 + k^2 + \dfrac{l^2}{c^2/a^2}}}$ for a tetragonal lattice.

where h, l, and k, are Miller's Indices.

$$\therefore a = \sqrt{h^2 + k^2 + \frac{l^2}{.644^2}} \qquad \left(\frac{c}{a} = \frac{4.58}{2.95} = 0.644 \right.$$

$$\left. \frac{c^2}{a^2} = 0.644^2 = 0.416 \right)$$

Distance between lines measured = 2l

and $4\theta = 360^\circ - \phi$. gives the value of θ.

The details of the calculations are shown in Figure 7. The mean values are approximately a = 4·58 Å and c = 2·95 Å (if last value left out).

Hence the specimen of titania must be in the form of Rutile.

Anatase is tetragonal also but has a = 3·73 Å, c = 9·37 Å while Brookite is orthorhombic and has a = 9·14 Å

b = 5·44 Å

c = 5·15 Å

and it was found that the spectrum obtained was inconsistent with these values.

Table 7.

2ℓ	ϕ	4θ	θ	sin θ	d	Planes	a	c
11·45 s	232·5°	127·5°	31·88°	0·5281	1·692	211	4·54	2·92
14·55 ww	295·4°	64·6°	16·15°	0·2781	3·21	110	4·54	2·92
9·55 ww	193·8°	166·2°	41·55°	0·6633	1·348	112	4·58	2·95
					β1·22	301	4·56	2·94
6·05 ww	122·8°	237·2°	59·30°	0·8599	1·039	420	4·64	2·98
4·45 ww	90·3	269·7°	67·43°	0·9235	0·9675	103	4·60	2·96
13·65 www	277·0°	83·0°	20·75°	0·3543	2·523	011	4·60	2·96
					β2·285			
11·20 www	227·5°	132·5°	33·13°	0·5466	1·635	220	4·61	2·97
6·85 ww	139·1°	220·9°	55·23°	0·8215	1·087	222	4·56	2·94
						330	4·61	2·97
10·25 www	208·1°	151·9°	37·98°	0·6155	1·450	310	4·58	2·95
12·05 www	244·1°	115·9°	28·98°	0·4846	1·846	201	4·66	3·00

In conclusion. I should like to express my thanks and indebtedness to Professor R. Hay, Ph.D., F.I.C.,for his interest in the work and his invaluable advice and encouragement, and also to J. White D.Sc., A.R.T.C., whose experience and advice in thermal technique was of great value. I should also like to thank the Department of Scientific and Industrial Research for the award of a grant which enabled me to participate in this research.

REFERENCES.

1. C.M.Dyson : Chemical Age, 1926, vol. 14, p.33.
2. Mathesius : British Patent No. 459, 432, 1935.
3. Comstock : Iron Age, 1924, vol. 114, p.1477.
4. Comstock : Chemical and Metallurgical Engineering, 1922, vol. 26, p.165.
5. Benedicks and Lofquist : Non-metallic Inclusions in Iron and Steel, Chapman and Hall, London, 1930.
6. Bogatzky : Metallurgist Russia, 1936, No.1, p.59.
7. Junker : Z. anorg. allegem. Chem., 1936, 228, 97-111.
8. Keizo Iwase and Usaburo Nisioka : Sci. Rep., Imperial Tokio Univ., Series 1, 26, No.4, 592.
9. Frankenheim : Ann. Physik., 1836, [ii] 39, 376.
   F.S.Schaffgotsch : ibid. 1857, 102, 293.
10. Osmond : Memoirs de l'Artillerie Marine, 1887, XV., 573.
    Journ. Iron and Steel Inst., 1890, I., 38.
11. Roberts - Austen : Fifth Report Alloys Research Committee, Proc. Instit. Mech. Engineers, 1899.
12. Rosenhain : Proc. Physical Soc., 1908, XXI., 180.
13. R.Schenck : Deut. Forschung, 3, 1928.
    Arch. Eisenhuttenwesen, 1928, 1, 494.
    Electrochem. 1915, 21, 48.
    Zeit. Anorg. Chem., 1926, 166, 113; 1932.
    208, 255.

14. Benedicks and Lofquist : Non-Metallic Inclusions in Iron and Steel . London, 1930: Chapman and Hall, Ltd.

15. Matheweson, Spire and Milligan : Amer. Soc. Steel Treaters 1931, 19, p.66.

16. H.Schenck and Hengler : Archiv. fur das Eisenhuttenwesen, 1931-32, 5, p.209.

17. Pfeil : Journ. Iron and Steel Inst., 1931, 123, p.237.

18. Jette and Foote : Contra. Amer. Inst. Min. Eng., 1933, 7. Journ. Chem. Phys., 1933, 1, 29.

19. Kanz and Scheil : Archiv. fur das Eisenhuttenwesen, 1938-39, 12, p.481.

20. Chaudron and Forestier : Comptes Rendus, 1924, 178, 2173.

21. Tritton and Hanson : Journ. Iron and Steel Inst., 1924, vol. CX., p.90.

22. Bowen and Schairer : American Journal of Science, 1932, 24, p,177.

23. White Hay and Graham : Journ. Iron and Steel Inst., 1935, 131, p.91.

24. White : Iron and Steel Inst., Carnegie Scholarship Memoirs, 1938, 27, p.1.

25. O.C.Ralston : Iron Oxide Reduction Equilibria, Washington, 1929. Bull U:S. Bur. Mines, 1929, 296.

26. Matsubara : Trans. Am. Inst. Min. Met. Eng. 1922, 67, 3. Z. Anorg. Chem., 1922, 124, 39.

27. Eastman and Evans : J. Am. Chem. Soc., 1924, 46, 888.

28. Hay, Howat and White : Journ. of the W. of Scotland, Iron and Steel Instit., 1933-34, 41, p.97.

29. Chimie Minerale : 1905, vol.4, p.399.

30. C.W.Blomstrand : Ber. 1875, 8, 130.
Geol. Forh. Stockholm, 1874, 2, 179;
1876, 3, 123.

31. Tiede and Birnbauer : ib. 1914, 87, 129, 162.

32. White, Howat and Hay : Jour. Royal Technical College, Glasgow, 1934, 3, p.231.

33. C.W.Scheele : Sevenska Akad. Handl., 1774, 35, 89, 177.
Abhand. Akad. Stockholm, 1774, 36, 95, 183.
Opuscula Chemica and Physica, Ripsiae London, 1901, 53.

34. E.G.L.Roberts and E.A.Wraight : Journ. Iron and Steel Inst., 1906, 70, ii, 229.

35. J. von Liebig : ib., 1885, 95, 116.

36. Oberhoffer and d Huart : K., St. Eisen, 1919, 39, 165, 196.

37. Andrews, Maddocks and Howat : Journ. Iron and Steel Inst., 1931, 125, ii, 283.

38. Oberhoffer and von Keil : O. I. St. Eisen, 1920, 40, 812.

39. H:E:Merwin and E.S.Larsen : Am. Journ. of Science, 1912, 34, p.42.

40. A.W.Hull : Amer. Phys. Soc. October, 1916.
Phys. Rev. 1917, 9, 84, 564; 1917, 10, 661.

41. P.Debeye and P.Scherrer : Nachr. Kgl. Wiss. Gottingen, 1915-16. Phys. Zeit., 1916, 17, 277; 1917, 18, 291-301.

42. King : J. Amer. Ceramic Soc., 1937, 16, 53.

43. Nobuyuki Nasu : Sci. Rep., Imperial Tokio Univ., Series 1, 25, No. 3, 510.

44. Emmett and Schultz : J. Amer. Ceramic Soc., 1933, 55, 1376.

45. Mc Cance : Trans. Far. Soc., 1925, 21, Part 2, 176. Symposium on Phys. Chem. of Steel-making.

46. Bowen and Schairer : Amer. Journ. of Science, 1932, 24.

47. Gibbs : Thermodynamische Studien. Trans. Connecticut Academy, III, 1874 bis 1878. Deutesche Ubersetzung von W.Oswald, 1892.

48. Roozeboom : Die Heterogenen Gleichgewichte vom Standpunkt der Phasenlehre.